DEVELOPMENT OF METHODS TO PREDICT AND ENHANCE THE PHYSICAL STABILITY OF HOT MELT EXTRUDED SOLID DISPERSIONS

Ziyi Yang, Msc Pharmaceutics

Thesis submitted for the degree of Doctor of Philosophy

University of East Anglia

June 2013

Acknowledgements

My PhD experience over the last three years at University of East Anglia has been enjoyable, rewarding and challenging. I would like to take this opportunity to express my gratitude to both my supervisors Dr Sheng Qi and Prof Duncan Craig for their excellent supervision, consideration, continuous encouragement and assistance throughout my PhD study. This work cannot be completed without the support and input from my industrial supervisors Dr Kathrin Nollenberger, Dr Jessica Albers and Mr George Smith from EvonikRöhm GmbH. Many thanks to Prof Peter Belton from the University of East Anglia for the solid state NMR work and many thanks to Dr Maximilian Skoda from Rutherford-Appleton Lab for the neutron reflectivity work. Thank you, Dr Jonathan Moffat from the University of East Anglia for the technical support and advice with AFM and ATR-FTIR work.

I would also like to thank all my fantastic friends, Xia Lin, Jonathan and Louise, Susan and Ricky, Dave and Kathy, Kate Bowman, Min Zhao, Jin Meng, Soik Chan and Fatama. Many thanks for all the laughs, beer and great company. Thanks to all the past and present members of the UEA Pharmaceutics research Group. In addition, I will not forget to mention the kindness of the staff and technicians from University of East Anglia for all their help and assistance throughout my PhD study. Many thanks to all those who have trained me on instruments taught me software and generally made my PhD life easier than it could have been.

I would like to extend my deepest gratitude to my wonderful parents, Tao Yang and Chunhua Shi. I would not be able to complete this endeavour task without your unconditional love, continuous support and encouragement.

Abstract

The application of amorphous solid dispersions is one of the most widely used formulation strategies for the enhancement of *in-vitro* and *in-vivo* performance of poorly water-soluble drugs. However, because of their meta-stable nature, the physical stability of amorphous solid dispersions has been considered to be the main obstacle for their formulation development and commercialisation by the pharmaceutical industry. The aim of this project was to understand, predict and enhance the physical stability of amorphous solid dispersions prepared by hot melt extrusion. Four model drugs felodipine, celecoxib, fenofibrate and carbamazepine and two polymeric matrices EUDRAGIT® EPO and Kollidon® VA 64 were formulated by hot melt extrusion and spin coating into solid dispersions. A series of physicochemical characterisation techniques including MTDSC, PXRD, SEM, ATR-FTIR and AFM-LTA were used to evaluate the systems. Physical characterisation of the model drugs and polymers, prediction of drug-polymer miscibility and solubility and real-time physical stability studies under different conditions were carried out. Across the project, several key achievements were obtained. It was revealed that the physical stability of the amorphous drugs alone and the predicted processing-related apparent drug-polymer solubility were the two dominant factors controlling the physical stability of the amorphous systems. A practical method, milling, was developed to provide a more accurate prediction of processing-related apparent drug-polymer solubility. Two methods were developed to enhance the physical stability of amorphous solid dispersions: one based on formulation design, use of immiscible polymer blends and the other based on a particular type of processing, spin coating. The achievements from the project are expected to contribute to the formulation development of amorphous solid dispersions in terms of screening suitable drug candidates, selecting “safe” (physically stable) drug loadings and identification of methodologies to improve the physical stability of formulations.

Table of Contents

Chapter 2 Materials and methods

Chapter 3: Physicochemical characterisation of model drugs and polymers

Chapter 6: Physical stability studies of hot melt extrudates on aging

List of Figures

List of Tables

Abbreviations

AFM	Atomic Force Miscroscopy
API	Acative Pharmaceutical Ingredient
ATR-FTIR	Attenuated Total Refelectance Fourier Transfom Infrared
DSC	Differential Scanning Calorimetry
DVS	Dynamic Vapor Sorption
HME	Hot Melt Extrusion
LTA	Locallized Thermal Analysis
MTDSC	Modulated temperature differential scanning calorimetry
PT-MS	Photothermal Microspectroscopy
PXRD	Powder X-Ray Diffraction
RH	Relative Humidity
SEM	Scanning Electron Microscopy
ssNMR	Solid State Nuclear Magnetic Resonance
T_g	Glass Transition Temperature
TGA	Thermogravimetric Analysis
TTM	Transition Temperature Mapping

Chapter 1 Introduction

1.1 Background of the project

The enhancement of oral bioavailability of poorly water-soluble drugs remains one of the most challenging aspects in the pharmaceutical industry with the increasing production of new active pharmaceutical ingredients (APIs) (1). It is commonly recognised in the pharmaceutical industry that, on average, around 30%-40% of newly discovered drug candidates are poorly water soluble (2-4). In 1995, the Biopharmaceutics Classification System (BCS) was introduced in the pharmaceutical industry, whereby APIs were divided into four groups based on their aqueous solubility and permeability. BCS II and IV (poor permeability) APIs are classified with poor aqueous solubility and have been attracting interests from formulation scientists on improving their dissolution performance (5). Briefly, an orally administered API will only be functional in bodies if it can be absorbed in the gastro-intestinal (GI) tract, for which the *in-vivo* dissolution of the API is the pre-requisite (6). Formulation strategies in overcoming the issue of poor aqueous solubility (especially BCS II APIs) in the pharmaceutical industry involves: particle size reduction; formation of complexes; formation of pro-drug (i.e. modify the drug into salt form or preparation of co-crystals); formulation of self-emulsifying drug delivery system and preparation of solid dispersions (7-12).

The application of solid dispersions has been proved to be highly effective in increasing dissolution rate of APIs with poorly aqueous solubility in a number of studies since the concept of solid dispersions was introduced decades ago (13-17). The first description of solid dispersions was introduced in a study using eutectic mixture of chloramphenicol and urea, and later in the same decade solid dispersions were defined as dispersing an API into polymeric matrices by various processes (13, 18). APIs can exist in solid dispersions in different states, such as crystalline or micro-crystalline and molecularly dispersed into the matrices, depending on the preparation techniques and conditions employed (6, 18, 19). Processes commonly applied to prepare solid dispersions include: solvent evaporation based method such as spray drying or film casting, melting based method such as hot melt extrusion, and milling (20-23).

Amorphous solid dispersions (solid solution) in which APIs are molecularly dispersed into polymeric matrices have been observed to show better dissolution performance in comparison to the corresponding solid dispersions containing crystalline APIs. Therefore, the application of amorphous solid dispersions is becoming popular amongst formulation scientists when attempting to improve drug release performance (24-26). The better dissolution performance has been well

explained by the reason that high-energy level amorphous materials had higher apparent solubility than their crystalline counterparts (27). However, this also brings the intrinsic drawback of amorphous solid dispersions having low physical stability. The high-energy level amorphous APIs in the solid dispersions tend to convert back to the more thermodynamically stable crystalline state (27). Physical instability of solid dispersions over aging can reduce the dissolution rate in comparison to the fresh sample due to the appearance crystalline drugs (28-30). Great effort has been devoted to the prediction and enhancement of the physical stability of amorphous solid dispersions (31-36). However, there have only been few products in the market despite the vast amount of existing articles (Table 1) (6). This is due to the incomplete understanding of the physical stability of amorphous solid dispersions, in particular concerning how to accurately predict and effectively enhance the physical stability of amorphous solid dispersions.

Table 1.1: Summary of currently available pharmaceutical products prepared using solid dispersions.

Product	Company	Year approved	Technology
GrisPEG	Pedinal Pharm Inc.	1975	Melt process
Cesamet	Eli Lilly	1985	Unknown
Sporanox	J&J	1996	Spray drying
Rezulin	Pfizer	1997	Melt extrusion
Kaletra	Abbot	2005	Melt extrusion
Torcetrapid	Pfizer	Phase III	Spray drying
Intelence	Tibotec	2008	Spray drying

Hot Melt Extrusion (HME) as a processing method can be superior over solvent evaporation based methods for certain systems due to the fast preparation, ease of scale up and solvent free (37, 38). In this project HME was selected as the main method for the preparation of amorphous solid dispersions. The key focus of this project is to predict and enhance the physical stability of amorphous solid dispersions. To achieve this goal, the project conducted studies on understanding factors controlling the physical stability, developing practical methods to predict drug-polymer solubility and developing methods to enhance the physical stability.

1.2 Amorphous materials

Changing crystalline drugs into the amorphous state can significantly increase the dissolution rate of poor water-soluble drugs (27). Therefore, amorphous solid dispersions are commonly considered to have superior performance over crystalline solid dispersions (6, 19). In some case studies, apparent aqueous solubility of drugs can be increased by hundreds folds by converting the original crystalline drug to its amorphous form (27, 39). Before the introduction of amorphous solid

dispersions, it is worth understanding the concept of amorphous materials and the mechanism of how the dissolution performance of poorly water-soluble drugs is improved.

1.2.1 Structure of amorphous materials

An amorphous material can be defined with the reference to its crystalline counterpart. A typical crystalline structure contains three long range order symmetry operators including translational, orientational and conformational (40). Structures of various crystalline materials are defined by these three operators whereas amorphous materials transformed from their crystalline counterparts are defined by the absence of all three operators (41). Position of molecules relative to one another in amorphous materials is random as in liquid state (27). Although lacking of the long range order, short range order have been confirmed to exist in amorphous materials. Ideally, amorphous materials are defined as isotropic having no order (translational, orientational and conformational) on any significant length scale. However, molecular structures of APIs can introduce local anisotropy to an amorphous system, which causes the local order and the order is termed as short range order (40). Therefore, an amorphous system has inherent short range order due to the local anisotropy but is still isotropic on a macroscopic scale (40). For most organic materials, the short range order is not expected to extend over distances significantly larger than nearest neighbour or next nearest neighbour, which is typically less than 20-25Å (a few molecular dimensions)(42). The illustration of structures of crystalline, amorphous and gaseous materials is shown in Figure 1.1.

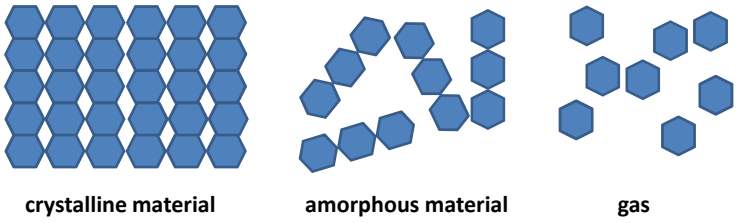

Figure 1.1: Illustration the structures of crystalline, amorphous and gas materials.

To dissolve a crystalline drug in a solution, a certain amount of energy is required to break the lattice structure to bring the drug molecules to a completely random state within the solution, and hence dissolution occurred. The more stable thermodynamically the lattice structure is, the more energy is needed. Therefore a poorly water-soluble drug could be expected if the dissolution energy barrier is high. However, as amorphous materials lack the long range order (typical lattice structure), less amount of energy is involved when dissolving amorphous materials in comparison to crystalline counterparts. Consequently, a higher dissolution rate can be achieved by changing a crystalline drug to amorphous state.

1.2.2 Thermodynamic properties of amorphous materials

To transform a crystalline material to its amorphous form, processes including precipitation from solution, milling and super-cooling from melt are commonly used (43-46). Amongst the three methods, super-cooling was the most effective and widely used method in preparing pure amorphous materials as the other two have limitations (i.e. the selection of solvent and anti-solvent in precipitation method can be limited) (43). The solid transformation from crystalline to amorphous state using super-cooling method has been well studied. The thermodynamic properties including enthalpy or specific volume (volume/mass) of a solid material as a function of its temperature are shown in Figure 1.2. For a crystalline material at very low temperatures, only a small increase of enthalpy was observed with increasing temperature (45). On heating to the temperature across the melting point of the crystalline drug, a discontinuity in both the enthalpy and specific volume of the crystalline drug at melting point (T_m) occurred, which represents the first order phase transition from solid to liquid (43). Upon rapid cooling from the melt, the values of enthalpy followed the equilibrium line into a "supercooled liquid" region. On further cooling, a change in slope can be seen at a characteristic temperature known as the glass transition temperature (T_g) of the material. From supercooled liquid (rubbery state) to glass state, the viscosity can significantly increase from 10^{-3} to 10^{12} Pa·s (43). It should be mentioned that fast cooling rate was required for the transformation into amorphous (glass) state as molecules did not have sufficient time to form crystalline structure.

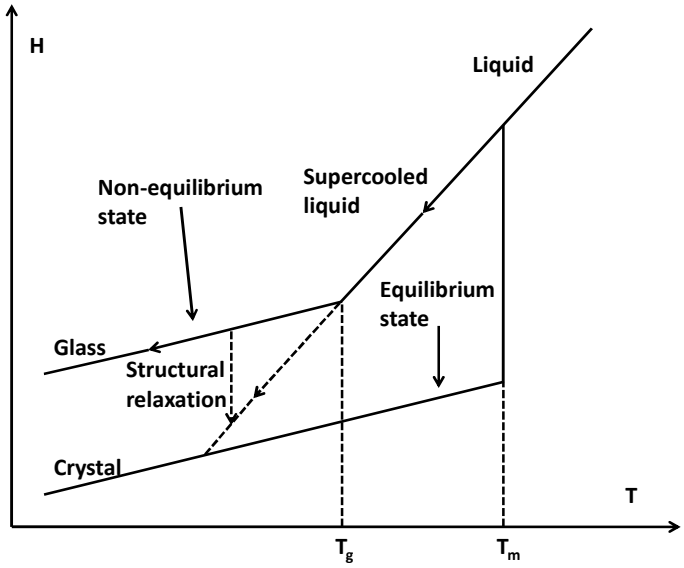

Figure 1.2: Schematic depiction of the formation of glass transition from a crystalline material.

Amorphous materials stay in a non-equilibrium state at the temperature below T_g and the thermodynamic properties (such as enthalpy and entropy in amorphous materials) are higher than

those in the corresponding crystalline materials at equilibrium state. If stored at the temperatures below T_g, structural relaxation in amorphous materials will occur (Figure 1.2) in the form of releasing the extra enthalpy or configurational entropy to approach the equilibrium (structural relaxation will be discussed later in this chapter). Amorphous materials prepared from their crystalline counterparts are intrinsically instable due to the high energy level, and they can only remain the amorphous state kinetically for a certain time period. However, it is also this high-energy level which mainly contributes to the improved dissolution rate in comparison to the corresponding crystalline materials. Therefore, in order to both obtain the enhanced dissolution rate and increase the physical stability of amorphous drugs, amorphous solid dispersions prepared with polymeric matrices and drugs were introduced in the pharmaceutical industry.

1.3 General introduction to solid dispersions

1.3.1 Definition of solid dispersions

The first preparation of solid dispersions can be dated back to 1961 when Sekiguchi and Obi prepared a eutectic mixture, of chloramphenicol and urea, whereby the drug and the matrices had specific composition and solidified together when cooling from melts and found the formulation showed enhanced dissolution rate and bioavailability (13). This eutectic mixture was later classified as one category of solid dispersions in the literature where solid dispersions were first defined: “the dispersion of one or more active ingredients in an inert carrier or matrix at solid state by the melting (fusion), solvent or melting-solvent method” (18).

Following the original concept, solid dispersion is now a broad concept which is commonly accepted by pharmaceutical researches as dispersing drugs into polymeric carriers via various preparation processes to form a drug-polymer mixture (19). In this mixture, drugs can remain in different states such as crystalline/micro-crystalline or molecularly dispersed into matrices. By formulating into solid dispersions with different matrices, drugs release can be modified: increasing dissolution rate of poorly water-soluble drugs, decreasing drug release rate of highly water-soluble drugs (6, 19).

Commonly employed preparation processes for solid dispersions consist of melting based methods such as: hot melt extrusion and solvent evaporation based methods such as spray drying (6, 37, 47). In comparison to other formulation strategies, such as pro-drug formulation and self-emulsifying drug delivery system for enhanced dissolution and absorption, solid dispersion can be superior in some aspects including: ease of scale up; low production cost and wide application to various drugs with different physical properties (14). Therefore, the solid dispersion technology has become a promising formulation strategy increasingly attracts interest from the pharmaceutical industry.

1.3.2 Classification of solid dispersions

The first classification of solid dispersions was introduced by Chiou and Riegelman in 1971 (18). Further on, in review articles concerning solid dispersions there are various methods for the classification of solid dispersions (14, 19). In this study, solid dispersions were assigned to two broad classes based on the physical state of the drug in the systems: crystalline drugs in solid dispersions and amorphous solid dispersions (solid solution) whereby drugs completely disperse into the polymer chain at molecular level. The mechanism of forming the two solid dispersions and their advantages and disadvantages will be discussed in the following sections.

1.3.2.1 Solid dispersions containing crystalline drug substances

1.3.2.1.1 Eutectic solid dispersions

The advantage of using solid dispersions containing crystalline drugs is this system can be more physically stable in comparison to amorphous solid dispersions (26). The most commonly used crystalline solid dispersion is the simple eutectic mixture which is composed of a crystalline drug and a water-soluble crystalline polymer. It is an intimate physical mixture of those two in which the crystalline drug and the crystalline polymer are completely miscible in the molten state (above their melting points). A eutectic mixture of fenofibrate and PEG 8000 with the ratio of 35:65 (w/w) was reported in the literature, and more than 90% drug release from the formulation was observed after 30min dissolution test under sink condition (48). To understand the mechanism of the formation of eutectic mixtures, a phase diagram was used to describe the composition of a eutectic mixture as seen in Figure 1.3. When a melted mixture composed of a crystalline drug (A) and a water soluble crystalline polymer (B) with the composition of E is cooled, the drug and the polymer crystallise out simultaneously together to form the eutectic mixture. However, when melted mixtures with other compositions are cooled, one of the components starts to crystallise before the other, leading to the formation of completely phase-separated materials instead of eutectic mixtures.

In dissolution, when a eutectic mixture is exposed to the media, the soluble carrier will dissolve rapidly and leave fine drug crystals (48). Due to the increased surface area brought by the small particle size, an increase of dissolution rate of the drug could be expected according to the Noyes-Whitney equation (49):

$$dW / dt = DA (C_s - C) / L \qquad Eq\ 1.1$$

where dW / dt is the dissolution rate, A is the surface area, C is the concentration of the drug in the bulk media, C_s is the solubility of the drug in the media and L is the diffusion layer thickness.

From the phase diagram of eutectic system, it can be seen that the feasibility of developing eutectic solid dispersions is dictated by the eutectic compositions (48, 50). Determination of eutectic compositions requires the generation of phase diagrams which can be time-consuming (48). In addition, due to the requirement of the specific composition in eutectic systems, its application can be limited since the clinical dose of different drug substances varies in a large range and it might be difficult to meet the specific eutectic drug-polymer composition. Therefore, despite the formation of a thermodynamically stable system, eutectic solid dispersions were not widely used in the pharmaceutical industry.

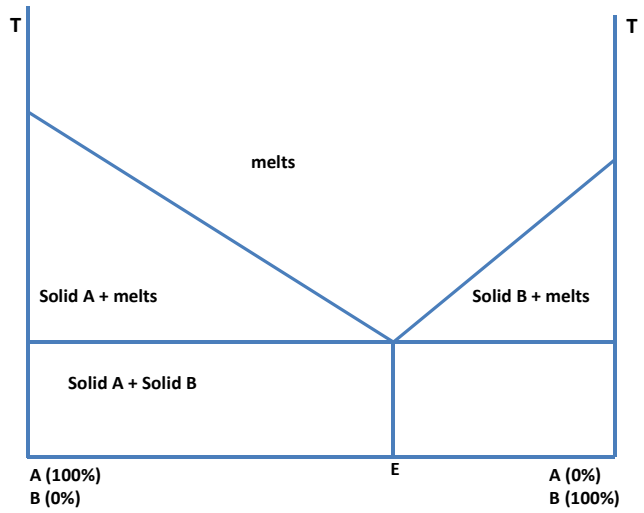

Figure 1.3: Phase diagram of the formation of eutectic mixture of a drug (A) and a polymer (B) with the composition of E.

1.3.2.1.2 Solid dispersions containing crystalline drugs

Besides the eutectic systems, crystalline solid dispersions prepared other methods such as spray drying have also been reported to be effective in improving dissolution performance of poorly water soluble drugs (22, 51, 52). A solid dispersion contained crystalline intraconazole was prepared using spraying (51). In the study, instead of using organic solution to dissolve drugs and polymers together, drugs was suspended in the water based solution with dissolved polymers before spray drying. The dissolution performance from the crystalline solid dispersions was similar to the commercial product (Sporanox®), and the in-vivo study in rats showed that the crystalline solid dispersion was bioequivalent to the commercial product (51). The enhanced dissolution and bioavailability was attributed to the structure of the crystalline solid dispersions in which drugs were covered by the hydrophilic polymer (PVP) and the surfactant (Poloxamer 188).

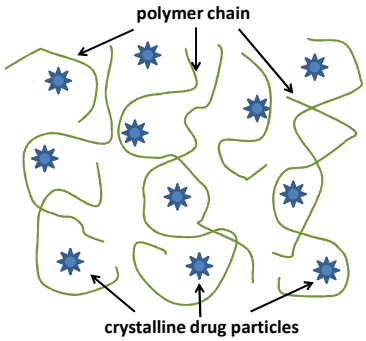

Figure 1.4: Proposed structure of crystalline solid dispersions prepared by wet media milling.

1.3.2.2 Amorphous solid dispersions (solid solutions)

As discussed above, amorphous drugs are physically instable, due to the higher energy level in comparison to their crystalline counterparts, and this physical instability is inevitable according to Gibbs free energy law:

$$\Delta G = \Delta H - T\Delta S \qquad Eq\ 1.2$$

Amorphous materials will tend to convert back to the low energy level crystalline form. However, physical stability of amorphous drugs can be improved if they are formulated with polymeric carriers into the amorphous solid dispersions. Mechanisms of enhanced physical stability by solid dispersions involve reducing molecular mobility of drugs by the interaction between drugs and polymers and increasing the diffusion length for the assembling of drug molecules to form drug-rich phase or recrystallization (53, 54).

Ideally, a miscible amorphous drug-polymer solid dispersion can be considered as a solid solution whereby, similar to aqueous solution, drug molecules act as solute dissolving into the solvate, polymer chains. Therefore, a solid solution is a single-phase drug-polymer solid dispersion. An intimate molecular mixing of the drug and polymer should be achieved if the amorphous solid dispersion is a solid solution (6). The structure of solid solutions is proposed in Figure 1.5. In solid solutions, drug molecules are molecularly dispersed into polymeric carriers, and therefore a higher dissolution rate can be expected in comparison to the crystalline counterparts. The structure of solid solutions can also potentially enhance the physical stability in comparison to pure amorphous drugs due to the increased diffusion length for the assembling of drug molecules. It should be mentioned that drug-polymer solid solutions are considered as liquid solutions (6, 19). Therefore, it can be expected that similar to liquid solutions, if the concentration of the drug in amorphous solid dispersions is below the drug-polymer solubility no recrystallization should be observed from the amorphous drug-polymer systems. Therefore, predicting/measuring the drug-polymer solubility is essential in the area of amorphous solid dispersions.

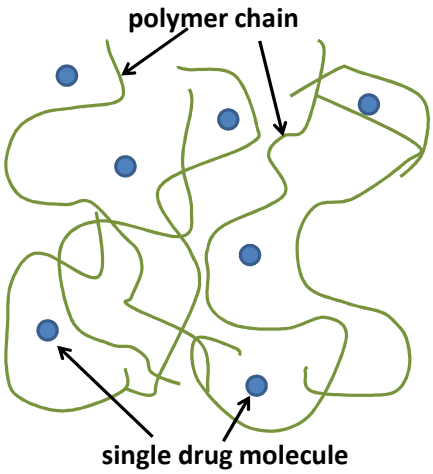

Figure 1.5: Theoretical scheme of miscible amorphous drug-polymer solid dispersions (solid solution).

The real physical state (drug-polymer distribution) of amorphous solid dispersions could be different from the proposed model (solid solution) (Figure 1.5) (39). Conventional characterisation techniques including MTDSC, FTIR, PXRD and ssNMR are useful for the detection of "global" phase separation in amorphous solid dispersions whereby the quantity of drug-rich phase or recrystallized drugs in systems are sufficiently high to be detected by these techniques. For instance, a typical amorphous phase separation in amorphous solid dispersions is reflected by the detection of two glass transitions in MTDSC (55). However, in some cases, phase separation could occur locally in amorphous solid dispersions at micro or sub-micrometre level, which cannot be detected using conventional tools, leading to the less correct judgement on the physical state of the system (56, 57).

Scanning probe microscopy based analytical techniques with high spatial resolution can be applied to detect local phase separation at low level (58, 59). For instance, Atomic Force Microscopy (AFM) combined with Local Thermal Analysis (LTA) is able to detect phase separation in solid dispersions at micron sub-micron level based on the thermal properties of the components in systems (58). Photothermal-FTIR allows operators to collect IR spectra at a highly specific point on the sample or even a single particle with micron dimension (60). These techniques will be discussed in detail in Chapter 2.

With the development of characterisation technology, the structure of amorphous solid dispersions will be understood in greater depth. However, to describe the composition and structure of amorphous solid dispersions accurately, it is recommended to characterise amorphous solid dispersion with global and local tools.

1.4 Preparation of solid dispersions

Processes for the preparation of solid dispersions can be divided into two categories: solvent evaporation based methods and non-solvent based methods (melting based method and milling) (14, 37, 47, 61). Typical solvent evaporation based methods in the pharmaceutical industry include spray drying, film casting, and co-precipitation. Recently, spin coating, a solvent evaporation base method, which is derived from semi-conductor industry, has been introduced to prepare solid dispersions (62-64). With regard to non-solvent preparation methods, hot melt extrusion and milling are the two main processes used. A brief introduction of each method is given in the following sections.

1.4.1 Spray-drying

Spray drying is a unit operation for transforming liquid solutions or suspensions into solid products by rapidly atomising the solutions/suspensions and drying with a hot gas. It has been widely used for preparing thermally-insensitive powder-form samples in food, dairy, ceramic, paints, fertilizers and pharmaceutical industry (65). In the pharmaceutical industry, spray-drying as a processing method, has been applied to prepare many systems, such as antibiotics, vitamins, vaccines, enzymes, plasma substitutes and excipients (47). It also has been widely used to prepare solid dispersions in the pharmaceutical industry to improve dissolution performance of poorly water-soluble drugs (66-70). The main procedure of spray-drying and the mass flow of the sample are depicted in Figure 1.6.

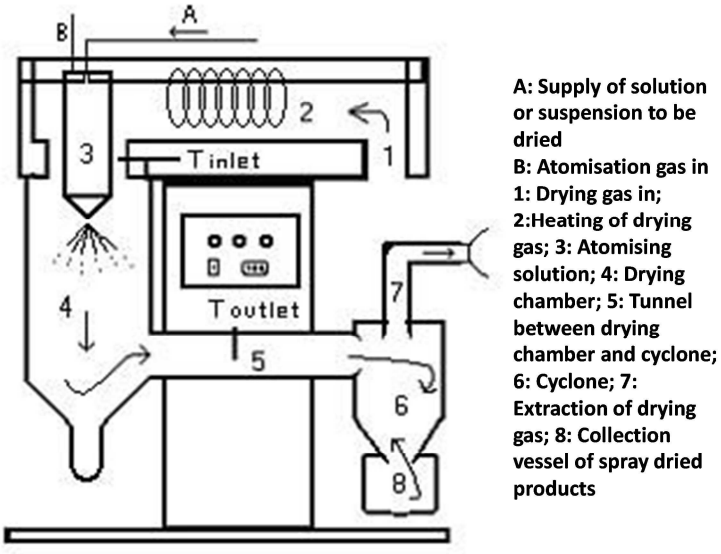

Figure 1.6: Schematic depiction of spray drying and the mass flow of samples in spray drying (71).

The general steps of using spray drying to prepare solid dispersions are described here (Figure 1.6) (72): 1) prepare the solution (or suspension) containing the drug and polymer; 2) the dissolved

or suspended sample solutions is fed from A; 3) air or nitrogen are heated when passing through section 2; 4) solutions are sprayed out from the heated nozzle in section 3 (the temperature in the nozzle should be higher than the boiling point of the solvent); 5) the solvent in the solution is evaporated, and the dried powders will be driven through section 5 and 6 by extraction effect from section 7 ; 6) samples are collected in section 8.

Spray drying has been proved as an effective processing method in preparation of amorphous solid dispersions to improve dissolution rate of poorly water-soluble drugs in many studies (66-70). Due to the pre-dissolution of drugs and polymers in the solvent or co-solvent, an intimate mixing between drugs and polymers at molecular level can be expected, which may assist to prepare amorphous solid dispersions by spray drying. Thus, improved dissolution performance and bioavailability of poorly water-soluble drugs can be achieved (65). In addition, compared with another commonly used solvent evaporation method, film casting, spray drying may have higher efficacy for the preparation of amorphous solid dispersions as the slow evaporation (73). This was attributed to the reason that solvent evaporation in film casting was relatively slow in comparison to spray drying (due to the hot air), which provided sufficient time for drugs to recrystallize from film-casted systems (73).

Although spray drying has demonstrated the capability of preparing amorphous solid dispersions, there are still limitations restricting the broad application of spray drying in the pharmaceutical industry (47). First, heat-sensitive drugs which are easily degraded at high temperatures are not appropriated for spray-drying as during spray drying solvent evaporation occurs by the hot air. Second, the application of organic solvent for dissolving water-insoluble drugs in solution preparation is not environment-friendly, and if scaled up to industry levels the recovery of organic solvents can be expensive. Finally, as the process depicted in Figure 1.6, during preparation, it is possible that part of the samples may deposit on the surface of the chambers (part 4, 5 and 6), leading to the material wastage and low yielding.

1.4.2 Co-precipitation

Co-precipitation is a typical solvent based method for preparing solid dispersions. It is a process in which drugs and polymeric carriers are dissolved together in a solvent to prepare a solution, and then the solution is added to an anti-solvent. Due to the significant difference of polarity between the solvent and anti-solvent, drugs and polymers will precipitate out simultaneously in the anti-solvent to form a solid dispersion. The difference of polarity between the solvent and anti-solvent should be high, and usually, the solvent is polar whilst the anti-solvent is non-polar (74). After the precipitation is completed, the suspension containing products can be treated by either filtration or solvent evaporation depending on the properties of the products and the solvent (75).

Due to the difficulties of selecting suitable solvent and anti-solvent, co-precipitation has not been widely used for the preparation for solid dispersions. Dong et al. compared the properties of solid dispersions prepared by hot-melt extrusion and co-precipitation. Both solid dispersions were confirmed as amorphous by PXRD and DSC (33). Solid dispersion prepared by co-precipitation showed faster drug release rate than that prepared by hot-melt extrusion. The reason was attributed to the larger surface area and porous structure achieved by using co-precipitation (33). Solid dispersions prepared by co-precipitation are normally particles with large surface to volume ratios and porous structures, which may significantly improve dissolution rate of poorly water-soluble drugs (76). However, as detailed previously, due to the limitations of solvent and anti-solvent selection co-precipitation has not been widely used for the preparation of solid dispersions.

1.4.3 Spin coating

Spin coating is a process to prepare a thin film with controllable thickness on a substrate. It has been widely used in microfabrication in the semiconductor industry (77). Spin coating is similar to film casting (another solvent evaporation based method), but unlike film casting in which solvent is evaporated under ambient condition or low vacuum, solvent evaporation in spin coating occurs at a rapid speed due to the fast spinning. The procedure of using spin coating to prepare a thin film (an amorphous drug-polymer solid dispersion) includes following steps: 1) prepare a solution which contains the desired concentration of drugs and polymers using a volatile solvent and co-solvent; 2) a substrate is placed on top of the chuck in the spin coater, and the substrate is attached to the chuck during the whole process by vacuum from underneath; 3) the substrate spins with the chuck at a pre-set rotation speed; 4) at the same time, sufficient amount of droplets of the prepared solution will be added onto the substrate; 5) the substrate is evenly covered by solutions due to the centrifugal force provided by high speed spinning; 6) solvent will evaporate during spinning and a thin solid film is formed on top of the substrate.

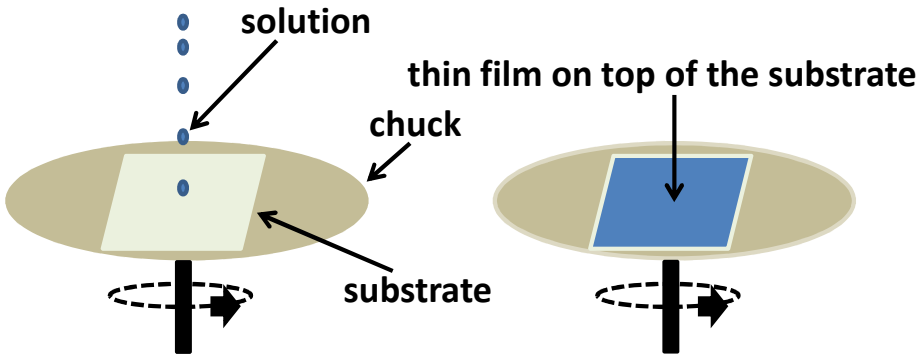

Figure 1.7: Procedure of using spin coating to prepare a thin film on a substrate.

With the advantages of high reproducibility, fast preparation and precise control during preparation, spin coating has been reported to be used to prepare solid dispersions for the

understanding of their physical stability behaviours (63, 64, 78, 79). By using spin coating to prepare solid dispersions containing model drugs including celecoxib, felodipine, fenofibrate and carbamazepine and polymers with different hygroscopicity, Ng et al (63) reported that key factors which affect physical stability of solid dispersions under stressed humidity were the physical stability of drugs alone and the hygroscopicity of polymers. In another study from the same group, drug migration of felodipine from the bulk towards the surface in the spin coated felodipine-PVP K29/32 thin films was discovered when the spin coated solid dispersion films were aged upon exposure to stressed humidity (64). The research mentioned above demonstrated that spin coating is an effective solid dispersion preparation process to stabilise amorphous drugs and to understand the physical stability behaviour of solid dispersions.

1.4.4 Milling

Milling has been proved to be an effective processing method to improve dissolution behaviour of poor water-soluble drugs (61, 80-83). The main properties brought by milling are: particle size reduction to sub-micron; crystalline drug transformation to amorphous state; and forming co-crystals (61, 84, 85). Milling can be processed with (wet milling) or without (dry milling) wet media depending on the purposes of the research (86, 87). Wet milling has been reported for the preparation of nano-suspensions whereby drugs and polymeric carriers are milled together (using ball milling) in wet media (surfactants solutions in water) for a certain time period to decrease the particle size of the drug to nanometre level (88). The reduced particle size can significantly enhance the dissolution rate of poorly water-soluble drugs and the polymeric carriers in the formulation can protect particles from agglomeration in the formulation by interacting with the drugs and increasing the viscosity of the nano-suspension (88).

Dry milling has been reported to show the ability to transform crystalline drugs to their amorphous state and hence improve the dissolution performance of the poorly water-soluble drugs (89). The solid state transformation by dry milling was reported to be affected by the milling temperature (90, 91). In a study, crystalline trehalose lactose and budesonide (an anti-inflammatory drug) were all transformed into amorphous state (confirmed using PXRD) after 20 hours milling at room temperature (below the T_g of all three amorphous materials) (90). In contrast, polymorphic transformation of mannitol and sorbitol were observed after 3 hours milling at room temperature (above the Tg of both amorphous materials) (90).

Solid dispersions can be prepared by both wet milling and dry milling methods (22, 92). For the preparation of solid dispersions using wet milling method to evaporate the media, downstream processes are required, such as lyophilisation. An anti-allergic drug, tranilast, was reported to be prepared into crystalline solid dispersions with HPC-SL using wet milling in water and followed by lyophilisation, and 60 folds increase of C_{max} was observed in rats in comparison to the physical

mixture with the same dose (22). Indomethacin with PVP were reported to form amorphous solid dispersions using dry milling, and the drug-polymer systems were confirmed as amorphous by PXRD with drug loadings up to 60% (w/w) (92). In the study, significantly increased dissolution rates were observed in all amorphous solid dispersions in comparison to pure drugs in the pH 6.8 buffer solutions (92).

Some disadvantages of using milling to improve dissolution rate of poorly water-soluble drugs have also been pointed out (93). First, particle size cannot decrease infinitely with increasing milling time due to the re-aggregation occurring during grinding (93). Therefore only a certain range of particle size reduction can be achieved depending on the properties of drugs and polymers. Second, milling is time-consuming whereby hours or days are required to achieve the desired amorphous solid dispersion.

1.4.5 Hot-melt extrusion (HME)

HME is a widely used non-solvent based method for the preparation of solid dispersions (37, 38). A great number of studies have been reported covering aspects such as the improvement of the design of extruder (i.e. specially designed meshes for rotating screws), investigation into the feasibility of the preparation of solid dispersions, and down-stream methods for further processing extrudates (37, 38). HME process can be simply described as conveying raw materials with a rotating screw under elevated temperatures, and products with a special shape (determined by the die) can be collected at the end of the extruder. The HME equipment is usually composed of several important parts including a control panel, inlet feeding hopper, steel barrel with different heating zones, screws for extrusion, a die attached to the end to specially shape the products and a cooling system. A detailed typical single screw hot melt extruder is shown in Figure 1.8.

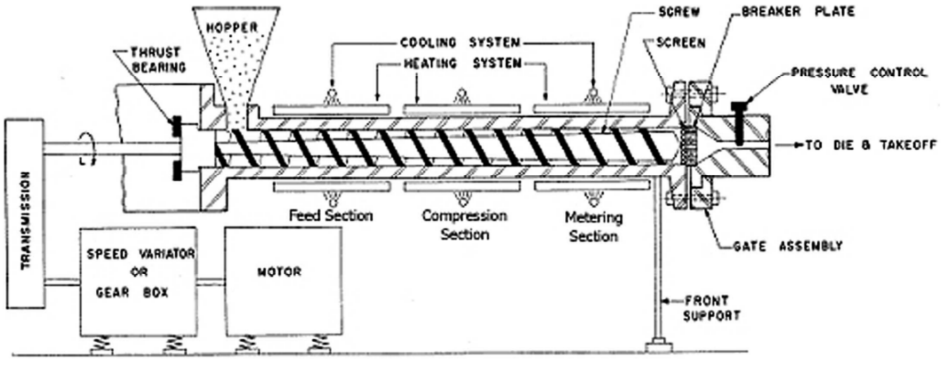

Figure 1.8: A schematic chart of a single screw hot-melt extruder (Crowley et al., 2007).

The speed of feeding depends on the rotating rate of the screw, and these two speeds must be compatible to avoid the formation of a melting bridge in the joint of the hopper and the barrel. The

barrel can be designed with different heating zones which can be set with different temperatures. Inside the barrel, the extrusion screws mix and convey the drug-polymer mixtures. Two main types of screw configuration are mainly used in HME in the pharmaceutical industry, single screw and twin screw extrusion. The single screw has a long history but may not provide sufficient mixing of different materials if the screw is not long enough (37). The twin-screw extruders utilize two screws usually arranged side by side, and they either rotate in the same or opposite directions (co-rotation and counter-rotation, respectively). The barrel with the screws is the key part of the extruder, not only for imposing high temperature and pressure on the materials to ensure them mix uniformly, but also to convey the mixtures as a continuous transportation. The energy for melting is obtained both from the heater and the shearing effect provided by screw rotating. At the end of each hot-melt extruder, a die with a special shape is attached. Extrudates can also be processed by downstream methods after extrusion, such as cutting into pellets, or being milled into powder after cooling.

For formulation design at lab scale, in order to avoid the wastage of expensive drugs, bench top hot-melt extruders were introduced. There have been two designs concerning the barrel. The first one is similar to industrial scale hot melt extruder which contains different heating zones as shown in Figure 1.9a. In addition, screws are specially designed with different shapes of meshes to assist complete mixing of drugs and polymers (Figure 1.9a). The other typical lab-scale hot melt extruder does not have different heating zones (Figure 1.9b). Instead, only one operation temperature can be applied during the whole process for this bench top extruder. To ensure the complete mixing of drugs and polymers in preparation, a particular valve is fixed at the end of the screw to block the outlet and lead the melted materials to a circulating route inside the constant-temperature heating zone (pointed in Figure 1.9b). Therefore, the melted materials can be circulated through the mixing zone several times before discharged from the extruder. In this project, the second bench top extruder was used for the preparation of amorphous solid dispersions.

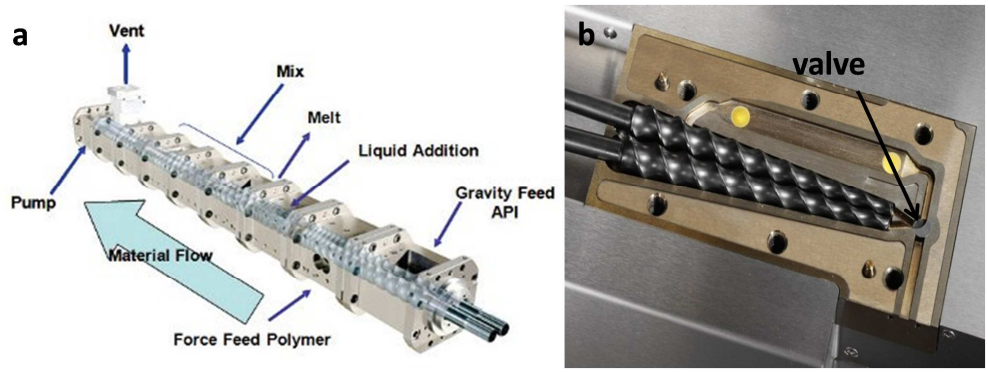

Figure 1.9: Inner structure of lab-scale extruder with (a: Thermo Scientific 16 Hot Melt Extruder) and without (b: Thermo Scientific HAAKE MiniLab II) different heating zones.

Generally, the components of HME formulations include drugs, polymers and plasticizers (in some cases). The polymers should be soften or molten during the HME process. Sometimes, plasticizers are necessary to ease the HME process if the systems are viscous. The main procedure for HME is described as follows:

1. Prior to HME, it is recommended that all components in the desired formulation should be dried to avoid absorbed moisture (store drug and polymer powders under 0%RH for a certain time period), since the moisture or water can function as plasticizer and have effect on the HME processing as well as the long term stability of the final solid dispersions.

2. Ingredients for the formulation are recommended to be pre-mixed before HME, i.e. using mortar and pestle.

3. Set the operating parameters of the HME including feed speed, different temperatures of different heating zones (if the extruder has) and rotation speed of the screws.

4. Collect all the extrudates and, if necessary, special-shaped dies can be attached to the end of the barrel to form varies types of extrudates such as rod shape or thin films.

5. All the extrudates are cooled down to room temperature and stored under different conditions according to the requirements.

1.5 Pharmaceutical applications of hot melt extrusion

Originally, the HME processing was mainly and widely employed in the plastic industry for the preparation of plastic products, and more than half of plastic products such as plastic bags, sheets and pipes are manufactured by this processing (94). The application of hot-melt extrusion in the pharmaceutical industry can be dated back as early as 1971 (95). Since then it has been widely used as a processing method for the preparation of solid dispersions and can be used to modify dissolution rate of drugs (37). In comparison to other solid dispersion preparation methods, such as solvent evaporation based method, HME can be superior in some aspects (38). Firstly, it is a solvent free method in which no organic solvent is required in preparation. The involvement of organic solvent can be problematic in terms of environmental pollution and high cost to recover. Secondly, it is a continuous single-step processing method which can be a highly efficient in preparing samples. Thirdly, scale up could be relatively easy. The disadvantage of hot melt extrusion is the potential thermal degradation of heat-sensitive drugs and polymers in preparation, which restricts the selection of drugs and polymers can be processed by HME. Nevertheless, hot melt extrusion is becoming increasingly popular in preparing solid dispersions in the pharmaceutical industry. The main applications of hot melt extrusion in the pharmaceutical

industry include fast release formulations, sustained release formulations and special formulation design and they will be discussed in the following sections.

1.5.1 Fast release formulations

Fast release formulations by hot melt extrusion are mainly based on the preparation of amorphous solid dispersions (23, 96-99). By using HME to process drug-polymer mixtures into amorphous solid dispersions, dissolution rate of poorly water-soluble drugs can be significantly enhanced. Itraconazole is a typical BSC Ⅱ drug with extremely low aqueous solubility (1.8μg/ml in pH 1.2 solution) (100). In one study, itraconazole and hydroxypropylmethyl-cellulose (HPMC) 2910 solid dispersions were prepared by HME and amorphous solid dispersions were confirmed by MTDSC and PXRD with drug loadings of up to 40% (w/w) (101). In this study, drug release of 90% was achieved after 120min even from 40% (w/w) loading formulation under sink condition (101). In a very recent study of using hot melt extrusion to improve dissolution performance of ketoprofen, another typical poorly water-soluble drug, hydroxypropylcellulose (HPC) was used (102). Amorphous solid dispersions were confirmed by DSC and PXRD up to 60% (w/w) drug loading in this study (102). In addition to enhancing the dissolution rate of the drug, the increased drug release rate can also be modified by using HPC with different grades. This was explained in the paper by the different swelling and erosion rates of different grades HPCs (two types of HPCs with the molecular weight of 60000 and 80000, respectively) (102). These successful applications of improving dissolution rates of poorly water-soluble drugs demonstrate that hot melt extrusion is an effective processing method for the enhancement of drug release via the preparation of amorphous solid dispersions.

The fast release mechanism of drugs from solid dispersions has been debatable (39). Two established models have been reported. In the first instance, a valuable contribution was provided by Corrigan in which not only the dissolution rate of the incorporated drug was measured but also the dissolution rate the polymer carrier (PEG) was assessed (103). The author found that the dissolution rate of the drug and the polymer was equivalent, which leads to the suggestion of carrier-controlled drug release whereby the dissolution rate of the drug is controlled by the inert carrier in the solid dispersion. This model was supported by other studies presenting similar results (104, 105). However, adisagreement issue was raised from Lloyd et al by arguing that if dissolution was dominated by the carrier rather than the drug, the physical form of the drug should be irrelevant (106). By examining the release of paracetamol from PEG 6000 solid dispersions, they found that formulations prepared with larger drug size fractions showed a higher drug release rate. With similar work from other groups, a drug-controlled dissolution was introduced whereby the dissolution rate of the drug is controlled by the drug dissolving and thus physical state of the drug (such as reduced particle size or changed into amorphous) can significantly affect the dissolution (107). Out of the two models, the dominant mechanism of drug release from solid dispersions is

dependent on whether the drug dissolves in the polymer diffusion layer rapidly in dissolution (carrier-controlled) or not (drug-controlled). The schematic illustration of the two mechanisms is shown in Figure 1.10.

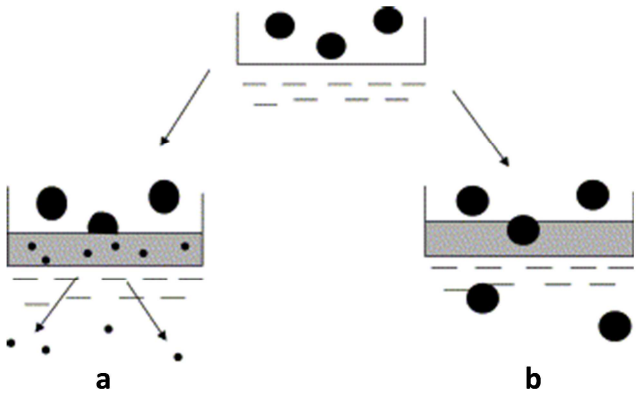

Figure 1.10: Schematic illustration of fast release mechanisms (a: carrier controlled dissolution whereby the drug dissolves into the concentrated carrier layer prior to release; b: drug-controlled dissolution whereby the drug is released effectively intact into the dissolution media) (39).

1.5.2 Modified release formulations

The preparation of solid dispersions, using hot melt extrusion with water insoluble polymeric carriers, may sustain drug release from formulations (108, 109). Miyagawa et al. used twin-screw hot-melt extruder to prepare controlled release diclofenacsodium formulations with different matrices (110). It was found that the dissolution rate can be controlled by adjusting the drug loadings. Recently, a series of studies using hot melt extrusion to prepare sustained release mini-matrices were carried out from the same research group (109, 111). Ethylcellulose was used as the main sustained release matrix in these studies (109, 111). In the first study, it was proved that using xanthamgum with different concentrations and different particle sizes in ethyl-cellulose based formulations, drug release of ibuprofen can be tailored to the required specifications (109). The dissolution of the drug was controlled by diffusion rather than erosion of polymers. Further research from the same group concluded that mechanical parameters including screw design, powder feed rate and screw rotation speed of hot melt extrusion in preparation had no influence on the homogeneity of products and drug release (metoprolol tartrate as model drug) profiles(111). This may demonstrate that hot melt extrusion is consistent and robust process for the preparation of solid dispersions in controlling drug release (111).

Form these studies, it can be concluded that the controlled release mechanism of a water-soluble drug from hot melt extruded solid dispersion is mainly dependent on the physical properties of the drug and the applied polymer carriers (112). If the polymer is hydrophilic, drug release is controlled by the swelling and erosion of the polymer in dissolution. If the drug is incorporated in

water-insoluble polymers, such as ethyl-cellulose, drug release is controlled by the diffusion of dissolution media into the matrix and followed by the diffusion of drug molecules through the polymer matrix into the dissolution media (113).

1.5.3 Other applications

In addition to the modification of drug release rate, two other typical applications of hot melt extrusion including the preparation of drug-loaded films and taste masking have been reported (37, 38). Polymeric films containing drugs are usually designed for local drug delivery systems such as transdermal and transmuscoal drug administration. Compared with other time-consuming casting techniques which may involve solvents and have environmental concerns, HME is a viable method for film based formulations (38). The film can be obtained by attaching a special roller unit to the end of the HME and the thickness of the film can be controlled. Film preparation using hot melt extrusion has been reported in articles (114-117). For example, lidocaine was prepared into film formulation by HME using hydroxypropyl cellulose (HPC) and hydroxypropyl methyl cellulose (HPMC) as matrices (115). In this study, the formation of an amorphous solid dispersion was confirmed by DSC and XRPD (115). A burst drug release at the early stage (to reach the required drug concentration in plasma within short time period) and a sustained drug release at later stage (to maintain the drug concentration in plasma) were achieved in the permeation test using diffusion cell (115).

Taste masking can be obtained through the formation of interaction (such as hydrogen bonding) between bitter drugs and polymer carriers (118). It has also been reported that the unpleasant flavour of the drugs can be masked if drugs can be molecularly dispersed into polymer carries (119). Therefore, hot melt extrusion as an effective preparation process for solid dispersions was introduced for taste masking. A case study reported using HME for the taste masking of paracetamol by formulating the drug with EUDRAGIT® EPO and Kollidon® VA64(120). *In-vivo* results by patients showed that both polymers can provide a taste masking effect with the drug loading up to 50% (w/w), and Kollidon® VA64 was slightly better (up to 60% w/w). This was likely attributed to the fact that paracetamol was partially crystalline in the EUDRAGIT® EPO melt extrudates whereas although phase separated, paracetamol was still amorphous in Kollidon® VA64 dispersions as confirmed by PXRD. However, in the paper it was not discussed why amorphous solid dispersions showed better taste masking effect than solid dispersions containing crystalline drugs. Nevertheless, the results still demonstrated that using HME as to prepare amorphous solid dispersions was an effective method for taste masking.

1.6 Physical stability of amorphous solid dispersions

Although amorphous solid dispersions have shown high potential of improving dissolution rate of poorly water-soluble drugs, the commercial application of solid dispersions is very limited (Table

1.1). There are still many hurdles for commercialising amorphous solid dispersions, such as: dosage form development; scale-up; and the chemical and physical stabilities of the formulations. Amoungst these hurdles, the physical stability of amorphous solid dispersions has been considered as the very key factor and has been the subject of most published reports in articles (6, 19, 37, 38, 65).

An amorphous drug-polymer solid dispersion is a thermodynamically instable delivery system since molecularly dispersed drugs (high energy level) in the system will tend to convert back to the more stable crystalline form (low energy level), leading to the physical stability issue. Freshly prepared amorphous solid dispersions may have the drug molecularly dispersed in the polymeric carriers. On aging the physical instability of amorphous solid dispersions could occur in the form of phase separation and recrystallization due to the relaxation of high energy-level drug molecules and molecular mobility of drugs (can be accelerated by storage condition i.e. stressed humidity or temperature). Phase separation refers to the procedure in amorphous solid solutions where molecularly dispersed drug molecules migrate together to form a drug-rich phase eventually containing a higher drug concentration than the average bulk drug concentration. Recrystallization could then occur within the drug-rich phase whereby high concentration amorphous drug recrystallize out to form the more stable crystalline state. A proposed procedure of the physical instability of amorphous solid dispersions on aging is shown in Figure 1.11.

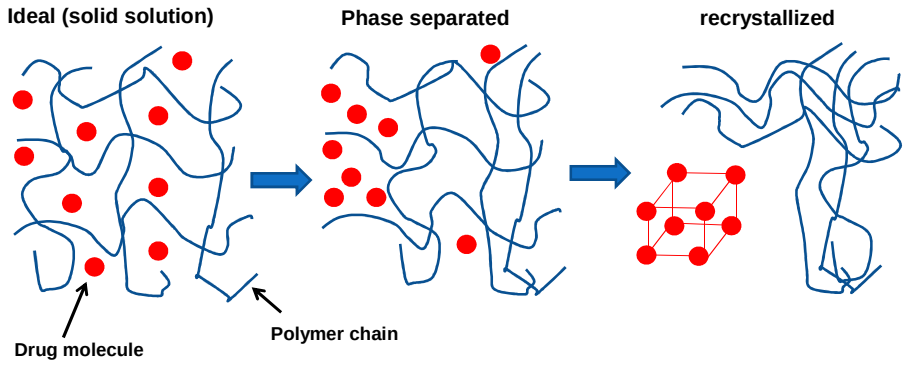

Figure 1.11: Proposed procedure of the physical instability of amorphous solid dispersions on aging.

Recrystallization could also take place if nuclei are provided. Nuclei can be the residual crystalline drug in the solid dispersion or foreign particles from the surrounding environment (121). With the occurrence of phase separation or recrystallization, the attempt to improve dissolution rate of poorly water-soluble drugs using amorphous solid dispersions will fail as the recrystallized drugs do not have as high dissolution rate as the amorphous form. Therefore, the understanding of the physical stability of amorphous solid dispersions is essential for the formulation development. Although phase separation might be inevitable in long time period on aging, with the development of methods for enhancing the physical stability, amorphous solid dispersions can still be extended

to a desired time length (acceptable shelf life). More importantly, the prediction of the physical stability of amorphous solid dispersions is highly demanded in the pharmaceutical industry at the early stage of the formulation design as this can save the time and decrease expense for the formulation development.

Factors which can potentially affect the physical stability of amorphous solid dispersions have been investigated widely, and glass transition temperatures, molecular mobility, physical stability of amorphous drugs alone, miscibility between drugs and polymers and solid solubility of drugs in polymers have been considered as key factors influencing the physical stability of solid dispersions (6, 31, 63, 122, 123). These factors will be discussed in the following sections in detail.

1.6.1 Glass transition temperature

Glass transition temperature (T_g) is a kinetic parameter associated with the molecular motion (viscosity) in amorphous state. Below T_g the amorphous materials are "kinetically frozen" (with great viscosity) into the thermodynamically unstable glassy state, and any further reduction in temperature has only a small effect on the decrease molecular motions of amorphous solids. Whereas above T_g, amorphous solids will enter rubbery state with significantly increased molecular motion and decreased viscosity (31). Molecular motion has been be related to the occurrence of the phase separation and recrystallization in amorphous solid dispersions (31, 124). This is because that molecular motion of drugs (drug migration) in amorphous solid dispersions can cause the formation of phase separation in amorphous solid dispersions and further recrystallization.

For amorphous solid dispersions, glass transition temperatures can be used as indicators to describe their physical state (125-127). If a binary drug-polymer system is miscible, only a single T_g can be observed using DSC. The presence of two glass transitions indicate that phase separation has occurred or the system is partially miscible (55). For miscible drug-polymer systems, if the T_g of the drug is lower than the T_g of the polymer, drugs can act as a plasticizer which can reduce the T_g of the system due to the ability of drugs as small molecules allowing the polymer chain segments to have greater freedom. But this also manifests the anti-plasticization effect provided by the polymer could increase the T_g to a higher value in comparison to that of pure amorphous drug. This may prolong the physical stability of amorphous solid dispersions compared with amorphous drugs alone (19). If the T_g of the drug is higher than the T_g of the polymer, anti-plasticizing of drugs effect could be expected, which may lead to less feasibilities for processes (i.e. in creased torque value in HME) (37).

The Gordon-Taylor (G-T) equation is a useful tool in predicting the glass transition temperatures of drug-polymer solid dispersions (126-128). For completely miscible binary drug-polymer solid dispersion, the glass transition temperature of the system can be calculated by:

$$T_{gmix} = [(w_1T_{g1}) + (Kw_2T_{g2})] / [w_1 + (Kw_2)] \quad Eq\ 1.3$$

where T_{g1}, T_{g2} and T_{gmix} are the glass transition temperatures (in Kelvin temperature) of component 1, 2 and the mixture, and w_1 and w_2 are the weight fractions of each component and K is a constant which can be calculated by:

$$K \approx (\rho_1 T_{g1}) / (\rho_2 T_{g2}) \quad Eq.1.4$$

where ρ_1 and $\rho_2$are the true densities of each component. The application of the equation in predicting the miscibility of solid dispersions lies in the comparison between the theoretical and experimental T_{gmix} values of the system. Gordon-Taylor equation is based on the assumption that the mixing processing is ideal in which the molecules from the two components are blended completely (126). Therefore, if the consistency of the comparison between the calculated and experimental T_{gmix} values is acquired, it may indicate that this system is miscible (129). However, exceptions have been reported in articles (126, 127, 130). The discrepancies of T_gs between the calculations from Gordon-Taylor equation and experimental data may be caused by two reasons. Firstly, interactions between drugs and polymers in amorphous solid dispersions can result in the deviation (127). Positive deviation whereby the experimental value is higher than the G-T predicted one could occur if the interaction between drugs and polymers are stronger that that between two drug molecules (130), whereas negative deviation could be observed if the drug-polymer interaction is weaker than that between two drug molecules (131). Secondly, water sorption in amorphous solid dispersions can decrease the T_g value of the system as water is a well-known plasticiser (129, 132).

1.6.2 Molecular mobility and structural relaxation of amorphous drugs

Molecular mobility of drugs is commonly considered to be a key factor associated with the stability of amorphous solid dispersions since high molecular mobility of drugs in the systems can lead to phase separation and recrystallization in amorphous solid dispersions on aging (31). As mentioned in former sections, amorphous materials which remains in the non-equilibrium state at the temperature below T_g have extra enthalpy and configurational entropy (results from the extra number of configurations of molecules in amorphous state in comparison to the corresponding crystalline state). Therefore, on aging the non-equilibrium amorphous materials will approach towards the equilibrium state by releasing those extra enthalpy and configurational entropy. This reducing extra energy process is termed as structural relaxation and the time length where the structural relaxation occurs is termed as relaxation time. Molecular mobility is in a reciprocal relationship to the relaxation time constant (τ). In the Adam-Gibbs model (133), it is calculated as:

$$\tau = \tau_0 exp(C / (TS_c)) \quad Eq\ 1.5$$

where τ is molecular relaxation time constant, τ_0 is a constant, T is the absolute temperature, S_c is the configurational entropy, and C is a material dependent constant. The equation was further modified as Adam-Gibbs-Vogel equation:

$$\tau = \tau_0 exp(D\ T_0 / (T\ (1 - T_0/T_f))) \qquad Eq.\ 1.6$$

where D is the strength parameter, $T_0$is the temperature of zero molecular mobility, and T_f is the fictive temperature (134). The fictive temperature is defined as the temperature of intersection between the equilibrium liquid line and the non-equilibrium glass line. In most cases, T_f values are very close to T_g values, and therefore in calculations the T_f value can be replaced by the T_g value (135, 136).

Two types of relaxations of amorphous materials have been defined at temperatures below and above the glass transition temperatures (43). For molecule with low M_w (such as drugs), at the temperature below T_g, the dominant relaxation procedure is β-structural relaxation (termed as local molecular mobility) which can take place by means of the spinning of atoms within the molecular structure. For amorphous polymers, at the temperature below T_g, β-structural relaxation refers to the vibrating of the side chains of the polymer (137). At the temperature higher than T_g, the dominant relaxation is α-structural relaxation (termed as global molecular mobility) (β-structural relaxation still occur at this temperature) which could occur for both amorphous drug and polymer whereby an intact molecule will be mobilised (137). These two types of relaxation can be detected by techniques such as DSC, Dynamic Mechanical Analysis (DMA) and dielectric spectroscopy (31, 138, 139). For instance, stored under ambient condition for a certain time period, relaxation enthalpy of amorphous indomethacin at the glass transition region can be detected on heating in DSC, and the detected relaxation enthalpy was a contribution of both α and β relaxations on aging (31). The detected relaxation enthalpy was attributed to the energy required to re-establish the liquid state on heating (31).

Both relaxations of drugs and polymers in amorphous solid dispersions are responsible for the physical instability on aging (31). As discussed above, molecular mobility of drugs were associated with temperature, and will decrease with decreasing aging temperature leading to the increased physical stability of amorphous solid dispersions. Therefore, this introduced the topic of the storage condition in terms of temperature for amorphous solid dispersions in the pharmaceutical industry. In a study, molecular mobility of typically applied pharmaceutical ingredients at different temperatures including amorphous indomethacin (representing drugs), PVP (representing polymer, naturally amorphous) and amorphous sucrose (representing sugars) were investigated (31). It was confirmed that at the temperatures 50K (and lower) below the glass transition temperature of individual material, no molecular motions can be detected by DSC for any tested material, and the

molecular mobility of amorphous materials could be neglected leading to materials remaining as amorphous for over a period of years (31). Consequently, it was suggested that amorphous solid dispersions should be stored at the temperature of T_g－50K to reduce the molecular mobility of drugs in amorphous solid dispersions and thus to increase the physical stability (31, 140).

In addition to the high storage temperature, stressed humidity can also increase molecular mobility of amorphous drugs in solid dispersions (141). Two potential effects of moisture uptake on the molecular mobility have been suggested. Firstly, absorbed water into the solid dispersions can act as a plasticiser (providing polymer chains with greater freedom resulting in the reduction of glass transition temperature of the intact system), and thus with the decreased T_g, a faster molecular mobility could be expected (142). Secondly, the formation of hydrogen bonding between drugs and polymers in solid dispersions has been considered as an effective formulation tactic to enhance the physical stability since molecular motion can be restricted if drugs are hydrogen-bonded with polymers. However, absorbed water molecules into the systems can disrupt the hydrogen bonding as the water molecule is highly potential hydrogen bonding donor and accepter (141), and therefore drug molecules can be forced to phase separate from the amorphous solid dispersions and further to recrystallize out.

1.6.3 Physical stability of amorphous drugs alone

Physical stability of amorphous drugs alone has been studied in various aspects including relaxation time of amorphous drugs under different storage conditions, bulk and surface recrystallisation rate and recrystallisation tendency of different amorphous drugs (143, 144). Amorphous nifedipine and indomethacin showed significant different recrystallisation rate between the bulk and the surface, and the surface recrystallisation rate of the two amorphous drugs was an order of magnitude faster than that of the bulk (145). Taylor et al used quench cooling and spin coating to prepare a variety of amorphous drugs, and classified them into three groups based on their recrystallisation tendency (78, 144). In Taylor et al studies, useful information concerning the "glass forming ability" and "glass stability" of amorphous drugs were provided and it was concluded that drugs with high glass forming ability were normally more physically stable (aged under ambient condition) than drugs with low glass forming ability. However, the crystallisation tendency of amorphous drugs prepared by melt-cool and spin coating in these studies was not completely the same whereby around 68% of cases showed the same trend (78). This may suggest that the physical stability of amorphous drugs can vary depending on the preparation methods.

Little studies correlated the physical stability of amorphous drugs alone with the physical stability of solid dispersions. Until recently, Ng et al (63) prepared amorphous solid dispersions using spin coating with felodipine, fenofibrate, celecoxib and carbamazepine and polymers with different hygroscopicity, and they found that the physical stability of these amorphous solid dispersions

showed the same order as the physical stability of the amorphous drugs alone. Therefore, it was suggested that the physical stability of amorphous drugs alone can be one of the significant factors affecting the physical stability of solid dispersions. Although the mechanism is still not completely understood, this observed correlation made a contribution to the formulation development of amorphous solid dispersions: the physical stability of amorphous drugs alone is a key factor influencing the physical stability of amorphous solid dispersions. In this project, the physical stability of amorphous model drugs were investigated aged under 0%RH/room temperature and 75%RH/room temperature. Moreover, to completely understand the physical behaviour of amorphous drugs alone and to avoid the effect of processing methods, samples were prepared by melt–cool and spin coating.

1.6.4 Miscibility between drugs and polymers

The significance of drug-polymer miscibility on the physical stability of amorphous solid dispersions has been emphasized by articles (122, 140, 146, 147). Miscibility is a concept originally applied in the liquid solution theory to describe the mixing of two liquids whereby if two liquids are miscible a homogeneous solution by mixing of the two should be formed with any proportions. In other words, a single phase solution which is thermodynamically stable should be formed at any ratios of the two liquids. Miscibility was further applied in the polymer and pharmaceutical industry to describe if the mixing of two polymers or drugs and polymers are thermodynamically favourable (34, 122, 148, 149). Evidently, if a drug and a polymer are miscible, a physically stable solid dispersion could be expected since it is a thermodynamically favourable single-phase system. Miscibility between drugs and polymers has been studied using different theoretical and practical methods including using solubility parameters, melting point depression and observation under hot stage microscope (34, 122, 140, 150-152).

1.6.4.1 Solubility parameters

Solubility parameter is a concept defined by the cohesive energy. The cohesive energy is the amount of energy required to separate the constituent atoms or molecules of the material to an infinite distance. It is a direct measurement of the attraction force that atoms or molecules have for one another. Cohesive energy is the whole effect of all the inter atomic/molecular interactions including: Van der Waals interactions; ionic bonds; hydrogen bonds and electrostatic interactions (150). Solubility parameter, δ, of a compound is defined as the square root of its cohesive energy density (153):

$$\delta = (\Delta E_v / V_m)^{0.5} \qquad \textit{Eq 1.7}$$

where ΔE_v is the energy of vaporization, and V_m is the molar volume. The units of the solubility parameter are $(J/m^3)^{0.5}$, $MPa^{0.5}$or $(cal/cm^3)^{0.5}$.

Solubility parameters of materials can be measured or predicted by different approaches. For materials which are stable above their boiling points, their solubility parameters can be directly determined by measuring their evaporation energy according to the definition in *Eq 1.7* (154). Another practical method of measuring solubility parameter is using inverse gas chromatographic experiments by the retention times of gases of known cohesive energies (155). However, these direct measurement methods were not widely applicable to materials with high molecular weight, such as polymers. In order to predict solubility parameters of high molecular weight materials, a theoretical approach based on group contribution was established. Basically, a chemical entity with complicated structure can be divided into different small groups, and the solubility parameters of those small groups can be measured by the vaporisation method (156). Therefore, the solubility parameter of the complicated materials with high molecular weight can be estimated. The group contribution methods were further developed and modified by different researchers such as the Hansen solubility parameters and the Fedor solubility parameters (157, 158). In case studies, the predicted solubility parameter value did not show significant differences between different methods (159). In this study, Fedor's group contribution method was used to calculate the solubility parameters of model drugs and polymers, and details of the application of this method are discussed in Chapter 4 (section 4.3.1.1).

The application of solubility parameter in predicting miscibility between drugs and polymers is based on the classic solution theory "likes dissolves likes" whereby if two solvents have similar solubility parameters they can be mixed to form a uniform solution with any ratios (i.e. mixing water and ethanol). Similarly, if drugs and polymers are predicted with close solubility parameters, a miscible drug-polymer solid dispersion could be prepared. It has been suggested empirically that compounds with a $\Delta\delta$ < 7.0 $MPa^{0.5}$ were likely to be miscible while compounds with a $\Delta\delta$ > 7.0 $MPa^{0.5}$ were likely to be immiscible (159).

The comparison of solubility parameters can be a rapid way to predict miscibility between drugs and polymers. However, exceptions have also been reported (122, 160). In a study regarding nifedipine-PVP solid dispersion, the system was predicted as immiscible which conflicted against the experimental results (122). This difference was attributed to the inappropriate use of the solubility parameter for systems containing specific interactions. Indeed, the hydrogen bonding was confirmed by FT-IR between the drug and the polymer. In another study, it was found that the $\Delta\delta$ between the components was not the decisive factor for prediction of miscibility of drug-polymer solid dispersions (160). In some cases in this study, a system (Vitamin E TPGS-EUDRAGIT® EPO) was immiscible even with a $\Delta\delta$ of 0.8 $MP_a^{0.5}$ where as another system (Tartaric acid- EUDRAGIT® EPO) with a $\Delta\delta$ of 19.8 $MP_a^{0.5}$ presented good miscibility and stability (160). The underpinning reason was the special acid-base interactions in Tartaric acid- EUDRAGIT® EPO systems (160). Although for systems with strong drug-polymer interaction, the solubility parameter is not

appropriate for miscibility prediction, it still can be a useful method for approximate estimation of drug-polymer miscibility in pre-formulation design (150).

1.6.4.2 Melting point depression

Melting point depression is a thermodynamic approach for studying miscible amorphous solid dispersion. The melting point of a pure drug occurs when the chemical potential of the crystalline drug equals to the chemical potential of the molten drug. If the drug is miscible with a polymer, then the chemical potential of the drug in the mixture with the polymer should be less than the chemical potential of the pure crystalline drug, and thus the reduced chemical potential will result in a depressed melting point of the drug with the existence of the miscible polymer (161). In contrast, if the drug and polymer are immiscible, no melting point depression is expected due to the unchanged chemical potential brought by the presence of polymers.

Briefly, the melting point depression approach could be a simple method to test the miscibility between drugs and polymers by running a physical mixture of the drug and the polymer in DSC on heating. The presence of the depressed melting may indicate the drug and the polymer are miscible. The melting point depression approach has been proved to be effective in predicting miscibility between felodipine and nifedipine with PVP in articles (122). In addition, combined with Flory-Huggins lattice based theory, the melting point depression method can be further applied to predict solid solubility of drugs in polymers (34). Melting point depression method was used in this project for the prediction of drug-polymer miscibility and solubility. Details of the application of this method are discussed in Chapter 4 (section 4.3.2.1).

1.6.4.3 Observation of miscibility using hot stage microscope

A hot stage microscope equipped with polarised lens can be also used to observe the miscibility between drugs and polymers (151, 152). Briefly, physical mixtures composed of crystalline drugs and polymers with different proportions are heated on hot stage microscope. At a temperature below the melting point of the drug, through polarised lens, birefringence from the crystalline drug should be seen. On heating to the temperature above the melting points of the drugs and glass transition temperatures of the polymers, if drugs and polymers are miscible two observations should be obtained (151, 152). First, at the temperature above the melting point of the drug, the birefringence will disappear due to the melting of the drug. Second, the physical mixture consisting of melted drugs and liquefied polymers should appear as a single phase without any boundaries (unlike the distribution of oil in water). Through the test of the physical mixture with the whole drug-polymer ratios, the range within which drugs are miscible with polymers can be achieved.

Although this method has been applied in studies regarding the miscibility between drugs and polymers, several factors may influence the observed results can be speculated. Local drug to

polymer ratio may differ from the desired ratio as incomplete mixing is very likely to occur when preparing physical mixtures with extreme drug-polymer ratios, which could lead to the incorrect miscible drug-polymer range. Moreover, bubbles left by the melting of drugs and softening of polymers under the microscope can confuse the judgement of the existence of the drug-polymer boundaries.

1.6.5 Solid solubility of drugs in polymers

Similar to the miscibility, drug-polymer solid solubility is also a concept derived from aqueous solution theory. But unlike miscibility regarding the mixing of two liquids, solubility is defined as dissolving a solid state material into a solvent until the equilibrium maximum concentration at a certain temperature under a certain pressure. Under a condition of a certain temperature and pressure, a solute can dissolve in a solvate if the amount of the solute is below the solubility in the solvate. After dissolution, no recrystallisation or precipitation of the solute should be observed as the concentration of the solution is below the solubility. Therefore, assuming drug-polymer solid dispersions as liquid solution, if the drug loading in the solid dispersion is below the solid solubility of the drug in the polymer, no phase separation or recrystallization should occur. Based on this hypothesis, a few studies have correlated the physical stability of solid dispersions with solid solubility of drugs in polymers (19, 34, 122, 162).

1.6.5.1 Prediction of solid solubility of drugs in polymers

Several theoretical methods have been reported for the prediction of solid solubility of drugs in polymers (56, 122, 162). Melting point depression combined with Flory-Huggins lattice based theory has been reported to predict solid solubility of felodipine and nifedipine in PVP (122). The interaction parameter χ from Flory-Huggins theory can be calculated using the detected depressed melting points from drug-polymer physical mixtures with different ratios, and by further using the obtained interaction parathion the solid solubility of drugs in polymers can be predicted. This method was applied in this project and details are discussed in Chapter 4 (section 4.3.2.1).

Another model based on the measurement of melting enthalpy of crystalline drugs in physical mixtures with polymers by DSC was recently developed by Qi et al(56). This model was a modification of a previous melting enthalpy based method (163). It assumed the dissolution of drugs in polymers on heating is endothermic and two extremes which involved drugs completely dissolved in polymers and *vice versa* were included in the model. The expected results did not agree with the model in that article, and it was attributed to the relatively high heating rate in DSC. This method was also utilised in the project and details of the model will be discussed in Chapter 4 (section 4.3.3.1).

In addition to the methods mentioned above, a rheology method was reported in articles to determine the solid solubility of drugs in polymers (164). This method involved the preparation of a series of drug-polymer physical mixtures. The viscosity of individual physical mixture was tested at the temperature above the glass transition temperature of the polymer but below the melting point of the drug. If the drug can dissolve in the polymer, the plasticising effect provided by the dissolved drug should decrease the viscosity of the physical mixture. With increasing drug loading, the viscosity should continue decreasing. However, if the drug loading was beyond the solid solubility, the non-dissolved drug as another phase in the physical mixture will increase the viscosity. Therefore, by plotting the viscosity against drug loading (drug-polymer ratios in physical mixtures) a negative slope should be seen until the turning point where the slope started to be positive, and the turning point was suggested as the solid solubility of the drug in the polymer.

Assume the dispersed particles (drugs) are single sized spheres, the reduced viscosity η/η_0 decreases with the increased volume fraction X of the drug in the mixtures (164):

$$\eta/\eta_0 = 1 + 2.5\,X \qquad \textit{Eq 1.8}$$

where η is the viscosity of the drug–polymer mixture, η_0 is the viscosity of the pure molten polymer and X is the volume fraction of the drug in the mixture. *Eq 1.8* suggests the viscosity of the mixture will increase when the drug-polymer ratio crosses the solubility of drug in polymer. This method was applied to pacacetamol-polyethylene systems in a study (164). The plot of measured viscosity against drug loading from the study is shown in Figure 1.12 (164). Measured solubility using different shearing rates are listed in the figure. The turning point as described in the method was clearly observed.

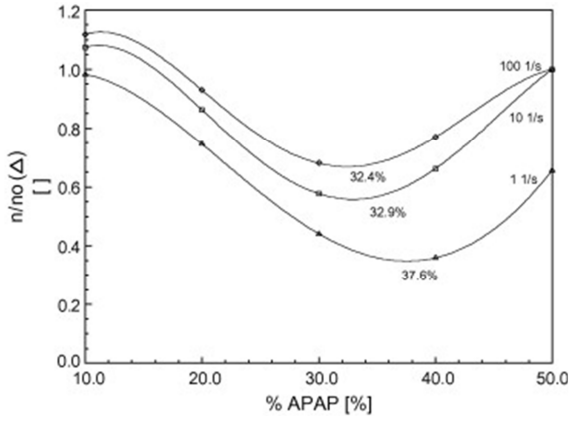

Figure 1.12: Measured viscosity of the mixture against drug loading at 120 °C at three different shear rates: 1, 10 and 100 1/s. The critical drug loadings are 37.6%, 32.9% and 32.4% for the shear rates of 1, 10 and 100 1/s, respectively (164).

However, this method can be limited as polymers still can be very viscous even at the temperature above their T_gs, and thus the method is highly relied on the rheological and thermal properties of drugs and polymers and may not be applied widely.

Recently, a new protocol to determine the solubility of drugs into polymer matrix using co-milling method was reported (162). In the study, super-saturated indomethacin-PVP K12 solid dispersions were prepared by using milling up to 8 hours. The super-saturated systems were heat-treated in DSC at high temperature (120^{o}C) for 2 hours to ensure the completion of de-mixing of drugs from the amorphous solid dispersions, and by re-scanning the same sample (after treated with heat at 120^{o}C) from room temperature an increased T_g value was detected in comparison to the T_g value in the fresh untreated sample. Using Gordon-Taylor equation, the drug concentration in the heat-treated sample can be estimated using the T_g value from re-scanning, and this drug concentration was considered as the solubility of indomethacin in PVP K12. Although this method made the contribution to faster drug-polymer solubility prediction, there still could be some potential issues concerning the accuracy and application of the method. Firstly, although milling has the potential to prepare amorphous solid dispersions with formulations containing PVP and drugs, it is not a processing method which can be generally and widely used to transform drug-polymer mixtures into super-saturated amorphous solid dispersions (61). This can restrict the application of this milling method to a broad range of drugs and polymers. Secondly, there was no physical stability study of amorphous solid dispersions to support the estimated solubility as amorphous solid dispersions with the drug loading below the predicted solubility were expected to be physically stable on aging. More importantly, this method did not take into account the effect of processing method on the drug-polymer solubility and it has been reported that apparent drug-polymer solubility may vary depending on preparation methods (73).

In this project, a practical milling method was specifically developed for the apparent solubility of drugs in melt extrudates. Details of this method are discussed in Chapter 5.

1.6.5.2 Limitations on the prediction of drug-polymer solid solubility

Although great efforts have been made to predict or measure the solid solubility of drugs in polymers, there still remain a few challenges. Firstly, solubility is a constant associated with temperature and pressure. Solid solubility predicted by approaches such as melting point depression method or rheology method is the value at the temperature significantly higher than room temperature, and therefore at room temperature where pharmaceutical products are normally stored the solid solubility could be lower as solubility can decrease with decreasing temperature. Secondly, predicted solid solubility by those approaches did not take into account the effect of preparation processes. For instance, practical solid solubility of drugs in solid dispersions prepared by hot melt extrusion can be higher than the predicted value by theoretical models as extra energy

in terms of high temperature and pressure during preparation is imposed on the system. It has been reported that the physical stability of solid dispersions with the same composition prepared by different processes varied significantly, which was attributed to the different apparent solid solubility in solid dispersions by different processes(73). Thirdly, those assumptions in the prediction models may underestimate the complication of the real drug-polymer system (such as the existing drug-polymer interactions), which can lead to the less accurate prediction.

1.6.6 Interactions between drug and polymer in solid dispersions

Interactions between drugs and polymers in solid dispersions have been reported as another important factor responsible for the physical stability of amorphous solid dispersions (165, 166). Firstly, the formed interaction between the drug molecules and the polymer chains in amorphous solid dispersions (such as hydrogen bonding) can restrict the molecular motion of drugs and hence it can increase the physical stability. Secondly, the formation of the interactions between drugs and polymers has been considered to be related to the drug-polymer miscibility and solid solubility of drugs in polymers. Therefore, it might be intended to select polymers which can potential interact with drugs when designing amorphous solid dispersions.

One of the common interactions between drugs and polymers is hydrogen bonding which is formed by the presence of proton acceptors and donors. Hydrogen-bonding is likely to occur among the carbonyl groups (acceptors), amine groups (donors) and hydroxyl groups (donors and accepters). Drugs and polymers with these groups have high tendency to form hydrogen bonding in amorphous solid dispersions. The effective tools for confirming the interaction are FT-IR and solid state NMR (126). In FT-IR, the frequency of vibrations within a chemical structure is very sensitive to how the atoms and molecules interact with neighboring functional groups. Variation of peak positions and intensities in the IR spectrum can be the indicators of the presence of hydrogen bonding (167). In solid state NMR, comparing the chemical shift of amorphous drugs and drugs in solid dispersion could be useful in judging the formation of hydrogen bonding. Hydrogen bonding was found to have significant effect on the physical stability of amorphous drug-polymer systems (168). The mechanism as suggested by those studies was the restriction on the molecular mobility of drug molecules and the enhancement of drug-polymer miscibility.

Besides hydrogen bonding, other interactions in solid dispersions such as acid-base were also discovered to be favourable for the enhancement of physical stability of solid dispersions(169). These interactions shared the same mechanism as hydrogen bonding which reduced the molecular mobility to prevent phase separation and recrystallization. However, this type of interaction could be very limited as it is dependent on the properties of drugs and polymers, and thus might not be widely utilised in solid dispersion formulation design.

Although the importance of hydrogen bonding in stabilising solid dispersions has been emphasized substantially, there is a concern on amorphous solid dispersions aged under stressed humidity. Certain polymers which contain carbonyl groups can be hygroscopic, such as PVP and PVPVA, and aged upon exposure to stressed humidity, it is very likely for amorphous solid dispersions prepared with them to absorb moisture (35, 63, 170). The moisture uptake can disrupt the formed hydrogen bonding between drugs and polymers since water molecule is strong hydrogen bonding acceptor and donor (35). Accordingly, the occurrence of phase separation followed by recrystallization is highly possible in these systems. This has already been proved in Qi et al paper that phase separation occurred in felodipine-PVP system within 24 hours aged under stressed humidity (64). Therefore, the formulation strategy of selecting hydrogen bonding donor polymers for solid dispersions might not be entirely correct. In order to balance the formation of hydrogen bonding and the issue of hygroscopicity, the application of polymer blends containing a hydrophilic and a hydrophobic polymer could be effective. Using immiscible polymer blends as a formulation strategy in melt extrudates to enhance the physical stability of amorphous solid dispersions was developed in this project and are discussed in Chapter 7.

1.7 Principal aims of the project

The application of amorphous solid dispersions has been proved to be effective in improving the dissolution performance of poorly water-soluble drugs in numerous studies in the pharmaceutical industry. Since the first application of solid dispersions was introduced in 1961, great effort has been input by pharmaceutical scientists to understand solid dispersions in various aspects such as preparation methods, physical properties of solid dispersions and development of polymeric carriers for solid dispersions. However, although the formulation conception of solid dispersions has been introduced for decades, there have only been few commercial products in market. The main issue lies in the intrinsic drawback of amorphous solid dispersions, the physical stability, as high energy level drug molecules in amorphous solid dispersions tend to revert back to the more stable crystalline form. The physical instability on aging in the form of phase separation and recrystallization can eventually affect the dissolution performance, resulting in the failure of the entire formulation strategy of using amorphous solid dispersions to improve dissolution rate.

This project was mainly designed to gain a greater depth of understanding of the physical stability of amorphous solid dispersions and a greater contribution to the prediction and enhancement of the physical stability of amorphous solid dispersions. In this project, hot melt extrusion was selected as the main method to prepare amorphous solid dispersions with model drugs (felodipine, fenofibrate, celecoxib and carbamazepine) polymers (EUDRAGIT® EPO and Kollidon® VA 64). The principal aims of this project are composed of three aspects:

1. By investigating physical properties of model drugs and polymers and combined with the real time physical stability study of amorphous solid dispersions prepared with them under different conditions, dominant factors which control the physical stability of amorphous solid dispersions can be revealed. Physical properties of model drugs are characterised in Chpater 3. Real-time physical stability studies of melt extruded systems prepared by hot melt extrusion are discussed in Chpater 6.

2. To develop a practical method (milling method) for the accurate prediction of drug-polymer solubility in amorphous solid dispersions prepared by hot melt extrusion. Drug-polymer solubilities (thermodynamic solubility) predicted by theoretical approaches are discussed in Chapter 4. Milling method which is developed for the prediction of processing-related drug-polymer solubility is discussed in Chpater 5. Comparing with the real-time physical stability studies (Chapter 6), the validation of the milling method can be tested. Meanwhile, out of the practical point of view in the pharmaceutical industry, the feasibility of the theoretical approaches in predicting drug-polymer solubility can be investigated.

3. To develop two novel formulation strategies for the enhancement of amorphous solid dispersions: using immiscible polymer blends (Chapter 7) in melt extruded formulations and using spin coating (Chapter 8) as processing method for the preparation of amorphous solid dispersions.

References

1. P.-C. Sheen, V.K. Khetarpal, C.M. Cariola, and C.E. Rowlings. Formulation studies of a poorly water-soluble drug in solid dispersions to improve bioavailability. International Journal of Pharmaceutics. 118:221-227 (1995).
2. R.A. Prentis, Y. Lis, and S.R. Walker. Pharmaceutical innovation by the seven UK-owned pharmaceutical companies (1964-1985). British Journal of Clinical Pharmacology. 25:387-396 (1988).
3. C.A. Lipinski. Drug-like properties and the causes of poor solubility and poor permeability. Journal of Pharmacological and Toxicological Methods. 44:235-249 (2000).
4. C.A. Lipinski, F. Lombardo, B.W. Dominy, and P.J. Feeney. Experimental and computational approaches to estimate solubility and permeability in drug discovery and development settings. Advanced Drug Delivery Reviews. 46:3-26 (2001).
5. G. Amidon, H. Lennernäs, V. Shah, and J. Crison. A Theoretical Basis for a Biopharmaceutic Drug Classification: The Correlation of in Vitro Drug Product Dissolution and in Vivo Bioavailability. Pharm Res. 12:413-420 (1995).
6. T. Vasconcelos, B. Sarmento, and P. Costa. Solid dispersions as strategy to improve oral bioavailability of poor water soluble drugs. Drug Discovery Today. 12:1068-1075 (2007).
7. S. Plakkot, M. de Matas, P. York, M. Saunders, and B. Sulaiman. Comminution of ibuprofen to produce nano-particles for rapid dissolution. International Journal of Pharmaceutics. 415:307-314 (2011).
8. T.R. Kommuru, B. Gurley, M.A. Khan, and I.K. Reddy. Self-emulsifying drug delivery systems (SEDDS) of coenzyme Q10: formulation development and bioavailability assessment. International Journal of Pharmaceutics. 212:233-246 (2001).
9. T. Yi, J. Wan, H. Xu, and X. Yang. A new solid self-microemulsifying formulation prepared by spray-drying to improve the oral bioavailability of poorly water soluble drugs. European Journal of Pharmaceutics and Biopharmaceutics. 70:439-444 (2008).

10. G.S. Basarab, P.J. Hill, A. Rastagar, and P.J.H. Webborn. Design of Helicobacter pylori glutamate racemase inhibitors as selective antibacterial agents: A novel pro-drug approach to increase exposure. Bioorganic & Medicinal Chemistry Letters. 18:4716-4722 (2008).
11. P. Srinarong, J.H. Faber, M.R. Visser, W.L.J. Hinrichs, and H.W. Frijlink. Strongly enhanced dissolution rate of fenofibrate solid dispersion tablets by incorporation of superdisintegrants. European Journal of Pharmaceutics and Biopharmaceutics. 73:154-161 (2009).
12. D. Mahlin, J. Berggren, G. Alderborn, and S. Engström. Moisture-induced surface crystallization of spray-dried amorphous lactose particles studied by atomic force microscopy. Journal of Pharmaceutical Sciences. 93:29-37 (2004).
13. O.N. Sekiguchi K. Studies on Absorption of Eutectic Mixture. I. A Comparison of the Behavior of Eutectic Mixture of Sulfathiazole and that of Ordinary Sulfathiazole in Man. Chem Pharm Bull:866-872 (1961).
14. C. Leunerand J. Dressman. Improving drug solubility for oral delivery using solid dispersions. European Journal of Pharmaceutics and Biopharmaceutics. 50:47-60 (2000).
15. N. Yüksel, A. Karataş, Y. Özkan, A. Savaşer, S.A. Özkan, and T. Baykara. Enhanced bioavailability of piroxicam using Gelucire 44/14 and Labrasol: in vitro and in vivo evaluation. European Journal of Pharmaceutics and Biopharmaceutics. 56:453-459 (2003).
16. V.B. Pokharkar, L.P. Mandpe, M.N. Padamwar, A.A. Ambike, K.R. Mahadik, and A. Paradkar. Development, characterization and stabilization of amorphous form of a low Tg drug. Powder Technology. 167:20-25 (2006).
17. G. Van den Mooter, I. Weuts, T. De Ridder, and N. Blaton. Evaluation of Inutec SP1 as a new carrier in the formulation of solid dispersions for poorly soluble drugs. International Journal of Pharmaceutics. 316:1-6 (2006).
18. W.L. Chiouand S. Riegelman. Pharmaceutical applications of solid dispersion systems. Journal of Pharmaceutical Sciences. 60:1281-1302 (1971).
19. A.T.M. Serajuddin. Solid dispersion of poorly water-soluble drugs: Early promises, subsequent problems, and recent breakthroughs. Journal of Pharmaceutical Sciences. 88:1058-1066 (1999).
20. S. Janssens, J.V. Humbeeck, and G.V.d. Mooter. Evaluation of the formulation of solid dispersions by co-spray drying itraconazole with Inutec SP1, a polymeric surfactant, in combination with PVPVA 64. European Journal of Pharmaceutics and Biopharmaceutics. 70:500-505 (2008).
21. A. Shanbhag, S. Rabel, E. Nauka, G. Casadevall, P. Shivanand, G. Eichenbaum, and P. Mansky. Method for screening of solid dispersion formulations of low-solubility compounds—Miniaturization and automation of solvent casting and dissolution testing. International Journal of Pharmaceutics. 351:209-218 (2008).
22. Y. Kawabata, K. Yamamoto, K. Debari, S. Onoue, and S. Yamada. Novel crystalline solid dispersion of tranilast with high photostability and improved oral bioavailability. European Journal of Pharmaceutical Sciences. 39:256-262 (2010).
23. A. Kalivoda, M. Fischbach, and P. Kleinebudde. Application of mixtures of polymeric carriers for dissolution enhancement of fenofibrate using hot-melt extrusion. International Journal of Pharmaceutics. 429:58-68 (2012).
24. W.L. Chiouand S. Riegelman. Preparation and dissolution characteristics of several fast-release solid dispersions of griseofulvin. Journal of Pharmaceutical Sciences. 58:1505-1510 (1969).
25. N.A. Urbanetz. Stabilization of solid dispersions of nimodipine and polyethylene glycol 2000. European Journal of Pharmaceutical Sciences. 28:67-76 (2006).
26. S.R. Vippagunta, Z. Wang, S. Hornung, and S.L. Krill. Factors affecting the formation of eutectic solid dispersions and their dissolution behavior. Journal of Pharmaceutical Sciences. 96:294-304 (2007).
27. L. Yu. Amorphous pharmaceutical solids: preparation, characterization and stabilization. Advanced Drug Delivery Reviews. 48:27-42 (2001).
28. S.-M. Khoo, C.J.H. Porter, and W.N. Charman. The formulation of Halofantrine as either non-solubilising PEG 6000 or solubilising lipid based solid dispersions: Physical stability

and absolute bioavailability assessment. International Journal of Pharmaceutics. 205:65-78 (2000).

29. B. Van Eerdenbrugh, M. Van Speybroeck, R. Mols, K. Houthoofd, J.A. Martens, L. Froyen, J. Van Humbeeck, P. Augustijns, and G. Van den Mooter. Itraconazole/TPGS/Aerosil®200 solid dispersions: Characterization, physical stability and in vivo performance. European Journal of Pharmaceutical Sciences. 38:270-278 (2009).
30. J.X. Wu, M. Yang, F.v.d. Berg, J. Pajander, T. Rades, and J. Rantanen. Influence of solvent evaporation rate and formulation factors on solid dispersion physical stability. European Journal of Pharmaceutical Sciences. 44:610-620 (2011).
31. B. Hancock, S. Shamblin, and G. Zografi. Molecular Mobility of Amorphous Pharmaceutical Solids Below Their Glass Transition Temperatures. Pharm Res. 12:799-806 (1995).
32. T. Miyazaki, Y. Aso, S. Yoshioka, and T. Kawanishi. Differences in crystallization rate of nitrendipine enantiomers in amorphous solid dispersions with HPMC and HPMCP. International Journal of Pharmaceutics. 407:111-118 (2011).
33. Z. Dong, A. Chatterji, H. Sandhu, D.S. Choi, H. Chokshi, and N. Shah. Evaluation of solid state properties of solid dispersions prepared by hot-melt extrusion and solvent co-precipitation. International Journal of Pharmaceutics. 355:141-149 (2008).
34. P. Marsac, T. Li, and L. Taylor. Estimation of Drug–Polymer Miscibility and Solubility in Amorphous Solid Dispersions Using Experimentally Determined Interaction Parameters. Pharm Res. 26:139-151 (2009).
35. A.C.F. Rumondorand L.S. Taylor. Effect of Polymer Hygroscopicity on the Phase Behavior of Amorphous Solid Dispersions in the Presence of Moisture. Molecular Pharmaceutics. 7:477-490 (2009).
36. I. Weuts, F. Van Dycke, J. Voorspoels, S. De Cort, S. Stokbroekx, R. Leemans, M.E. Brewster, D. Xu, B. Segmuller, Y.T.A. Turner, C.J. Roberts, M.C. Davies, S. Qi, D.Q.M. Craig, and M. Reading. Physicochemical properties of the amorphous drug, cast films, and spray dried powders to predict formulation probability of success for solid dispersions: Etravirine. Journal of Pharmaceutical Sciences. 100:260-274 (2011).
37. M.M. Crowley, F. Zhang, M.A. Repka, S. Thumma, S.B. Upadhye, S. Kumar Battu, J.W. McGinity, and C. Martin. Pharmaceutical Applications of Hot-Melt Extrusion: Part I. Drug Development and Industrial Pharmacy. 33:909-926 (2007).
38. M.A. Repka, S.K. Battu, S.B. Upadhye, S. Thumma, M.M. Crowley, F. Zhang, C. Martin, and J.W. McGinity. Pharmaceutical Applications of Hot-Melt Extrusion: Part II. Drug Development and Industrial Pharmacy. 33:1043-1057 (2007).
39. D.Q.M. Craig. The mechanisms of drug release from solid dispersions in water-soluble polymers. International Journal of Pharmaceutics. 231:131-144 (2002).
40. S. Bates, G. Zografi, D. Engers, K. Morris, K. Crowley, and A. Newman. Analysis of Amorphous and Nanocrystalline Solids from Their X-Ray Diffraction Patterns. Pharm Res. 23:2333-2349 (2006).
41. B. Wunderlich. A classification of molecules, phases, and transitions as recognized by thermal analysis. Thermochimica Acta. 340–341:37-52 (1999).
42. M.P. Fontana, R. Burioni, and D. Cassi. The generalized Peierls–Landau instability: a novel perspective on the nature of glasses? Philosophical Magazine. 84:1307-1311 (2004).
43. B.C. Hancockand G. Zografi. Characteristics and significance of the amorphous state in pharmaceutical systems. Journal of Pharmaceutical Sciences. 86:1-12 (1997).
44. D.Q.M. Craig, P.G. Royall, V.L. Kett, and M.L. Hopton. The relevance of the amorphous state to pharmaceutical dosage forms: glassy drugs and freeze dried systems. International Journal of Pharmaceutics. 179:179-207 (1999).
45. L.R. Hildenand K.R. Morris. Physics of amorphous solids. Journal of Pharmaceutical Sciences. 93:3-12 (2004).
46. J.M. Saiter, J. Grenet, E. Dargent, A. Saiter, and L. Delbreilh. Glass Transition Temperature and Value of the Relaxation Time at Tg in Vitreous Polymers. Macromolecular Symposia. 258:152-161 (2007).
47. J. Broadhead, S.K. Edmond Rouan, and C.T. Rhodes. The spray drying of pharmaceuticals. Drug Development and Industrial Pharmacy. 18:1169-1206 (1992).

48. D. Law, W. Wang, E.A. Schmitt, Y. Qiu, S.L. Krill, and J.J. Fort. Properties of rapidly dissolving eutectic mixtures of poly(ethylene glycol) and fenofibrate: The eutectic microstructure. Journal of Pharmaceutical Sciences. 92:505-515 (2003).
49. A.A. Noyesand W.R. Whitney. THE RATE OF SOLUTION OF SOLID SUBSTANCES IN THEIR OWN SOLUTIONS. Journal of the American Chemical Society. 19:930-934 (1897).
50. D. Law, W. Wang, E. Schmitt, and M. Long. Prediction of Poly(Ethylene) Glycol-Drug Eutectic Compositions Using an Index Based on the van't Hoff Equation. Pharm Res. 19:315-321 (2002).
51. Y.-J. Park, J. Xuan, D. Oh, P. Balakrishnan, H.-J. Yang, W. Yeo, M.-K. Lee, H.-G. Choi, and C. Yong. Development of novel itraconazole-loaded solid dispersion without crystalline change with improved bioavailability. Arch Pharm Res. 33:1217-1225 (2010).
52. Y.-D. Yan, J.H. Sung, K.K. Kim, D.W. Kim, J.O. Kim, B.-J. Lee, C.S. Yong, and H.-G. Choi. Novel valsartan-loaded solid dispersion with enhanced bioavailability and no crystalline changes. International Journal of Pharmaceutics. 422:202-210 (2012).
53. A. Ito, T. Watanabe, S. Yada, T. Hamaura, H. Nakagami, K. Higashi, K. Moribe, and K. Yamamoto. Prediction of recrystallization behavior of troglitazone/polyvinylpyrrolidone solid dispersion by solid-state NMR. International Journal of Pharmaceutics. 383:18-23 (2010).
54. H. Al-Obaidiand G. Buckton. Evaluation of griseofulvin binary and ternary solid dispersions with HPMCAS. AAPS PharmSciTech. 10:1172-1177 (2009).
55. D.M. Craig, M. Barsnes, P. Royall, and V. Kett. An Evaluation of the Use of Modulated Temperature DSC as a Means of Assessing the Relaxation Behaviour of Amorphous Lactose. Pharm Res. 17:696-700 (2000).
56. S. Qi, P. Belton, K. Nollenberger, N. Clayden, M. Reading, and D.M. Craig. Characterisation and Prediction of Phase Separation in Hot-Melt Extruded Solid Dispersions: A Thermal, Microscopic and NMR Relaxometry Study. Pharm Res. 27:1869-1883 (2010).
57. D.C. Sheng Qi. Detection of Phase Separation in Hot Melt Extruded Solid Dispersion Formulations Global vs. Localized Characterization. American Pharmaceutical Review. 13:757-764 (2010).
58. L. Harding, S. Qi, G. Hill, M. Reading, and D.Q.M. Craig. The development of microthermal analysis and photothermal microspectroscopy as novel approaches to drug–excipient compatibility studies. International Journal of Pharmaceutics. 354:149-157 (2008).
59. X. Dai, J.G. Moffat, J. Wood, and M. Reading. Thermal scanning probe microscopy in the development of pharmaceuticals. Advanced Drug Delivery Reviews. 64:449-460 (2012).
60. L.C. Grisedale, J.G. Moffat, M.J. Jamieson, P.S. Belton, S.A. Barker, and D.Q.M. Craig. Development of Photothermal FTIR Microspectroscopy as a Novel Means of Spatially Identifying Amorphous and Crystalline Salbutamol Sulfate on Composite Surfaces. Molecular Pharmaceutics. 10:1815-1823 (2013).
61. H. Al-Obaidi, M.J. Lawrence, S. Shah, H. Moghul, N. Al-Saden, and F. Bari. Effect of drug–polymer interactions on the aqueous solubility of milled solid dispersions. International Journal of Pharmaceutics. 446:100-105 (2013).
62. T. Ogi, L.B. Modesto-Lopez, F. Iskandar, and K. Okuyama. Fabrication of a large area monolayer of silica particles on a sapphire substrate by a spin coating method. Colloids and Surfaces A: Physicochemical and Engineering Aspects. 297:71-78 (2007).
63. Y.C. Ng, Z. Yang, W.J. McAuley, and S. Qi. Stabilisation of amorphous drugs under high humidity using pharmaceutical thin films. European Journal of Pharmaceutics and Biopharmaceutics. 84:555-565 (2013).
64. S. Qi, J.G. Moffat, and Z. Yang. Early Stage Phase Separation in Pharmaceutical Solid Dispersion Thin Films under High Humidity: Improved Spatial Understanding Using Probe-Based Thermal and Spectroscopic Nanocharacterization Methods. Molecular Pharmaceutics. 10:918-930 (2013).

65. A. Paudel, Z.A. Worku, J. Meeus, S. Guns, and G. Van den Mooter. Manufacturing of solid dispersions of poorly water soluble drugs by spray drying: Formulation and process considerations. International Journal of Pharmaceutics. 453:253-284 (2012).
66. B. Chauhan, S. Shimpi, and A. Paradkar. Preparation and evaluation of glibenclamide-polyglycolized glycerides solid dispersions with silicon dioxide by spray drying technique. European Journal of Pharmaceutical Sciences. 26:219-230 (2005).
67. J.E. Patterson, M.B. James, A.H. Forster, R.W. Lancaster, J.M. Butler, and T. Rades. Preparation of glass solutions of three poorly water soluble drugs by spray drying, melt extrusion and ball milling. International Journal of Pharmaceutics. 336:22-34 (2007).
68. M. Vogt, K. Kunath, and J.B. Dressman. Dissolution enhancement of fenofibrate by micronization, cogrinding and spray-drying: Comparison with commercial preparations. European Journal of Pharmaceutics and Biopharmaceutics. 68:283-288 (2008).
69. J.-S. Kim, M.-S. Kim, H.J. Park, S.-J. Jin, S. Lee, and S.-J. Hwang. Physicochemical properties and oral bioavailability of amorphous atorvastatin hemi-calcium using spray-drying and SAS process. International Journal of Pharmaceutics. 359:211-219 (2008).
70. Y.K. Choi, B.K. Poudel, N. Marasini, K.Y. Yang, J.W. Kim, J.O. Kim, H.-G. Choi, and C.S. Yong. Enhanced solubility and oral bioavailability of itraconazole by combining membrane emulsification and spray drying technique. International Journal of Pharmaceutics. 434:264-271 (2012).
71. D. Chiouand T.A.G. Langrish. Crystallization of Amorphous Components in Spray-Dried Powders. Drying Technology. 25:1427-1435 (2007).
72. K. Sollohuband K. Cal. Spray drying technique: II. Current applications in pharmaceutical technology. Journal of Pharmaceutical Sciences. 99:587-597 (2010).
73. S. Janssens, A. Zeure, A. Paudel, J. Humbeeck, P. Rombaut, and G. Mooter. Influence of Preparation Methods on Solid State Supersaturation of Amorphous Solid Dispersions: A Case Study with Itraconazole and Eudragit E100. Pharm Res. 27:775-785 (2010).
74. F. Usui, K. Maeda, A. Kusai, M. Ikeda, K. Nishimura, and K. Yamamoto. Dissolution improvement of RS-8359 by the solid dispersion prepared by the solvent method. International Journal of Pharmaceutics. 170:247-256 (1998).
75. G. Sertsou, J. Butler, J. Hempenstall, and T. Rades. Solvent change co-precipitation with hydroxypropyl methylcellulose phthalate to improve dissolution characteristics of a poorly water-soluble drug. Journal of Pharmacy and Pharmacology. 54:1041-1047 (2002).
76. G. Sertsou, J. Butler, A. Scott, J. Hempenstall, and T. Rades. Factors affecting incorporation of drug into solid solution with HPMCP during solvent change co-precipitation. International Journal of Pharmaceutics. 245:99-108 (2002).
77. K. Norrman, A. Ghanbari-Siahkali, and N.B. Larsen. 6 Studies of spin-coated polymer films. Annual Reports Section "C" (Physical Chemistry). 101:174-201 (2005).
78. B. Van Eerdenbrugh, J.A. Baird, and L.S. Taylor. Crystallization tendency of active pharmaceutical ingredients following rapid solvent evaporation—classification and comparison with crystallization tendency from undercooled melts. Journal of Pharmaceutical Sciences. 99:3826-3838 (2010).
79. B. Van Eerdenbrughand L.S. Taylor. Small Scale Screening To Determine the Ability of Different Polymers To Inhibit Drug Crystallization upon Rapid Solvent Evaporation. Molecular Pharmaceutics. 7:1328-1337 (2010).
80. S. Mallick, S. Pattnaik, K. Swain, P.K. De, A. Saha, G. Ghoshal, and A. Mondal. Formation of physically stable amorphous phase of ibuprofen by solid state milling with kaolin. European Journal of Pharmaceutics and Biopharmaceutics. 68:346-351 (2008).
81. J.E. Kipp. The role of solid nanoparticle technology in the parenteral delivery of poorly water-soluble drugs. International Journal of Pharmaceutics. 284:109-122 (2004).
82. E. Merisko-Liversidgeand G.G. Liversidge. Nanosizing for oral and parenteral drug delivery: A perspective on formulating poorly-water soluble compounds using wet media milling technology. Advanced Drug Delivery Reviews. 63:427-440 (2011).
83. M.L. Branham, T. Moyo, and T. Govender. Preparation and solid-state characterization of ball milled saquinavir mesylate for solubility enhancement. European Journal of Pharmaceutics and Biopharmaceutics. 80:194-202 (2012).

84. A. Hedoux, A.A. Decroix, Y. Guinet, L. Paccou, P. Derollez, and M. Descamps. Low- and High-Frequency Raman Investigations on Caffeine: Polymorphism, Disorder and Phase Transformation. Journal of Physical Chemistry B. 115:5746-5753 (2011).
85. J.F. Willart, L. Carpentier, F. Dannede, and M. Descamps. Solid-state vitrification of crystalline griseofulvin by mechanical milling. Journal of Pharmaceutical Sciences. 101:1570-1577 (2012).
86. M. Juhnke, D. Märtin, and E. John. Generation of wear during the production of drug nanosuspensions by wet media milling. European Journal of Pharmaceutics and Biopharmaceutics. 81:214-222 (2012).
87. V. Caron, J.F. Willart, R. Lefort, P. Derollez, F. Danede, and M. Descamps. Solid state amorphization kinetic of alpha lactose upon mechanical milling. Carbohydrate Research. 346:2622-2628 (2011).
88. S.K. Singh, K.K. Srinivasan, K. Gowthamarajan, D.S. Singare, D. Prakash, and N.B. Gaikwad. Investigation of preparation parameters of nanosuspension by top-down media milling to improve the dissolution of poorly water-soluble glyburide. European Journal of Pharmaceutics and Biopharmaceutics. 78:441-446 (2011).
89. A. Otte, Y. Zhang, M.T. Carvajal, and R. Pinal. Milling induces disorder in crystalline griseofulvin and order in its amorphous counterpart. CrystEngComm. 14:2560-2570 (2012).
90. M. Descamps, J.F. Willart, E. Dudognon, and V. Caron. Transformation of pharmaceutical compounds upon milling and comilling: The role of Tg. Journal of Pharmaceutical Sciences. 96:1398-1407 (2007).
91. K.J. Crowleyand G. Zografi. Cryogenic grinding of indomethacin polymorphs and solvates: Assessment of amorphous phase formation and amorphous phase physical stability. Journal of Pharmaceutical Sciences. 91:492-507 (2002).
92. R.T.Y. Lim, W.K. Ng, and R.B.H. Tan. Dissolution enhancement of indomethacin via amorphization using co-milling and supercritical co-precipitation processing. Powder Technology. 240:79-87 (2013).
93. J. Pirttimäki, E. Laine, J. Ketolainen, and P. Paronen. Effects of grinding and compression on crystal structure of anhydrous caffeine. International Journal of Pharmaceutics. 95:93-99 (1993).
94. E.M. Pearce. Introduction to polymer science and technology: An SPE text-book, Herman S. Kaufman and Joseph J. Falcetta, Eds., Wiley-Interscience, New York, Journal of Polymer Science: Polymer Letters Edition. 16:55-55 (1978).
95. S.M. El-Egakey MA, Speiser P. Hot extruded dosage forms. I. Technology and dissolution kinetics of polymeric matrices. Pharm Acta Helv. 46:31-52 (1971).
96. M. Yang, P. Wang, C.Y. Huang, M.S. Ku, H.J. Liu, and C. Gogos. Solid dispersion of acetaminophen and poly(ethylene oxide) prepared by hot-melt mixing. International Journal of Pharmaceutics. 395:53-61 (2010).
97. I. Ghosh, J. Snyder, R. Vippagunta, M. Alvine, R. Vakil, W.Q. Tong, and S. Vippagunta. Comparison of HPMC based polymers performance as carriers for manufacture of solid dispersions using the melt extruder. International Journal of Pharmaceutics. 419:12-19 (2011).
98. M. Maniruzzaman, M.M. Rana, J.S. Boateng, J.C. Mitchell, and D. Douroumis. Dissolution enhancement of poorly water-soluble APIs processed by hot-melt extrusion using hydrophilic polymers. Drug Development and Industrial Pharmacy. 39:218-227 (2013).
99. Y.F. Luo, L.S. Xu, M. Xu, X.G. Tao, R.T. Ai, and X. Tang. Improvement of dissolution and bioavailability of Ginsenosides by hot melt extrusion and cogrinding. Drug Development and Industrial Pharmacy. 39:109-116 (2013).
100. J.-Y. Jung, S.D. Yoo, S.-H. Lee, K.-H. Kim, D.-S. Yoon, and K.-H. Lee. Enhanced solubility and dissolution rate of itraconazole by a solid dispersion technique. International Journal of Pharmaceutics. 187:209-218 (1999).
101. B. Rambali, G. Verreck, L. Baert, and D.L. Massart. Itraconazole Formulation Studies of the Melt-Extrusion Process with Mixture Design. Drug Development and Industrial Pharmacy. 29:641-652 (2003).

102. N. Mohammed, S. Majumdar, A. Singh, W. Deng, N. Murthy, E. Pinto, D. Tewari, T. Durig, and M. Repka. Klucel™ EF and ELF polymers for immediate-release oral dosage forms prepared by melt extrusion technology. AAPS PharmSciTech. 13:1158-1169 (2012).
103. O.I. Corrigan. Mechanisms of Dissolution of Fast Release Solid Dispersions. Drug Development and Industrial Pharmacy. 11:697-724 (1985).
104. J.-L. Duboisand J.L. Ford. Similarities in the release rates of different drugs from polyethylene glycol 6000 solid dispersions. Journal of Pharmacy and Pharmacology. 37:494-495 (1985).
105. O.I. Corrigan. Retardation of Polymeric Carrier Dissolution by Dispersed Drugs: Factors Influencing the Dissolution of Solid Dispersions Containing Polyethlene Glycols. Drug Development and Industrial Pharmacy. 12:1777-1793 (1986).
106. G.R. Lloyd, D.Q.M. Craig, and A. Smith. A calorimetric investigation into the interaction between paracetamol and polyethlene glycol 4000 in physical mixes and solid dispersions. European Journal of Pharmaceutics and Biopharmaceutics. 48:59-65 (1999).
107. E.S. Saersand D.Q.M. Craig. An investigation into the mechanisms of dissolution of alkyl p-aminobenzoates from polyethylene glycol solid dispersions. International Journal of Pharmaceutics. 83:211-219 (1992).
108. R. Yang, Y.J. Wang, X. Zheng, J. Meng, X. Tang, and X.F. Zhang. Preparation and evaluation of ketoprofen hot-melt extruded enteric and sustained-release tablets. Drug Development and Industrial Pharmacy. 34:83-89 (2008).
109. E. Verhoeven, T.R.M. De Beer, E. Schacht, G. Van den Mooter, J.P. Remon, and C. Vervaet. Influence of polyethylene glycol/polyethylene oxide on the release characteristics of sustained-release ethylcellulose mini-matrices produced by hot-melt extrusion: in vitro and in vivo evaluations. European Journal of Pharmaceutics and Biopharmaceutics. 72:463-470 (2009).
110. H. Sato, Y. Miyagawa, T. Okabe, M. Miyajima, and H. Sunada. Dissolution mechanism of diclofenac sodium from wax matrix granules. Journal of Pharmaceutical Sciences. 86:929-934 (1997).
111. E. Verhoeven, T.R.M. De Beer, G. Van den Mooter, J.P. Remon, and C. Vervaet. Influence of formulation and process parameters on the release characteristics of ethylcellulose sustained-release mini-matrices produced by hot-melt extrusion. European Journal of Pharmaceutics and Biopharmaceutics. 69:312-319 (2008).
112. M. Zahiruland I. Khan. Dissolution testing for sustained or controlled release oral dosage forms and correlation with in vivo data: Challenges and opportunities. International Journal of Pharmaceutics. 140:131-143 (1996).
113. M.M. Crowley, B. Schroeder, A. Fredersdorf, S. Obara, M. Talarico, S. Kucera, and J.W. McGinity. Physicochemical properties and mechanism of drug release from ethyl cellulose matrix tablets prepared by direct compression and hot-melt extrusion. International Journal of Pharmaceutics. 269:509-522 (2004).
114. M.M. Crowley, A. Fredersdorf, B. Schroeder, S. Kucera, S. Prodduturi, M.A. Repka, and J.W. McGinity. The influence of guaifenesin and ketoprofen on the properties of hot-melt extruded polyethylene oxide films. European Journal of Pharmaceutical Sciences. 22:409-418 (2004).
115. M.A. Repka, K. Gutta, S. Prodduturi, M. Munjal, and S.P. Stodghill. Characterization of cellulosic hot-melt extruded films containing lidocaine. European Journal of Pharmaceutics and Biopharmaceutics. 59:189-196 (2005).
116. C.R. Palem, S.K. Battu, S. Maddineni, R. Gannu, M.A. Repka, and M.R. Yamsani. Oral transmucosal delivery of domperidone from immediate release films produced via hot-melt extrusion technology. Pharmaceutical Development and Technology. 18:186-195 (2013).
117. D.X. Li, G. Guo, R.R. Fan, J. Liang, X. Deng, F. Luo, and Z.Y. Qian. PLA/F68/Dexamethasone implants prepared by hot-melt extrusion for controlled release of anti-inflammatory drug to implantable medical devices: I. Preparation, characterization and hydrolytic degradation study. International Journal of Pharmaceutics. 441:365-372 (2013).
118. D. Douroumis. Practical approaches of taste masking technologies in oral solid forms. Expert Opinion on Drug Delivery. 4:417-426 (2007).

119. D. Douroumis. Orally disintegrating dosage forms and taste-masking technologies; 2010. Expert Opinion on Drug Delivery. 8:665-675 (2011).
120. M. Maniruzzaman, J.S. Boateng, M. Bonnefille, A. Aranyos, J.C. Mitchell, and D. Douroumis. Taste masking of paracetamol by hot-melt extrusion: An in vitro and in vivo evaluation. European Journal of Pharmaceutics and Biopharmaceutics. 80:433-442 (2012).
121. C.D. Bruce, K.A. Fegely, A.R. Rajabi-Siahboomi, and J.W. McGinity. The influence of heterogeneous nucleation on the surface crystallization of guaifenesin from melt extrudates containing Eudragit® L10055 or Acryl-EZE®. European Journal of Pharmaceutics and Biopharmaceutics. 75:71-78 (2010).
122. P. Marsac, S. Shamblin, and L. Taylor. Theoretical and Practical Approaches for Prediction of Drug–Polymer Miscibility and Solubility. Pharm Res. 23:2417-2426 (2006).
123. S. Dudduand P. Dal Monte. Effect of Glass Transition Temperature on the Stability of Lyophilized Formulations Containing a Chimeric Therapeutic Monoclonal Antibody. Pharm Res. 14:591-595 (1997).
124. D. Zhou, G.G.Z. Zhang, D. Law, D.J.W. Grant, and E.A. Schmitt. Thermodynamics, Molecular Mobility and Crystallization Kinetics of Amorphous Griseofulvin. Molecular Pharmaceutics. 5:927-936 (2008).
125. J.F. Willartand M. Descamps. Solid State Amorphization of Pharmaceuticals. Molecular Pharmaceutics. 5:905-920 (2008).
126. M. Tobyn, J. Brown, A.B. Dennis, M. Fakes, Q. Gao, J. Gamble, Y.Z. Khimyak, G. McGeorge, C. Patel, W. Sinclair, P. Timmins, and S. Yin. Amorphous drug–PVP dispersions: Application of theoretical, thermal and spectroscopic analytical techniques to the study of a molecule with intermolecular bonds in both the crystalline and pure amorphous state. Journal of Pharmaceutical Sciences. 98:3456-3468 (2009).
127. G. Van den Mooter, M. Wuyts, N. Blaton, R. Busson, P. Grobet, P. Augustijns, and R. Kinget. Physical stabilisation of amorphous ketoconazole in solid dispersions with polyvinylpyrrolidone K25. European Journal of Pharmaceutical Sciences. 12:261-269 (2001).
128. M. Gordonand J.S. Taylor. Ideal copolymers and the second-order transitions of synthetic rubbers. i. non-crystalline copolymers. Journal of Applied Chemistry. 2:493-500 (1952).
129. B. Hancockand G. Zografi. The Relationship Between the Glass Transition Temperature and the Water Content of Amorphous Pharmaceutical Solids. Pharm Res. 11:471-477 (1994).
130. K. Khougazand S.-D. Clas. Crystallization inhibition in solid dispersions of MK-0591 and poly(vinylpyrrolidone) polymers. Journal of Pharmaceutical Sciences. 89:1325-1334 (2000).
131. S.L. Shamblin, L.S. Taylor, and G. Zografi. Mixing behavior of colyophilized binary systems. Journal of Pharmaceutical Sciences. 87:694-701 (1998).
132. Y.H. Roos. Frozen state transitions in relation to freeze drying. Journal of Thermal Analysis. 48:535-544 (1997).
133. I.M. Hodge. Effects of annealing and prior history on enthalpy relaxation in glassy polymers. 6. Adam-Gibbs formulation of nonlinearity. Macromolecules. 20:2897-2908 (1987).
134. Y. Aso, S. Yoshioka, and S. Kojima. Molecular mobility-based estimation of the crystallization rates of amorphous nifedipine and phenobarbital in poly(vinylpyrrolidone) solid dispersions. Journal of Pharmaceutical Sciences. 93:384-391 (2004).
135. P. Claudy, S. Jabrane, and J.M. Létoffé. Annealing of a glycerol glass: Enthalpy, fictive temperature and glass transition temperature change with annealing parameters. Thermochimica Acta. 293:1-11 (1997).
136. P. Badrinarayanan, W. Zheng, Q. Li, and S.L. Simon. The glass transition temperature versus the fictive temperature. Journal of Non-Crystalline Solids. 353:2603-2612 (2007).
137. K.L.N. R. Böhmer, C. A. Angell, D. J. Plazek Nonexponential relaxations in strong and fragile glass formers. Journal of Chemical Physics. 99:9 (1993).
138. C. Bhugra, R. Shmeis, S. Krill, and M. Pikal. Predictions of Onset of Crystallization from Experimental Relaxation Times I-Correlation of Molecular Mobility from Temperatures

Above the Glass Transition to Temperatures Below the Glass Transition. Pharm Res. 23:2277-2290 (2006).
139. S. Hasegawa, P. Ke, and G. Buckton. Determination of the structural relaxation at the surface of amorphous solid dispersion using inverse gas chromatography. Journal of Pharmaceutical Sciences. 98:2133-2139 (2009).
140. F. Qian, J. Huang, and M.A. Hussain. Drug–polymer solubility and miscibility: Stability consideration and practical challenges in amorphous solid dispersion development. Journal of Pharmaceutical Sciences. 99:2941-2947 (2010).
141. H. Konnoand L. Taylor. Ability of Different Polymers to Inhibit the Crystallization of Amorphous Felodipine in the Presence of Moisture. Pharm Res. 25:969-978 (2008).
142. C. Ahlneckand G. Zografi. The molecular basis of moisture effects on the physical and chemical stability of drugs in the solid state. International Journal of Pharmaceutics. 62:87-95 (1990).
143. T. Wuand L. Yu. Surface Crystallization of Indomethacin Below T g. Pharm Res. 23:2350-2355 (2006).
144. J.A. Baird, B. Van Eerdenbrugh, and L.S. Taylor. A classification system to assess the crystallization tendency of organic molecules from undercooled melts. Journal of Pharmaceutical Sciences. 99:3787-3806 (2010).
145. L. Zhu, L. Wong, and L. Yu. Surface-Enhanced Crystallization of Amorphous Nifedipine. Molecular Pharmaceutics. 5:921-926 (2008).
146. J. Liand D. Chiappetta. An investigation of the thermodynamic miscibility between VeTPGS and polymers. International Journal of Pharmaceutics. 350:212-219 (2008).
147. K. Kawakami. Miscibility analysis of particulate solid dispersions prepared by electrospray deposition. International Journal of Pharmaceutics. 433:71-78 (2012).
148. P.J. Flory. Thermodynamics of High Polymer Solutions. Journal of Chemical Physics. 10:11 (1942).
149. J.S. Higgins, M. Tambasco, and J.E.G. Lipson. Polymer blends; stretching what we can learn through the combination of experiment and theory. Progress in Polymer Science. 30:832-843 (2005).
150. B.C. Hancock, P. York, and R.C. Rowe. The use of solubility parameters in pharmaceutical dosage form design. International Journal of Pharmaceutics. 148:1-21 (1997).
151. M. Yang, P. Wang, C.-Y. Huang, M.S. Ku, H. Liu, and C. Gogos. Solid dispersion of acetaminophen and poly(ethylene oxide) prepared by hot-melt mixing. International Journal of Pharmaceutics. 395:53-61 (2010).
152. S.M. Maru, M. de Matas, A. Kelly, and A. Paradkar. Characterization of thermal and rheological properties of zidovidine, lamivudine and plasticizer blends with ethyl cellulose to assess their suitability for hot melt extrusion. European Journal of Pharmaceutical Sciences. 44:471-478 (2011).
153. C.M. Hansen. The universality of the solubility parameter. Industrial & Engineering Chemistry Product Research and Development. 8:2-11 (1969).
154. C. Sunwooand H. Eisen. Solubility parameter of selected sulfonamides. Journal of Pharmaceutical Sciences. 60:238-244 (1971).
155. J.W. King. Determination of the solubility parameter of soybean oil by inverse gas chromatography. Lebensm Wiss Technol. 28:190-195 (1995).
156. M. Dunkel. Z Physik Chem. 42:(1928).
157. R.F. Fedors. A method for estimating both the solubility parameters and molar volumes of liquids. Supplement. Polymer Engineering & Science. 14:472-472 (1974).
158. C.M. Hansen. 50 Years with solubility parameters—past and future. Progress in Organic Coatings. 51:77-84 (2004).
159. D.J. Greenhalgh, A.C. Williams, P. Timmins, and P. York. Solubility parameters as predictors of miscibility in solid dispersions. Journal of Pharmaceutical Sciences. 88:1182-1190 (1999).
160. S.-u. Yoo, S.L. Krill, Z. Wang, and C. Telang. Miscibility/stability considerations in binary solid dispersion systems composed of functional excipients towards the design of multi-component amorphous systems. Journal of Pharmaceutical Sciences. 98:4711-4723 (2009).

161. T. Nishiand T.T. Wang. Melting Point Depression and Kinetic Effects of Cooling on Crystallization in Poly(vinylidene fluoride)-Poly(methyl methacrylate) Mixtures. Macromolecules. 8:909-915 (1975).
162. A. Mahieu, J.F. Willart, E. Dudognon, F. Danede, and M. Descamps. A New Protocol To Determine the Solubility of Drugs into Polymer Matrixes. Molecular Pharmaceutics. 10:560-566 (2013).
163. T. Felix, H. Anwar, and H. Takeru. Quantitative analytical method for determination of drugs dispersed in polymers using differential scanning calorimetry. Journal of Pharmaceutical Sciences. 63:427-429 (1974).
164. H. Suwardie, P. Wang, D.B. Todd, V. Panchal, M. Yang, and C.G. Gogos. Rheological study of the mixture of acetaminophen and polyethylene oxide for hot-melt extrusion application. European Journal of Pharmaceutics and Biopharmaceutics. 78:506-512 (2011).
165. C. Wiranidchapong, I.G. Tucker, T. Rades, and P. Kulvanich. Miscibility and interactions between 17β-estradiol and Eudragit® RS in solid dispersion. Journal of Pharmaceutical Sciences. 97:4879-4888 (2008).
166. A.F. Rumondor, I. Ivanisevic, S. Bates, D. Alonzo, and L. Taylor. Evaluation of Drug-Polymer Miscibility in Amorphous Solid Dispersion Systems. Pharm Res. 26:2523-2534 (2009).
167. X. Tang, M. Pikal, and L. Taylor. A Spectroscopic Investigation of Hydrogen Bond Patterns in Crystalline and Amorphous Phases in Dihydropyridine Calcium Channel Blockers. Pharm Res. 19:477-483 (2002).
168. J. Huang, R.J. Wigent, and J.B. Schwartz. Drug–polymer interaction and its significance on the physical stability of nifedipine amorphous dispersion in microparticles of an ammonio methacrylate copolymer and ethylcellulose binary blend. Journal of Pharmaceutical Sciences. 97:251-262 (2008).
169. C. Telang, S. Mujumdar, and M. Mathew. Improved physical stability of amorphous state through acid base interactions. Journal of Pharmaceutical Sciences. 98:2149-2159 (2009).
170. H. Konnoand L.S. Taylor. Influence of different polymers on the crystallization tendency of molecularly dispersed amorphous felodipine. Journal of Pharmaceutical Sciences. 95:2692-2705 (2006).

Chapter 2 Materials and methods

2.1 Introduction

With the increasing application of amorphous solid dispersions in the pharmaceutical industry, the enhancement and prediction of the physical stability is becoming more and more significant as the physical stability of amorphous solid dispersions is one of the key challenges associated with the formulation development of solid dispersion (1-3). In order to investigate the dominant factors which control the physical stability of solid dispersions and to further enhance the physical stability of amorphous solid dispersions, four model drugs including felodipine, celecoxib, fenofibrate and carbamazepine with different physicochemical properties, such as different glass transition temperatures different melting points and different crystallization tendency of individual amorphous drugs, were selected in this project (4-6). EUDRAGIT® EPO as the main model polymer was mainly used to formulate with the model drugs by hot melt extrusion. EUDRAGIT® EPO is a hydrophobic polymer and thus it might protect amorphous drugs from recrystallization under stressed humidity (7). Kollidon® VA 64 was also used in this project and it was formulated with EUDRAGIT® EPO together (immiscible polymer blends) in hot melt extrusion to enhance the physical stability of amorphous solid dispersions (discussed in Chapter 7).

To understand the physicochemical properties of amorphous solid dispersions, different characterisation technologies were employed. For instance, Powder X-Ray Diffraction (PXRD) results presenting amorphous halo rather than peaks indicate the majority of components in the solid dispersion was mainly amorphous (8). A single glass transition detected by Differential Scanning Calorimetry (DSC) in binary drug-polymer dispersion may indicate a single-phase amorphous solid solution (9). Fourier Transform Infrared Spectroscopy (FTIR) alone with solid state NMR (ssNMR) can be used to judge if interactions (e.g. hydrogen bonding) have been formed between drugs and polymers in solid dispersions based on the analysis of peak positions (10, 11). Besides these conventional characterisation techniques, some analytical technologies with high spatial resolution, such as Atomic Force Microscopy combined with Localised Thermal Analysis (AFM-LTA) and Photothermal Microspectroscopy (PT-MS), were used to map the drug-polymer distribution of amorphous solid dispersions at a micron to sub-micron scale (12).

In this project, conventional technologies including DSC, PXRD, ATR-FTIR, ssNMR and localised technologies with high spatial resolution including Scanning Electron Microscope (SEM), AFM-LTA and PT-MS were applied to characterise solid dispersions. Thermal gravimetric analysis (TGA) was used to test the thermal stability of materials for hot melt extrusion. Dynamic Vapour

Sorption (DVS) was used to investigate the behaviour of water sorption of samples upon exposure to stressed humidity.

2.2 Materials

Felodipine, fenofibrate, celecoxib, carbamazepine and EUDRAGIT® EPO were kindly donated by Evonik Industries AG, Darmstadt Germany. Kollidon® VA 64 (PVPVA) was received as a gift BASF, Ludwigshafen, Germany.

2.2.1 Felodipine

Felodipine (ethyl methyl 4-(2, 3-dichlorophenyl)-1, 4-dihydro-2, 6-dimethyl-3, 5-pyridinedicarboxylate), as shown in Figure 2.1, is a Ca^{2+} antagonist and a member of the dihydropyridine family with analogues including nifedipine, nitrendipine and nicardipine (13). It has been widely used to treat hypertension. Commercial products containing felodipine are available in market such as Plendil® (AstraZeneca Pharmaceuticals, dose includes 2.5, 5 and 10mg/tablet). Felodipine is a typical BCS II drug with a low aqueous solubility of 0.5mg/L at room temperature (14). Three polymorph of crystalline felodipine has been reported with the onset value of melting points of 144.9^{o}C for form I, 141.5^{o}C for form II and 133.9^{o}C for form III and amongst these polymorphs form III was most stable (15). Solid state transition of different polymorphs of crystalline felodipine has been reported whereby heating the melt-cooled amorphous felodipine at 10^{o}C/min melting points of different polymorphs were detected (4). However, it was not further discussed if using different heating rates recrystallization of polymorphs could controlled specifically (4). In another study, crystallising out from the felodipine solution in co-solvent (n-hexane: methanol 10:1) at room temperature, form III (with the melting point of 133.9^{o}C was successfully prepared) (16). The Glass transition temperature of amorphous felodipine has also been reported as 45^{o}C (14).

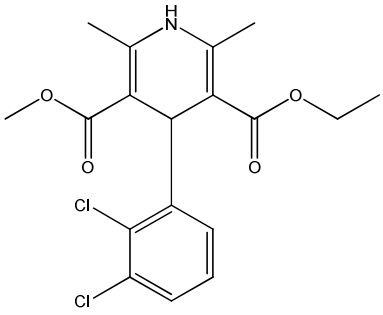

Figure 2.1: Chemical structure of felodipine.

2.2.2 Celecoxib

Celecoxib is a non-steroidal anti-inflammatory drug (NSAID) and selective cyclo-oxygenase (COX-2) inhibitor used in the treatment of osteoarthritis, rheumatoid arthritis, acute pain (17). The commercial product of celecoxib was manufactured by Pfizer and was named as Celebrex® (dose 100mg/tablet). The chemical structure of celecoxib is shown in Figure 2.2. Celecoxib is a BCS II drug that has low water solubility of 5mg/L at room temperature but good permeability (18). Three polymorphs of crystalline celecoxib have been reported in literature with the onset melting points of 162.8°C for form I, 161.5°C for from II and 160.8°C for form III and form III is the thermodynamically stable form under ambient condition (19, 20). There were few articles discussing the solid state transformation between different celecoxib polymorphs, and thus it was not clearly understood the recrystallization behaviour of amorphous celecoxib. In this project, celecoxib polymorphs with different melting point were detected on heating the melt-cooled amorphous celecoxib (discussed in Chapter 3). However, the mechanism was not understood. The glass transition temperature of amorphous celecoxib has been reported as 58°C (5).

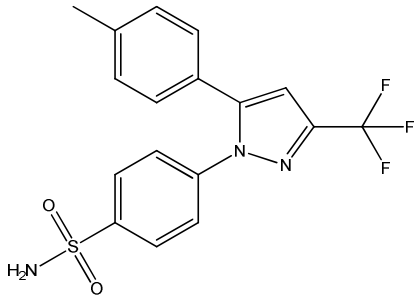

Figure 2.2: Chemical structure of celecoxib.

2.2.3 Fenofibrate

Fenofibrate is clinically administrated to control cholesterol levels in patients at risk of cardiovascular disease by reducing low-density lipoprotein and very low density lipoprotein and increasing high density lipoprotein (21). Fenofibrate has a broad clinical dose ranging from 48mg/capsule (i.e. Trictor® by Abbots) to 200mg/capsule (Lofibra® by Teva Pharmaceuticals). The chemical structure of fenofibrate is shown in Figure 2.3. It has been reported in literature that as classified into BSC II, the aqueous solubility of fenofibrate is extremely low (below 0.5mg/L) (22). Two polymorphs of crystalline fenofibrate have been reported in literature with the stable form I (melting point 80°C) and metastable form II (melting point 73°C) (23).Transformation between the two polymorphs has been reported (23). By maintaining melt-cooled amorphous fenofibrate at the temperature of 40°C and 70°C, respective, recrystallized form I and II were detected using DSC (23). Glass transition temperature of amorphous fenofibrate was reported as -19°C (5).

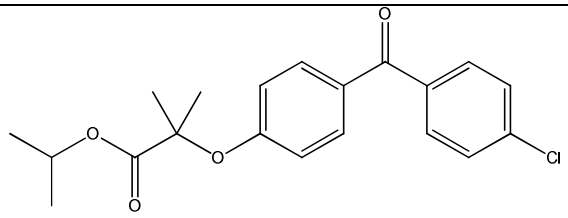

Figure 2.3: Chemical structure of fenofibrate.

2.2.4 Carbamazepine

Carbamazepine (CBZ) is an anticonvulsant and mood-stabilizing drug used primarily in the treatment of epilepsy and bipolar disorder (24). There have been a few carbamazepine branded products in different countries and the dose varies from 100mg/tablet to 400mg/tablet (i.e. Tegretol by Novartis Pharma with both doses). At least four anhydrous polymorphs of crystalline carbamazepine and a dihydrate have been confirmed (25-28). Thermodynamically, form III has been reported as the most stable form and on heating in DSC a double melting could be detected with the first one being a combination of melting of form III at 161^{o}C and transformation into form I and with the second one being the melting of form I at 191^{o}C (29). The dihydrate form was reported to form by using form III of to directly contact with water and the water (30). The water content in dehydrates was circa 13% (w/w) (30). The solubility and bioavailability of carbamazepine has been reported to vary depending on polymorphs. Form III, the most commonly available on the market, presents a very low aqueous solubility of 17.7mg/L (31, 32). The chemical structure of carbamazepine is shown in Figure 2.4. The glass transition temperature of amorphous carbamazepine was reported as 55^{o}C (5).

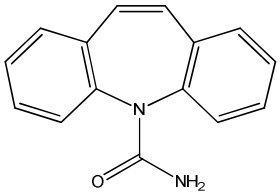

Figure 2.4: Chemical structure of carbamazepine.

2.2.5 EUDRAGIT® EPO

EUDRAGIT® EPO is a cationic copolymer which is composed of dimethylaminoethyl methacrylate and neutral methacrylic ester units as shown in Figure 2.5. It is a pH-dependent soluble polymer that dissolves at the pH below 5. EUDRAGIT® EPO is naturally amorphous with a glass transition temperature of approximately 50^{o}C (33). EUDRAGIT® EPO has been widely applied in pharmaceutical industry in taste masking via the preparation of solid dispersions or microspheres with bitter drugs (13, 34-36). Due to its non-hygroscopicity, EUDRAGIT® EPO was

also used to protect amorphous solid dispersions from moisture uptake to enhance the physical stability (7).

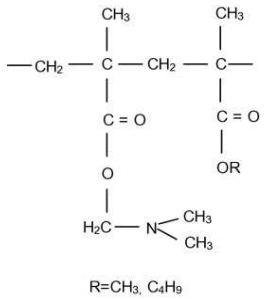

Figure 2.5: Chemical structure of EUDRAGIT® EPO.

Recently, EUDRAGIT® EPO was used in amorphous solid dispersions to increase the dissolution rate of poorly water-soluble drugs (15, 37, 38). An ibuprofen tablet prepared from compressing ibuprofen-EUDRAGIT® EPO melt extrudates was reported to show a similar dissolution profile to the commercial Nurofen® (39). Increasing the drug loadings in the tablet (up to 40% w/w) a faster dissolution rate was observed and it was attributed to the faster disintegration of the tablet due to the higher loading of talc (39). In another research, an efravirenz-EUDRAGIT® EPO melt extrudate was prepared and compared with the physical mixture with the same drug-polymer ratio, the dissolution rate from the solid dispersions increased two times higher (15). These studies demonstrated the feasibility of EUDRAGIT® EPO in the hot melt extrusion and its ability of dissolution enhancement of some poorly water-soluble drugs.

In addition, phase separation behaviour of EUDRAGIT® EPO based amorphous solid dispersions was also studied (13, 17, 36, 40, 41). Hot melt extrudates prepared with paracetamol and EUDRAGIT® EPO were studied by Qi et al, and it was reported that crystalline drug could be detected even in 10% (w/w) drug loading sample (17). Phase separation including molecular drug-polymer dispersion and crystalline drug were very likely to present in the solid dispersions (17). Felodipine-EUDRAGIT® EPO solid dispersions prepared by hot melt extrusion was studied by the same group (41). After 2 month aging under 20%RH/40^{o}C, only little amount of crystalline felodipine was detected in 70% (w/w) drug loading sample. These finds indicate that drug-polymer solid solubility is drug-dependent and different drugs formulated with the same polymer can present significantly different physical stability. In addition, a very recent study on the investigation of the physical stability of spin coated solid dispersions showed that EUDRAGIT® EPO can strongly protect solid dispersions from phase separation under stressed humidity in comparison to PVP K30 and Soluplus. This was attributed to the low hygroscopicity of EUDRAGIT® EPO and moisture uptake has been suggested as a key factor causing physical instability of the studied solid dispersions (7). Consequently, based on the good processibility of EUDRAGIT® EPO in hot melt extrusion and its low-hygroscopicity nature, it was selected as the

main model polymer to formulate solid dispersions with model drugs by hot melt extrusion in this project.

2.2.6 Kollidon® VA64

Kollidon® VA64 (PVPVA64) is a hydrophylic polymer which is composed of 6 parts of N-vinylpyrrolidone and 4 parts of vinyl acetate (Figure 2.6). It is an amorphous polymer with a glass transition temperature of 106°C (42). Kollidon® VA64 was originally invented as a binder for wet granulation or dry binder for direct compression. Due to the suitable glass transition temperature and good thermoplasticity, Kollidon® VA64 was introduced as polymeric carriers in hot melt extrusion (43). Amorphous solid dispersions prepared by hot melt extrusion with Kollidon® VA64 have been reported to show enhanced dissolution performance (44-46). In a study regarding the improvement of a model poorly water-soluble drug (a cannabinoid antagonist, newly synthesised), the formulation prepared with 10% w/w drug and 90% (w/w) Kollidon® VA64 showed 100% drug release whereas only 3% of the pure drug dissolved under non-sink condition within the same time period (21). The formulation was still confirmed as amorphous after 15 days aged under 75%RH/40°C. In another study, bifendate was prepared into melt extrudates with Kollidon® VA64 (47). In comparison to the commercial product, a significant increase of dissolution rate was observed in the melt extrudates with 10% (w/w) drug loading. In addition, a relative bioavailability of 145.3±35.3% compared with commercial product was achieved.

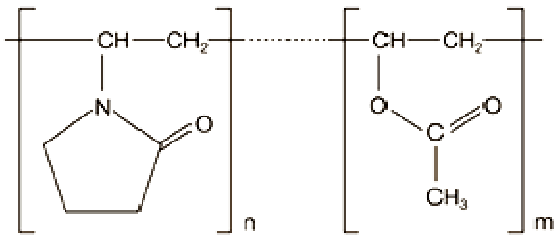

Figure 2.6: Chemical structure of Kollidon® VA64

As can be seen in the chemical structure (Figure 2.6), Kollidon® VA64 contains exposed carbonyl groups indicating its strong potential as an acceptor to form hydrogen bonding with drugs contain donor groups (i.e. NH or OH) in solid dispersions. This may lead to a high drug-polymer solubility in amorphous solid dispersions (48). Although in comparison to PVP K30, 40% of hydrophilic components, vinylpyrrolidone, has been replaced by hydrophobic group, vinyl acetate, moisture uptake by solid dispersions prepared with Kollidon® VA64 was reported (49, 50). In this project, Kollidon® VA64 was used with EUDRAGIT® EPO as an immiscible polymer blend matrix to stabilise melt extruded solid dispersions with felodipine. The hypothesis can be described as follows. Firstly, the ability of Kollidon® VA64 to form hydrogen bonding with model drugs may potential increase the overall drug-polymer solubility. Secondly, moisture uptake of solid

dispersions prepared with Kollidon® VA64 can be reduced with the addition of EUDRAGIT® EPO. Therefore, combined the two effects, the physical stability of amorphous solid dispersions can be enhanced if formulated with the immiscible polymer blends. The application of the immiscible polymer blends is discussed in Chapter 7.

2.3 Methods

Solid dispersions were prepared by hot melt extrusion and spin coating in this study. In order to investigate drug-polymer miscibility and solubility as well as characterise model drugs and solid dispersions, several conventional characterisation technologies were used in this study including MTDSC, ATR-FTIR and PXRD. Modulated temperature differential scanning calorimetry (MTDSC) has been widely used in the pharmaceutical industry to provide the thermal properties of materials in heating. Attenuated total reflectance Fourier-transform infrared spectroscopy (ATR-FTIR) has been used to gain chemical information on drug-polymer solid dispersions. Powder X-Ray diffraction (PXRD) can be used to distinguish a system from crystalline to amorphous state. Besides these technologies mentioned above which provide bulk properties of solid dispersions, microscopy based technology including scanning electronic microscopy (SEM) and atomic force microscopy (AFM) combined with local thermal analysis (LTA) and photothermal microscopy (PT-MS) were also used in this study to understand the form, distribution and physical stability occurred on a spatially resolved basis.

2.3.1 Preparation of drug-polymer solid dispersions

2.3.1.1 Hot melt extrusion

The principle and application of hot melt extrusion in the pharmaceutical industry has been described in detail in Chapter 1 (section 1.4.5). In this study, all melt extruded formulations were carried out on a Thermo Scientific HAAKE MiniLab II (Thermo Scientific, UK) with co-rotating twin screws. In this study, the rotation speed of the twin screws was set at 100r/min unless otherwise stated. The barrel temperature was generally set higher (~5^{o}C) than the melting points of model drugs (it was specified in the case, if different operation temperature was used). The dwell time was maintained for 5 min for all formulations to ensure the complete mixing and melting of drug and polymer powder mixtures.

2.3.1.2 Spin coating

The mechanism and principle of spin coating has been discussed in Chapter 1 (section 1.4.3). In this project, spin coating was used to prepare pure amorphous drugs to investigate theircrystallisation tendency and physical stability. Solid dispersions were also prepared by spin coating in order to compare the physical stability with solid dispersions prepared by hot melt

extrusion and evaluate whether the physical stability of the solid dispersions with the same drug-polymer composition varies depending on different preparation processes.

A G3P-8 spin coater (Specialty Coating System, Surrey, UK) as shown in Figure 2.7 was used to prepare samples in this study. Generally a mixture of ethanol and dichloromethane with the ratio of 50:50 was used as the solvent to prepare solutions for spin coating since model drugs and polymers all have high solubilities in this mixed solvent. In addition, the selection of the solvent ensures the fast evaporation during spin coating as the boiling point of dichloromethane is only 39.6^{o}C. This can bring the boiling point of the solvent mixture (dichloromethane and ethanol) to the value in between 39.6^{o}C and 78.4^{o}C (boiling point of ethanol). Solid concentration of all solutions was 15% (w/v) which provides the viscosity to form the thin film with suitable thickness (approximately 10µm). In spin coating, a piece of square-cut microscopy glass slide with the size of 25mm×25mm was placed on the chuck (Figure 2.7). Vacuum was provided underneath the chuck to ensure the substrate was attached tightly during spinning. For all sample preparations, the spinning speed was maintained at 2000 r/min with a duration time of 2min. With this set of parameters, no residue solvent was detected when testing the sample by ATR-FTIR (no typical solvent peak was observed).

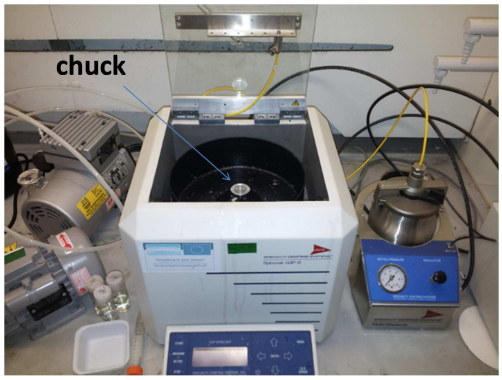

Figure 2.7: A G3P-8 spin coater (Specialty Coating System, Surrey, UK).

2.3.1.3 Milling

In this project, milling was used for two purposes. First, it was used as a downstream method to process strand form melt extrudates into powder for the dissolution test (particle size was controlled using sieve to the size between 63 and 106µm). Second, milling was developed into a practical method for the accurate prediction of the apparent solubility of model drugs in melt extrudates (details are discussed in Chapter 5). A vibrating ball milling (Retsch MM 400 Ball Milling, Haan, Germany) was used in this project (Figure 2.8). The milling balls were made of stainless steel with a diameter of 7mm. Parameters including milling vibrating frequency and milling time is discussed in the related chapters.

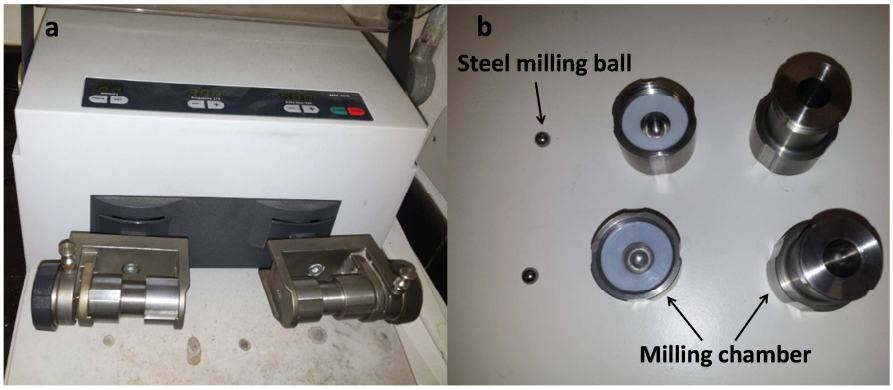

Figure 2.8: Retsch MM 400 ball milling (a); milling chamber and the steel balls for milling (b).

2.3.2 Physicochemical characterisation techniques

2.3.2.1 Differential scanning calorimetry (DSC)

2.3.2.1.1 Basic principles

Differential scanning calorimetry (DSC) is a thermal analysis technique which was first commercially introduced in 1963 (24). It provides qualitative and quantitative information as a function of time and temperature regarding thermal transitions in materials that involve endothermic or exothermic processes, or changes in heat capacity (51). Generally, there are two types DSC instruments: power compensation and heat flux. Power compensation DSC involves two separated furnaces for the reference and for the sample. The common principle of power compensation DSC is to heat both the reference and the sample simultaneously in such a way that the temperature of the two is kept identical, and the extra powder supply to maintain the temperature is measured (52). Unlike power compensation DSC using two furnaces, heat flux DSC uses two crucibles for the sample and for the reference within one furnace as seen in Figure 2.9. They are both heated from the same source and the temperature difference between the sample and the reference is measured (52). The signal is then converted into the power difference as shown in the following equation:

$$dQ / dt = \Delta T / R \qquad Eq\ 2.1$$

where Q is the heat, t is the time ΔT is the temperature difference between the sample and the reference and R is the thermal resistance of the heat paths between the furnace and the crucible. Therefore, if heat paths are identical, the heat flow difference can reflect the temperature difference between the sample and the reference.

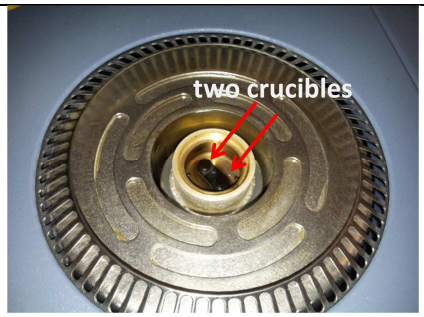

Figure 2.9: Opened furnace with two crucibles in Q-2000 MTDSC.

The total heat content of a material is in linear relationship to its heat capacity (C_p J/g·^{o}C) which is the quantity of heat required to change the temperature of the material by 1K:

$$C_p = dQ / dT \qquad \textit{Eq 2.2}$$

Rearranging this equation with time:

$$dQ / dt = C_p\,(dT / dt) \qquad \textit{Eq 2.3}$$

where dQ / dt is the heat flow and dT / dt is the heating rate. With this equation, the differential heat flow can be a measure of the sample heat capacity. DSC data is normally expressed with the heat flow as a function of the temperature. A typical DSC thermograph is shown in Figure 2.10.

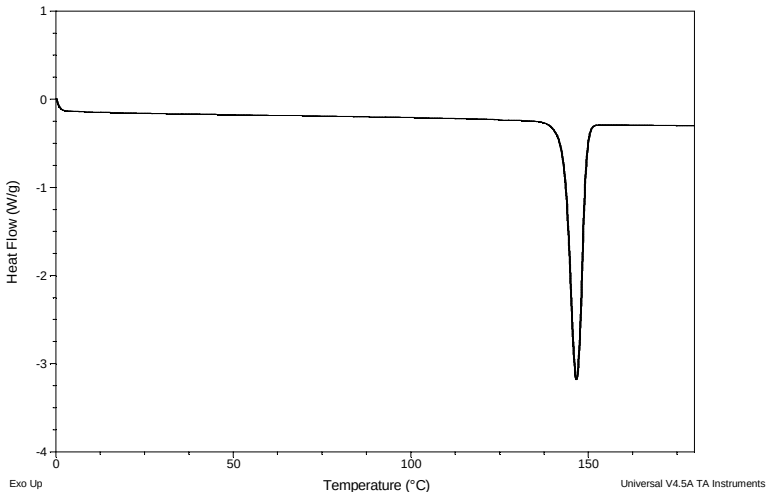

Figure 2.10: DSC result of felodipine measured at the heating rate of 10^{o}C/min.

2.3.2.1.2 Modulated temperature differential scanning calorimetry (MTDSC)

Conventional DSC mentioned above is a powerful tool to measure thermal event such as melting accurately. However it cannot distinguish overlapping thermal events: glass transition and relaxation could occur within the same temperature range for some amorphous drugs and polymer

(53). MT DSC was designed to separate overlapping thermal events. Compared with conventional DSC, a sinusoidal modulation is overlaid on the linear ramp, namely, a perturbed heating or cooling process. As a result, there are three variables related to DSC results and they are average heating rate (underlying heat rate), amplitude of modulation and frequency of modulation. With effects of these variables, the equation describing heat flow can be reorganised as follows:

$$dQ / dt = C_p (dT / dt + f''(t,T)) + f(t,T) \qquad Eq\ 2.4$$

where dQ / dt is the total heat flow comprises two contributions, dT / dt is the heating rate, C_p is the heat capacity, $f''(t,T)$ is the thermodynamic heat flow component, and $f(t,T)$ is kinetically limited heat flow (12). This equation shows that total heat flow comprises two contributions: one is function of heating rate (heating rate dependent) and the other one is a function of time and temperature (temperature and time dependent). Heating rate dependent transitions tend to be larger when evaluated using faster heating rates and are reversing. For instance, the transition (i.e. heat capacity) can be cycled by altering heating and cooling (termed as reversing transition). Temperature and time dependent transitions cannot be reversed once initiated and these transitions are termed as non-reversing transitions, such as relaxation or decomposition. Consequently, by separating signals into reversing and non-reversing responses, overlapping thermal events can be distinguished.

In addition to separating reversing and non-reversing thermal events, MTDSC is also able to measure the heat capacity more accurately in comparison to the conventional DSC. In MTDSC, the heat capacity data (C_p) is calculated (54):

$$C_p = K_c A_{HF} / A_{HR} \qquad Eq\ 2.5$$

where K_c is the heat capacity calibration constant, A_{HF} is the amplitude of the modulated heat flow and A_{HR} is the modulated heating rate. Therefore, the application of large amplitude in MTDSC can increase the heat capacity precision by reducing noise (54). For amorphous drugs, heat capacity value normally increased when crossing the glass transition region on heating in DSC, and thus with the high precision of the detection of heat capacity, MTDSC can be highly sensitive in detecting glass transitions of amorphous materials (54).

2.3.2.1.3 Calibration and experimental parameters

A Q-2000 MTDSC (TA Instruments, Newcastle, USA) was used in this study. It is a heat flux MTDSC. As mentioned above, two crucibles were set within one furnace for this type of DSC. In any measurement, the thermal behaviour of the reference is compared with that of the sample. Therefore factors which will affect the accuracy such as heat adsorption by the two crucibles and

heat loss through convection need to be minimised. In order to provide accurate and consistent results by DSC, it is necessary to calibrate DSC before it is used.

For the Q-2000 MTDSC in this study, in standard mode (used as conventional DSC), three basic calibrations were required and carried out. They were baseline calibration, cell constant calibration and temperature calibration. The baseline calibration involved two stages and the first stage was running DSC with empty cell (furnace) at a wide temperature range from -80 to 400˚C at the ramp of 20˚C/min. The second stage was performed with running two sapphire disks placed on sample and reference crucibles, respectively. After baseline calibration, results will be saved in the machine which can ensure the temperature variation on scanning be minimised. Cell constant calibration (enthalpy calibration) was performed with running indium through its melting transition. The measured heat flow was compared with the value stored in the machine and the ratio from those two was the cell constant. Temperature calibration is designed to correct the thermalcouple readings of temperature under experimental conditions. Three standards (n-octadecane with T_m of 28.24˚C, indium with T_m of 156.60˚C and Tin with T_m of 231.93˚C) with high purity were used to calibrate temperatures.

For MTDSC, addition heat capacity calibration is required. In order to run MTDSC, three parameters are required to set up including amplitude, underlying heating rate and period. The relationship between these three parameters is recommended by the manufacturer (55):

$$amplitude = (heating\ rate \times period) / (2\pi \times 60) \qquad Eq\ 2.6$$

where the unit of heating rate is ^{o}C/min, the unit of period is s, and the number of 60 is to adjust the second into miniute. By changing the parameters, MTDSC measurement can be improved, i.e. larger amplitude can increase sensitivity of detecting thermal events such as glass transition as described above (56). In this study, an aluminium oxide sapphire was used for heat capacity calibration for modulated mode. The modulation parameters used were ±0.318˚C/60 sec with a 2˚C/min underlying heating rate. With this set of parameters, thermal events such as glass transition and recrystallization of model drugs and polymers can be clearly detected. In this study, all samples were tested in TA standard crimped pans. For each sample, measurements were repeated at least three times (n=3).

2.3.2.2 Thermogravimetric analysis (TGA)

Thermogravimetry is one of the oldest thermal analytical procedures and has been used extensively in the study of polymeric systems (Bolland et al, 1946). The technique involves monitoring the weight loss of the sample in a chosen atmosphere (usually nitrogen or air) as a function of temperature. It is a combination of a suitable electronic microbalance with a furnace, a

temperature programmer and computer for control, which allows the sample to be simultaneously weighted and heated in a controlled manner, and the mass, time and temperature to be captured. In the pharmaceutical industry, TGA is applied to compositional analysis of drugs, the volatile components of substances, effects of water vapour on the stability of crystalline drugs and excipients, and the determination of the water content, both free and bound, of a wide variety of materials (57).

In this study, TGA was used to determine the thermal stability of the drugs and polymers upon heating to assist with selecting the operation temperature in hot melt extrusion to avoid thermal degradation occurred in process. It was also used to detect the quantity of water uptake by solid dispersions upon exposure to high humidity. It is significantly important to measure the water content in solid dispersions since water can act as a plasticizer that can increase molecular mobility of amorphous drugs and compete against drugs in forming hydrogen bonding with polymers to increase physical instability of solid dispersions.

2.3.2.3 Dynamic vapour sorption (DVS)

2.3.2.3.1 Basic principles

Dynamic vapour sorption is a gravimetric technology which measures the water uptake of samples upon exposure to humidity as a function of time. It is a powerful tool to study the kinetics of moisture uptake of samples. DVS is normally used in two modes to investigate the kinetics of water adsorption and absorption. The first one is termed as isohumidity whereby samples are exposed to certain humidity at a fixed temperature for a certain time length until the equilibrium is obtained. The second one is termed as isothermal which involves a step increase of the provided humidity at a certain temperature and monitor the mass change of the sample against time.

DVS has been widely used in the food and pharmaceutical industry to evaluate the behaviour of moisture sorption onto samples as water is a well-known plasticiser which can affect physical property of materials (25, 28, 31). The application of DVS is to investigate the kinetics of moisture sorption of materials and use different fitting mathematical models to evaluate the process of waster uptake. The water uptake by materials or drug delivery systems (i.e. solid dispersions) can be complex, and is typically divided into two steps adsorption (where moisture covers the surface of the samples) and absorption (where moisture penetrates into the bulk of the samples). Different models have been developed to describe the two stages. The classic Brunauer-Emmett-Teller (BET) theory is applied to the adsorption of molecules onto the surface and was typically depicted as sigmoidal shape (33, 35). However, it only applies to the materials with water activity up to 0.4. For more complex systems with water activity range of 0-0.9, the semi-empirical Guggenheim-Anderson-de Boer was introduced (34). In the field of solid dispersions, the Fickian Diffusion and Case II Diffusion are mainly the two widely used models as the process of moisture uptake of

amorphous materials is dominated by either of them (36, 58). Through fitting the DVS using different models, the process of moisture uptake can be better understood which could be beneficial for the selection of storage condition for samples (i.e. food or pharmaceutical dosage forms), especially for developing formulation using hygroscopic materials.

2.3.2.3.2 Experimental parameters

In this study, A Q-5000 SA dynamic vapour sorption (TA Instruments, Newcastle, USA) was applied for the investigation of moisture uptake by samples. Isohumic test were performed on samples including EUDRAGIT® EPO, Kollidon® VA 64 raw powder and different melt extrudates with and without drugs. The samples were exposed to 75%RH at 25°C in DVS up to 10 hours to study their kinetics of moisture uptake.

2.3.2.4 Attenuated total reflectance fourier transform infrared spectroscopy (ATR-FTIR)

2.3.2.4.1 Basic principles

Fourier transform infrared spectroscopy (FTIR) is a spectroscopic technique that can be used to identify chemical bonds within a sample. An electromagnetic wave in the infrared region (wavelength between 750nm and 1mm) can stimulate molecular vibrations and rotations at specific frequencies which depend on the chemical nature of the functional groups. This allows generating a characteristic spectrum which is unique for individual chemical entity.

There are several modes in which FTIR measurements can be made. The commonly used transmission mode requires specific sample preparation for solid samples, that is grinding samples into a fine powder with potassium bromide (KBr) and being compressed into thin disk. This restricts the application of transmission FTIR as the material may change structure during grinding and compressing stages. The mode of attenuated total reflectance (ATR) when applied to FTIR can be used to probe a sample at or near a surface, which makes it possible to obtain FTIR spectra for a surface of a sample without any additional sample preparation (59). The principle of ATR-FTIR is shown in Figure 2.11. ATR method uses a high refractive index crystal such as diamond (59). The sample which could be liquid or solid is placed in contact with the diamond, and infrared light from an FTIR source is allowed entering the diamond at a specific angle and reflecting at the surface (59). The light can penetrate the sample. The depth of penetration d_{ir}, defined as the distance normal to the interface which the intensity falls to 1/e of the intensity at the surface, is expressed (60):

$$d_{ir} = \lambda / (2\pi n_1 (\sin^2 \theta - n_{12}^2)^{1/2}) \qquad \textit{Eq 2.7}$$

where λ is the wavelength of the light, the angle of incidence of the beam is θ and n_{12} is the refractive index ratio (n_2 / n_1) of two media (air and diamond). Specific frequencies of the incoming

radiation, corresponding to the fundamental vibrational frequencies and vibrational overtones of the sample material, are absorbed, and the rest of the light is reflected through the diamond and into a detector. The resulting spectrum is very similar to a FTIR transmission spectrum.

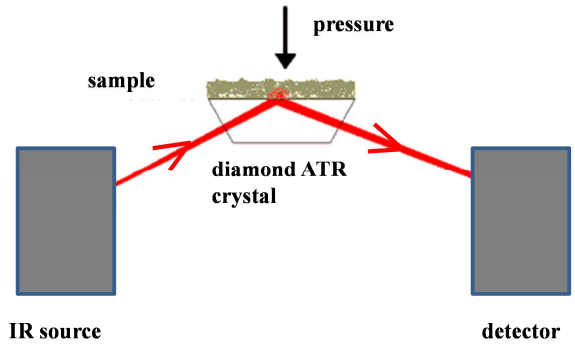

Figure 2.11: Schematic illustration of using ATR-FTIR method to test a solid form sample.

FTIR is one of most commonly used technique in understanding solid dispersions. It can distinguish some chemical groups from drug molecule present differently in a FTIR spectrum when changed from crystalline form to amorphous form. It is also capable to detect the formation of hydrogen bonding between drug and polymer molecules in solid dispersions. Some articles have reported that the drug-polymer inter-molecule hydrogen bonding in solid dispersions is essential to stabilise solid dispersions on aging by inhibiting phase separation and crystallisation of amorphous drugs (61, 62). This is due to the decreased molecular mobility of amorphous drug molecules when hydrogen bonded with the polymer molecules (61).

2.3.2.4.2 Experimental parameters

In this study, ATR-FTIR spectroscopic experiments were carried out on a IFS 66/S FTIR spectrometer (Bruker Optics Ltd, Coventy, UK) fitted with a Golden Gate® ATR accessory with heated top plate (Orpington, UK). The crystal is a single reflection diamond element. The resolution was 2 cm^{-1}, and 32 scans were taken for each sample.

2.3.2.5 Powder X-Ray diffraction (PXRD)

2.3.2.5.1 Basic principles

Powder X-ray diffraction (PXRD) is widely used for the identification of structures of different crystalline materials. In the pharmaceutical industry, PXRD is commonly employed to in the identification of crystalline and amorphous compounds by their diffraction pattern (63, 64). The diffraction will occur if a crystalline material is interacted with a focused X-ray beam according to Bragg's law,

$$n\lambda = 2d\sin\theta \qquad \text{Eq 2.8}$$

where the integer n is the order of the diffracted beam, λ is the wavelength of the incident X-ray beam, d is the distance between adjacent planes of atoms (the d-spacing), and θ is the angle of incidence of the X-ray beam. By altering θ during scanning, different d-spacing can be obtained. The characteristic set of d-spacing generated by a typical PXRD scan is unique for individual crystalline material. Therefore, the "fingerprint" of each crystalline material can be obtained, which is useful in identifying unknown materials.

PXRD is a fundamental tool for the investigation of pharmaceutical solid dispersions whereby the physical state of a solid dispersion can be rapidly tested being amorphous or crystalline (65-67). Simply, if no peaks are detected in a PXRD spectrum, the system can be considered as amorphous initially. In addition, PXRD is also useful for the detection of solid transformation (amorphous drugs crystallised into different polymorphs) in solid dispersions (68).

However, as a global characterisation technique, the issue of relatively low sensitivity of detecting crystalline drugs in amorphous solid dispersions have been reported (69). A report by Lin et al (69) concluded that PXRD failed in detecting acetaminophen crystals if the crystalline impurities were below 5% (w/w). Furthermore, in general sample preparation (i.e. prepare original samples into powder form) are required in PXRD, which may result in inconvenience and uncertainty if samples were prepared by hot-melt extrusion, since the state of extrudates may alter by grinding after melt extrusion. This effect has been confirmed in this project and is discussed in Chapter 5. Nevertheless, PXRD still remains a useful tool in evaluating amorphous solid dispersions due to the simplicity and efficiency.

2.3.2.5.2 Experimental parameters

In this study, PXRD tests were performed at room temperature with a Thermol-ARL Xtra diffractormeter (Thermo scientific, UK). Strand form extrudates were milled by mortar and pestle before testing. Samples were placed on a zero background samples holder and incorporated onto a spinner stage. Cu $K\alpha_1$ was used as the X-Ray source (voltage: 45 kV, current: 40 mA). It was mounted with the wavelength of 1.54 Å. The angular range (3-80˚ 2θ) was scanned with a step size of 0.01˚ and 0.5s per step.

2.3.2.6 Scanning electron microscopy (SEM)

2.3.2.6.1 Basic principles

Scanning electron microscope (SEM) is a type of electron microscope that produces images of a sample with higher magnification than normal light microscopes. Basically, by scanning the sample with a high energy electron beam, the interactions between the beam and the atoms in the sample can be detected (26). The scanning electrons in SEM can be produced by a thermal emission source such as the tungsten filament (most commonly used) or a field emission cathode (provide the

brightest beam with highest resolution but expensive). There are many possible interactions generated by the scanning electron beam such as secondary electrons, back-scattered electrons, characteristic X-rays and Auger electron. These generated interactions can be collected by various detectors in the SEM chamber. The signal from each detector is then fed to the monitor which is rastered in synchronisation with the electron beam. In theory, in addition to the observation of the topography of samples, structural information can be achieved if switching between different detection technologies, (27).

SEM is commonly used as an auxiliary tool to study solid dispersions mainly focusing on the morphology of samples (70, 71). It has been reported that heterogeneity on the surface of melt extrudated strand can be a sign of phase separation since the freshly prepared melt extrudates present a smooth surface (41).

2.3.2.6.2 Experimental parameters

In this study, the samples were sputter coated with Au/Pd prior to SEM experaments. The images of the samples were taken using a Phillips XL20 SEM (Phillips Electron Optics, Netherlands).

2.3.2.7 Scanning probe microscopy based compositional analysis methods

2.3.2.7.1 Basic Principles of Atomic Force Microscope (AFM)

Atomic-Force Microscope (AFM) is a tool for visualizing sample surfaces with micron or sub-micro special resolution which belongs to the family of microscopes known as scanning probe microscope (SPM). It was first invented in 1986 by Binning et al as an extension of another technique known as scanning tunnelling microscopy (STM) (42, 72). An AFM consists of a sharp tip at the end of a cantilever (probe) being brought into close proximity with the sample. As the probe scans the surface the deflection of the cantilever is monitored by an optical lever arrangement formed by reflecting a laser beam from the back of the cantilever onto a photodetector. Changes in the deflection of the cantilever provide the height of the sample at each x,y position (73). The schematic diagram of AFM is depicted in Figure 2.12. An AFM experiment can be operated with the tip either touching the sample (contact mode) or off the sample (non-contact).

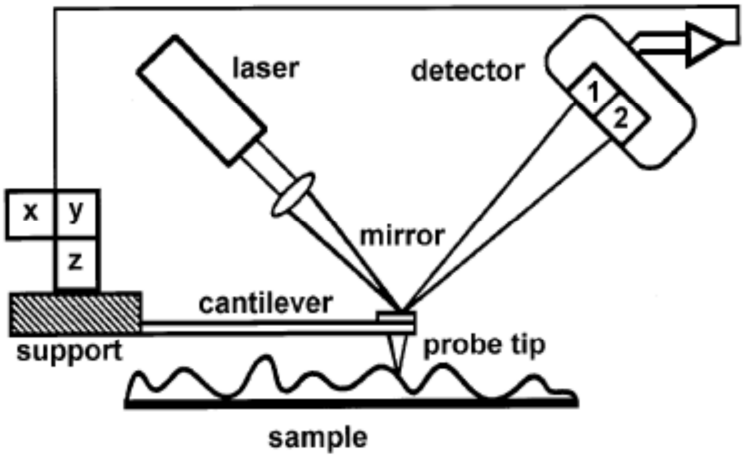

Figure 2.12: Illustration of instrumental design of Atomic-Force Microscope (73).

2.3.2.7.2 AFM contact mode

Contact mode is the simplest way to achieve topographic images of the sample. As the name suggests, the probe is in contact with the sample during scanning. The deflection of the probe (and so the force applied to the sample) is maintained constant (setpoint value) as the probe scanning over the sample surface. As the tip is moved across the sample, the cantilever will be bent or deflected due to the imposed force (setpoint value) in response to the change of height. The signal which is generated by adjusting the position of the probe to the setpoint value is collected and used to create the topographical image. Contact mode is ideal for rigid samples such as solid materials but not for soft samples such as biological samples.

2.3.2.7.3 AFM tapping mode

To avoid physical contact of the tip to the samples in contact mode, AFM can be also operated in tapping mode. In tapping mode, an oscillation is imposed on the probe. The probe to sample distance is set so that the probe tip only lightly contacts (taps) with the sample. During scanning, the interaction (i.e. probe dragged by the sample due to the stickness) between the sample and the probe will cause the change of the imposed oscillation. This change of oscillation amplitude or phase will be monitored and can be used to generate the phase image. In addition to normal topographic image, phase image can be achieved if samples were scanned in tapping mode. Due to the different mechanical properties of different materials within the scanning area (assume the sample is a mixture with different components), the contact time of the probe with different components will be different, which leads to the different phase constant change (74). Therefore, materials with different mechanical properties such as stiffness and viscosity can be distinguished within the sample appearing as different phases in the phase image. This can useful in probing the distribution of materials in a sample (74).

2.3.2.7.4 Basic principles of localised thermal analysis (LTA)

Localised thermal analysis (LTA) is an extension of the conventional AFM by replacing conventional probes with thermal probes. The tips of these probes are composed of material with high resistance to electrical current. When an electrical current is applied, it causes the tip of the probe to heat up (75). The probes have unique advantage that not only can be used as normal probes to generate topographical images but can also be used as a localised heating source. The first LTA probe (named as Wollaston probe) was developed in 1994 and first used in 1996 by Hammiche et al (76). The probe consists of a 75µm diameter silver wire with a 5µm platinum filament core. The wire is manipulated to form a sharp point at which the silver is electrochemically removed to expose the filament (Figure 2.13). This V-shaped wire is then used as the sensor to perform the functions mentioned above. Due to its micron spatial resolution of the technique, it is termed as micro-thermal analysis (µTA). There are several modes in which heated probes can be used but one of the most common is to carry out the thermal analysis on specific locations on a sample surface (77). The probe is placed in contact with the desired point. The system monitors the position of the probe above the surface as the voltage is applied. Once the temperature at the end of the tip is sufficiently high to meet the softening temperature of the tested sample, such as glass transition or melting, penetration of the tip into the sample will occur, which is reflected as a decreased deflection of the probe voltage. Other applications of heated probe have also been reported (74, 75). The LTA probe can be used at a constant temperature as it is scanning across the sample. Differences of thermal properties of materials will cause the changes of heat flow between the probe and the sample. The current needs to be adjusted to maintain the constant temperature. Therefore a map of relative thermal conductivity can be generated by monitoring these changes (74).

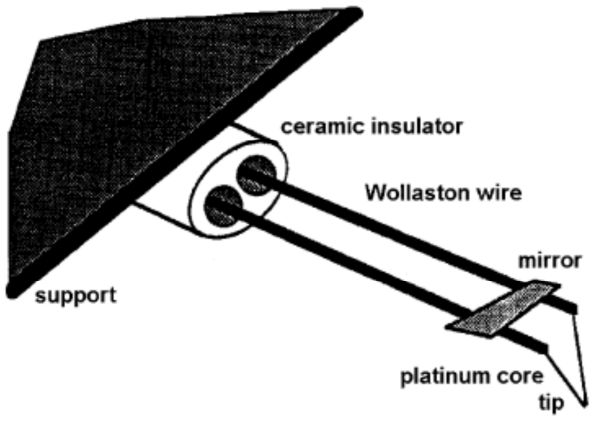

Figure 2.13: Schematic design of Wollaston wire thermal probe (Price et al, 1999).

Recently, thermal probes with the similar dimension to conventional tapping mode probes were invented, which allows the application of LTA studies at a increase spatial resolution (sub-micron)

in comparison to the Wollaston probe (77). The probe has a length of circa 200µm and the height of the tip is below 1 µm (75). This provides the probe with a topographic spatial resolution of 5nm (78). The probe is made of highly doped silica with boron or phosphorus which has a high electrical resistance (75). This allows the tip to be heated when an electrical current is applied. Due to sub-micron resolution, it is named as nano-thermal analysis (nanoTA). A typical nanoTA tip is shown in Figure 2.14.

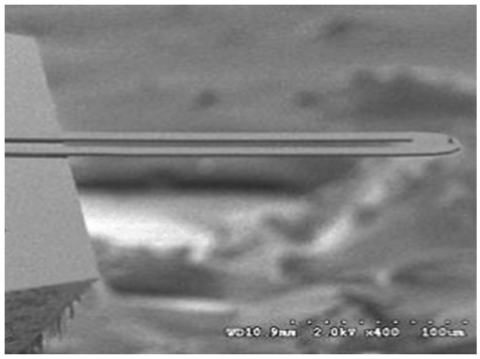

Figure 2.14: SEM images of a nanoTA probe (Image provided by Analysis Instrument).

Localised thermal analysis can be used to identify materials (or same material with different physical state, crystalline and amorphous) with different thermal transition temperature. Especially in the area of solid dispersions, LTA has been used to investigate phase separation at a micron to sub-micrometre level (77). Bulk analysis techniques such as DSC and PXRD may lack the ability to detect localised phase separation or recrystallization in solid dispersions (40, 79). For instance, a DSC or PXRD level amorphous solid solution may contain low quantity of drug crystals which cannot be detected by bulk analysis technology. However, with the high spatial resolution provided by LTA, phase separation and recrystallization can be clearly confirmed (this has been proved in this study and is discussed in Chapter 8). Overall, LTA can be used as a powerful tool combined with conventional characterisation technologies to understand the physical behaviour of solid dispersions with greater depth.

2.3.2.7.5 Basic principles of transition temperature mapping (TTM)

Based on the principles of LTA, a major development has been reported recently, transition temperature mapping (TTM), which is an extension of the localised thermal analysis (53). Instead of manually selecting the tested locations across the sample surface in normal LTA test, a defined region of the sample can be detected in pixels. A pixel is defined as a LTA tested point, and the test at a certain pixel will stop once a thermal transition is detected. Subsequent, the probe will be located to the adjacent pixel to carry on the LTA test until all pixels are completed within the region. The distance between the two consecutive pixels can be as close as 1µm (53). The detected transition temperatures within that area are assigned a colour based on a particular palette and

hence the coloured image is assembled based on different transition temperatures. A typical TTM result is shown in Figure 2.15.

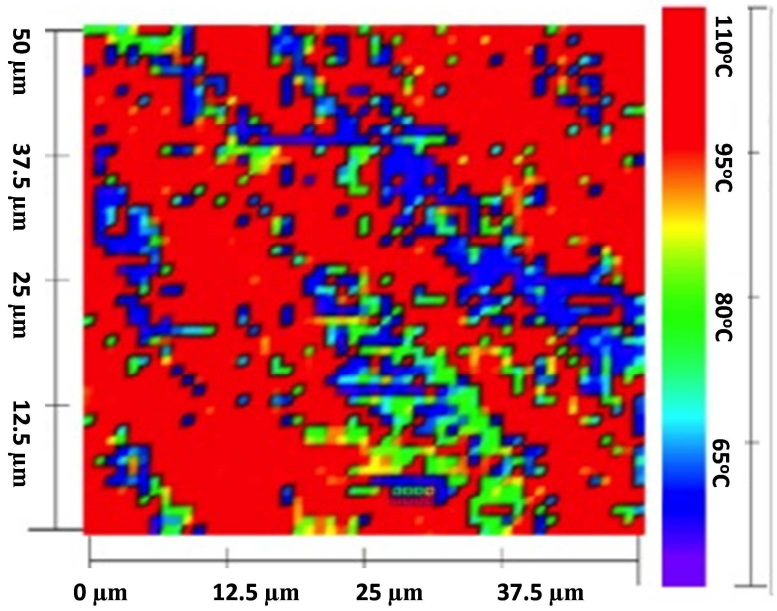

Figure 2.15: TTM result of the surface of hot melt extruded EUDRAGIT® EPO-Kollidon® VA 64 (50:50 w/w).

In comparison to LTA, TTM can not only distinguish different materials or phases in the same sample within a small area (i.e. 50µm×50µm), it can also "draw" the borderline between different phases in the same sample (as shown in Figure 2.14). Therefore, it can be useful to investigate the distribution of different materials within the sample at a sub-micrometre level (7).

2.3.2.7.6 Basic principles of photothermal microspectroscopy (PT-MS)

Another main development of LTA is the photothermal microspectroscopy (PT-MS) in which LTA probe is used as a temperature sensor (80, 81). Small temperature changes will occur if the sample absorbs infrared radiation. In PT-MS these small temperature changes can be detected using the thermal probe (normally the Wollaston probe). PT-MS was first invented in 1999 by Hammiche et al (56). The technique is implemented by interfacing a conventional FTIR spectrometer with an AFM equipped with the thermal probe. The signal detected by the thermal probe can be Fourier transformed to generate a spectrum which is very similar to a conventional IR spectrum of the material. Figure 2.16 shows a PTMS and a conventional IR spectrum of EUDRAGIT® EPO. It can be seen that all peaks present in the absorbance IR spectrum are detected by PTMS, but the relative peak intensities are different. This is because the two techniques are measuring different entities: temperature changes for PT-MS and the amount of light transmitted for FTIR.

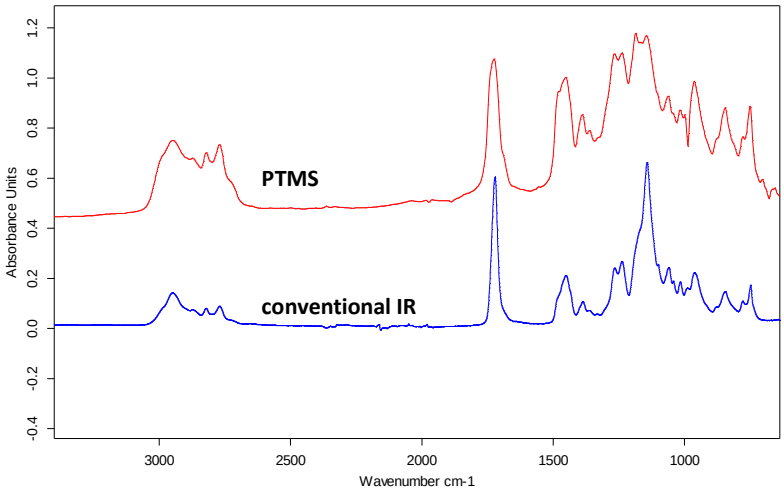

Figure 2.16: PTMS and conventional IR spectrum of EUDRAGIT® EPO.

PTMS can be operated by either placing the probe in contact with the sample surface or the probe is attached with a single particle (80, 82). The benefit of using PTMS in comparison to conventional FTIR is PT-MS is a localised technique which can be used to collect local spectroscopic information of the sample. The conventional IR spectrometer is a tool to investigate the composition of a sample at a global level. PTMS can be used as a localised technique to achieve photothermal spectrum of a sample at micron to sub-micron level. The resolution of PTMS is dependent on two aspects: the size of the applied thermal probe and the thermal diffusion length of the sample (56). Using Wollaston probe as the PTMS detector, a micron level of spatial resolution can be expected. The thermal conductivity can also affect the resolution. Materials with high thermal conductivity can have a long thermal diffusion length. This may result in the detection of average temperature changes of an area (the area surround the contacting point of the probe) rather than the temperature changes at the contacting point (56). Despite the potential resolution issue, PTMS has already shown the capability to be used as a compositional imaging tool. For instance, it has been reported that PT-MS is a powerful tool to evaluate drug distribution in hot melt extruded solid dispersions (12).

2.3.2.7.7 Calibration and experimental parameters of LTA and TTM

In this study, nano-TA and TTM were applied to test samples. Scanning topography images were acquired at room temperature on samples using a Caliber AFM (Veeco Instruments, Santa Barbara, USA) equipped with a nano-thermal probe (EXP-AN2-200, Asylum Research, Santa Barbara, USA). TTM was carried out on a VESTA System (Anasys Instruments, Santa Barbara, USA). In order to detect the transition temperature accurately by LTA, the temperature calibration is necessary. The nano-thermal probe was calibrated for temperatures by supplying a scanning voltage profile whilst in contact with polymeric materials with known melting points (poly(e-caprolactone) with T_m at 60°C, polyethylene with T_m at 130°C and polyethylene terephthalate with

T_m at 238°C). All LTA measurements were carried out at a heating rate of 10°Cs^{-1}. For each tested sample, at least three areas were selected to be measured using LTA.

TTM was operated with the same probe (EXP-AN2-200, Asylum Research, Santa Barbara, USA). The temperature calibration for TTM was the same as LTA by using the three standards. The tested area is mentioned in the section where TTM is applied.

For tapping mode, the phase image was obtained using a Caliber AFM (Veeco Instruments, Santa Barbara, USA) equipped with a silicon cantilever (AC-160TS, Asylum Research, Santa Barbara, USA). The spring constant of the probe was 42 N/m with the oscillation frequency of 300 kHz at an amplitude of 2.5 V.

2.3.2.7.8 Experimental parameters of PTMS

In this study, PT-MS experiments were performed by interfacing (using a dedicated optical interface) a Thermo-microscopes Explorer AFM (Vecco, CA, USA) equipped with a Wollaston wire thermal probe (Vecco, CA, USA) and a FTIR spectrometer (IFS66/S model from Bruker Optics limited, Coventry, UK). A single particle from the milled extrudates powder was immobilised on the tip by placing the tip and particle in contact. For each measurement 200 scans were acquired at a resolution of 8cm-1.

2.3.2.8 Solid state nuclear magnetic resonance (ssNMR)

2.3.2.8.1 Basic rinciples

Nuclear magnetic resonance (NMR) occurs because some nuclei have a property termed as spin. This spin can result in the nuclei having magnetic moments which can re-orient themselves if a large magnetic field is imposed on the sample containing those spinning nuclei (83). Nuclei that can spin are the isotopes which contain an odd number of protons and/or of neutrons. When exposed to a magnetic field, NMR active nuclei can absorb electromagnetic radiation at a characteristic frequency of the isotope. The resonance frequency, energy of the absorption and the intensity of the signal are proportional to the imposed magnetic field. The most commonly studied nuclei are ^{1}H and ^{13}C (84).

Based on the NMR phenomenon, NMR spectroscopy was developed and widely used in physics, chemistry, medicine and pharmacy to investigate chemical structure of a material combined with other spectroscopy techniques such as IR (85). Two main parameters can be achieved from the NMR spectroscopy: chemical shift and relaxation time. Chemical shift is measured based on the interaction between the imposed large magnetic field and the magnetic field generated by the spinning nuclei. It can provide information on the structure of molecules. Relaxation refers to the

process that the nuclei return to the thermal equilibrium state after excited by absorbing energy from imposed magnetic field. This process is also termed as "spin-lattice" (T_1). It is used to describe the mean time of this relaxation process. Excitation can be not only caused by the external magnetic field, but also induced by the adjacent spins, and the process from the excited state induced by adjacent spins to the non-precessing field is termed as transverse relaxation (T_2).

Solid state NMR (ssNMR) is an extensional development of conventional solution NMR for studying solid samples. In solution NMR, the spectra consist of very sharp transitions due to averaging of anisotropic interactions by fast isotropic molecular tumbling, whereas in solid state this motion usually is absent. Consequently, the resonances become very broad as the full effects of anistropic interactions are observed. These anisotropic interactions can significantly lower the resolution. However, with the development of special techniques such as magic-angle spinning, cross polarisation and special pulse sequences, high resolution ssNMR has become possible and widely used in solid state material characterisation (86).

In the field of solid dispersions, ssNMR has been used to investigate the phase behaviour of solid dispersions, the interaction between drugs and polymers and miscibility between drugs and polymers. The hydrogen bonding was confirmed between BMS-488043 and PVP in spray dried solid dispersions by ssNMR. The study concluded that the formed hydrogen bonding showed stabilising effect on the physical stability of the system against high temperature (87). In another study, by measuring the relaxation time of solid dispersions prepared by spray drying, miscibility between nifedipine and hydrophilic polymers was obtained (11). It was suggested in the study that if two components were miscible, the relaxation decay of the mixture should be described by a mono-exponential model, whereas an immiscible mixture should be described by a bi-exponential model. Their results showed good agreement with the DSC results that PVP had better miscibility with nifedipine than PHPA (11). In a study of hot melt extruded felodipine-EUDRAGIT® EPO systems, phase separation was confirmed in aged solid dispersions with high drug loadings (70% w/w) by the detected double relaxations using ssNMR (41). These studies showed that SSNMR can be a useful tool in characterising solid dispersions.

2.3.2.8.2 Experimental parameters

In this study, solid state NMR was applied to investigate phase behaviour of melt extrudates. The high resolution ^{13}C CPMAS (Cross Polarization Magic Angle Spinning) was carried out on a Varian Infinity Plus 300 spectrometer operating at 299.75 and 73.85MHz for ^{1}H and ^{13}C, respectively. Proton relaxation times of melt extrudates were measured on a Bruker Mq-20 spectrometer (19.95 MHz) with a proton 90^{o} pulse-length of 2.85μs.

Reference

1. I. Weuts, D. Kempen, G. Verreck, A. Decorte, K. Heymans, J. Peeters, M. Brewster, and G.V.d. Mooter. Study of the physicochemical properties and stability of solid dispersions of loperamide and PEG6000 prepared by spray drying. European Journal of Pharmaceutics and Biopharmaceutics. 59:119-126 (2005).
2. B. Van Eerdenbrugh, M. Van Speybroeck, R. Mols, K. Houthoofd, J.A. Martens, L. Froyen, J. Van Humbeeck, P. Augustijns, and G. Van den Mooter. Itraconazole/TPGS/Aerosil®200 solid dispersions: Characterization, physical stability and in vivo performance. European Journal of Pharmaceutical Sciences. 38:270-278 (2009).
3. J. Yang, K. Grey, and J. Doney. An improved kinetics approach to describe the physical stability of amorphous solid dispersions. International Journal of Pharmaceutics. 384:24-31 (2010).
4. S. Srčič, J. Kerč, U. Urleb, I. Zupančič, G. Lahajnar, B. Kofler, and J. Šmid-Korbar. Investigation of felodipine polymorphism and its glassy state. International Journal of Pharmaceutics. 87:1-10 (1992).
5. J.A. Baird, B. Van Eerdenbrugh, and L.S. Taylor. A classification system to assess the crystallization tendency of organic molecules from undercooled melts. Journal of Pharmaceutical Sciences. 99:3787-3806 (2010).
6. B. Van Eerdenbrugh, J.A. Baird, and L.S. Taylor. Crystallization tendency of active pharmaceutical ingredients following rapid solvent evaporation—classification and comparison with crystallization tendency from undercooled melts. Journal of Pharmaceutical Sciences. 99:3826-3838 (2010).
7. Y.C. Ng, Z. Yang, W.J. McAuley, and S. Qi. Stabilisation of amorphous drugs under high humidity using pharmaceutical thin films. European Journal of Pharmaceutics and Biopharmaceutics(2013).
8. W.L. Chiou. Pharmaceutical applications of solid dispersion systems: X-ray diffraction and aqueous solubility studies on griseofulvin-polyethylene glycol 6000 systems. Journal of Pharmaceutical Sciences. 66:989-991 (1977).
9. S.L. Law, W.Y. Lo, F.M. Lin, and C.H. Chaing. Dissolution and absorption of nifedipine in polyethylene glycol solid dispersion containing phosphatidylcholine. International Journal of Pharmaceutics. 84:161-166 (1992).
10. C. Dohertyand P. York. Evidence for solid- and liquid-state interactions in a furosemide-polyvinylpyrrolidone solid dispersion. Journal of Pharmaceutical Sciences. 76:731-737 (1987).
11. Y. Aso, S. Yoshioka, T. Miyazaki, T. Kawanishi, K. Tanaka, S. Kitamura, A. Takakura, T. Hayashi, and N. Muranushi. Miscibility of Nifedipine and Hydrophilic Polymers as Measured by ¹H-NMR Spin–Lattice Relaxation. Chemical and Pharmaceutical Bulletin. 55:1227-1231 (2007).
12. S. Qi, P. Belton, K. Nollenberger, A. Gryczke, and D.M. Craig. Compositional Analysis of Low Quantities of Phase Separation in Hot-Melt-Extruded Solid Dispersions: A Combined Atomic Force Microscopy, Photothermal Fourier-Transform Infrared Microspectroscopy, and Localised Thermal Analysis Approach. Pharm Res. 28:2311-2326 (2011).
13. K. Wingstrand, B. Abrahamsson, and B. Edgar. Bioavailability from felodipine extended-release tablets with different dissolution properties. International Journal of Pharmaceutics. 60:151-156 (1990).
14. J. Kerc, S. Srcic, M. Mohar, and J. Smid-Korbar. Some physicochemical properties of glassy felodipine. International Journal of Pharmaceutics. 68:25-33 (1991).
15. S.K. Sathigari, V.K. Radhakrishnan, V.A. Davis, D.L. Parsons, and R.J. Babu. Amorphous-state characterization of efavirenz—polymer hot-melt extrusion systems for dissolution enhancement. Journal of Pharmaceutical Sciences. 101:3456-3464 (2012).
16. J.M. Rollingerand A. Burger. Polymorphism of racemic felodipine and the unusual series of solid solutions in the binary system of its enantiomers. Journal of Pharmaceutical Sciences. 90:949-959 (2001).
17. S. Qi, A. Gryczke, P. Belton, and D.Q.M. Craig. Characterisation of solid dispersions of paracetamol and EUDRAGIT® E prepared by hot-melt extrusion using thermal,

microthermal and spectroscopic analysis. International Journal of Pharmaceutics. 354:158-167 (2008).
18. G.S. Geis. Update on clinical developments with celecoxib, a new specific COX-2 inhibitor: What can we expect? Scandinavian Journal of Rheumatology. 28:31-37 (1999).
19. S.K. Paulson, L. Engel, B. Reitz, S. Bolten, E.G. Burton, T.J. Maziasz, B. Yan, and G.L. Schoenhard. Evidence for Polymorphism in the Canine Metabolism of the Cyclooxygenase 2 Inhibitor, Celecoxib. Drug Metabolism and Disposition. 27:1133-1142 (1999).
20. P.S.M. Leonard J. Ferro. Polymorphic crystalline forms of celecoxib, US Pataent, 2000.
21. L.S. Ranzani, J. Font, F. Galimany, A. Santanach, A.M. Gomez-Gomar, G. Casadevall, and A. Gryczke. Enhanced in vivo absorption of CB-1 antagonist in rats via solid solutions prepared by hot-melt extrusion. Drug Development and Industrial Pharmacy. 37:694-701 (2011).
22. D. Zhou, G.G.Z. Zhang, D. Law, D.J.W. Grant, and E.A. Schmitt. Physical stability of amorphous pharmaceuticals: Importance of configurational thermodynamic quantities and molecular mobility. Journal of Pharmaceutical Sciences. 91:1863-1872 (2002).
23. A. Heinz, K.C. Gordon, C.M. McGoverin, T. Rades, and C.J. Strachan. Understanding the solid-state forms of fenofibrate – A spectroscopic and computational study. European Journal of Pharmaceutics and Biopharmaceutics. 71:100-108 (2009).
24. F. Theeuwes, A. Hussain, and T. Higuchi. Quantitative analytical method for determination of drugs dispersed in polymers using differential scanning calorimetry. Journal of Pharmaceutical Sciences. 63:427-429 (1974).
25. D.J. Burnett, F. Thielmann, and J. Booth. Determining the critical relative humidity for moisture-induced phase transitions. International Journal of Pharmaceutics. 287:123-133 (2004).
26. K.D. Vernon-Parry. Scanning electron microscopy: an introduction. III-Vs Review. 13:40-44 (2000).
27. G.W. Kammlott. Some aspects of scanning electron microscopy. Surface Science. 25:120-146 (1971).
28. L. Mackin, R. Zanon, J.M. Park, K. Foster, H. Opalenik, and M. Demonte. Quantification of low levels (<10%) of amorphous content in micronised active batches using dynamic vapour sorption and isothermal microcalorimetry. International Journal of Pharmaceutics. 231:227-236 (2002).
29. C. Rustichelli, G. Gamberini, V. Ferioli, M.C. Gamberini, R. Ficarra, and S. Tommasini. Solid-state study of polymorphic drugs: carbamazepine. Journal of Pharmaceutical and Biomedical Analysis. 23:41-54 (2000).
30. L.E. McMahon, P. Timmins, A.C. Williams, and P. York. Characterization of dihydrates prepared from carbamazepine polymorphs. Journal of Pharmaceutical Sciences. 85:1064-1069 (1996).
31. N.E. Hunter, C.S. Frampton, D.Q.M. Craig, and P.S. Belton. The use of dynamic vapour sorption methods for the characterisation of water uptake in amorphous trehalose. Carbohydrate Research. 345:1938-1944 (2010).
32. Y. Roosand M. Karel. Plasticizing Effect of Water on Thermal Behavior and Crystallization of Amorphous Food Models. Journal of Food Science. 56:38-43 (1991).
33. S. Brunauer, P.H. Emmett, and E. Teller. Adsorption of Gases in Multimolecular Layers. Journal of the American Chemical Society. 60:309-319 (1938).
34. G.I.W. De Jong, C. Van den Berg, and A.J. Kokelaar. Water vapour sorption behaviour of original and defatted wheat gluten. International Journal of Food Science & Technology. 31:519-526 (1996).
35. E.O. Timmermann, J. Chirife, and H.A. Iglesias. Water sorption isotherms of foods and foodstuffs: BET or GAB parameters? Journal of Food Engineering. 48:19-31 (2001).
36. A.M. Ribeiro, T.P. Sauer, C.A. Grande, R.F.P.M. Moreira, J.M. Loureiro, and A.r.E. Rodrigues. Adsorption Equilibrium and Kinetics of Water Vapor on Different Adsorbents. Industrial & Engineering Chemistry Research. 47:7019-7026 (2008).
37. J. Feng, L.S. Xu, R.C. Gao, Y.F. Luo, and X. Tang. Evaluation of polymer carriers with regard to the bioavailability enhancement of bifendate solid dispersions prepared by hot-melt extrusion. Drug Development and Industrial Pharmacy. 38:735-743 (2012).

38. C.-W. Park, N.-T. Tung, D.-D. Son, J.-Y. Kim, Y.-S. Rhee, S.-Y. Kang, S.-A. Park, K.-M. Hwang, T.-O. Oh, J.-M. Ha, S.-C. Chi, and E.-S. Park. Preparation and in vivo evaluation of immediate-release pellet containing celecoxib solid dispersion. Journal of Pharmaceutical Investigation. 42:121-126 (2012).
39. A. Gryczke, S. Schminke, M. Maniruzzaman, J. Beck, and D. Douroumis. Development and evaluation of orally disintegrating tablets (ODTs) containing Ibuprofen granules prepared by hot melt extrusion. Colloids and Surfaces B: Biointerfaces. 86:275-284 (2011).
40. J. Zhang, M. Bunker, A. Parker, C.E. Madden-Smith, N. Patel, and C.J. Roberts. The stability of solid dispersions of felodipine in polyvinylpyrrolidone characterized by nanothermal analysis. International Journal of Pharmaceutics. 414:210-217 (2011).
41. S. Qi, P. Belton, K. Nollenberger, N. Clayden, M. Reading, and D.M. Craig. Characterisation and Prediction of Phase Separation in Hot-Melt Extruded Solid Dispersions: A Thermal, Microscopic and NMR Relaxometry Study. Pharm Res. 27:1869-1883 (2010).
42. G. Binnig, C.F. Quate, and C. Gerber. Atomic Force Microscope. Physical Review Letters. 56:930-933 (1986).
43. F.Z. Michael M. Crowley, Michael A. Repka,Sridhar Thumma,Sampada B. Upadhye,Sunil Kumar Battu,James W. McGinity,Charles Martin. Pharmaceutical Applications of Hot-Melt Extrusion: Part I. Drug Development and Industrial Pharmacy. 33:909-926 (2007).
44. J.J. Fu, L.S. Xu, X.L. Wang, S. Zhang, X.G. Tao, X.N. Zhao, H.B. He, and X. Tang. Nimodipine (NM) tablets with high dissolution containing NM solid dispersions prepared by hot-melt extrusion. Drug Development and Industrial Pharmacy. 37:934-944 (2011).
45. M. Maniruzzaman, M.M. Rana, J.S. Boateng, J.C. Mitchell, and D. Douroumis. Dissolution enhancement of poorly water-soluble APIs processed by hot-melt extrusion using hydrophilic polymers. Drug Development and Industrial Pharmacy. 39:218-227 (2013).
46. Y. Song, L. Wang, P. Yang, R.M. Wenslow, Jr., B. Tan, H. Zhang, and Z. Deng. Physicochemical characterization of felodipine-kollidon VA64 amorphous solid dispersions prepared by hot-melt extrusion. Journal of pharmaceutical sciences. 102:(2013).
47. J. Feng, L. Xu, R. Gao, Y. Luo, and X. Tang. Evaluation of polymer carriers with regard to the bioavailability enhancement of bifendate solid dispersions prepared by hot-melt extrusion. Drug Development and Industrial Pharmacy. 38:735-743 (2012).
48. P. Marsac, S. Shamblin, and L. Taylor. Theoretical and Practical Approaches for Prediction of Drug–Polymer Miscibility and Solubility. Pharm Res. 23:2417-2426 (2006).
49. I. Weuts, D. Kempen, A. Decorte, G. Verreck, J. Peeters, M. Brewster, and G. Van den Mooter. Phase behaviour analysis of solid dispersions of loperamide and two structurally related compounds with the polymers PVP-K30 and PVP-VA64. European Journal of Pharmaceutical Sciences. 22:375-385 (2004).
50. I. Weuts, D. Kempen, A. Decorte, G. Verreck, J. Peeters, M. Brewster, and G. Van den Mooter. Physical stability of the amorphous state of loperamide and two fragment molecules in solid dispersions with the polymers PVP-K30 and PVP-VA64. European Journal of Pharmaceutical Sciences. 25:313-320 (2005).
51. E. Verdonck, K. Schaap, and L.C. Thomas. A discussion of the principles and applications of Modulated Temperature DSC (MTDSC). International Journal of Pharmaceutics. 192:3-20 (1999).
52. M.R. Duncan Q. M. Craig Thermal Analysis of Pharmaceuticals. Edited by Duncan Q. M. Craig and Mike Reading. ChemMedChem. 3:1139-1140 (2008).
53. M. Reading. personal communication(2007).
54. V.L. Hill, D.Q.M. Craig, and L.C. Feely. The effects of experimental parameters and calibration on MTDSC data. International Journal of Pharmaceutics. 192:21-32 (1999).
55. T. Instruments. DSC 2920 Differential Scanning Calorimeter Operator's Manual. (1993).
56. A.P. Hammiche, H.M.; Reading, M.; Claybourn, M.; Turner, P.H.; Jewkes, K. Photothermal FT-IR Spectroscopy: A Step Towards FT-IR Microscopy at a Resolution Better Than the Diffraction Limit. Applied Spectroscopy 53:(1999).

57. G. Pyramides, J.W. Robinson, and S. William Zito. The combined use of DSC and TGA for the thermal analysis of atenolol tablets. Journal of Pharmaceutical and Biomedical Analysis. 13:103-110 (1995).
58. H.M.L. Thijs, C.R. Becer, C. Guerrero-Sanchez, D. Fournier, R. Hoogenboom, and U.S. Schubert. Water uptake of hydrophilic polymers determined by a thermal gravimetric analyzer with a controlled humidity chamber. Journal of Materials Chemistry. 17:4864-4871 (2007).
59. J.D. Schuttlefieldand V.H. Grassian. ATR–FTIR Spectroscopy in the Undergraduate Chemistry Laboratory. Part I: Fundamentals and Examples. Journal of Chemical Education. 85:279 (2008).
60. H.E. Johnsonand S. Granick. Exchange kinetics between the adsorbed state and free solution: poly(methyl methacrylate) in carbon tetrachloride. Macromolecules. 23:3367-3374 (1990).
61. L. Taylorand G. Zografi. Spectroscopic Characterization of Interactions Between PVP and Indomethacin in Amorphous Molecular Dispersions. Pharm Res. 14:1691-1698 (1997).
62. H. Takeuchi, S. Nagira, H. Yamamoto, and Y. Kawashima. Solid dispersion particles of amorphous indomethacin with fine porous silica particles by using spray-drying method. International Journal of Pharmaceutics. 293:155-164 (2005).
63. A.T.M. Serajuddin. Solid dispersion of poorly water-soluble drugs: Early promises, subsequent problems, and recent breakthroughs. Journal of Pharmaceutical Sciences. 88:1058-1066 (1999).
64. T. Vasconcelos, B. Sarmento, and P. Costa. Solid dispersions as strategy to improve oral bioavailability of poor water soluble drugs. Drug Discovery Today. 12:1068-1075 (2007).
65. M.V. Margarit, I.C. Rodríguez, and A. Cerezo. Physical characteristics and dissolution kinetics of solid dispersions of ketoprofen and polyethylene glycol 6000. International Journal of Pharmaceutics. 108:101-107 (1994).
66. M.M. de Villiers, D.E. Wurster, J.G. Van der Watt, and A. Ketkar. X-Ray powder diffraction determination of the relative amount of crystalline acetaminophen in solid dispersions with polyvinylpyrrolidone. International Journal of Pharmaceutics. 163:219-224 (1998).
67. J.J. García-Rodriguez, P.M. de la Torre-Iglesias, M.C. Vegas-Sánchez, S. Torrado-Durán, F. Bolás-Fernández, and S. Torrado-Santiago. Changed crystallinity of mebendazole solid dispersion: Improved anthelmintic activity. International Journal of Pharmaceutics. 403:23-28 (2011).
68. C.R.-E. M. C. Martínez-Ohárriz, C. Martín,M. M. Goñi,M. C. Tros-Ilarduya,M. Sánchez. Solid Dispersions of Diflunisal–PVP: Polymorphic and Amorphous States of the Drug. Drug Development and Industrial Pharmacy. 28:717-725 (2002).
69. M.-C. Linand W.C. Duncan-Hewitt. Deformation kinetics of acetaminophen crystals. International Journal of Pharmaceutics. 106:187-200 (1994).
70. E. Karavas, M. Georgarakis, A. Docoslis, and D. Bikiaris. Combining SEM, TEM, and micro-Raman techniques to differentiate between the amorphous molecular level dispersions and nanodispersions of a poorly water-soluble drug within a polymer matrix. International Journal of Pharmaceutics. 340:76-83 (2007).
71. C. Duret, N. Wauthoz, T. Sebti, F. Vanderbist, and K. Amighi. Solid dispersions of itraconazole for inhalation with enhanced dissolution, solubility and dispersion properties. International Journal of Pharmaceutics. 428:103-113 (2012).
72. G. Binnig, H. Rohrer, C. Gerber, and E. Weibel. Surface Studies by Scanning Tunneling Microscopy. Physical Review Letters. 49:57-61 (1982).
73. D.M. Price, M. Reading, A. Hammiche, and H.M. Pollock. Micro-thermal analysis: scanning thermal microscopy and localised thermal analysis. International Journal of Pharmaceutics. 192:85-96 (1999).
74. Y.T.A. Turner, C.J. Roberts, and M.C. Davies. Scanning probe microscopy in the field of drug delivery. Advanced Drug Delivery Reviews. 59:1453-1473 (2007).
75. L. Harding, W. King, X. Dai, D.M. Craig, and M. Reading. Nanoscale Characterisation and Imaging of Partially Amorphous Materials using Local Thermomechanical Analysis and Heated Tip AFM. Pharm Res. 24:2048-2054 (2007).

76. M.R. A. Hammiche, H. M. Pollock, M. Song, and D. J. Hourston. Localized thermal analysis using a miniaturized resistive probe. Rev Sci Instrum. 67:(1996).
77. M. Reading, D.M. Price, D.B. Grandy, R.M. Smith, L. Bozec, M. Conroy, A. Hammiche, and H.M. Pollock. Micro-thermal analysis of polymers: current capabilities and future prospects. Macromolecular Symposia. 167:45-62 (2001).
78. V.L. Sedman, S. Allen, X. Chen, C.J. Roberts, and S.J.B. Tendler. Thermomechanical Manipulation of Aromatic Peptide Nanotubes. Langmuir. 25:7256-7259 (2009).
79. S. Qi, J.G. Moffat, and Z. Yang. Early Stage Phase Separation in Pharmaceutical Solid Dispersion Thin Films under High Humidity: Improved Spatial Understanding Using Probe-Based Thermal and Spectroscopic Nanocharacterization Methods. Molecular Pharmaceutics. 10:918-930 (2013).
80. X. Dai, J.G. Moffat, A.G. Mayes, M. Reading, D.Q.M. Craig, P.S. Belton, and D.B. Grandy. Thermal Probe Based Analytical Microscopy: Thermal Analysis and Photothermal Fourier-Transform Infrared Microspectroscopy Together with Thermally Assisted Nanosampling Coupled with Capillary Electrophoresis. Analytical Chemistry. 81:6612-6619 (2009).
81. J.G. Moffat, A.G. Mayes, P.S. Belton, D.Q.M. Craig, and M. Reading. Compositional Analysis of Metal Chelating Materials Using Near-Field Photothermal Fourier Transform Infrared Microspectroscopy. Analytical Chemistry. 82:91-97 (2009).
82. X. Dai, P. Belton, D. de Cogan, J.G. Moffat, and M. Reading. Thermally induced movement of micro particles observed on a rough surface: A novel observation and its implications for high throughput analysis and synthesis. Thermochimica Acta. 517:121-125 (2011).
83. I.I. Rabi, J.R. Zacharias, S. Millman, and P. Kusch. A New Method of Measuring Nuclear Magnetic Moment. Physical Review. 53:318-318 (1938).
84. L.M.K. Vandersypen, M. Steffen, G. Breyta, C.S. Yannoni, M.H. Sherwood, and I.L. Chuang. Experimental realization of Shor's quantum factoring algorithm using nuclear magnetic resonance. Nature. 414:883-887 (2001).
85. J.M. Tyszka, S.E. Fraser, and R.E. Jacobs. Magnetic resonance microscopy: recent advances and applications. Current Opinion in Biotechnology. 16:93-99 (2005).
86. D.D. Laws, H.-M.L. Bitter, and A. Jerschow. Solid-State NMR Spectroscopic Methods in Chemistry. Angewandte Chemie International Edition. 41:3096-3129 (2002).
87. M. Tobyn, J. Brown, A.B. Dennis, M. Fakes, Q. Gao, J. Gamble, Y.Z. Khimyak, G. McGeorge, C. Patel, W. Sinclair, P. Timmins, and S. Yin. Amorphous drug–PVP dispersions: Application of theoretical, thermal and spectroscopic analytical techniques to the study of a molecule with intermolecular bonds in both the crystalline and pure amorphous state. Journal of Pharmaceutical Sciences. 98:3456-3468 (2009).

Chapter 3: Physicochemical characterisation of model drugs and polymers

3.1 Introduction

Amorphous solid dispersions have been widely used in the pharmaceutical industry to improve dissolution rate of poorly water-soluble drugs. As discussed in Chapter 1, the main issue in this research domain still lies in the physical stability since the phase separation and recrystallization of amorphous solid dispersions can eventually affect the dissolution performance (1). Factors which can potentially affect the physical stability of solid dispersions have been listed in Chapter 1: the physicochemical properties of drugs and polymers such as glass transition temperature, miscibility between drugs and polymers and solid solubility of drugs in polymers (2-4). The aim of this chapter is focusing on the characterisation of physicochemical properties of model drugs as this is pre-requisite for a comprehensive understanding of the factors which can affect the physical stability of amorphous solid dispersions.

Four model drugs including felodipine, celecoxib, fenofibrate and carbamazepine and two model polymers including EUDRAGIT® EPO and Kollidon® VA 64 were used in this study. The model drugs have very different thermal properties. For instance, the glass transition temperature of amorphous felodipine was reported as circa 45^{o}C whereas the T_g of amorphous fenofibrate was -19^{o}C (5). Additionally, the four model drugs have been reported to have significantly different recrystallization tendency, which may indicate the different molecular mobility between the four model drugs and different physical stability of amorphous drugs alone (5, 6). These diverse physicochemical properties of the four model drugs can assist understanding of the contribution of amorphous drug intrinsic physical stability to the overall physical stability of amorphous solid dispersions.

The two polymers also have different thermal properties: the T_g of EUDRAGIT® EPO was reported as 50^{o}C whereas the T_g of Kollidon® VA 64 was reported as 106^{o}C (7, 8). EUDRAGIT® EPO has been reported to have the ability to protect amorphous solid dispersions from moisture sorption whereas Kollidon® VA 64 was reported to be hydrophilic (9, 10). Therefore amorphous solid dispersions prepared with the two polymers respectively may show significantly different physical stability behaviour if aged under stressed humidity. Structurally, EUDRAGIT® EPO and Kollidon® VA 64 both have carbonyl groups as shown in Figure 2.5 and 2.6 which indicates that they can potentially form hydrogen bonding with drugs containing donor groups. It also can be noted that the carbonyl group in Kollidon® VA 64 is more exposed than that in EUDRAGIT® EPO, which can possibly result in a stronger potential to form hydrogen bonding with drugs than

EUDRAGIT® EPO. This may lead to the difference of drug-polymer miscibility and the solid solubility of the model drugs in polymers, which may further cause difference in the physical stability of solid dispersions prepared by the two polymers. In summary, the characterisation of the physicochemical properties of the model drugs and polymers are essential for the understanding of physical stability behaviour of solid dispersions.

Research objectives

1. To characterise the physicochemical properties of model drugs and polymers.

2. To assess the physical stability of amorphous drugs alone prepared by melt-cool and spin coating under 0%RH and 75%RH at room temperature.

3. To compare the thermodynamic behaviours of the model drugs.

3.2 Experimental methods

3.2.1 Modulated temperature differential scanning calorimetry (MTDSC)

Instrumental information and the parameters used in MTDSC refer to Chapter 2 (section 2.2.2.1.3).Melting points of crystalline model drugs were determined by DSC in standard mode at a heating ramp of 10^{o}C/min.

3.2.2 Determination of glass transition temperatures of model drugs

In order to determine glass transition temperatures (T_g) of model drugs, a heat-cool-reheat process in MTDSC mode was applied to transform drugs from crystalline form to amorphous form and then further tested T_g values. Crystalline drugs were accurately weighed into TA standard pans, and then the sample pan was crimped and tested in MTDSC mode at the underlying heating ramp of 2˚C/min until 5 degree higher than the melting point of the crystalline drug. The above melting point temperature was maintained for 3min, and then the sample was cooled down at the same heating ramp to -10˚C. For fenofibrate, it was cooled down to -40˚C since it has been reported amorphous fenofibrate has a glass transition temperature below -20^{o}C (11). After isothermal for 3min, the sample was reheated to melting point at the same ramp. The glass transition temperature was determined in the reheating process to remove the potential factors, such as the amount of trapped moisture, preparation methods and thermal history, which could affect glass transition of materials (12). EUDRAGIT® EPO was tested by the same method.

3.2.3 Determination of fragility of model drugs

Different heating ramps of 1, 2, 5, 10 and 20˚C/min were applied to scan the sample to calculate fragility. To summarise, crystalline drugs were heated and cooled at the same scanning rate, and

the T_g value from cooling was used to calculate the fragility parameter (13). For each heating rate, triplicated samples were tested. For carbamazepine, amorphous drugs were prepared using melt-cool method whereby crystalline carbamazepine was melted inside a DSC pan by hot plate at the temperature 5 degrees higher than the melting point (191^{o}C) for 10 seconds, and then samples were removed from the hot plate to be cooled down under ambient condition. The melt cooled carbamazepine was heated to 70^{o}C in DSC and then cooled down to -10^{o}C at different rates including.

3.2.4 Preparation of melt-cool amorphous drugs for physical stability test

Amorphous model drugs were prepared to test their physical stability under dry and high humidity conditions at room temperature. Crystalline model drugs were weighed into DSC standard pans and were melted on a hotplate (IKA LABORATECHNIK Basic RCT stirrer hotplate, Germany) at the temperatures 5 degree above their melting points for 10sec, and then samples were removed from the hotplate and cooled down under ambient conditions. Melt-cool amorphous drugs were then stored under 0%RH (provided by P_2O_5) and 75%RH (provided by over-saturated sodium chloride water solution), respectively, at room temperature, and were tested by MTDSC in 1, 3, 7 and 14 days.

3.2.5 Preparation of spin coated amorphous drugs for the physical stability test

The spin coated amorphous drugs were prepared on the SCS G3P-8 spin-coater (Specialty Coating Systems, Surry, USA). The solvent for the spin coated solution consisted of a mixture of ethanol and dichloramethane with the ratio of 50:50. Crystalline drugs were dissolved in the solvent to prepare drug solutions with solid concentrations of 15% (w/v) for all samples. The spinning speed was set at 2000 r/min. The acceleration was 5 second and the duration time of spinning was 2min. The drops of the solution were deposited by a glass pipette manually on a cut microscope glass slide with size of 25mm×25mm. Spin coated samples were stored under 0% and 75%RH, respectively, at room temperature and were tested by polarised microscopy and ATR-FTIR spectroscopy.

3.2.6 Observation of model drug crystals on spin coated amorphous drugs using polarised light microscopy

Polarised light microscopy studies were conducted using a Leica DM LS2 polarised light microscope (Wetzlar GmbH, Germany) connected to a video capture system. Fresh and aged spin coated amorphous drugs were tested under the polarised microscopy for the observation of recrystallised drugs.

3.2.7 Attenuated Total Reflection – Fourier Transform Infrared Spectrometer (ATR-FTIR)

ATR-FTIR spectroscopy was used to investigate the physical state of the spin coated amorphous drugs. Spectra were collected in absorbance mode using spectrometer IFS/66S from Bruker Instruments (Coventry, UK) equipped with a Golden Gate® ATR accessory (Specac Ltd, Coventry, UK). 64 scans were collected at a resolution of 2 cm^{-1} for each sample over the wavelength region from 550 to 4000 cm^{-1}.

3.3 Results and discussion

3.3.1 Thermodynamic properties of model drugs

Preparation of amorphous model drugs including felodipine, celecoxib and fenofibrate has been discussed in section 3.2.2.2. Evident glass transitions can be observed in MTDSC results for felodipine, celecoxib and fenofibrate as shown in Figure 3.1. However, for carbamazepine, recrystallization occurred in cooling, which results in the failure of detecting glass transition temperature in reheating. This may be due to the poor glass forming property of carbamazepine which makes it difficult to be transformed to amorphous form (5).

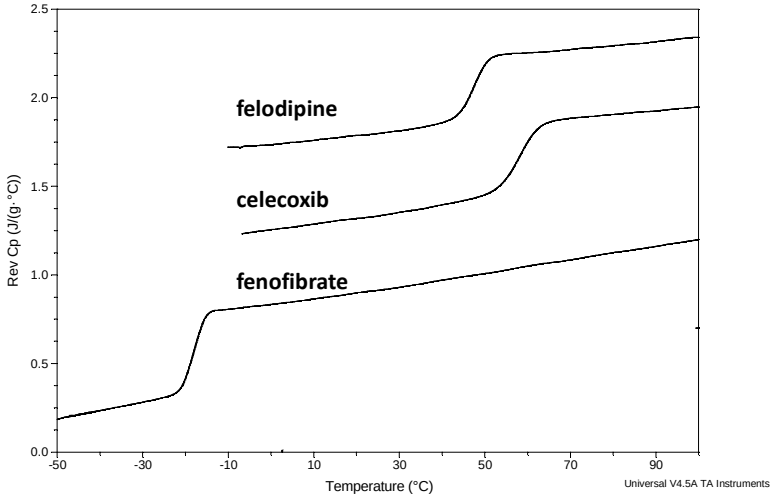

Figure 3.1: Glass transition of amorphous felodipine, celecoxib and fenofibrate detected by MTDSC.

The failure of preparing amorphous carbamazepine by DSC can be attributed to the applied slow cooling rate. Cooling from melts is one the most commonly used method to transform materials from crystalline to amorphous state (14). Upon cooling a melt, the material can behave in two ways (15). At a slow cooling rate, the melted liquid can transform back to the crystalline structure. However, at a fast cooling rate, molecules do not have sufficient time to re-establish the crystalline structure, leading to the formation of the amorphous material. Thus the cooling rate is essential for the preparation of amorphous materials. Crystalline carbamazepine was weighed into standard DSC pan, instead of melting and cooling in MTDSC, the sample was heated to melt on top of a hot plate

at the temperature 5 degree above the melting point for 10s, and then it was cooled down under ambient conditions. The pan was then immediately crimped and tested in MTDSC mode at the underlying heating rate of 2˚C/min. With this method, glass transition of amorphous carbamazepine was clearly detected (Figure 3.2), and the glass transition temperature was determined as 50.02^{o}C.

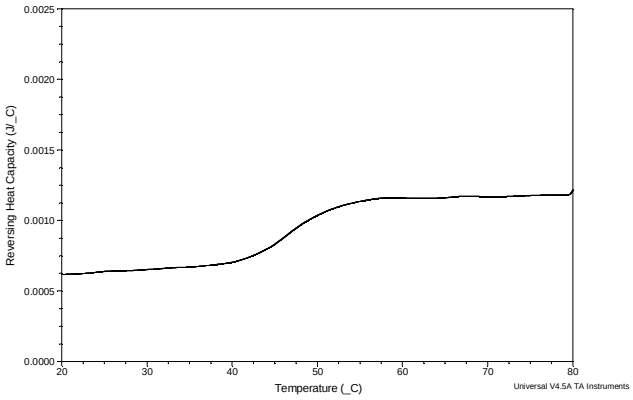

Figure 3.2: Glass transition of amorphous carbamazepine detected by MTDSC.

Glass transition temperatures (midpoints of glass transition area in MTDSC results) of amorphous model drugs and melting points of crystalline model drugs are summarised in Table 3.1. As can be seen from the table that T_g values of selected model drugs vary in a relatively large range from -19.7 to 58.2˚C, which will possibly enable the understanding of the effect of T_g values of amorphous drugs on the physical stability of solid dispersions prepared by hot melt extrusion with them. This will be discussed in Chapter 6.

Table 3.1: Thermodynamic properties of model drugs (n=3).

Materials	felodipine	celecoxib	fenofibrate	carbamazepine
Mid point of T_g (^{o}C)	46.5±0.2	58.2±0.2	-19.7±0.4	50.1±0.3
Onset of T_m (^{o}C)	143.1±0.1	160.8±0.3	80.4±0.1	189.5±0.2
Peak of T_m (^{o}C)	146.6±0.1	163.1±0.3	81.6±0.1	190.5±0.2

3.3.2 Thermodynamic properties of model polymers

Glass transition temperatures of the two model polymers were studied using heat-cool-reheat method at a scanning rate of 2^{o}C. Clear glass transitions were detected for both polymers as shown in Figure 3.3. The T_g value of EUDRAGIT® EPO was determined as 51.1^{o}C and the T_g value of Kollidon® VA64 was determined as 106.8^{o}C. In comparison to EUDRAGIT® EPO, Kollidon®

VA64 has a significantly higher glass transition temperature, which may possibly improve the physical stability of solid dispersions (16). This is attributed to the reason that polymers with high T_g can increase the T_g of the amorphous drug-polymer solid dispersion in comparison to polymers to the T_g of the drug, and thus the molecular mobility in solid dispersions can be reduced, leading to enhanced physical stability (17). The comparison of the physical stability of solid dispersions prepared by different polymers is discussed in Chapter 7.

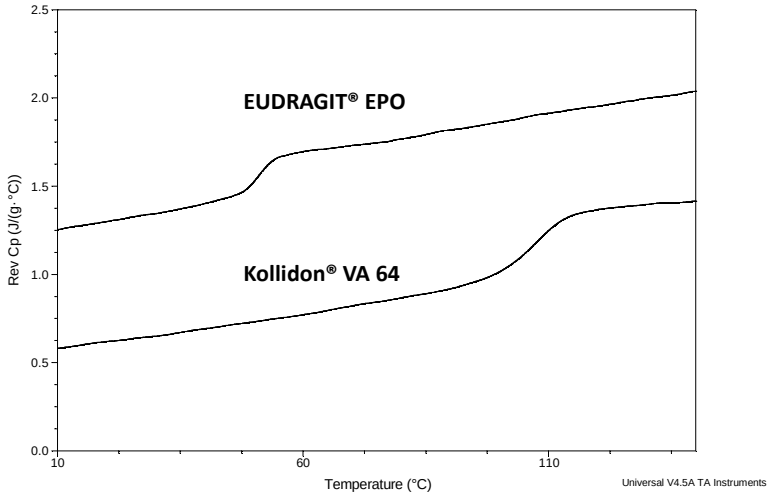

Figure 3.3: glass transition of EUDRAGIT® EPO and Kollidon® VA64 detected by MTDSC.

3.3.3 Fragility of amorphous model drugs

The concept of fragility is of interest in research field of formation of amorphous drugs since it is considered as one of the key factors that correlate with glass forming ability and physical stability of amorphous systems (18, 19). The fragility parameter *m* is related to an average degree of molecular mobility reflected in the structural relaxation near glass transition. If the fragility parameter *m*, also called steepness index, is smaller than 100 the glass is defined as a strong glass or a strong glass former. If the value of *m* is in between 100 and 200, the glass is defined as a weak glass or a weak glass former(20). Fragile glass formers have a molecular mobility that increases drastically at temperatures across T_g in comparison to that occurring in strong glass formers. It has been suggested that strong glass is more physically stable than a fragile glass (21).

Fragilities of amorphous model drugs in this study were calculated by using the theory of extrapolating configurational entropy to zero (20). As discussed in Chapter 1, T_g is a kinetic parameter of amorphous material whereby using different cooling rate form the melts, different T_g values can be obtained. The activation energy of the structural relaxation at the glass transition was estimated by using different scanning rates to achieve different T_g values as expressed in the following equation:

$$m = E_a^* / (2.303RT_g) \qquad Eq.\ 3.1$$

where m is the fragility parameter of the material, E_a^* is the activation energy and R is gas constant(13). E_a^*/R is the slope of plotting $1/T_f$ against $ln(q)$ (q is heating or cooling rate) as shown in Eq.3.2:

$$dln(q) / d(1/T_f) = -E_a^*/R \qquad Eq.\ 3.2$$

where q is heating rate, and T_f is the fictive temperature defined as the temperature of intersection between the equilibrium volume or entropy/temperature liquid curve and the linear extrapolation of glassy curve. However, as discussed in Chapter 1, it has been proved that T_f has a very similar value to T_g, therefore T_f was replaced by T_g in this study (20).

The plots of heating rates against detected T_g (1000/ T_g) of individual amorphous model drug is shown in Figure 3.4 (regression plot using *Eq. 3.2*). By using activation energy values calculated using *Eq. 3.2*, fragility parameters of felodipine, celecoxib, fenofibrate and carbamazepine were calculated as 52.6, 106.7, 56.8 and 116.7. This indicates that felodipine and fenofibrate are more capable of forming a glass than celecoxib and carbamazepine.

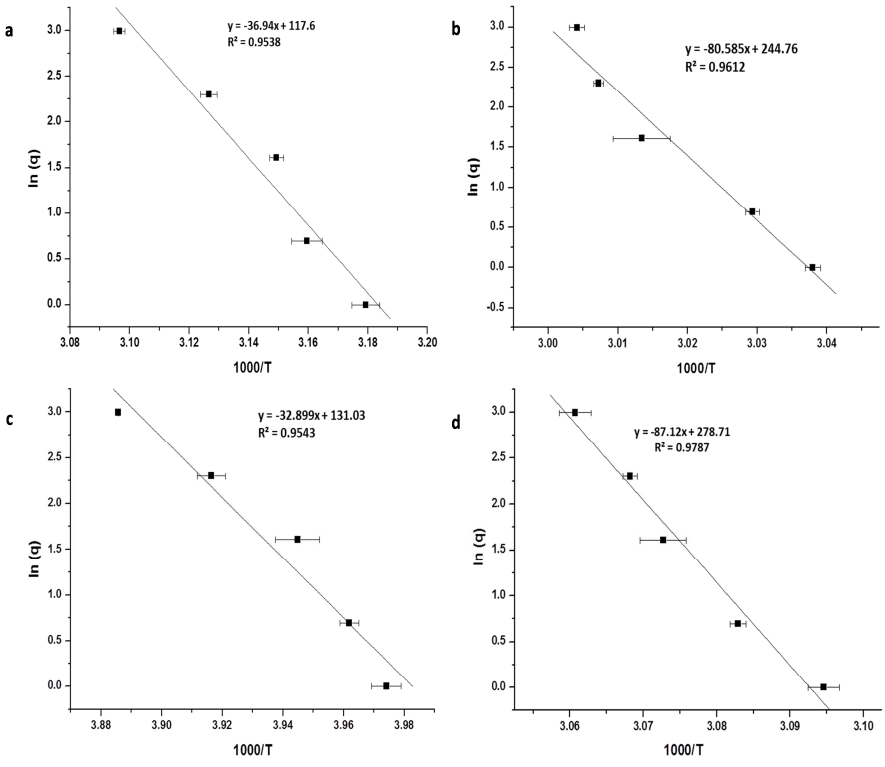

Figure 3.4: Plots of ln (q) against inverse glass transition temperature (K) of amorphous felodipine (a), celecoxib (b), fenofibrate (c) and carbamazepine (d).

The different glass forming ability between the four model drugs were also evident in the heat-cool-reheat test using DSC. After being melted in first heating, no melting can be detected in cooling and reheating for felodipine and fenofibrate, whereas recrystallization followed by melting was observed for celecoxib (recrystallization in reheating) and carbamazepine (recrystallization in cooling) (Figure 3.5 a and b).

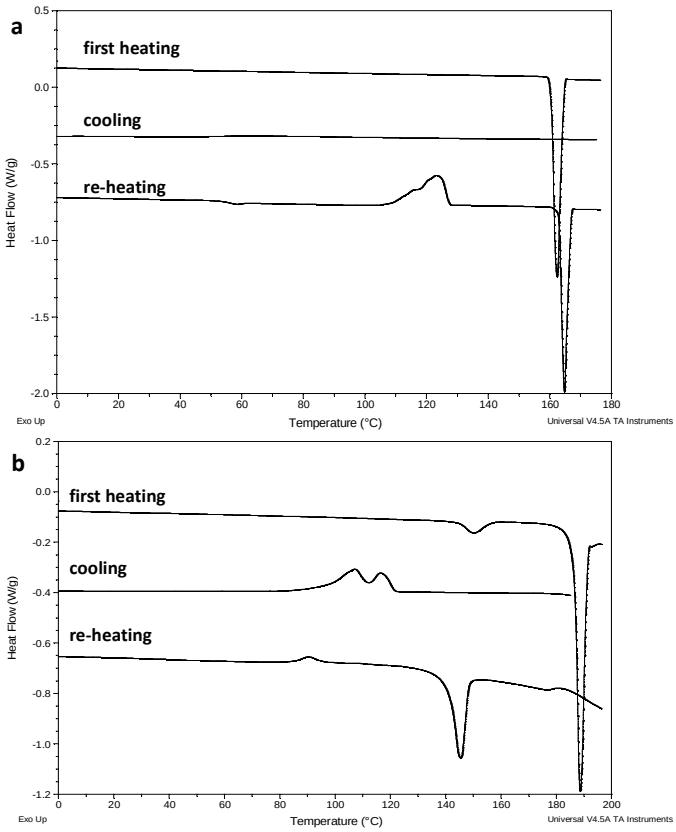

Figure 3.5: MTDSC thermograph of celecoxib (a) and carbamazepine (b) tested by heating-cooling-reheating.

In summary, by evaluating the fragility of amorphous model drugs, the order of the glass forming ability of model drugs used in this study is felodipine ≈ fenofibrate > celecoxib ≥ carbamazepine. The fragility (glass forming ability) may have no direct relationship with the physical stability of amorphous drugs alone or the physical stability of amorphous solid dispersions, but it is a useful parameter for the calculation of molecular mobility of amorphous material. This is discussed in the following section.

3.3.4 Calculation of relaxation time of amorphous model drugs

Many crystalline drugs are poorly water soluble resulting in low bioavailability (22). Transformation of crystalline drugs into their amorphous form can improve the apparent aqueous solubility up to hundreds of folds for certain drugs (23). As mentioned in Chapter 1, amorphous drugs remained at non-equilibrium state and tended to convert back to more stable crystalline form. This procedure of approaching the equilibrium is termed as structural relaxation, and relaxation

time is the time length where relaxation occurs (21, 24, 25). Relaxation is caused by molecular mobility of amorphous drugs which is reciprocal to relaxation time. It has been suggested that molecular mobility was associated with the physical stability of pure amorphous materials whereby high molecular mobility could lead to poor physical stability of amorphous materials, and this has been discussed in Chapter 1 (17). The calculation of relaxation time has been well described in articles such as using empirical Kohlrausch-Williams-Watts (KWW) equation with endothermic enthalpy measured at relaxation by DSC or the Adam-Gibbs-Vogel (AGV) equation (26-30). In this study, in order to compare physical stability of pure amorphous model drugs, the relaxation times of model drugs were calculated using the Adam-Gibbs-Vogel (AGV) equation. The model has been briefly introduced in Chapter 1, and is described more in more detail here as shown below:

$$\tau = \tau_0 exp\ (DT_0/(T(1-T_0/T_f))) \qquad Eq.3.3$$

where τ is the relaxation time at temperature T, τ_0 is a constant (about 10^{-14}second) (31), D and T_0 are the Vogel-Tammann-Fulcher (VTF) equation parameters which can be calculated as follows(24, 32, 33):

$$D=2.303(m_{min}^2)/(m-m_{min}) \qquad Eq.3.4$$

$$m_{min}=log(\tau_{Tg}/\tau_0)= log(100/10^{-14})=16 \qquad Eq.3.5$$

$$T_0=T_g(1- m_{min}/m) \qquad Eq.3.6$$

where τ_{Tg} represent the relaxation time at T_g and were assumed to be 100s as suggested in articles(for most super-cooled liquids, m_{min} takes values between 16 and 17), and m is the fragility index (31). As mentioned above, fictive temperature T_f has a very similar value to T_g, therefore T_g is used in relaxation calculation instead of T_f.

Results of calculated relaxation time values at different temperatures (25^{o}C is considered as normal room temperature and 40^{o}C is the temperature generally used for accelerate storage test) of the amorphous model drugs are summarised in Table 3.2. It can be seen that felodipine, celecoxib and carbamazepine have similar relaxation times, whereas fenofibrate showed a relatively fast relaxation time, indicating amorphous felodipine, celecoxiband carbamzepine may have lower molecular mobilities than fenofibrate and hence may be more physically stable. The order of the level of molecular mobility of amorphous model drugs is celecoxib ≤ carbamazepine ≈ felodipine < fenofibrate .

Table 3.2: Calculated relaxation times of amorphous model drugs

Drugs	felodipine	celecoxib	fenofibrate	carbamazepine
τ at 25°C (s)	2.47×10^{3}	1.31×10^{4}	3.51×10^{-1}	1.78×10^{3}
τ at 40°C (s)	1.91×10^{2}	9.11×10^{2}	7.92×10^{-2}	2.63×10^{2}

3.3.5 Physical stability of amorphous model drugs on aging

Little research has been carried out to investigate the relationship between physical stability of solid dispersions and physical stability of amorphous drugs alone. It was reported in a study that physical stability of amorphous solid dispersions prepared by spin coating (aged under high humidity) showed the same order as the physical stability of amorphous drugs (9). It may indicate that physical stability of amorphous drugs alone may be a key factor influencing the physical stability of amorphous solid dispersions. Therefore, in order to gain a comprehensive understanding of the factors which control the physical stability of amorphous solid dispersions, the physical stability study of pure amorphous drugs were carried out in this project. It has been reported that, physical stability of pure amorphous drugs varied depending on the processing methods (melt-cool and spin coating) (5, 6). Therefore, in this study in order to avoid the influence of the processing methods and to understand the physical stability behaviour of amorphous drugs more completely, amorphous model drugs were prepared by melt-cool (a melting based method) and spin coating (a solvent evaporation based method), respectively. Melt-cooled and spin coated amorphous drugs were stored under dry (0%RH) and high humidity conditions (75%RH) at room temperature, respectively, to evaluate and compare their physical stabilities. In addition, the calculation of relaxation time showed that amorphous felodipine, celecoxib and carbamazepine should have similar physical stability and they should be more stable than amorphous fenofibrate. By investigating the real-time physical stability of amorphous drugs alone, the accuracy of the relaxation calculation can be tested.

3.3.5.1 Physical stability of melt-cooled amorphous model drugs

3.3.5.1.1 Physical stability of melt-cooled model drugs aged under 0%RH/room temperature

3.3.5.1.1.1 Felodipine

MTDSC results of melt-cooled amorphous felodipine on aging under 0%RH/room temperature is shown in Figure 3.6. It can be seen that after two weeks aging under 0%RH at room temperature, no recrystallization or melting can be detected for amorphous felodipine, indicating amorphous felodipine can be stable for at least two weeks under dry condition at room temperature. Relaxation enthalpy of amorphous felodipine increased with increasing aging time. Amorphous materials often

experience a gradual loss in energy in terms of enthalpy due to the effect of molecular motions occurring on aging (34). The amount of lost energy in amorphous materials on aging can be compensated on heating in DSC across T_g due to the requirement of re-establishing the liquid state above T_g (35). The detected relaxation was the contribution from molecular mobility of amorphous felodipine on aging. Therefore, the increased relaxation enthalpy of amorphous felodipine on aging reflects an increased molecular mobility.

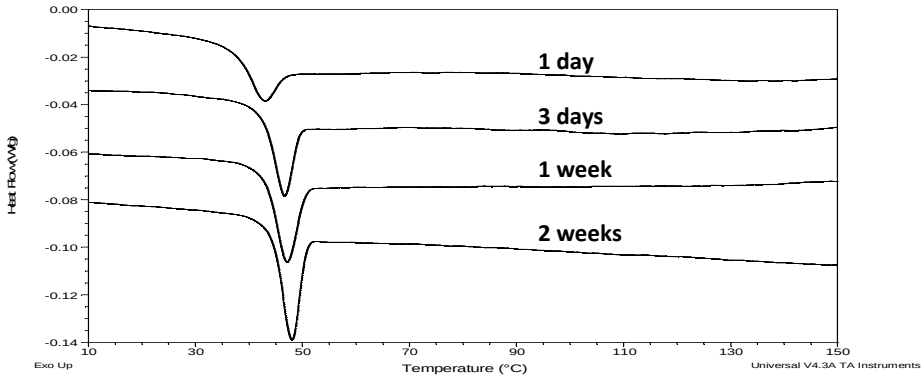

Figure 3.6: Results of MTDSC test of melt-cooled amorphous felodipine on aging under 0%RH/room temperature.

Relaxation enthalpy of amorphous feldopine against time is shown in Figure 3.7. KWW equation has been reported to calculate the relaxation time of amorphous drugs using the measured relaxation enthalpy on aging (17). The empirical equation can be expressed by (17):

$$\Phi(t) = \exp(-(t/\tau)^{\beta}) \qquad \text{Eq 3.7}$$

where $\Phi(t)$ is the extent of relaxation at time t (can be calculated using the measured enthalpy by DSC on aging at time t), τ is the mean molecular relaxation time and β is a constant. However, the data did not fit in the KWW equation. Nevertheless, the increased relaxation enthalpy on aging still indicates the increased molecular mobility of melt-cooled felodipine on aging under 0%RH/room temperature.

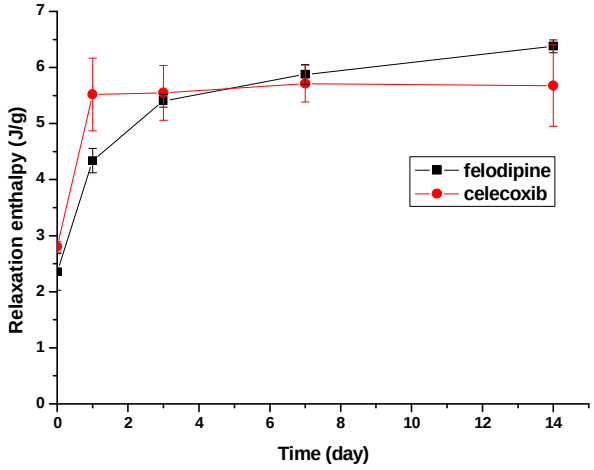

Figure 3.7: Relaxation enthalpy of amorphous feldopine and celecoxib against time on aging under 0%RH at room temperature

3.3.5.1.1.2 Celecoxib

Recrystallization and melting on heating were detected by DSC for melt-cooled amorphous celecoxib (Figure 3.6) suggesting the transformation of celecoxib from amorphous form to crystalline form occurred very fast during heating. In comparison to amorphous felodipine, this indicates that recrystallization of amorphous celecoxib is sensitive to heat treatment. It also can be seen that temperatures of the exothermic peaks (very likely to be recrystallisation) and the following melting points for crystalline celecoxib do not show any particular trend. For example, as shown in Figure 3.8, after one day aging, amorphous celecoxib recrystallized into a mixture of form I (majority) (with a onset melting point of 162.6^{o}C) and III (with a onset melting point of 160.2^{o}C) , but after 3 days aging, recrystallized celecoxib in heating was a pure Form I. Even within the same testing time point, results were not reproducible amongst three repeats. The reason of this phenomenon was still not clearly understood. Relaxation enthalpy of amorphous celecoxib at glass transition on aging is also summarised in Figure 3.5. It can be seen that relaxation enthalpy did not increase with increasing storage time, indicating molecular mobility reached a high level only after 1 day aging under 0%RH/room temperature. The relaxation pattern did not fit in the KWW equation.

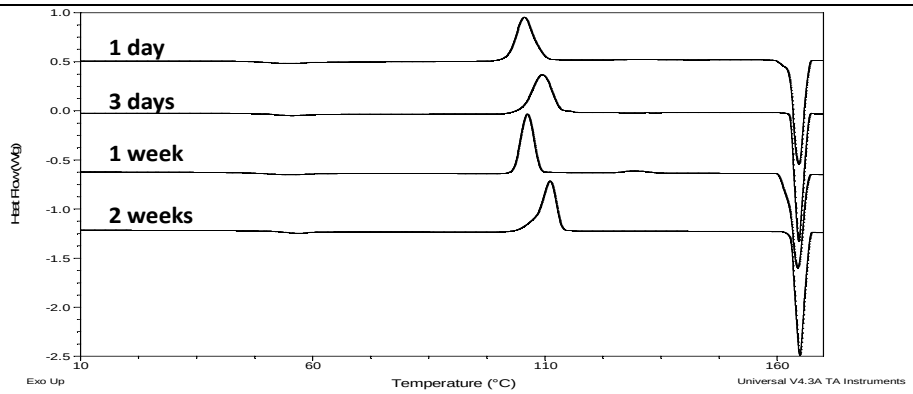

Figure 3.8: Results of MTDSC test of melt-cooled amorphous celecoxib on aging under 0%RH/room temperature.

3.3.5.1.1.3 Carbamazepine

Consistent melting points were achieved for melt-cooled amorphous carbamazepine aged for different time periods under 0%RH/room temperature as shown in Figure 3.9. After 1 day aging under 0%RH/room temperature, recrystallization followed with melting was detected in melt-cool amorphous carbamazepine. This indicates that amorphous carbamazepine can be triggered to recrystallize on heating and it was less stable than amorphous felodipine.

In comparison of the melting point to the value from the literature (36), it was confirmed the recrystallized carbamazepine was form I. It has been reported that form III of carbamazepine was the most stable form at room temperature, although heating form III in DSC can lead to a solid transformation at 175^{o}C and the melting of form I at 192^{o}C (37). Form III with lower melting point but higher physical stability than form I was explained by the "density rule" (38, 39) whereby if a modification of a molecule crystal has a lower density than the other, it may assumed to be less stable at absolute zero (0K), and this is the case for carbamazepine that form I has lower density than form III (37). No solid transformation at 175^{o}C was detected in the any aged melt-cooled carbamazepine (Figure 3.7), and combined with the exothermic peak detected at circa 90^{o} (recrystallization) it indicates all amorphous carbamazepine was recrystallized into form I on heating. The DSC study showed that melt-cooled amorphous carbamazepine on aging under 0%RH/room temperature had a strong tendency of recrystallization on heating, which was similar to the results of celecoxib.

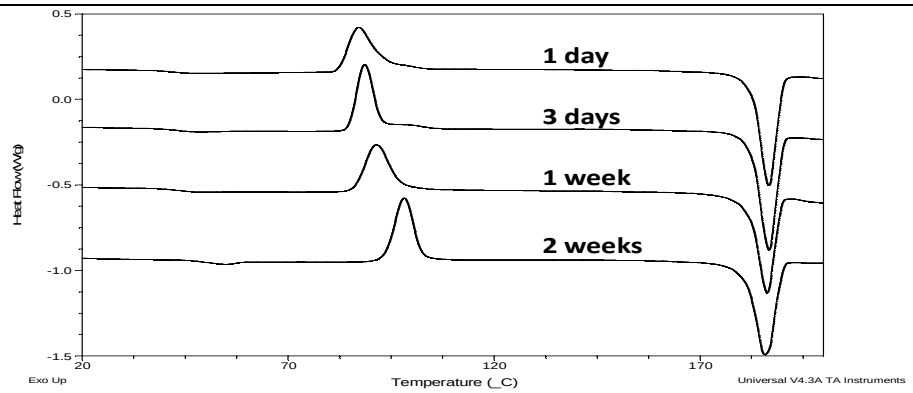

Figure 3.9: Results of MTDSC test of melt-cooled amorphous carbamazepine on aging under 0%RH/room temperature.

3.3.5.1.1.4 Fenofibrate

Results of physical stability study of amorphous fenofibrate under 0%RH/room temperature were different from other model drugs. As described above, fenofibrate has a very low glass transition temperature (-19.7^{o}C) leading to a high molecular mobility at room temperature, which can result in a fast recrystallsation. In this study, it was discovered that crystalline fenofibrate was very easy to be transformed into amorhopus form by melt-cool method, and can be physically stable for very long time if recrystallization was not triggered. Pure amorphous fenofibrate at room temperature is a liquid-like due to the low T_g value, and its recrystallization can be triggered by many external factors such as surface disruption (touched by tweezers) and high humidity. Freshly prepared melt-cooled feofibrate showed no birefringence under polarised microscopy (Figure 3.10a). Once the recrystallization was triggered, the crystals grew at a fast rate. Figure 3.10 (b and c) shows the crystals growth recorded by polarised microscope within 5min. Evident birefringence can be seen under polarised microscope, proving recrystallization of fenofibrate. As can be seen in Figure 3.10, within 5min, a relatively large area of amorphous fenofibrate was chaged into crystalline form. Some preliminary work showed the results that after prepared by melt-cooled method some samples were still amorphous detected by DSC after 3days storage under 75%RH/at room temperature. But some samples recrystallised within one day aged under 0%RH/room temperature. These observations indicate that amorphous fenofibrate has low nucleation rate but high crystal growth rate. The accurate control of the recrystallization was difficult to achieve and no further experiment was carried out as this was not of the scope of the study. Therefore, the physical stability test of melt-cool fenofibrate cannot be carried out precisely. However, these studies of fenofibrate still proved its high recrystallization tendency.

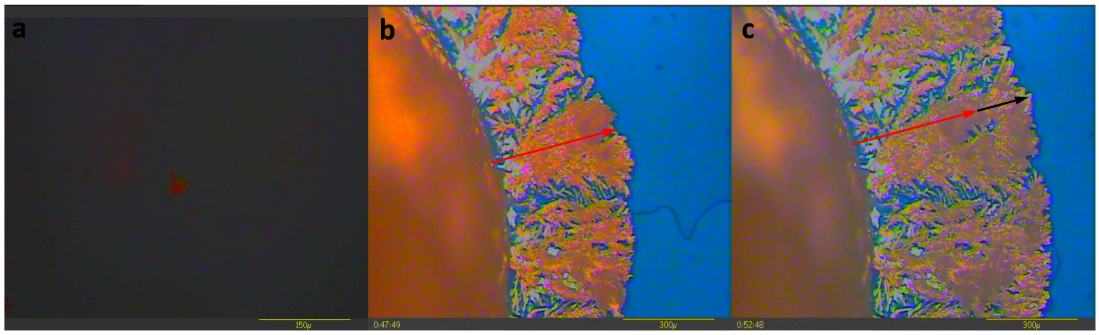

Figure 3.10: Freshly prepared melt-cooled fefibrate (a) and a 5min period of the recrystallisation of amorphous fenofibrate recorded under polarised light microscopy (b and c).

Aging under 0%RH/room temperature up to 2 weeks, the order of the physical stability of melt-cooled amorphous drugs is felodipine > celecoxib ≈ carbamazepine > fenofibrate. This is different from the molecular mobility predicted using the AGV model, which may indicate it is necessary to carry out the real-time physical stability study of amorphous drugs to compare their physical stabilities.

3.3.5.1.2 Physical stability of melt-cooled model drugs aged under 75%RH/ room temperature

3.3.5.1.2.1 Felodipine

MTDSC results of the melt-cooled amorphous felodipine aged under 75%RH/room temperature are shown in Figure 3.11. Melting can be detected for amorphous felodipine after 1 week aging. This indicates that the physical stability of amorphous felodipine can be affected by high humidity. This is very likely to be attributed to the water uptake of amorphous felodipine under high humidity. The moisture uptake can increase molecular mobility, leading to the recrystallisation of amorphous drugs as reported in articles that the plasticising effect of absorbed water in solid dispersions can significantly decrease physical stability (24, 40-42). Water uptake in amorphous felodipine was reflected by a decrease in T_g values on aging. Freshly prepared amorphous felodipine showed a T_g of 45.5^{o}C, and after 2 weeks aging under 75%RH T_g decreased to 40.9^{o}C. Using Gordon–Taylor equation as described in Chapter 1 (*Eq 1.1* and *1.2*) the quantity of water uptake in amorphous felodipine was calculated as 0.95% (w/w) after 2 weeks aging under 75%RH/room temperature. It also should be noted that after 2 weeks aging under 75%RH/room temperature, a relatively large recrystallization peak was detected (Figure 3.11), which suggests there were still certain amount of amorphous felodipine left.

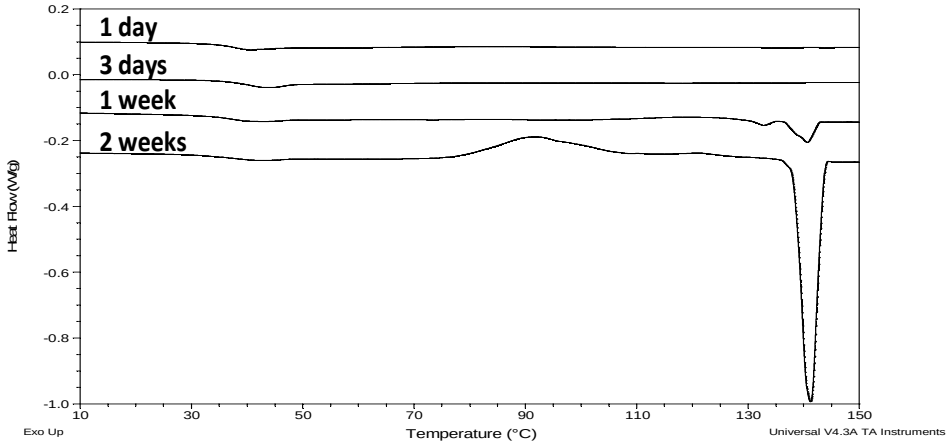

Figure 3.11: Results of MTDSC test of melt-cooled amorphous felodipine on aging under 0%RH/room temperature.

The relaxation enthalpy of melt-cooled amorphous felodipine on aging under 75%RH/room temperature was measured as shown in Figure 3.12. It can be seen that relaxation of amorphous felodipine almost reached a plateau after 1 day aging. The decreased relaxation enthalpy after 1 week aging was due to partial recrystallised felodipine within the sample.

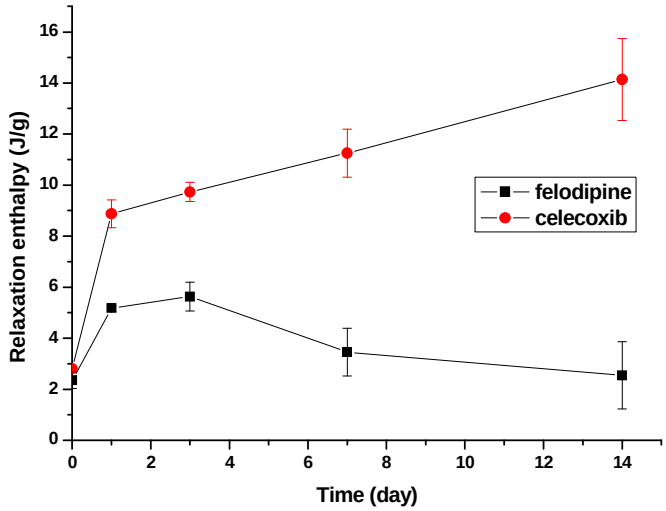

Figure 3.12: Relaxation enthalpy of amorphous feldopine and celecoxib against time on aging under 75%RH/room temperature.

3.3.5.1.2.2 Celecoxib

Amorphous celecoxib aged under 75%RH/room temperature showed similar results to that under dry condition (Figure 3.13). Recrystallisation on heating followed by melting was detected after one day aging. The irregular recrystallisation temperatures of amorphous celecoxib were detected. A decrease in T_g of amorphous celecoxib was observed from 58.2°C (fresh) to 51.2°C (after 2

weeks aging) due to the water sorption on aging. By using Gordon-Taylor equation, the water uptake was calculated as 1.51% (w/w) after 2 weeks aging.

The relaxation enthalpy of celecoxib continued increasing with increasing aging time as depicted in Figure 3.11, indicating increased molecular mobility on aging under high humidity. In comparison to the results of the relaxation enthalpy of the samples aged under 0%RH/room temperature, the physical instability of amorphous celecoxib was significantly increased under 75%RH/room temperature.

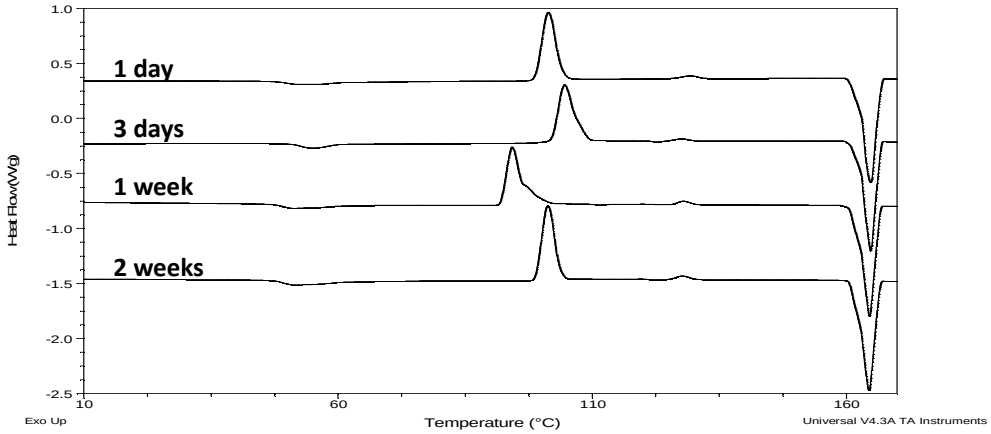

Figure 3.13: Results of MTDSC test of melt-cool amorphous celecoxib on aging under 0%RH/room temperature.

3.3.5.1.2.3 Carbamazepine

Amorphous carbamazepine aged under 75%RH/room temperature showed similar results to that aged under 0%RH/room temperature as shown in Figure 3.14. Recrystallisation on heating followed by melting was detected after one day aging. Same to the results of amorphous carbamazepine aged under 0%RH/room temperature, all amorphous carbamazepine recrystallized into form I on heating as proved by the detected melting point (190.5^{o}C). A decrease in T_g with increasing aging time was observed from 50.1^{o}C (fresh) to 33.6^{o}C (after 2 weeks aging). Using Gordon-Taylor equation, the water uptake was calculated as 5.18% (w/w). It has been reported that carbamazepine can form a dihydrate if the drug was in contact with water directly (43, 44). However, as all detected melting peaks on aging showed consistent value of the melting point of form I, it can conclude that amorphous carbamazepine still recrystallised into form I after 2 weeks aging under 75%RH/room temperature.

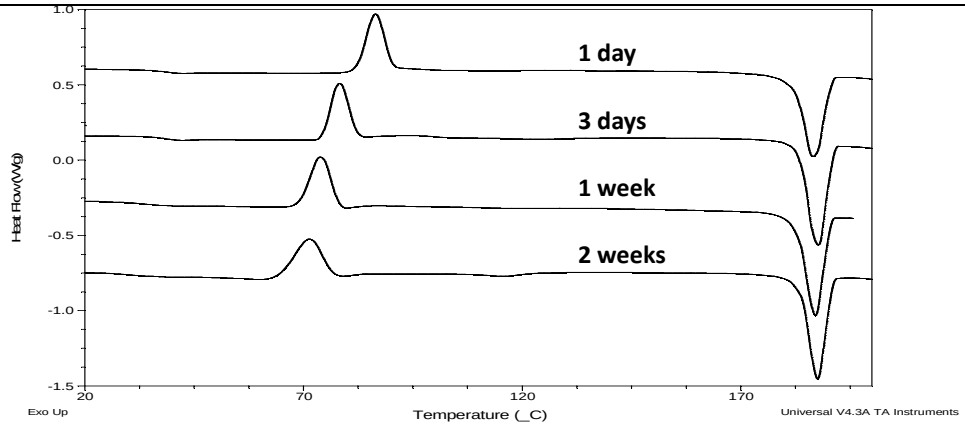

Figure 3.14: Results of MTDSC test of melt-cool amorphous carbamazepine on aging under 0%RH/room temperature.

In short summary, the order of physical stability of amorphous drugs aged under 75%RH/room temperature is still felodipine > celecoxib ≈ carbamazepine > fenofibrate. However, in comparison to the amorphous model drugs aged under 75%RH/room temperature, a decreased physical stability was observed for amorphous drugs aged under 75%RH/room temperature. This indicates the physical stability of amorphous drugs can be significantly affected by stressed humidity.

3.3.5.2 Physical stability of amorphous drugs prepared by spin coating

Results of the physical stability of melt-cooled amorphous drugs showed that felodipine were the most stable amorphous drug under both dry and 75%RH conditions. Celecoxib and carbamazepine showed similar and less stable physical stability behaviour than felodpine. However, it was noted that on aging under 75%RH/room temperature, melt-cooled celecoxib was still translucent after 3 days aging. Melt-cooled carbamazepine changed from translucent to cloudy after 1 day aging under 75%RH/room temperature. These observations indicate that amorphous celecoxib may have better physical stability than carbamazepine at room temperature. It is very likely that recrystallization of amorphous celecoxib is sensitive to temperature, and thus recrystallization and melting were observed by DSC. In addition, as mentioned earlier, the physical stability of amorphous drugs was reported to be dependent on processing methods (5, 6). Therefore, in order to gain a comprehensive understanding of the physical stability of amorphous drugs, amorphous drugs were prepared using spin coating for the physical stability study. Spin coated amorphous drugs was stored under 0%RH/room temperature and 75%RH/room temperature, respectively.

3.3.5.2.1 Physical stability of spin-coated amorphous drugs aged under 0%RH/room temperature

3.3.5.2.1.1 Felodipine

Images of spin coated amorphous felodipine aged under 0%RH/room temperature taken by polarised microscopy are shown in Figure 3.15. It can be seen that no evident birefringence can be observed for freshly spin coated felodipine, indicating felodipine was amorphous after fresh spin coating. After two weeks aging, areas with birefringence were observed, suggesting the occurrence of recrystallization on storage. Freshly prepared and aged spin coated felodipine was also tested by ATR-FTIR. The ATR-FTIR results showed that after 2 weeks aging felodipine was still amorphous (Figure 3.16). For felodipine, the transformation from crystalline form to amorphous form after spin coating can be identified by NH peak shift from 3365 to 3331cm^{-1}(45). After two weeks aging, despite felodipine crystals were observed by polarised microscope, the NH peak position remained the same. This suggests the low level of recrystallisation of spin coated felodipine was possibly below the detection limit of IR.

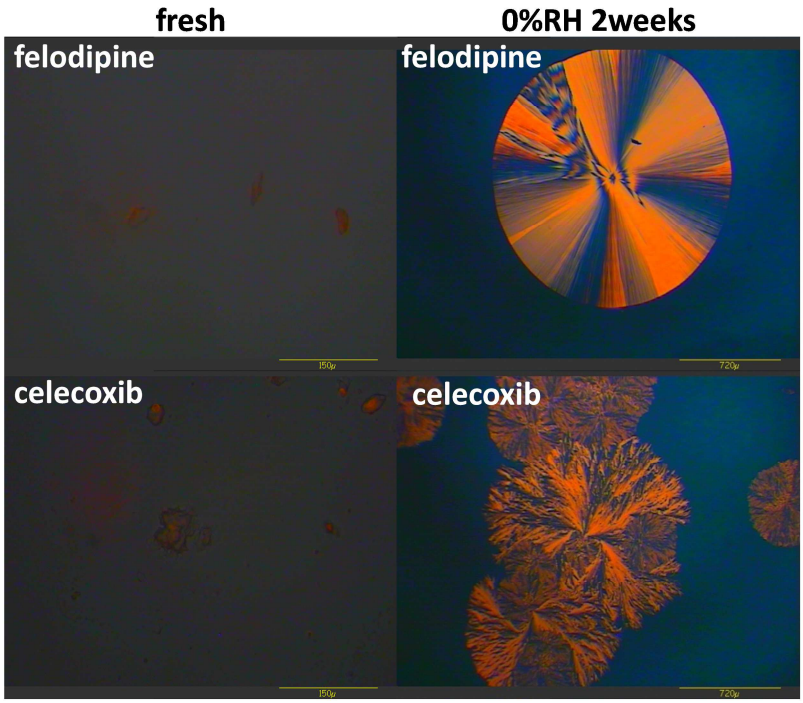

Figure 3.15: Images of spin coated felodipine and celecoxib taken by polarised light microscopy on aging under 0%RH/room temperature.

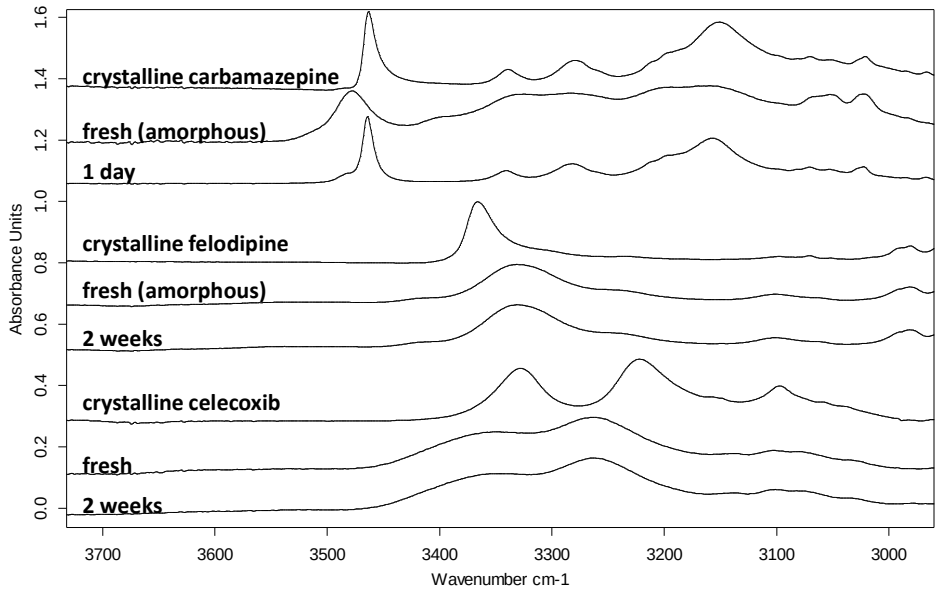

Figure 3.16: ATR-FTIR results of NH (felodipine) and NH_2 (celecoxib, carbamazepine) groups from spin coated amorphous model drugs aged under 0%RH/room temperature for different time periods.

3.3.5.2.1.2 Celecoxib

Figure 3.15 shows the images of spin coated amorphous celecoxib aged under 0%RH/room temperature taken by polarised microscopy. Similar to the spin coated felodipine, no evident birefringence was observed for the freshly spin coated celecoxib, indicating celecoxib amorphous after fresh spin coating. After two weeks aging under 0%RH/room temperature, areas with birefringence were seen, indicating the occurrence of recrystallization of amorphous celecoxib on storage. However the recrystallized celecoxib was not detected using ATR-FTIR (Figure 3.16). The ATR-FTIR results of spin coated celecoxib showed that after 2 weeks aging celeocixb was still amorphous (Figure 3.16). A doublet peaks at 3222 and 3329cm^{-1} in IR spectra of crystalline celecoxib form III were attributed to the N-H stretching vibration of NH_2 group (46). After spin coating, the two peaks shifted to 3264 and 3362$cm^{-1,}$ respectively, with broader peak bands. Similar to spin coated felodipine, spin coated celecoxib was still amorphous after 2 weeks aging according to the ATR-FTIR spectra, which indicates the majority of the sample remained amorphous.

3.3.5.2.1.3 Carbamazepine

Compared with spin coated felodipine and celecoxib, spin coated carbamazepine present very poor physical stability under the same storage condition. As seen in Figure 3.17, a large area with birefringence was observed on spin coated carbamazepine after 1 day aging under 0%RH/room temperature, indicating a high level of recrystallisation occurred within a short time period. This was also confirmed by ATR-FTIR spectroscopy as shown in Figure 3.16. NH_2 group represented by a band at 3463cm^{-1} from aged spin coated carbamazepine showed an identical position in IR

spectrum to original crystalline form III carbamazepine, whereas the peak from freshly prepared amorphous drug was at 3478cm^{-1}. A shoulder peak at 3483cm^{-1} next to 3463cm^{-1} also can be seen, and this peak indicates the presence of form I compared with the peak position from the literature (37). Therefore, on aging under dry condition, spin coated carbamazepine recrystallized rapid into a mixture of Form I and III with the majority of Form III.

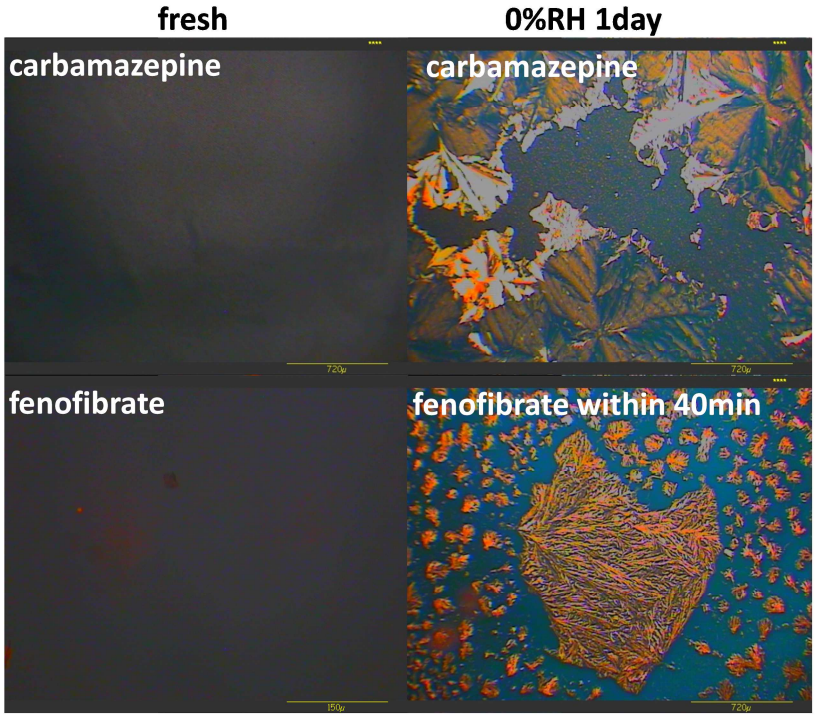

Figure 3.17: Images of spin coated carbamazepine (a) and fenofibrate (b) taken by polarised light microscopy on aging for different time periods under 0%RH/room temperature.

3.3.5.2.1.4 Fenofibrate

For fenofibrate, although freshly prepared sample was amorphous as confirmed by polarised microscopy, recrystallization continued and almost accomplished within 40min as shown in Figure 3.17. ATR-FTIR measurements of spin coated fenofibrate confirmed its fast recrystallsation as depicted in Figure 3.18. Originally positioned at 1648cm^{-1}, the carbonyl group from fenofibrate shifted to 1656cm^{-1} after changed from crystalline form to amorphous form. Spectra of spin coated fenofibrate were taken continuously with an interval of 2min. A peak shift from 1656cm^{-1} to 1648cm^{-1} was completed in 40min indicating the solid transformation from amorphous state to crystalline state was accomplished in 40min. Aging under 0%RH/room temperature up to 2 weeks, the order of the physical stability of spin coated amorphous drugs is felodipine ≥ celecoxib > carbamazepine > fenofibrate.

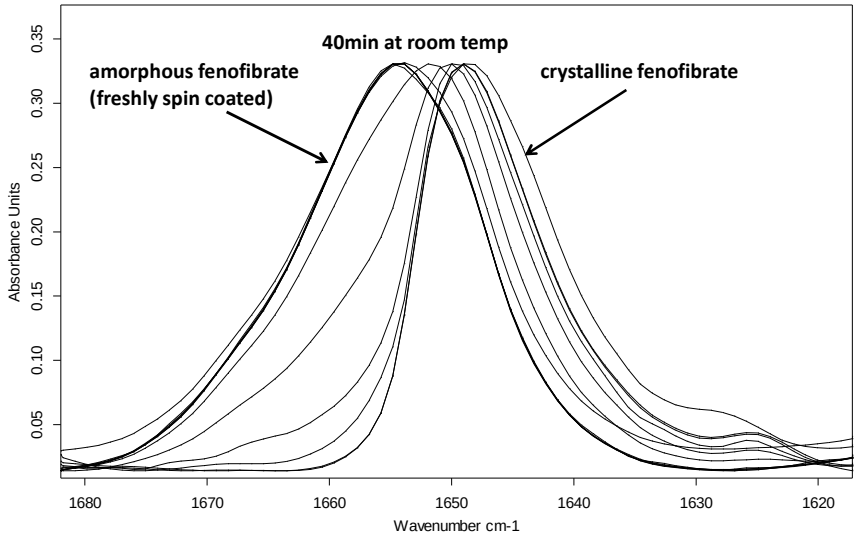

Figure 3.18: ATR-FTIR results of carbonyl group from spin coated fenofibrate tested at ambient environment for 40min.

3.3.5.2.2 Physical stability of spin coated amorphous drugs aged under 75%RH/room temperature

3.3.5.2.2.1 Felodipine

Areas with birefringence in spin coated felodipine were observed by polarised microscope after 3 days aging under 75%RH/room temperature as shown in Figure 3.19a, indicating high humidity can accelerate recrystallization of amorphous felodipine in comparison to the samples aged under 0%RH/room temperature. The results were similar to the melt-cooled amorphous felodipine whereby recrystallization was detected by DSC for samples only aged under 75%RH/room temperature. Recrystallisation of aged spin coated felodipine was also detected by ATR-FTIR (Figure 3.20). After 2 weeks aging under 75%RH/room temperature, the NH peak from freshly spin coated felodipine shifted from 3331cm^{-1} back to 3365 cm^{-1} (crystalline felodipine form I). This indicates that a higher level of recrystallization occurred in comparison to samples aged under 0%RH/room temperature.

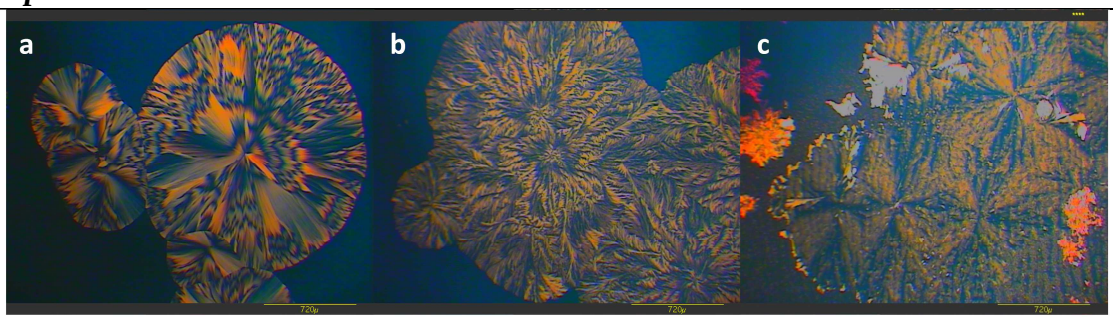

Figure 3.19: Polarised light microscopy images of spin coated felodipine (a) and celecoxib (b) aged for 2 weeks and carbamazepine (c) aged for 1 day upon exposure to 75%RH at room temperature.

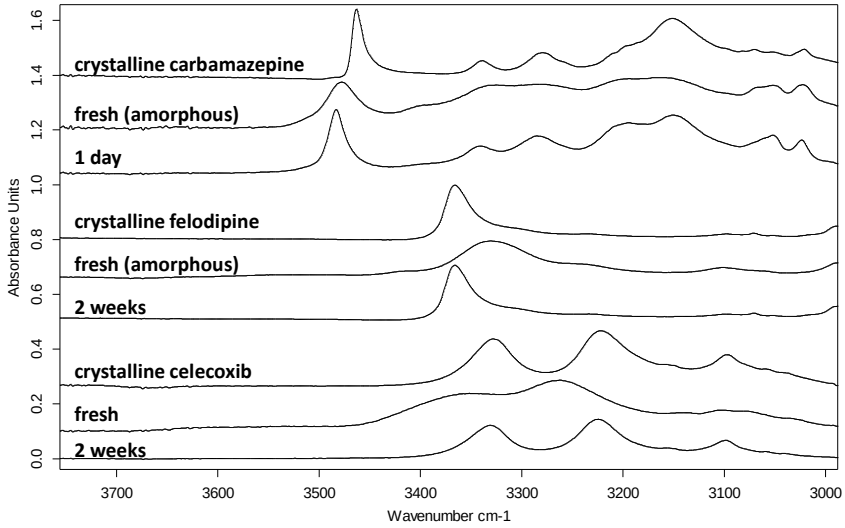

Figure 3.20: ATR-FTIR results of NH (felodipine) and NH_2 (celecoxib, carbamazepine) groups from spin coated amorphous model drugs aged under 75%RH at room temperature for different time periods.

3.3.5.2.2.2 Celecoxib

Areas with birefringence in spin coated celecoxib were observed after 3 days aging under 75%RH/room temperature (Figure 3.19b), indicating the occurrence of recrystallization. In comparison to the same samples aged under 0%RH/room temperature, recrystallization of spin coated celecoxib aged under 75%RH/room temperature occurred at a greater level. Physical stability studies of melt-cooled celecoxib only showed an increased molecular mobility as demonstrated by the increased relaxation enthalpy measured by DSC on aging. However, by using spin coating, it clearly proved that stressed humidity (75%RH) can induce recrystallization for amorphous celecoxib. Recrystallisation of spin coated celecoxib was also detected by ATR-FTIR after 2 weeks aging under 75%RH/room temperature as seen in Figure 3.20. The doublet NH peaks at 3264 and 3362 cm^{-1} from freshly spin coated celecoxib shifted to 3222 and 3329 cm^{-1} after 2

weeks aging, indicating a higher level of recrystallization compared with the same sample stored under 0%RH/room temperature.

3.3.5.2.2.3 Carbamazepine

Carbamazepine showed large birefringent area only after 1 day aging as shown in Figure 3.19c. The sizes of the observed birefringent areas in samples aged under 75%RH/room temperature was similar to that in samples aged under 0%RH/room temperature. This indicates amorphous carbamazepine has high potential to recrystallize, which is less affected by the aging condition. Recrystallization of spin coated carbamazepine was also studied by ATR-FTIR (Figure 3.20). It can be seen that the recrystallization of spin coated carbamazepine under 75%RH/room temperature was different from the results under 0%RH/room temperature. Unlike the detection of both recrystallized form I and III in samples aged under 0%RH/room temperature, only form I was detected after 2 weeks aging under 75%RH/room temperature. This indicates that the aging condition can affect the solid state transformation of carbamazepine. Furthermore, recrystallisation behaviour between melt-cool and spin coated carbamazepine are different since only form I can be detected by MTDSC for melt-cool samples. This is possibly because although aged under different conditions (dry and humid), heating induced recrystallisation of amorphous carbamazepine in the MTDSC test tend to configure molecules into form I (43).

3.3.6 Summary of the physicochemical characterisation of model drugs

Thermodynamic properties of the four model drugs varied in a broad range. For instance, the T_g of fenofibrate was -19.7^{o}C but the T_g of celecoxib was 58.2^{o}C measured by DSC. The four model drugs also showed different glass forming ability. Using the AGV equation, relaxation time of the four amorphous was calculated and results showed that the four amorphous model drugs had different molecular mobility. In addition to these commonly evaluated physical properties of drugs, the real-time physical stability of amorphous drugs were studied under 0%RH/room temperature and 75%RH/ room temperature. In order to avoid the effect of processing methods, amorphous drugs were prepared using melt-cool and spin coating, respectively. Results showed that irrespective of the preparation methods, the order of the physical stability of amorphous was felodipine > celecoxib > carbamazepine > fenofibrate. The results of the physical stability study also showed that stressed humidity can induce recrystallization of amorphous model drugs.

Factors including glass transition temperatures of amorphous drugs, molecular mobility of amorphous drugs and the physical stability of amorphous drug have been reported to be associated with the physical stability of amorphous solid dispersions (9, 17, 47). However, there have been few studies combining these factors to disclose which of them are most relevant to the physical stability of amorphous solid dispersions. In Chapter 6, the real-time physical stability studies of amorphous solid dispersions prepared with these model drugs are evaluated. Therefore, comparing

the physical stability of amorphous solid dispersions with the physical properties of model drugs, dominating factors affecting the physical stability of amorphous solid dispersions may be revealed, which can be potentially helpful for the enhancement of the physical stability of amorphous solid dispersions.

3.4 Conclusions

In this chapter, physicochemical properties of model drugs and polymers were investigated, and these properties have been considered to be related to the physical stability of solid dispersions. These properties including glass transition temperature, fragility and molecular mobility, varied in a wide range as proved by the calculation. Physical stability of amorphous drugs prepared by different methods was tested under dry and high humidity condition. Although prepared and aged differently, the order of the physical stability of amorphous drugs was felodipine > celecoxib > carbamazepine > fenofibrate in all cases. The achieved characterisation results could be further used in combination with miscibility/solid solubility prediction at the next stage for fulfilling the method development of predicting and enhancing physical stability of solid dispersions prepared by hot melt extrusion.

Reference

1. A.T.M. Serajuddin. Solid dispersion of poorly water-soluble drugs: Early promises, subsequent problems, and recent breakthroughs. Journal of Pharmaceutical Sciences. 88:1058-1066 (1999).
2. S. Yoshiokaand Y. Aso. Correlations between molecular mobility and chemical stability during storage of amorphous pharmaceuticals. Journal of Pharmaceutical Sciences. 96:960-981 (2007).
3. G. Van den Mooter. The use of amorphous solid dispersions: A formulation strategy to overcome poor solubility and dissolution rate. Drug Discovery Today: Technologies. 9:e79-e85 (2012).
4. D.J. Greenhalgh, A.C. Williams, P. Timmins, and P. York. Solubility parameters as predictors of miscibility in solid dispersions. Journal of Pharmaceutical Sciences. 88:1182-1190 (1999).
5. J.A. Baird, B. Van Eerdenbrugh, and L.S. Taylor. A classification system to assess the crystallization tendency of organic molecules from undercooled melts. Journal of Pharmaceutical Sciences. 99:3787-3806 (2010).
6. B. Van Eerdenbrugh, J.A. Baird, and L.S. Taylor. Crystallization tendency of active pharmaceutical ingredients following rapid solvent evaporation—classification and comparison with crystallization tendency from undercooled melts. Journal of Pharmaceutical Sciences. 99:3826-3838 (2010).
7. K. Six, G. Verreck, J. Peeters, M. Brewster, and G.V.d. Mooter. Increased physical stability and improved dissolution properties of itraconazole, a class II drug, by solid dispersions that combine fast- and slow-dissolving polymers. Journal of Pharmaceutical Sciences. 93:124-131 (2004).
8. A.L. Sarode, H. Sandhu, N. Shah, W. Malick, and H. Zia. Hot melt extrusion (HME) for amorphous solid dispersions: Predictive tools for processing and impact of drug–polymer interactions on supersaturation. European Journal of Pharmaceutical Sciences. 48:371-384 (2013).
9. Y.C. Ng, Z. Yang, W.J. McAuley, and S. Qi. Stabilisation of amorphous drugs under high humidity using pharmaceutical thin films. European Journal of Pharmaceutics and Biopharmaceutics(2013).

10. H. Konnoand L.S. Taylor. Influence of different polymers on the crystallization tendency of molecularly dispersed amorphous felodipine. Journal of Pharmaceutical Sciences. 95:2692-2705 (2006).
11. A. Górniak, A. Wojakowska, B. Karolewicz, and J. Pluta. Phase diagram and dissolution studies of the fenofibrate–acetylsalicylic acid system. J Therm Anal Calorim. 104:1195-1200 (2011).
12. N. Passeriniand D.Q.M. Craig. An investigation into the effects of residual water on the glass transition temperature of polylactide microspheres using modulated temperature DSC. Journal of Controlled Release. 73:111-115 (2001).
13. S. Qi, P. Avalle, R. Saklatvala, and D.Q.M. Craig. An investigation into the effects of thermal history on the crystallisation behaviour of amorphous paracetamol. European Journal of Pharmaceutics and Biopharmaceutics. 69:364-371 (2008).
14. M.D. Ediger, C.A. Angell, and S.R. Nagel. Supercooled Liquids and Glasses. The Journal of Physical Chemistry. 100:13200-13212 (1996).
15. J. Kerčand S. Srčič. Thermal analysis of glassy pharmaceuticals. Thermochimica Acta. 248:81-95 (1995).
16. T. Vasconcelos, B. Sarmento, and P. Costa. Solid dispersions as strategy to improve oral bioavailability of poor water soluble drugs. Drug Discovery Today. 12:1068-1075 (2007).
17. B. Hancock, S. Shamblin, and G. Zografi. Molecular Mobility of Amorphous Pharmaceutical Solids Below Their Glass Transition Temperatures. Pharm Res. 12:799-806 (1995).
18. P. Gupta, G. Chawla, and A.K. Bansal. Physical Stability and Solubility Advantage from Amorphous Celecoxib: The Role of Thermodynamic Quantities and Molecular Mobility. Molecular Pharmaceutics. 1:406-413 (2004).
19. A.M. Kaushaland A.K. Bansal. Thermodynamic behavior of glassy state of structurally related compounds. European Journal of Pharmaceutics and Biopharmaceutics. 69:1067-1076 (2008).
20. B. Borde, H. Bizot, G. Vigier, and A. Buleon. Calorimetric analysis of the structural relaxation in partially hydrated amorphous polysaccharides. I. Glass transition and fragility. Carbohydrate Polymers. 48:83-96 (2002).
21. K. Grzybowska, M. Paluch, A. Grzybowski, Z. Wojnarowska, L. Hawelek, K. Kolodziejczyk, and K.L. Ngai. Molecular Dynamics and Physical Stability of Amorphous Anti-Inflammatory Drug: Celecoxib. The Journal of Physical Chemistry B. 114:12792-12801 (2010).
22. C.A. Lipinski. Drug-like properties and the causes of poor solubility and poor permeability. Journal of Pharmacological and Toxicological Methods. 44:235-249 (2000).
23. L. Yu. Amorphous pharmaceutical solids: preparation, characterization and stabilization. Advanced Drug Delivery Reviews. 48:27-42 (2001).
24. B.C. Hancock, S.L. Shamblin, and G. Zografi. Molecular Mobility of Amorphous Pharmaceutical Solids Below Their Glass Transition Temperatures. Pharmaceutical Research. 12:799-806 (1995).
25. S.L. Shamblin, B.C. Hancock, Y. Dupuis, and M.J. Pikal. Interpretation of relaxation time constants for amorphous pharmaceutical systems. Journal of Pharmaceutical Sciences. 89:417-427 (2000).
26. I.M. Hodge. Enthalpy relaxation and recovery in amorphous materials. Journal of Non-Crystalline Solids. 169:211-266 (1994).
27. M. Yoshioka, B.C. Hancock, and G. Zografi. Crystallization of indomethacin from the amorphous state below and above its glass transition temperature. Journal of Pharmaceutical Sciences. 83:1700-1705 (1994).
28. D. Zhou, G.G.Z. Zhang, D. Law, D.J.W. Grant, and E.A. Schmitt. Thermodynamics, Molecular Mobility and Crystallization Kinetics of Amorphous Griseofulvin. Molecular Pharmaceutics. 5:927-936 (2008).
29. L.R. Hildenand K.R. Morris. Prediction of the relaxation behavior of amorphous pharmaceutical compounds. I. Master curves concept and practice. Journal of Pharmaceutical Sciences. 92:1464-1472 (2003).

30. J.H.G. Gerold Adam On the Temperature Dependence of Cooperative Relaxation Properties in Glass-Forming Liquids. J Chem Phys. 43:(1965).
31. I.M. Hodge. Strong and fragile liquids — a brief critique. Journal of Non-Crystalline Solids. 202:164-172 (1996).
32. A. Yukio, Y. Sumie, and K. Shigeo. Explanation of the crystallization rate of amorphous nifedipine and phenobarbital from their molecular mobility as measured by 13C nuclear magnetic resonance relaxation time and the relaxation time obtained from the heating rate dependence of the glass transition temperature. Journal of Pharmaceutical Sciences. 90:798-806 (2001).
33. A. Yukio, Y. Sumie, and K. Shigeo. Molecular mobility-based estimation of the crystallization rates of amorphous nifedipine and phenobarbital in poly(vinylpyrrolidone) solid dispersions. Journal of Pharmaceutical Sciences. 93:384-391 (2004).
34. V. Kakumanuand A. Bansal. Enthalpy Relaxation Studies of Celecoxib Amorphous Mixtures. Pharm Res. 19:1873-1878 (2002).
35. S. Qi, A. Gryczke, P. Belton, and D.Q.M. Craig. Characterisation of solid dispersions of paracetamol and EUDRAGIT® E prepared by hot-melt extrusion using thermal, microthermal and spectroscopic analysis. International Journal of Pharmaceutics. 354:158-167 (2008).
36. C. Rustichelli, G. Gamberini, V. Ferioli, M.C. Gamberini, R. Ficarra, and S. Tommasini. Solid-state study of polymorphic drugs: carbamazepine. Journal of Pharmaceutical and Biomedical Analysis. 23:41-54 (2000).
37. A.L. Grzesiak, M. Lang, K. Kim, and A.J. Matzger. Comparison of the four anhydrous polymorphs of carbamazepine and the crystal structure of form I. Journal of Pharmaceutical Sciences. 92:2260-2271 (2003).
38. A. Burgerand R. Ramberger. On the polymorphism of pharmaceuticals and other molecular crystals. II. Mikrochim Acta. 72:273-316 (1979).
39. A. Burgerand R. Ramberger. On the polymorphism of pharmaceuticals and other molecular crystals. I. Mikrochim Acta. 72:259-271 (1979).
40. I. Weuts, D. Kempen, G. Verreck, A. Decorte, K. Heymans, J. Peeters, M. Brewster, and G.V.d. Mooter. Study of the physicochemical properties and stability of solid dispersions of loperamide and PEG6000 prepared by spray drying. European Journal of Pharmaceutics and Biopharmaceutics. 59:119-126 (2005).
41. S. Janssens, C. Roberts, E.F. Smith, and G. Van den Mooter. Physical stability of ternary solid dispersions of itraconazole in polyethyleneglycol 6000/hydroxypropylmethylcellulose 2910 E5 blends. International Journal of Pharmaceutics. 355:100-107 (2008).
42. H. Bley, B. Fussnegger, and R. Bodmeier. Characterization and stability of solid dispersions based on PEG/polymer blends. International Journal of Pharmaceutics. 390:165-173 (2010).
43. Y. Kobayashi, S. Ito, S. Itai, and K. Yamamoto. Physicochemical properties and bioavailability of carbamazepine polymorphs and dihydrate. International Journal of Pharmaceutics. 193:137-146 (2000).
44. L.E. McMahon, P. Timmins, A.C. Williams, and P. York. Characterization of dihydrates prepared from carbamazepine polymorphs. Journal of Pharmaceutical Sciences. 85:1064-1069 (1996).
45. X. Tang, M. Pikal, and L. Taylor. A Spectroscopic Investigation of Hydrogen Bond Patterns in Crystalline and Amorphous Phases in Dihydropyridine Calcium Channel Blockers. Pharm Res. 19:477-483 (2002).
46. G. Chawla, P. Gupta, R. Thilagavathi, A.K. Chakraborti, and A.K. Bansal. Characterization of solid-state forms of celecoxib. European Journal of Pharmaceutical Sciences. 20:305-317 (2003).
47. B.C. Hancockand G. Zografi. Characteristics and significance of the amorphous state in pharmaceutical systems. Journal of Pharmaceutical Sciences. 86:1-12 (1997).

Chapter 4: Prediction of drug-polymer miscibility and solubility using different theoretical approaches

4.1 Introduction

The application of amorphous solid dispersions has been proved to be effective in enhancing dissolution rate of poorly water-soluble drugs (1, 2). However, as mentioned in Chapter 1, the physical stability of amorphous solid dispersions is still the main challenge for the formulation development in the pharmaceutical industry (3-5). The occurrence of physical instability in amorphous solid dispersions, including phase separation or recrystallization can lead to the appearance of drug crystals in formulations, which may further affect dissolution rate and bioavailability as crystalline drugs do not have as high dissolution rate as amorphous forms (4, 6).

Several factors such as molecular mobility, glass transition temperature, miscibility between drugs and polymers and drug-polymer solid solubility have been evaluated to correlate their relationship with the physical stability of solid dispersions (7-11). It has been proposed by articles that drug-polymer miscibility and solid solubility of drugs in polymers was one of the most significant factors in impacting the physical stability of amorphous solid dispersions (9, 12-14). Therefore, to fulfil the development of prediction methods for physical stability of solid dispersions, drug-polymer miscibility and solubility is evaluated by theoretical approaches in this chapter.

Miscibility originally is a property to describe mixing of liquids to form a homogeneous solution, for instance mixing of phenol and water depicted a typical miscibility phase diagram of a A-B binary system with the “inversed U” shape as discussed in the literature (Figure 4.1) (15). Above the critical temperature, A and B are completely miscible with each other, whereas below the critical temperature the mixed system becomes partially miscible containing A-rich phase or B-rich phase. The compositions of A-rich phase, B-rich phase and the miscible phase can be determined from the phase diagram. In amorphous drug-polymer solid dispersions, miscibility is applied to the mixing property of drugs and polymers at a certain temperature (16). If within a certain range of drugs to polymers ratios at a certain temperature, a single phase system can be achieved by mixing, it may indicate that the amorphous drug and the amorphous polymer are miscible within the range. An amorphous solid dispersion prepared with drug loadings falling into the miscible drug-polymer ratios is likely to be thermodynamically stable (16-18).

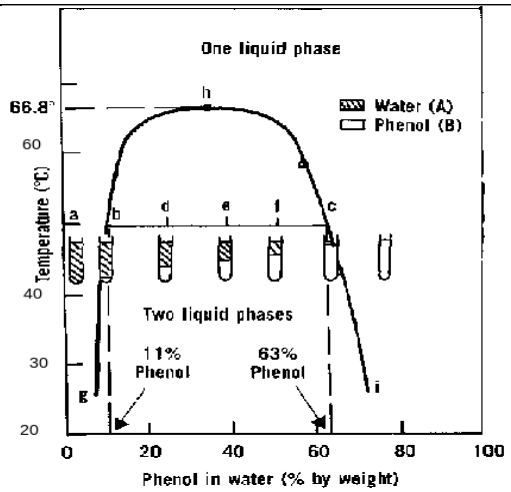

Figure 4.1: Liquid-liquid phase diagram of phenol and water (miscibility gap between phenol and water) (19).

Drug-polymer solid solubility is also a concept derived from aqueous solution theory. Unlike miscibility regarding the mixing of two liquids, solubility is defined as dissolving a solid state material into a solvent until the equilibrium maximum concentration at a certain temperature under a certain pressure. In amorphous drug-polymer solid dispersions, the maximum amount of drug molecules which can be molecularly dispersed into polymer chains to form a single phase system (at a certain temperature under a certain pressure) is considered as the solid solubility of the drug in the polymer (16). It can be expected that if the drug loading is below the solid solubility of the drug in the polymer, the amorphous solid dispersions can be physically stable as the drug concentration is not sufficiently high to recrystallize out. Therefore, the determination and prediction of solid solubility of drugs in polymers are essential for the formulation development of amorphous solid dispersions.

In this chapter, several most widely used theoretical approaches in predicting drug-polymer miscibility and solubility including solubility parameter, melting point depression and recently developed enthalpy methods were applied to predict the drug-polymer miscibility and solubility between model drugs and EUDRAGIT® EPO (20-22). The predicted miscibility and solubility may assist formulation design of melt extruded solid dispersions with enhanced physical stability.

Research objectives

1. To predict drug-polymer miscibility and solubility using the solubility parameter approach.

2. To predict drug-polymer miscibility and solubility using the melting point depression approach.

3. To predict drug-polymer solid solubility using the enthalpy method.

4.2 Experimental methods

4.2.1 Preparation of physical mixtures of crystalline model drugs and EUDRAGIT® EPO

Physical mixtures of model drugs and EUDRAGIT® EPO with different drug-polymer ratios were prepared in standard DSC pans with a total mass approximately of 3mg. The drug-polymer physical mixtures with drug concentrations from 10% to 90% (w/w) were prepared by weighing the drugs and the polymer together within the DSC aluminium standard pans. After mixing by gently tapping, the lid was crimped and tested by DSC immediately.

4.2.2 Standard differential scanning calorimetry (DSC)

Instrumental information of DSC refers to Chapter 2 (section 2.2.2.1.3). Different heat rates including 0.2,1 and 10^{o}C/min were used to different samples.

4.3 Results and discussion

4.3.1 Solubility parameters approach

4.3.1.1 Theoretical background

The detailed development of solubility parameter (δ) has been described in Chapter 1. In this chapter, details of using the group contribution method to calculate solubility parameters of model drugs and EUDRAGIT® EPO will be discussed. Originating from polymer science, so far the employment of solubility parameter in the pharmaceutical industry has been mainly focused on the comparison of solubility parameters of drugs and polymers to evaluate miscibility between them (20, 23). It has been suggested that compounds with a solubility parameter difference smaller than 7.0 MPa$^{1/2}$ were likely to be miscible, otherwise were likely to be immiscible (23).

Solubility parameters of low molecular weight material can be directed measured by their evaporation energy according to the definition of solubility parameter as mentioned in Chapter 1. However, this cannot be applied to the materials with high molecular weight, such as polymers. In 1928, Dunkel suggested that for low molecular weight materials, cohesive energy E_{coh}, was an additive property, and therefore the cohesive energy of liquids at room temperature can be divided into different functional groups (group contribution) (24). Following the conception of the group contribution method, Hayes, Di Benidetto, and Fedors applied the group contribution method to predict solubility parameters of high molecular weight molecules (25-27). In this study, Fedors group contribution method was applied to calculate solubility parameters of model drugs and EUDRAGIT® EPO (20, 27). As mentioned in Chapter 1, solubility parameter is the square root of cohesive energy density (E_{coh}). Fedors calculated contributions to E_{coh} for a great number of structural groups and their molar volume (V) at 298.15K dividing the structure of a compound into these functional groups, the solubility parameter can be predicted (27). An example of the calculation of solubility parameter of a model drug, fenofibrate (Table 4.1), is given as follows.

Table 4.1: Group contributions to fenofibrate by Fedors method (27).

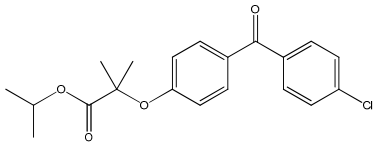

Fenofibrate

Groups	Quantity	E_{coh} (kJ/mol)	V (cm^3/mol)
CH_3	4	4.71	33.5
C	1	1.47	-19.2
CO_2	1	18	18
O	1	3.35	3.8
Phenyl	2	31.94	71.4
CO	1	17.37	10.8
Cl	1	11.55	24
CH	1	3.43	-1

Therefore, solubility parameter of fenofibrate:

$$\delta = (\Sigma E_{coh} / \Sigma V)^{1/2} = 20.98 MP_a^{1/2} \qquad Eq\ 4.1$$

$$\Sigma E_{coh} = (4.71\times4 + 1.47\times1 + 18\times1 + 3.35\times1 + 31.94\times2 + 17.37\times1 + 11.55\times1 + 3.43\times1) = 137.89\times10^3 J/mol$$

$$\Sigma V = (33.5\times4 - 19.2\times1 + 18\times1 + 3.8\times1 + 71.4\times2 + 10.8\times1 + 24\times1 - 1\times1) = 313.2\ cm^3/mol$$

4.3.1.2 Prediction of miscibility and solid solubility by the solubility parameter approach

The calculated solubility parameters of model drugs and EUDRAGIT® EPO are summarised in Table 4.2. It can be seen that the difference of solubility parameters between the model drugs and the monomer of EUDRAGIT® EPO is very little. The highest discrepancy of solubility parameter of model drugs to EUDRAGIT® EPO occurs in carbamazepine, which is 4.07 $MP_a^{1/2}$. According to the discrepancy value mentioned above that if two materials have difference of solubility parameters smaller than 7 $MP_a^{1/2}$, they are very likely to be miscible (23). Therefore, via comparing predicted solubility parameters between model drugs and EUDRAGIT® EPO, it suggests that the model drugs are likely to be miscible with EUDRAGIT® EPO.

Table 4.2: Calculated solubility parameters of model drugs and EUDRAGIT® EPO by Fedors group contribution method.

Materials	ΣE_{coh} (kJ/mol)	ΣV (cm^3/mol)	δ ($MP_a^{1/2}$)
felodipine	143.8	287.4	22.37
celecoxib	124.75	285	20.92
enofibrate	137.98	313.2	20.98
carbamazepine	106.2	190.8	23.59
EUDRAGIT® EPO (monomer)	96.32	252.7	19.52

The predicted solubility parameter may theoretically suggest a high likelihood of miscibility between model drugs and polymers. By further developing this method, the solid solubility of model drugs in EUDRAGIT® EPO can be calculated. Flory-Huggins lattice-based theory derived in 1953 was established to depict thermodynamics of polymer solutions based on the Gibbs free energy law (28). It assumed that the polymer solution had a structure similar to crystalline lattice as schemed in Figure 4.2. Basically, the solution is considered to be composed by lattices and the monomer of the polymer and the solvent molecule will occupy a single lattice in the whole structure. A polymer chain with a polymerisation degree of x will occupy x lattices.

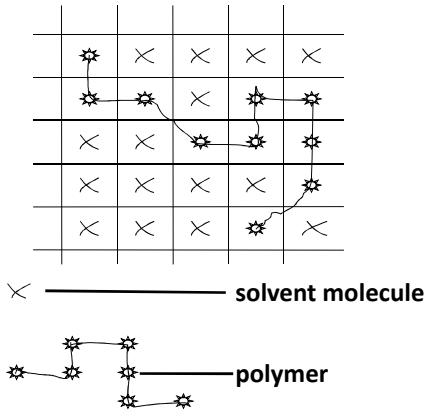

Figure 4.2: Schematic model of Flory-Huggins lattice based theory of polymer solution.

The thermodynamics of mixing a polymer with a solvent based on the Flory-Huggins lattice theory can be described by (28):

$$\Delta G = \Delta H - T\Delta S = RT\,(n_1 \ln \Phi_1 + n_2 \ln \Phi_2 + n_1 \Phi_2 \chi_{12}) \qquad Eq\ 4.3$$

$$\Delta H = RT\, n_1 \Phi_2 \chi_{12} \qquad Eq\ 4.4$$

$$T\Delta S = -RT\,(n_1 \ln \Phi_1 + n_2 \ln \Phi_2) \qquad Eq\ 4.5$$

where ΔG is the free energy change of mixing the polymer with the solvent, ΔH is the enthalpy change of mixing the polymer with the solvent, ΔS is the entropy change of mixing the polymer with the solvent, n_1 is the number of moles of the solvent molecule, n_2 is the number of moles of the polymer, Φ_1 is volume fraction of the solvent, Φ_2 is volume fraction of the polymer, and χ_{12} is called Flory-Huggins interaction parameter between the solvent and the polymer (28). This lattice-based theory was further developed to describe drug-polymer mixing by Taylor's group assuming the drug molecule is the single lattice (21). Considering the amorphous drug molecule as a solute molecule, the Flory-Huggins equation can be written by:

$$\Delta G_M/(RT) = n_{drug} \ln \Phi_{drug} + n_{polymer} \ln \Phi_{polymer} + n_{drug} \Phi_{polymer} \chi \qquad Eq\ 4.6$$

where ΔG_M is the free energy change in the mixing process, n_{drug} is the number of moles of drug, $n_{polymer}$ is the number of moles of polymer, Φ_{drug} is the volume fraction of the drug, $\Phi_{polymer}$ is the volume fraction of the polymer, R is the gas constant, χ is the Flory-Huggins interaction parameter between the drug and the polymer, and T is the temperature at which the mixing of drugs and polymers occurs. The relationship between the interaction parameter and the solubility parameters of drugs and polymers is described by:

$$\chi = V_{site} / RT \, (\delta_{drug} - \delta_{polymer})^2 \qquad \textit{Eq 4.7}$$

where V_{site} is the volume of the hypothetical lattice, and since the volume of the polymer chain is significantly larger than that of the drug, the molar volume of the drug is used as the site volume (21). Results of calculated interaction parameters of model drugs with EUDRAGIT® EPO are summarised in Table 4.3.

Table 4.3: Calculated interaction parameters of model drugs with EUDRAGIT® EPO

materials	feldoipine	celecoxib	fenofibrate	carbamazepine
χ	0.9417	0.4712	0.2603	1.2705

Combining the calculated solubility parameter and the interaction parameter, the free energy of drug-polymer mixing can be calculated by using *Eq 4.6*. One should note that cohesive energy and molar volume from Fedors method were calculated at 25°C (298.15K) under standard pressure, and thus the resultant free energy of mixing by this method can only be applied at room temperature (298K) under standard pressure. The plot of drug ratios in drug-polymer mixtures against calculated free energy of mixing between model drugs and EUDRAGIT® EPO is shown in Figure 4.3. It can be seen that through the entire drug-polymer ratio range, from 5% to 95% (w/w), the mixing of model drugs and EUDRAGIT® EPO is thermodynamically favourable at room temperature (298.15K) since the calculated free energies of mixing are all negative. This indicates a good miscibility between model drugs and EUDRAGIT® EPO, which is in agreement with the prediction by the comparison of solubility parameters between model drugs and EUDRAGIT® EPO. It also can be noted that there exists a lowest value of the calculated free energy change of mixing for individual model drug in a certain drug weight percentage. With the drug-polymer ratio equals to that value the mixing process of amorphous model drugs and EUDRAGIT® EPO is most thermodynamically favourable. This may suggest that amorphous solid dispersions prepared with model drugs and EUDRAGIT® EPO are very likely to be physically stable if the drug loadings are close to these values. Consequently, it can be proposed that this particular value can be used for the mixing of individual drug in EUDRAGIT® EPO in the preparation of amorphous solid dispersions since the demixing of drugs and EUDRAGIT® EPO will not occur spontaneously. This value (solid solubility of the drug in EUDRAGIT® EPO) is circa 25% (w/w) for felodipine, 35% (w/w) for

celecoxib, 35% (w/w) for fenofibrate and 15% (w/w) for carbamazepine. It should be noted that the observed value where the mixing of drugs and the polymer are most thermodynamically favourable might not be the thermodaynamic drug-polymer solubility. However, in the view of fomulaton development for amorphous solid dispersions, the value may be considered as apparent drug-polymer solubility.

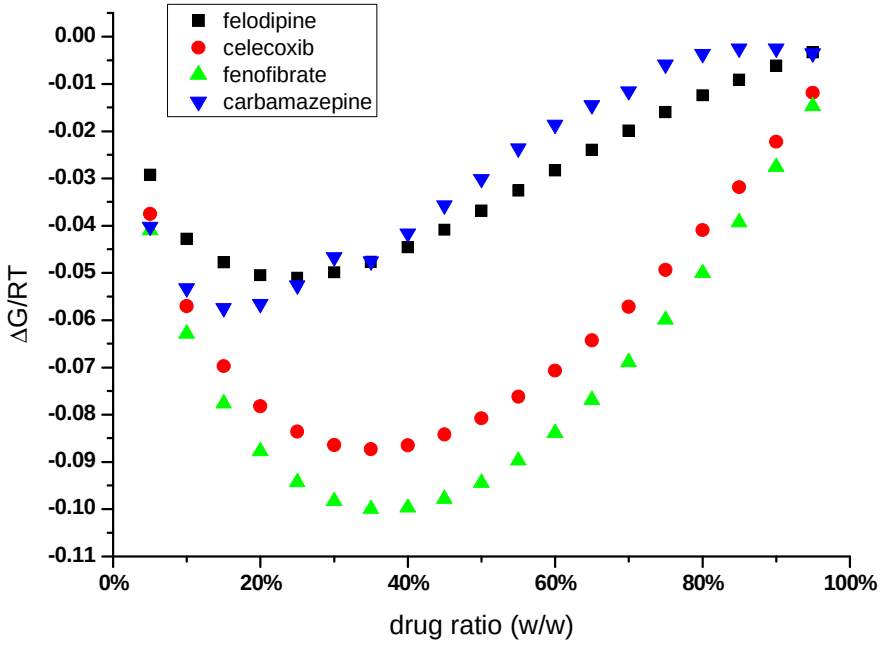

Figure 4.3: Plot of drug ratios in drug-polymer mixtures against calculated free energy change (*ΔG/RT*) of mixing of model drugs and EUDRAGIT® EPO.

Although the predicted model drugs-EUDRAGIT® EPO miscibility and solubility can be applied to room temperature, some potential issues regarding the accuracy of the method should be clarified. Solubility parameter theory only accounts for the direct contact energies between components and does not take into account the effects of entropy or the free volume of amorphous solids (29). It also should be noted that this theory is based on regular solution theory and deviations from solution behaviours such as changes in volume on mixing must be accounted for (23). Therefore, the factors mentioned above might be responsible for the inaccurate prediction of drug-polymer miscibility and solubility in comparison to real drug-polymer cases.

4.3.2 Melting point depression approach

4.3.2.1 Theoretical background

The melting point depression method was first introduced to be applied to predict the solid-solid miscibility between two polymers in 1975 (30). From then on, it was widely used in polymer science to investigate whether the crystalline polymer and the amorphous one were miscible when being mixed together on heating (31-33).

In the field of polymer science regarding the investigation of the miscibility between two polymers, the interaction parameter, χ, from the Flory-Huggins lattice-based theory was correlated with the melting point depression. Basically, on melting of a physical mixture of a crystalline polymer and an amorphous polymer alone in equilibrium state, the solid–liquid chemical potential (calculated as partial differential of the free energy from Flory-Huggins model) change of the crystalline polymer should be equivalent to the chemical potential difference (change) of the crystalline polymer in liquid state and in the amorphous polymer phase. Therefore the relationship between melting point depression and Flory-Huggins model was established by *Eq 4.8:* (30, 33, 34)

$$(1/T^{mix}_{M} - 1/T^{pure}_{M}) = -R/\Delta H_{fus} [ln\Phi_1 + (1/m_1 - 1/m_2)\Phi_2 + \chi\Phi_2^2] \qquad Eq\ 4.8$$

where T^{mix}_{M} is the melting temperature of the crystalline polymer in the mixture with another amorphous polymer, T^{pure}_{M} is the melting temperature of the crystalline material, ΔH_{fus} is the heat of fusion of the polymer crystal, and m_1 and m_2 are the degree of polymerization (the number of lattice of the individual polymer chain occupies) and R is the universal gas constant. A negative interaction parameter may indicate the two polymers are miscible as the negative interaction parameter can lead to a negative free energy change of mixing (*Eq 4.3*), whereas a positive interaction parameter may indicate the two polymers are immiscible or partially miscible.

The melting point depression method was further developed and applied in amorphous solid dispersions to predict the drug-polymer miscibility and solid solubility by Taylor's group (12, 21). The melting of a pure drug occurs when the chemical potential of the crystalline drug equals to the chemical potential of the molten drug (35). If the drug is miscible with a polymer, the mixing of the drug and the polymer is thermodynamically favourable, which is reflected by a negative free energy change of the mixture. Thus the chemical potential (partial Gibbs free energy) of the drug in the mixture with the polymer on melting will be smaller than the chemical potential of the pure crystalline drug on melting without the existence of the miscible polymer, resulting in the melting point depression of the crystalline drug Chemical potential is a function composed of pressure, temperature and Gibbs free energy and thus a decreased chemical potential can lead to a decreased melting point (34). In contrast, if the drug and polymer are immiscible, no melting point depression is expected because of unchanged chemical potential of the melted drug.

In amorphous drug-polymer solid dispersions, since the volume of a drug molecule is significantly smaller than a polymer chain, *Eq 4.8* was modified assuming the lattice size is the size of a single drug molecule (21):

$$(1/T^{mix}_{M} - 1/T^{pure}_{M}) = -R/\Delta H_{fus} [ln\Phi_{drug} + (1 - 1/m)\Phi_{polymer} + \chi\Phi_{polymer}^2] \qquad Eq\ 4.9$$

where T^{mix}_{M} is the melting temperature (depressed melting point) of the crystalline drug in the mixture with the amorphous polymer, T^{pure}_{M} is the standard melting point, ΔH_{fus} is the heat of fusion of the crystal, m is the ratio of the volume of the polymer to that of a single lattice site (defined here by the volume of the drug). Rearranging *Eq 4.9*, one can easily notice the linear relationship:

$$(1/T^{mix}_{M} - 1/T^{pure}_{M}) \times (\Delta H_{fus}/-R) - ln(\Phi_{drug}) - (1 - 1/m)\Phi_{polymer} = \chi\Phi_{polymer}^{2} \qquad Eq\ 4.10$$

The interaction parameter, χ, can be calculated as the slope of the linear regression between the left (calculated by the detected depressed melting points and the physical properties of drugs and polymers) and the right ($\Phi_{polymer}^{2}$) of *Eq 4.10*. The achieved interaction parameter can be used to judge whether an amorphous drug and a polymer are miscible by calculating the free energy change of mixing the drug and the polymer using *Eq 4.6*.

To further use the melting point depression method to calculate the drug-polymer solubility, it is essential to understand classic thermodynamic solubility in liquid theory. In liquid solutions, solubility occurs at equilibrium state where the chemical potential of the solute in solid state should be equivalent to that in the solution. Based on this theory, the relationship between the solubility and temperature can be written by:

$$dlnS/dT = \Delta H_{fus} / (RT^{2}) \qquad Eq\ 4.11$$

where S is the solubility of the material at temperature T in the solution, ΔH_{fus} is the heat of fusion of the solid. One can easily rewrite *Eq 4.11*with certain temperatures into:

$$lnS = -\Delta H_{fus} /R\ (1/T_2 - 1/T_1) \qquad Eq\ 4.12$$

Therefore, considering T_2 and T_1 as T^{mix}_{M} and T^{pure}_{M} from *Eq 4.9*, respectively, the solubility of the drug in the polymer can be calculated by combining *Eq 4.9* and *Eq 4.12* (21):

$$lnS_{drug} = ln\Phi_{drug} + (1 - 1/m)\Phi_{polymer} + \chi\Phi_{polymer}^{2} \qquad Eq\ 4.13$$

where S_{drug} is solubility of a drug in a polymer at the temperature at which solubility parameter is calculated, and in terms of melting point depression approach the temperature should be the depressed meting points under standard pressure.

4.3.2.2 Prediction of miscibility and solid solubility by the melting point depression approach

4.3.2.2.1 Effect of heating rate on the melting point depression

The influence of heating rates on the melting points of felodipine in the 50% (w/w) physical mixture with EUDRAGIT® EPO is shown in Figure 4.4. It can be seen that the onset value of the melting points of felodipine decreased from 141.3°C to 138.1°C, as well as the melting enthalpy decreased from 35.16 to 25.88J/g, as the heating rate reduced from 10 to 0.2°C/min. It indicates that melting point depression can be significantly affected by the applied heating rate. This is because the low heating rate may provide the drug with sufficient time to interact with the polymer. Based on these results, the heat rate of 0.2°C/min was used for the melting point depression study of felodipine as the most significant depressed melting point was achieved at this rate.

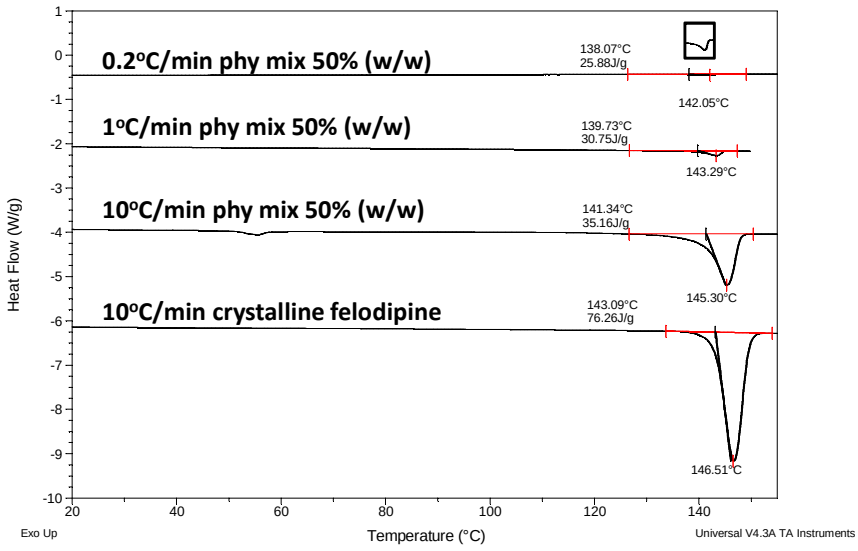

Figure 4.4: Influence of heating rate on melting points and melting enthalpy of felodipine in 50% (w/w) felodipine-EUDRAGIT® EPO physical mixture.

Melting point depression of celecoxib and carbamazepine in EUDRAGIT® EPO detected by DSC at the ramp of 1°C/min is shown in Figure 4.5. It can be seen that evident depressed melting points can be achieved for both drugs. The onset value of melting decreased from 160.5°C to 155.7°C for celecoxib and from 186.4°C to 180.5°C for carbamazepine. This demonstrates that the heating rate of 1°C/min was sufficiently low for investigating the melting point depression of celecoxib and carbamazepine in this project. Compared with felodipine, the degree of depressed melting points of celecoxib and carbamazepine were more significant, even felodipine was tested at a heating rate of 0.2°C/min. Physical mixtures of fenofibrate and EUDRAGIT® EPO were tested by DSC as well. However, no melting point depression was observed for 50% (w/w) fenofibrate-EUDRAGIT® EPO even with the lowest heating rate (0.2°C/min). The absence of melting point depression of fenofibrate indicates a low miscibility between fenofibrate and EUDRAGIT® EPO by this approach.

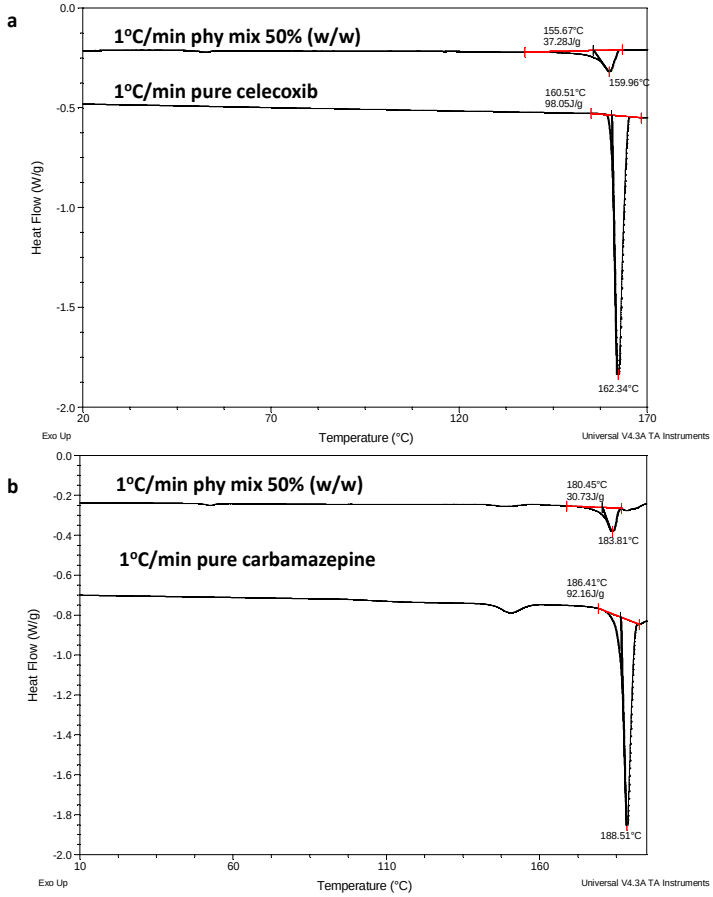

Figure 4.5: DSC results of 50% (w/w) physical mixture of (a) celecoxib and EUDRAGIT® EPO, and (b) carbamazepine and EUDRAGIT® EPO at the heating ramp of 10°C/min.

Different melting point behaviours of physical mixtures of model drugs with EUDRAGIT® EPO were observed. As mentioned earlier, melting point depression is caused by the miscibility between the two components. It has been reported that this miscibility was associated with interactions between the two components (21). As can be seen in the chemical structures of model drugs and EUDRAGIT® EPO (Chapter 2), felodipine, celecoxib and carbamazepine all have hydrogen bonding donor groups and EUDRAGIT® EPO contains carbonyl groups which can act hydrogen bonding acceptors. However, this is not the case for fenofibrate. Therefore it is possible that felodipine, celecoxib and carbamazepine at melted state with high mobility can interact with EUDRAGIT® EPO stronger than fenofibrate, leading to the greater depressed melting points. The reason why celecoxib and carbamazepine showed more depressed melting point values than felodipine at the same heating rate is not clear. However, according to the definition of the interaction parameter, it demonstrates that the interaction between carbamazepine, celecoxib and EUDRAGIT® EPO are stronger than that between felopdipine and EUDRAGIT® EPO (36).

4.3.2.2.2 Predicted drug-polymer miscibility and solid solubility by the melting point depression approach

Physical mixtures of model drugs and EUDRAGIT® EPO with drug-polymer ratios from 10% to 90% (w/w) were tested by DSC at 1°C/min for celecoxib and carbamazepine, and at 0.2°C/min for felodipine. As no melting point depression was detected for the physical mixture of fenofibrate and EUDRAGIT® EPO at the heating rate of 0.2°C/min, the melting point depression method was not applicable to fenofibrate. The physical properties of model drugs and EUDRAGIT® EPO required for the melting point depression method are listed in Table 4.4.

Table 4.4: Physical properties of model drugs and EUDRAGIT® EPO required for the melting point depression method.

Materials	Mw (g/mol)	Density (g/cm^3)[b]	ΔH_{fus} (kJ/mol)[c]
Felodipine	384.26	1.28	30.7±0.1
Celecoxib	381.37	1.52	37.2±0.2
Carbamazepine	236.27	1.30	24.0±0.1
EUDRAGIT® EPO	4840.00[a]	1.16[d]	-

a: assume 20 repeat units in the polymer (12).
b: obtained from Cambridge Structure Database
c: measured by DSC (n=3)
d: obtained from the instruction of commercial EUDRAGIT® EPO product

Felodipine- EUDRAGIT® EPO physical mixtures are discussed here as an example of using the melting point depression method. Using *Eq 4.10* with the detected depressed melting points from physical mixtures of felodipine and EUDRAGIT® EPO, the plot of $(1/T^{mix}_M - 1/T^{pure}_M) \times (\Delta H_{fus}/-R) - ln(\Phi_{drug}) - (1-1/m)\Phi_{polymer}$ against $\Phi_{polymer}^2$ was carried out as seen in Figure 4.6. It should be noted that the linearity can only be achieved with high drug concentration physical mixtures. The absence of linearity across the entire concentration range (data not shown) may reflect the well-known composition dependence of the interaction parameter as well as the increasingly unfavourable kinetics of the drug-polymer (12). With the acceptable linearity coefficient, according to the theory aforementioned, the interaction parameter can be achieved as the slope of the regression analysis, -1.0267 (felodipine).

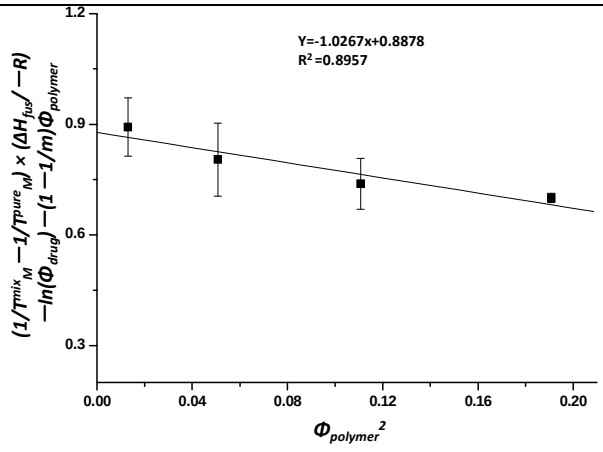

Figure 4.6: Regression analysis of melting point depression approach with low polymer volume fraction square.

Applying the same method to celecoxib and carbamazepine, interaction parameters were calculated as -0.9247 for celecoxib and -0.8549 for carbamazepine. Predicted negative solubility parameters for felodipine, celecoxib and carbamazepine indicate that three model drugs present good miscibility with EUDRAGIT® EPO (12, 21).

The good miscibility between felodipine, celecoxib and carbamazepine with EUDRAGIT® EPO can also be proved by using *Eq 4.6* to calculate free energy change of mixing drugs and EUDRAGIT® EPO (Figure 4.7). Through entire drug-polymer ratios, mixing is thermodynamically favourable as demonstrated by the negative free energy change values. Although interaction parameters predicted by solubility parameter and melting point depression approaches are different, they mutually suggest good miscibility between felodipine, celecoxib and carbamazepine with EUDRAGIT® EPO. Despite predicted high miscibility and solubility between fenofibrate and EUDRAGIT® EPO by solubility parameter approach, it is very likely that they are immiscible or partially miscible, since no melting point depression was observed. As mentioned earlier, this immiscibility between fenofibrate and EUDRAGIT® EPO on heating is very likely to be associated with the incapability of the formation of strong interaction (hydrogen bonding) between them. The study of the formation of hydrogen bonding in amorphous solid dispersions between model drugs and EUDRAGIT® EPO will be discussed in Chapter 6.

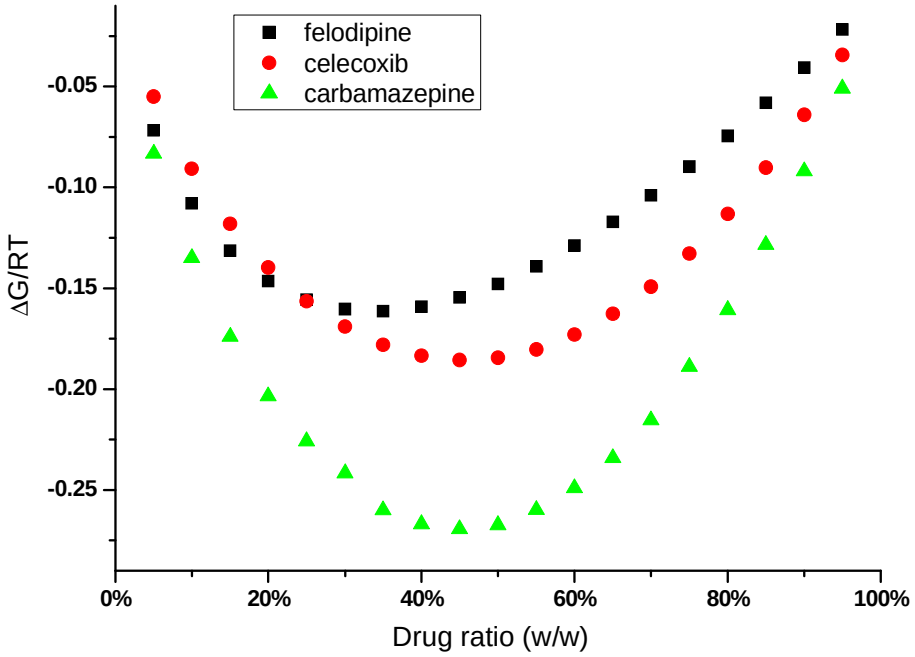

Figure 4.7: Free energy change (*ΔG/RT*) of mixing calculated using interaction parameter predicted by melting point depression approach.

It can be noted that the calculated values of free energy change of mixing model drugs with EUDRAGIT® EPO was different between the solubility parameter method and the melting point depression method. This is because the Flory-Huggins interaction parameter applied in the two methods was calculated in different ways (*Eq 4.7* for the solubility parameter method and *Eq 4.10* for melting point depression method). The free energy change of mixing model drugs and EUDRAGIT® EPO was dependent on the enthalpy change of mixing and the entropy change of mixing. The solubility parameter was associated with the enthalpy change of mixing (*Eq 4.4*). The entropy change of mixing always thermodynamically favoured the mixing as after mixing the system was more disordered than the individual drug and polymer. Therefore even with a positive interaction parameter (as calculated by the solubility parameter method), the mixing of drugs and polymer could still be thermodynamically favoured if the entropy change of mixing was superior over the enthalpy change of mixing. This result was also reported in the literature that nifedipine was miscible with PVP k29/30 even with a calculated interaction parameter of 0.5 (21).

Using *Eq 4.12* combined with calculated interaction parameters from the melting point depression approach, solid solubility of model drugs in EUDRAGIT® EPO can be predicted. The predicted solubility of model drugs in EUDRAGIT® EPO is listed in Table 4.5. Since the interaction parameter was obtained from melting point depression approach, the calculated solubility listed in Table 4.5 should be considered under the DSC running condition, more specifically, at the temperature close to the melting point of the crystalline drug. It also can be seen from Table 4.5 that the predicted solubility increased with increasing temperature, which can be considered as a

reasonable phenomenon that the solubility is likely to increase if temperature is increased. Moreover, e.g. at the temperature close to melting point of crystalline felodipine (409.74 to 413.50K), the variation of predicted solubility is very limited, ranging from 29.02% to 32.20% (w/w), which indicates that the equilibrium solid solubility of felodipine in EUDRAGIT® EPO is likely to be within this range, and averagely circa 31% (w/w). Using the same calculation method, solid solubility of celecoxib and carbamazepine in EUDRAGIT® EPO was calculated as 41% (w/w) for celecoxib and 46% (w/w) for carbamazepine.

Table 4.5: Predicted solid solubility of felodipine in EUDRAGIT® EPO by melting point depression approach.

drug	felodipine		celecoxib		carbamazepine	
concentration in the mixture (w/w)	temperature[a] (K)	Solubility (w/w)	temperature[a] (K)	Solubility (w/w)	temperature[a] (K)	Solubility (w/w)
10%	407.28	14.01%	415.42	13.74%	442.58	13.58%
20%	409.38	22.36%	419.82	16.64%	446.72	23.14%
30%	408.35	27.38%	423.25	24.32%	448.75	27.96%
40%	410.40	30.31%	426.92	31.10%	451.90	35.38%
50%	411.42	31.78%	427.14	36.57%	453.59	41.18%
60%	411.58	32.20%	428.34	40.38%	454.22	45.11%
70%	413.22	31.74%	432.01	42.26%	455.89	47.04%
80%	413.50	30.65%	433.40	42.06%	457.27	46.98%
90%	414.33	29.97%	434.32	41.81%	459.43	45.08%

a: the measured depressed melting temperature of the drug in the physical mixture by DSC

Using the melting point depression approach, carbamazepine was predicted to have the highest solid solubility (46% w/w) amongst model drugs, whereas using the solubility parameter method the solubility of which was the lowest (15% w/w). In addition, solid solubility of felodipine and celecoxib in EUDRAGIT® EPO predicted by the melting point depression method were both higher than that predicted by the solubility parameter method. In addition to the limitation of the

solubility parameter approach mentioned in 4.3.1.2, the restriction of the melting point depression approach should also be discussed. The results from the melting point depression approach can only be valid to describe the drug-polymer miscibility and solubility to a narrow temperature range which was close to the melting points of model drugs as the interaction parameter was calculated at that temperature range. At temperatures close to the melting points of model drugs, equilibrium of drug-polymer miscibility and solubility can be established rapidly as both the drugs and the polymer were in the liquid state with low viscosity. This can possibly lead to the accurate prediction of drug-polymer miscibility and solubility (16). At temperatures below T_g or at room temperature, the establishment of the equilibrium can take very long time period due to the high viscosity of drugs and polymers. Therefore using the melting point depression approach may overestimate the drug-polymer miscibility and solubility in comparison to using the solubility parameter approach.

It can be noted in Figure 4.4 and 4.5 that melting enthalpies of felodipine, celecoxib and carbamazepine detected by DSC from their 50% (w/w) physical mixture with EUDRAGIT® EPO are disproportional to those of pure crystalline drugs. This may indicate the occurrence of dissolution of model drugs into EUDRAGIT® EPO on heating whereby the exothermic enthalpy from the drug dissolving into the polymer offsets the endothermic melting enthalpy of the crystalline drug, leading to the disproportional melting enthalpy of the crystalline drug. Based on this phenomenon, a model was established by accurately describing the behaviour of drug-polymer physical mixture on heating to predict the drug-polymer solubility (22). This recently developed model was also applied in this project and will be discussed as in the following section.

4.3.3 Melting enthalpy approach

4.3.3.1 Theoretical background

The estimation of the solubility of drugs in polymers using the melting enthalpy of crystalline drugs in drug-polymer mixtures measured by DSC can be dated back to 1974 (37). The principle of the method can be described simply as that the fraction of the drug dissolved in the polymer does not contribute to the melting endotherm associated with the dispersed drug fraction. Accordingly, through plotting the measured melting enthalpy values as a function of a series of drug concentrations in physical mixtures and extrapolating to zero enthalpy, the solubility of the drug in the polymer could be estimated as the x-intercept of the plotted line. However, the validation of this method required a rapid heating rate to avoid the dissolution of the drug into the polymer on heating, and hence the exothermic dissolution will not offset the melting endotherm. This was further confirmed by the study in which a hyper DSC was used with different heating rates to determine the solubility of metronidazole (a crystalline drug) in silicone elastomer (38). In that study, different heating rate from 20 to 400^{o}C/min was applied to test the physical mixtures, and it

was found that the determined solubility was dependent on the heating rates: the higher the heating rate, the more accurate the determined solubility. The predicted solubility increased with increasing heating rates. This demonstrated that the dissolution of crystalline drugs into polymers in the physical mixture was difficult to be avoided on heating even at a relatively high heating rate (100°C/min).

This melting enthalpy measurement based approach was applied in this study to calculate the solubility of felodipine in EUDRAGIT® EPO using the DSC data obtained by testing their physical mixtures with different ratios at the heating rate of 10˚C/min. The plot of the melting enthalpy verses drug-polymer ratios is illustrated in Figure 4.8. It can be seen that the solubility is below 10% and after calculation the exact value is as low as 2.41% (w/w). However, tested at the heating rate of 0.2°C/min, no melting can be observed for 5% (w/w) physical mixture (data not shown), indicating solid solubility should at least be higher than 5% (w/w), which in turn proved the inaccuracy of this method.

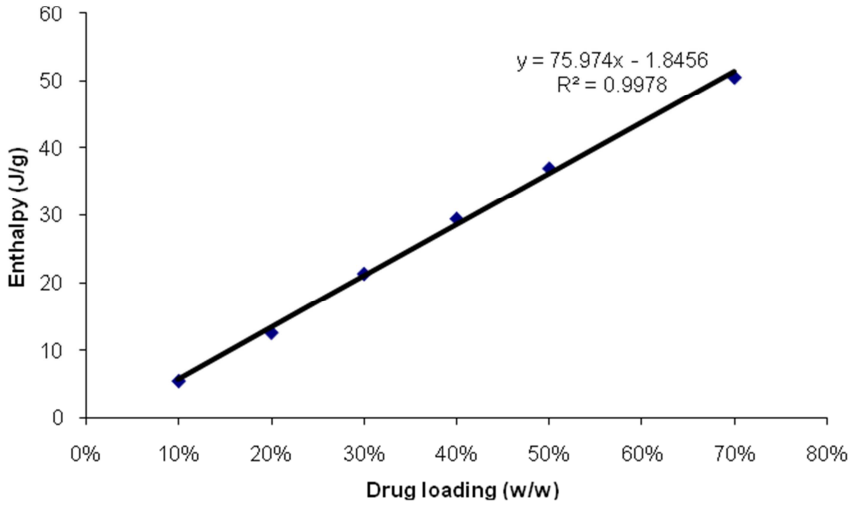

Figure 4.8: Melting enthalpy as a function of different drug loadings in the physical mixture of felodipine and EUDRAGIT® EPO at the heating rate of 10˚C/min.

Qi et al modified the melting enthalpy method and developed a new model predicting the solubility of the drug in the polymer (22). They assumed that the enthalpy value of the endothermic peak was composed of the energy involved the drug dissolution into the softened polymer and the melting of the crystalline drug. In this theory, it was suggested that different drug-polymer dissolution behaviours may occur depending on the drug concentrations in the physical mixtures. Firstly, if the drug concentration is considerably lower than the solubility of the drug in the polymer, drugs will completely dissolve into the polymer on heating and the linear relationship of the measured endothermic enthalpy against drug concentration should cross the (0,0) point (Figure 4.8). Secondly, for the extremely high drug concentration systems in which the polymer

concentration is lower than the solubility of the polymer in the melted drug, the polymer will completely dissolve into the drug and the linear relationship of the measured endothermic enthalpy against drug concentration still exists but with an intercept (Figure 4.8). Thirdly, with the drug concentration in the physical mixtures in between the two extremes, both the drug dissolution into the polymer and the polymer dissolution into the drug will take place simultaneously and this gives another linear relationship of measured endothermic enthalpy against drug concentration (Figure 4.8). Given the three situations mentioned above, ideally, one should expect to see three areas of drug-polymer behaviours as demonstrated in Figure 4.9. The two values on the x-axis from the two breaking points on the curve are the solubility of the drug in the polymer and the solubility of the polymer in the drug (depicted as P_A and P_B).

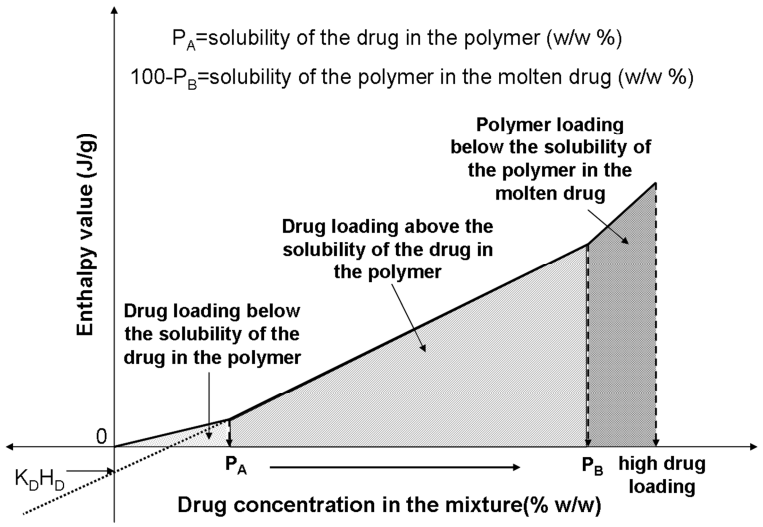

Figure 4.9: Three possible regions of drug-polymer mixing behaviour (22).

The detailed calculation of the drug-polymer behaviour is described as follows. The process occurring at low drug loading region can be expressed by:

$$H_t / (M_D + M_P) = X_D (H_f + H_D) \qquad \textit{Eq 4.14}$$

where H_t is the total amount of heat change of the exothermic peak, M_D is the mass of the drug dissolved in the polymer, M_P is the mass of the polymer, X_D is the weight fraction of the drug in the whole mixture, H_f is the heat fusion of the drug and H_D is the heat of dissolution of the drug in the polymer (assumed to be exothermic).

The intermediate region is represented by:

$$H_t / (M_D + M_P) = X_D (H_f - K_D H_D + K_P H_P) + K_D H_D \qquad \textit{Eq 4.15}$$

where K_D is the solubility of the drug in the polymer, K_P is the solubility of the polymer in the melted drug and H_P is the enthalpy of dissolution of the polymer in the drug.

The high drug ratio region can be written by:

$$H_t / (M_D + M_P) = X_D (H_f - H_P) + H_P \qquad Eq\ 4.16$$

4.3.3.2 Solid solubility predicted by the enthalpy approach

The same data sets used in the melting point depression approach was also used for this approach (physical mixtures of fenofibrate and EUDRAGIT® EPO were tested at the heating rate of 1°C/min). The plot of melting enthalpies of model drugs in physical mixtures with EUDRAGIT® EPO against drug ratios is shown in Figure 4.10. Three drug-polymer behaviours were observed for all physical mixtures of model drugs and EUDRAGIT® EPO. According to the theory mentioned above, two breaking points in the regression line are defined as solid solubility of the drug in the polymer and solid solubility of the polymer in the drug. Therefore, solid solubility of model drugs in EUDRAGIT® EPO is circa 20% (w/w) for felodipine, 20% (w/w) for fenofibrate, 30% (w/w) for carbamazepine and 40% (w/w) for fenofibrate.

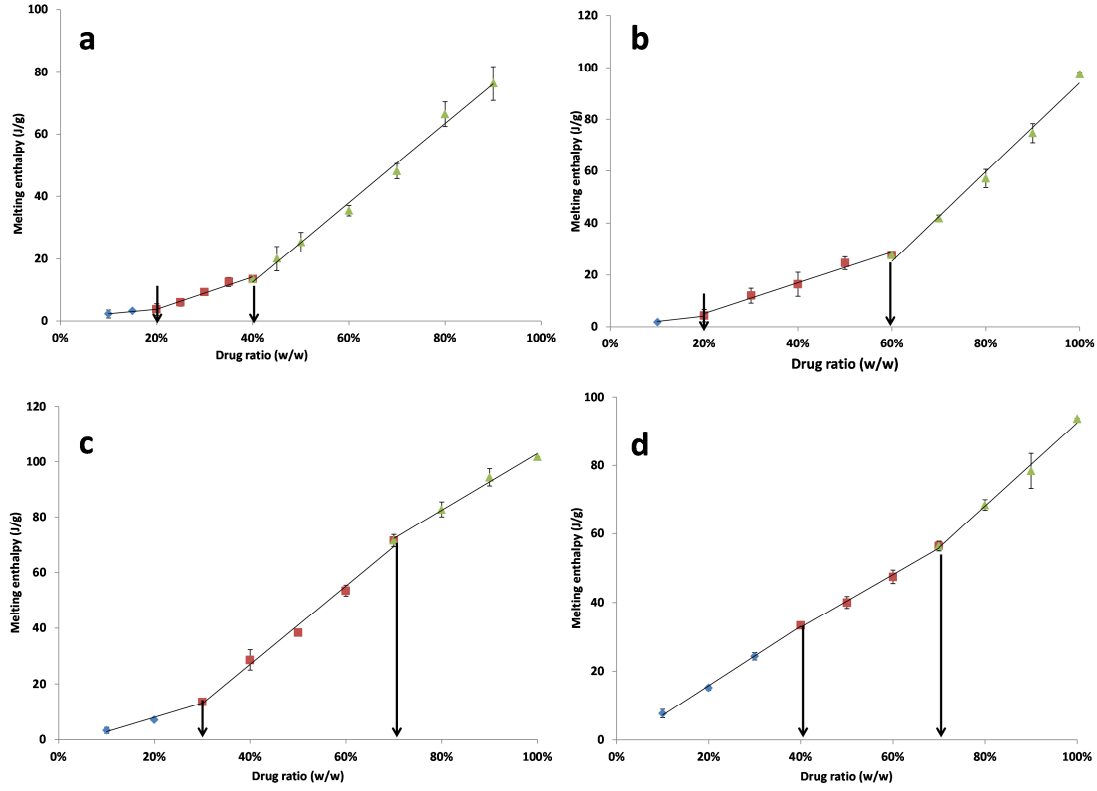

Figure 4.10: Plot of melting enthalpies of model drugs in physical mixtures against drug ratios (a: felodipine; b: celecoxib; c: carbamazepine; d: fenofibrate).

Solid solubility of model drugs in EUDRAGIT® EPO predicted by this approach was still restricted to a high narrow temperature range which is close to the melting points of the crystalline model drugs. This is because the drug-polymer behaviours mentioned in the theory occurred at high temperatures where the equilibrium of the dissolution of model drugs into the polymer can be established rapidly due to their low viscosity at high temperature. Therefore, there may still be deviation from the true drug-polymer solubility at room temperature.

Solid solubility of model drugs in EUDRAGIT® EPO predicted by different theoretical approaches are summarised in Table 4.6. It can be seen that the predicted solid solubility of individual drugs in EUDRAGIT® EPO varies significantly depending on the method applied. For instance, predicted solid solubility of carbamazepine in EUDRAGIT® EPO varies ranging from 15% to 46% (w/w) by different approaches. Several factors can contribute to the discrepancy of predicted solid solubility. Firstly, the applied approaches are all based on different assumptions and they all have limitations and restrictions, which may be far different from real drug-polymer cases. Secondly, solubility is a parameter associated with temperature and pressure, and it is reasonable that solid solubility predicted by the solubility parameter method is different form that by melting point depression method since the former is on the basis at room temperature and the latter is applied at the temperature close to melting points of model drugs. Thirdly, predicted solid solubility by theoretical approaches are thermodynamic solubility which is not related to the preparation process, for instance apparent solid solubility of drugs in polymers can vary significantly between prepared by film casting and by spray drying (39). Therefore, the application of theoretical approaches may not be accurate in predict the physical stability of amorphous solid dispersions prepared by different processing methods.

Table 4.6: Predicted solid solubility of model drugs in EUDRAGIT® EPO by different theoretical approaches.

APIs	Solubility by solubility parameter (w/w)[a]	Solubility by melting point depression (w/w)[b]	Solubility by thermal detection method (w/w)[c]
felodipine	25%	31%	20%
celecoxib	35%	41%	20%
carbamazepine	15%	46%	30%
fenofibrate	35%	-	40%

a:condition of 298.15K, standard pressure; b: condition of temperature close to melting points of individual drug, standard pressure; c: condition of temperature close to melting points of individual drug, standard pressure.

4.4 Conclusions

In this chapter, three commonly used theoretical approaches, including solubility parameter, melting point depression and a enthalpy method, were applied to predict model drugs-EUDRAGIT® EPO miscibility and solubility. Discrepancies of predicted results can be found due to the fact that the applied approaches are based on different assumptions and solid solubility was also predicted at different temperatures. It has been agreed that solid solubility is one of the key factors which plays important impact on physical stability of solid dispersions. However, predicted drug-polymer solubilities by different theoretical approaches vary in a relatively large range, which may indicate these methods are less accurate. More significantly, these theoretical approaches did not take into account the effect of processing method on the drug-polymer solubility. Therefore, in order to predict drug-polymer solubility more accurately, processing related prediction method is required to be established. Accordingly, in the next chapter, a practical method for the prediction of the solubility of drugs in melt extrudates is developed.

Reference

1. K. Kogermann, A. Penkina, K. Predbannikova, K. Jeeger, P. Veski, J. Rantanen, and K. Naelapaa. Dissolution testing of amorphous solid dispersions. International Journal of Pharmaceutics. 444:40-46 (2013).
2. M. Maniruzzaman, M.M. Rana, J.S. Boateng, J.C. Mitchell, and D. Douroumis. Dissolution enhancement of poorly water-soluble APIs processed by hot-melt extrusion using hydrophilic polymers. Drug Development and Industrial Pharmacy. 39:218-227 (2013).
3. F. Kedzierewicz, F. Villieras, C. Zinutti, M. Hoffman, and P. Maincent. A 3 year stability study of tolbutamide solid dispersions and β-cyclodextrin complex. International Journal of Pharmaceutics. 117:247-251 (1995).
4. A.T.M. Serajuddin. Solid dispersion of poorly water-soluble drugs: Early promises, subsequent problems, and recent breakthroughs. Journal of Pharmaceutical Sciences. 88:1058-1066 (1999).
5. M.M. Smikallaand N.A. Urbanetz. The influence of povidone K17 on the storage stability of solid dispersions of nimodipine and polyethylene glycol. European Journal of Pharmaceutics and Biopharmaceutics. 66:106-112 (2007).
6. T. Vasconcelos, B. Sarmento, and P. Costa. Solid dispersions as strategy to improve oral bioavailability of poor water soluble drugs. Drug Discovery Today. 12:1068-1075 (2007).
7. D.J. van Drooge, W.L.J. Hinrichs, M.R. Visser, and H.W. Frijlink. Characterization of the molecular distribution of drugs in glassy solid dispersions at the nano-meter scale, using differential scanning calorimetry and gravimetric water vapour sorption techniques. International Journal of Pharmaceutics. 310:220-229 (2006).
8. Y.B. Pawar, G. Shete, D. Popat, and A.K. Bansal. Phase behavior and oral bioavailability of amorphous Curcumin. European Journal of Pharmaceutical Sciences. 47:56-64 (2012).
9. J.A. Bairdand L.S. Taylor. Evaluation of amorphous solid dispersion properties using thermal analysis techniques. Advanced Drug Delivery Reviews. 64:396-421 (2012).
10. P. Ke, S. Hasegawa, H. Al-Obaidi, and G. Buckton. Investigation of preparation methods on surface/bulk structural relaxation and glass fragility of amorphous solid dispersions. International Journal of Pharmaceutics. 422:170-178 (2012).
11. S.L. Shamblin, X. Tang, L. Chang, B.C. Hancock, and M.J. Pikal. Characterization of the Time Scales of Molecular Motion in Pharmaceutically Important Glasses. The Journal of Physical Chemistry B. 103:4113-4121 (1999).

12. P. Marsac, T. Li, and L. Taylor. Estimation of Drug–Polymer Miscibility and Solubility in Amorphous Solid Dispersions Using Experimentally Determined Interaction Parameters. Pharm Res. 26:139-151 (2009).
13. P.H.-L. Tran, T.T.-D. Tran, J.-B. Park, D.H. Min, H.-G. Choi, H.-K. Han, Y.-S. Rhee, and B.-J. Lee. Investigation of physicochemical factors affecting the stability of a pH-modulated solid dispersion and a tablet during storage. International Journal of Pharmaceutics. 414:48-55 (2011).
14. M. Maniruzzaman, D.J. Morgan, A.P. Mendham, J.Y. Pang, M.J. Snowden, and D. Douroumis. Drug-polymer intermolecular interactions in hot-melt extruded solid dispersions. International Journal of Pharmaceutics. 443:199-208 (2013).
15. A.N. Campbelland A.J.R. Campbell. Concentrations, Total and Partial Vapor Pressures, Surface Tensions and Viscosities, in the Systems Phenol—Water and Phenol—Water—4% Succinic Acid. Journal of the American Chemical Society. 59:2481-2488 (1937).
16. F. Qian, J. Huang, and M.A. Hussain. Drug–polymer solubility and miscibility: Stability consideration and practical challenges in amorphous solid dispersion development. Journal of Pharmaceutical Sciences. 99:2941-2947 (2010).
17. D. Linand Y. Huang. A thermal analysis method to predict the complete phase diagram of drug–polymer solid dispersions. International Journal of Pharmaceutics. 399:109-115 (2010).
18. H. Al-Obaidi, M.J. Lawrence, N. Al-Saden, and P. Ke. Investigation of griseofulvin and hydroxypropylmethyl cellulose acetate succinate miscibility in ball milled solid dispersions. International Journal of Pharmaceutics. 443:95-102 (2013).
19. Martin's Physical Pharmacy and Pharmaceutical Sciences 2006.
20. D.J. Greenhalgh, A.C. Williams, P. Timmins, and P. York. Solubility parameters as predictors of miscibility in solid dispersions. Journal of Pharmaceutical Sciences. 88:1182-1190 (1999).
21. P. Marsac, S. Shamblin, and L. Taylor. Theoretical and Practical Approaches for Prediction of Drug–Polymer Miscibility and Solubility. Pharm Res. 23:2417-2426 (2006).
22. S. Qi, P. Belton, K. Nollenberger, N. Clayden, M. Reading, and D.M. Craig. Characterisation and Prediction of Phase Separation in Hot-Melt Extruded Solid Dispersions: A Thermal, Microscopic and NMR Relaxometry Study. Pharm Res. 27:1869-1883 (2010).
23. B.C. Hancock, P. York, and R.C. Rowe. The use of solubility parameters in pharmaceutical dosage form design. International Journal of Pharmaceutics. 148:1-21 (1997).
24. M. Dunkel. Z Physik Chem. 42:(1928).
25. R.A. Hayes. The relationship between glass temperature, molar cohesion, and polymer structure. Journal of Applied Polymer Science. 5:318-321 (1961).
26. A.T. DiBenedetto. Molecular properties of amorphous high polymers. I. A cell theory for amorphous high polymers. Journal of Polymer Science Part A: General Papers. 1:3459-3476 (1963).
27. R.F. Fedors. A method for estimating both the solubility parameters and molar volumes of liquids. Supplement. Polymer Engineering & Science. 14:472-472 (1974).
28. P.J. Flory. Priciples of polymer chemistry. Cornell University Press, Ithaca(1953).
29. B. Rudolf, H.A. Schneider, and H.J. Cantow. Pressure-volume-temperature behaviour of molten polymers. Polymer Bulletin. 34:109-116 (1995).
30. T. Nishiand T.T. Wang. Melting Point Depression and Kinetic Effects of Cooling on Crystallization in Poly(vinylidene fluoride)-Poly(methyl methacrylate) Mixtures. Macromolecules. 8:909-915 (1975).
31. Y. Hoei, K. Yamaura, and S. Matsuzawa. A lattice treatment of crystalline solvent-amorphous polymer mixtures on melting point depression. The Journal of Physical Chemistry. 96:10584-10586 (1992).
32. B. Borde, H. Bizot, G. Vigier, and A. Buleon. Calorimetric analysis of the structural relaxation in partially hydrated amorphous polysaccharides. I. Glass transition and fragility. Carbohydrate Polymers. 48:83-96 (2002).
33. E. Meaurio, E. Zuza, and J.-R. Sarasua. Miscibility and Specific Interactions in Blends of Poly(l-Lactide) with Poly(Vinylphenol). Macromolecules. 38:1207-1215 (2005).

34. P.B. Rimand J.P. Runt. Melting point depression in crystalline/compatible polymer blends. Macromolecules. 17:1520-1526 (1984).
35. M. Born. Thermodynamics of Crystals and Melting. Journal of chemical Physics(1939).
36. S. Cimmino, E. Pace, E. Martuscelli, and C. Silvestre. Crystallization of Multicomponent Polymer Systems. In M. Dosière (ed.), Crystallization of Polymers, Vol. 405, Springer Netherlands1993, pp. 381-402.
37. T. Felix, H. Anwar, and H. Takeru. Quantitative analytical method for determination of drugs dispersed in polymers using differential scanning calorimetry. Journal of Pharmaceutical Sciences. 63:427-429 (1974).
38. D. Gramaglia, B.R. Conway, V.L. Kett, R.K. Malcolm, and H.K. Batchelor. High speed DSC (hyper-DSC) as a tool to measure the solubility of a drug within a solid or semi-solid matrix. International Journal of Pharmaceutics. 301:1-5 (2005).
39. S. Janssens, A. Zeure, A. Paudel, J. Humbeeck, P. Rombaut, and G. Mooter. Influence of Preparation Methods on Solid State Supersaturation of Amorphous Solid Dispersions: A Case Study with Itraconazole and Eudragit E100. Pharm Res. 27:775-785 (2010).

Chapter 5 Development of milling method for the prediction of apparent drug-polymer solubility in hot melt extruded solid dispersions

5.1 Introduction

The prediction of solid solubility of drugs in polymers has attracted increasing amount of interests from pharmaceutical researchers since it has been considered as one of the most significant factors in affecting physical stability of amorphous solid dispersions (1-3). Several methods including Flory-Huggins lattice based theory, solubility parameter method, rheology test based method and melting enthalpy measurement based method, have been reported to be used to predict drug-polymer solid solubility (4-7). The involved assumptions and limitations of those methods may lead to a less accurate prediction in comparison to the real value. For instance, using melting point depression method may lead to the over estimation of drug-polymer solubility in comparison to the true solubility at room temperature as the method was only applied to the prediction of the solubility at temperatures close to the melting points of crystalline drugs. More significantly, theoretical based predictions do not take into account the effect of preparation process, whereby the apparent solid solubility can be significantly higher than the theoretical value (thermodynamic solubility) since the extra energy imposed by preparation process can disperse drug molecules evenly into polymer chains forming solid solution (8). This has been demonstrated by studies that the physical stability of solid dispersions prepared by different processing methods can be significantly different and this could be associated with the different apparent drug-polymer solubility caused by the different processing methods (9, 10).

Mechanical milling has been widely used in the pharmaceutical manufacturing, mainly for particle size reduction (11, 12). Recently, the use of milling to create amorphous pharmaceuticals and solid dispersions has been increasingly explored (13-19). However, although the effects of milling on crystalline drugs in terms of solid transformation, physical stability has been substantially studied, the effect of milling on the physical stability of amorphous solid dispersions on aging is still poorly understood (13, 20-22). Milling is an essential downstream process for hot melt extruded products (5, 23-25). So far, there is no systematic study reporting how milling can affect the stability of hot melt extruded solid dispersions, and how the milling process should be controlled to minimize any negative effects if they exist. In this chapter, firstly the impact of mechanical milling on the physical stability of felodipine-EUDRAGIT® EPO was investigated. By studying this model system, an effective and practical method to predict drug-polymer solid solubility in melt extrudates was proposed and applied to other model drugs including celecoxib, fenofibrate and carbamazepine.

Previously, solid solubility of model drugs in EUDRAGIT® EPO was predicted by theoretical approaches in Chapter 4. However, as mentioned above, theoretically predicted solid solubility can deviate significantly from the values in solid dispersions prepared by different processes. Therefore, in order to measure the solid solubility more accurately (taking into account of the physical stability), a practical method, mechanical milling, was developed and applied in predicting the apparent solid solubility of drugs in hot-melt extrudates. In combination with theoretical values, it is anticipated that this approach will provide an accurate and reliable measurement of solid solubility that can be practically applied in hot melt extruded formulations in the pharmaceutical industry.

Research objectives

1. To investigate the effect of milling on the physical stability of felodipine-EUDRAGIT® EPO melt extrudates.

2. To develop a milling based method for the prediction of apparent drug-polymer solubility in melt extrudates.

3. To predict apparent apparent solid solubility of model drugs in melt extrudates using milling method.

5.2 Experimental methods

5.2.1 Hot melt extrusion

Hot melt extrusion was performed using a Thermo Scientific HAAKE MiniLab II (Thermo Scientific, UK) with co-rotating twin screws. Crystalline model drugs and EUDRAGIT® EPO powder with ratios from 10:90 to 70:30 (w/w) were pre-mixed in mortar and pestle before melt extrusion. The operation temperature was set at 1 to 5 degree higher than the melting points of crystalline model drugs with a dwell time in the extruder of 5 minutes. The rotating speed of the screws was 100rotation/min. A round shape die with diameter of 2mm was attached to the extruder.

5.2.2 Ball milling

Strand form extrudates were milled by Retsh MM400 Ball Milling (RETSH, Haan, Germany). For felodipine-EUDRAGIT® EPO systems, samples were milled for 5, 10, 30, and 60 minutes at the frequency of 30HZ by a single 7mm stainless steel ball to investigate the effect of milling periods. For other model drugs-EUDRAGIT® EPO systems, samples were milled for 10min. The particle size of the milled powders used for testing was controlled by sieve to between 63 and 106μm.

The strand form and milled felodipine-EUDRAGIT® EPO extrudates were stored under 75%RH at room temperature for up to 6 months and were characterised by modulated temperature differential scanning calorimetry (MTDSC), powder X-Ray diffraction (PXRD), attenuated total reflectance-fourier transform infrared spectroscopy (ATR-FTIR) and scanning electron microscopy (SEM) at regular intervals. For other systems including milled celecoxib-EUDRAGIT® EPO and carbamazepine-EUDRAGIT® EPO extrudates, samples were stored under 75%RH at room temperature for different time periods and were tested by MTDSC.

5.2.3 Physicochemical characterisation

Parameters of characterisation technology including MTDSC, PXRD, ATR-FTIR and SEM refers to Chapter 2 (2.2.2.1.3 for MTDSC, 2.2.2.4.2 for ATR-FTIR, 2.2.2.5.2 for PXRD, 2.2.2.6.2 for SEM)

5.3 Results and discussion

For an amorphous molecular dispersion based formulation, having a drug loading lower than the solid solubility of the drug in the polymer has been suggested as the safest option for minimizing the physical instability of amorphous solid dispersions on aging (4, 26). However, so far it is still difficult to accurately measure the solid solubility of drugs in amorphous solid dispersions. In addition, although the effects of milling on the behaviours of crystalline drugs, such as solid state transformation, have been substantially investigated (13, 20-22), very few studies have been carried out to evaluate the effect of milling on the behaviours of amorphous solid dispersions. Therefore, firstly in this chapter, the effect of mechanical milling on the recrystallization behaviour of milled hot melt extrudates was investigated. Secondly, via the evaluation of the impact of milling on the physical stability of melt extruded felodipine-EUDRAGIT® EPO systems, a practical approach to predict apparent solid solubility of drugs in melt extrudates, mechanical milling, was developed.

5.3.1 Effects of milling on the physical stability of felodipine-EUDRAGIT® EPO melt extrudates

5.3.1.1 Effect of drug loading

Felodipine-EUDRAGIT® EPO melt extrudates with drug loadings from 10% to 70% (w/w) were milled for 5min. PXRD results of freshly prepared and milled samples are shown in Figure 5.1. It can be seen that samples with all drug loadings showed amorphous halos rather than crystalline peak features, indicating no significant amount of recrystallized felodipine was generated immediately after 5min milling.

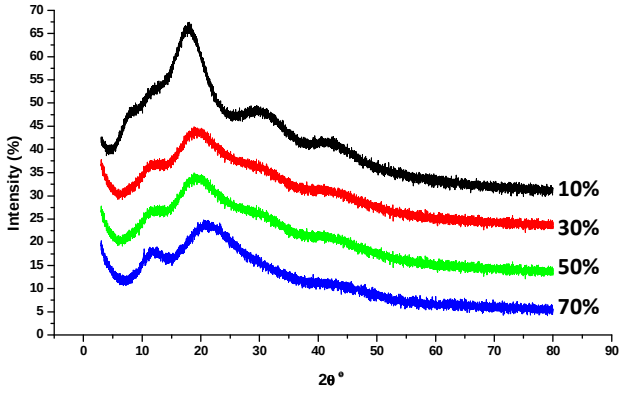

Figure 5.1: PXRD results of freshly prepared and milled (5min) felodipine-EUDRAGIT® EPO melt extrudates.

Freshly milled felodipine-EUDRAGIT® EPO melt extrudates were also tested by MTDSC. No recrystallization or melting can be detected for fresh formulations with the drug loadings below 50% (w/w), and the MTDSC results of freshly milled 10%-50% (w/w) extrudates were identical to the corresponding freshly prepared strand from extrudates (Figure 5.2). This suggests milling has no instant effect on the physical state of felodipine-EUDRAGIT® EPO melt extrudates with drug loadings at and below 50% (w/w).

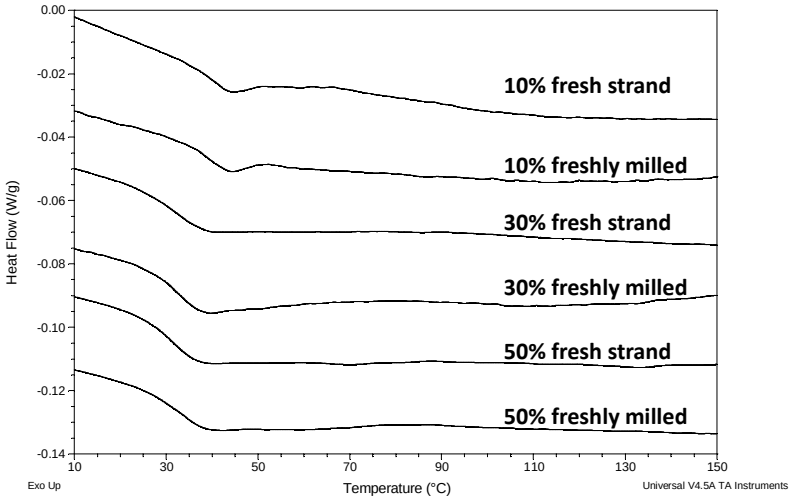

Figure 5.2: MTDSC results of 10%-50% (w/w) freshly prepared and milled (for 5min) and fresh strand form extrudates.

However, MTDSC measurements of 70% (w/w) extrudates gave significantly different results as seen in Figure 5.3. In comparison to 70% (w/w) strand form extrudate, the freshly milled 70% (w/w) extrudate (milled for 5min) was detected with an evident recrystallization and a subsequent

melting. To calculate the amount of recrystallized felodipine in the extrudates measured by MTDSC, the following equation can be used:

$$W_{crys}\% = (\Delta H_{extrudate} / \Delta H_{drug}) \times W_{drug\ loading} \qquad Eq\ 5.1$$

where $W_{crys}\%$ is the percentage of the detected crystalline drug by DSC in the system, $\Delta H_{extrudate}$ is the melting enthalpy of crystalline drug in the extrudates measured by DSC, ΔH_{drug} is the melting enthalpy of the pure drug (felodipine) measured by DSC, $W_{drug\ loading}$ is the drug loading in the extrudate and $W_{drug}\%$ is the amount of crystalline drug in the extrudates. Using *Eq 5.1* the total amount of crystalline felodipine measured increased from 0.1% (un-milled strand) to 21.5% (w/w) (5min milled powder).

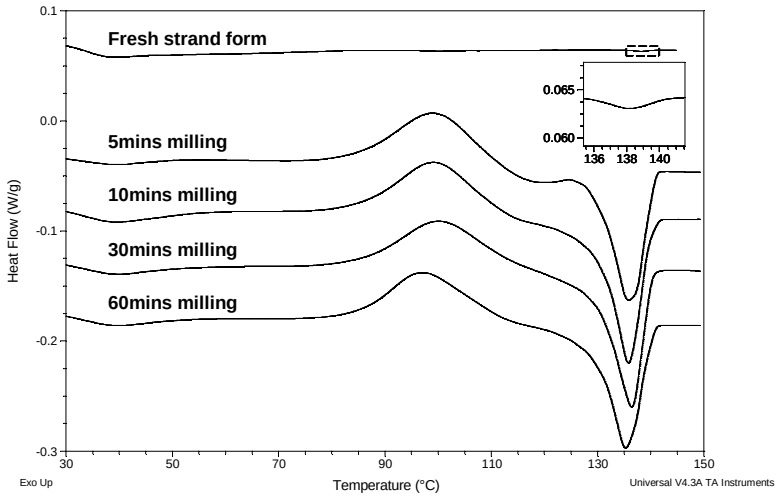

Figure 5.3: MTDSC results of 70% (w/w) strand form and milled for different time periods felodipine-EUDRAGIT® EPO samples.

It can be seen in Figure 5.3 that no recrystallization was detected in the 70% (w/w) freshly prepared strand form sample, and thus the detected low amount (0.6% w/w) of melted crystalline felodipine by DSC was highly likely to be the undissolved crystalline drug in the preparation of hot melt extrusion. In contrast, a large amount of recrystallization followed by melting was observed in the 5min milled 70% (w/w) extrudates. This indicates that milling can instantly affect the physical state of 70% (w/w) felopdipine-EUDRAGIT® EPO extrudates. The detected recrystallization of amorphous felodipine in the milled extrudates demonstrates that after milling, a certain portion of amorphous felodipine had already phase separated from the bulk amorphous solid dispersions. This separated amorphous felodipine phase can instantly recrystallize if treated by heating (such as the heating during a DSC scan). The amorphous felodipine (the amount of instable felodipine in amorphous solid dispersions) generated by milling may not recrystallize instantly at room temperature after milling, but it may have a high potential to convert back to crystalline form on

aging under stressed conditions (stressed humidity or temperature), and may consequently affect dissolution performance.

In summary of the milling effect on extrudates with different drug loadings, milling only had impact on the physical state of felopdipine-EUDRAGIT® EPO melt extrudates with high drug loading (70% w/w). It can instantly generate a certain level of amorphous phase separation in the 70% (w/w) extrudates. Compared with the predicted solubility by different theoretical approaches in Chapter, it can be concluded that those method underestimated the apparent solubility of felodipine in melt extrudates. Even for 50% (w/w) extrudates (higher than all predicted solubility), there was no instant effect of the physical behaviour of this sample.

5.3.1.2 Effect of milling time

Milling was proved to have the potential to affect the physical stability of 70% felodipine-EUDRAGIT® EPO extrudates. In order to understand the milling effect on the physical stability more thoroughly, the study of different milling duration time on freshly prepared 10%-70% (w/w) felodipine-EUDRAGIT® EPO extrudates was carried out as the prolonged milling time may influence the physical state more significantly. Freshly prepared 10%-70% (w/w) samples were milled for different time periods up to 60min. However, even with 1 hour milling time, no recrystallization or melting was detected by DSC in the freshly milled 10%-50% (w/w) extrudates, which indicates prolonged milling time (as long as 1 hour) has little instant effect on the physical state of these samples. The DSC results of 10-50% (w/w) extrudates milled for 1 hour were identical to those milled for 5min.

Freshly prepared 70% (w/w) extrudates milled for different time periods showed significantly different results. As can be seen in Figure 5.3, samples milled with different duration time (from 5min to 1h) all showed exothermic recrystallization peaks at 96-99^{o}C suggesting milling can increase physical instability of 70% (w/w) extrudates instantly as mentioned above. The calculated crystallinity of felodipine in the system using *Eq 5.1* showed that after 10min milling, no further increase of the amount of recrystallized felodipine was observed and the crystallinity reached plateau (Figure 5.4). This possibly indicates in 70% (w/w) extrudates only a certain amount of felodipine can be made instable by milling. The exothermic enthalpy of recrystallization of 70% (w/w) samples milled for different time length were also studied as seen in Figure 5.4. The enthalpy values of the recrystallization peak show reductions with increasing milling time periods from 5 to 30min, and seem to reach a plateau after 30min. The melting enthalpy of crystalline felodipine was mainly contributed by the recrystallization of amorphous felodipine induced by milling as discussed above. Therefore, given the very close values of crystallinity of felodipine in sample milled for different time periods (10min to 1h), the reduced recrystallization enthalpy may

suggest that the amount of felodipine crystals already present in the system after milling (before heating by MTDSC) increases slightly with the milling time.

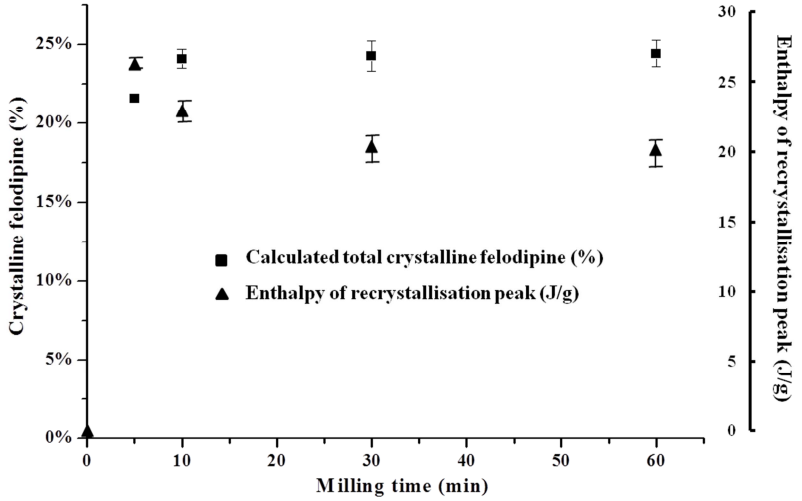

Figure 5.4: Calculated crystallinity in 70% (w/w) HME felodipine-EUDRAGIT® EPO systems milled for different timeperiods based on the total melting enthalpy and their corresponding recrystallization enthalpy.

10%-70% (w/w) felodipine-EUDRAGIT® EPO melt extrudates milled for different time periods were further studied by ATR-FTIR. ATR-FTIR results of 10%-50% (w/w) samples milled for 1h showed identical spectra to the corresponding fresh strand samples (Figure 5.5), indicating long milling time did not destabilise felodipine-EUDRAGIT® EPO melt extrudates with these drug loadings. The ATR-FTIR results showed good agreement with the DSC results for 10-50% (w/w) milled extrudates.

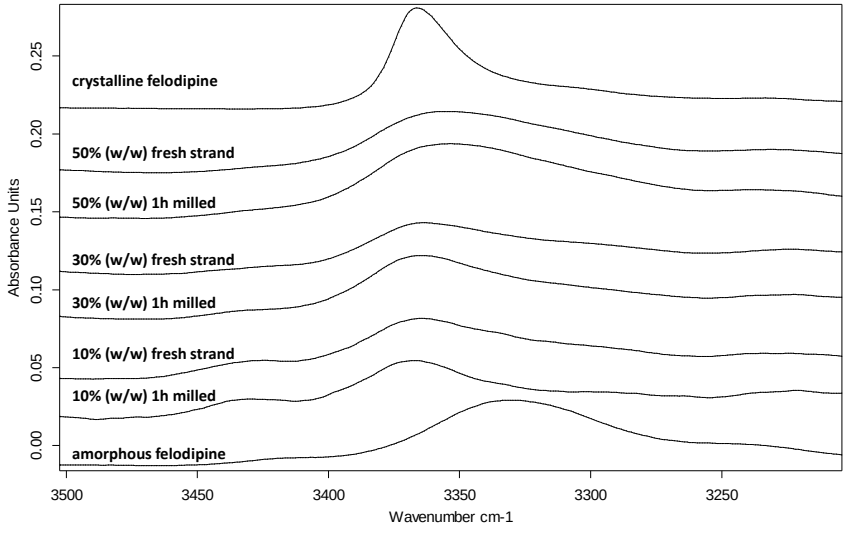

Figure 5.5: NH group from felodipine in 10-50% (w/w) felodipine-EUDRAGIT® EPO freshly prepared strand form and 1 hour milled melt extrudates.

ATR-FTIR results of 70% (w/w) freshly milled extrudates for different time periods also showed good agreement with MTDSC results. It has been reported that NH group from felodipine was an evident indicator of the drug being amorphous or crystalline (27). As seen in Figure 5.6, freshly prepared 70% (w/w) strand form extrudates before milling shows a single NH peak at 3343cm^{-1} which is in between the NH peak from crystalline felodipine (3367cm^{-1}) and the NH peak from amorphous felodipine (3333cm^{-1}). This NH peak position in the solid dispersions is likely because that the carbonyl groups from the polymer can affect the hydrogen bonding formed between two felodipine molecules via competition with the carbonyl groups from felodipine molecules. It has been discussed that hydrogen bonding between two felodipine molecules was stronger in amorphous form than in crystalline form (27). Therefore, although lack of the evidence of forming hydrogen bonding between felodipine and EUDRAGIT® EPO, this competition effect is possible to weaken the hydrogen bonding between two drug molecules leading to the NH peak shift.

After 5min milling, the original single 3341cm^{-1} peak (from 70% w/w strand form extrudates) separated into two peaks, 3367cm^{-1} representing crystalline felodipine and 3335cm^{-1} representing amorphous felodipine. The occurrence of phase separation proved that milling could significantly affect the physical stability of 70% (w/w) extrudates even without the treatment of heat.

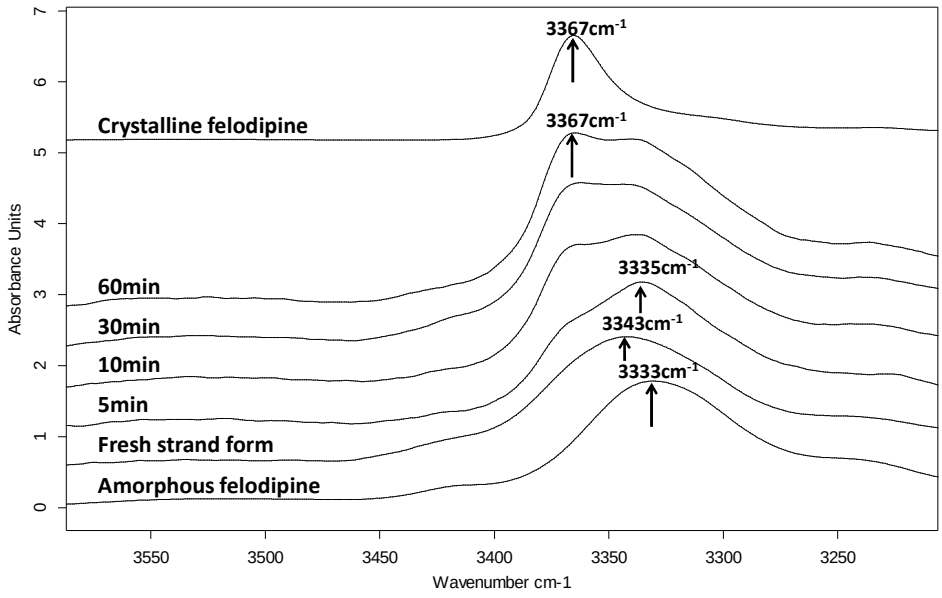

Figure 5.6: NH group from felodipine in 70% (w/w) felodipine-EUDRAGIT® EPO melt extrudates milled for different time periods (from top to bottom: crystalline felodipine, milled for 60 min, milled for 30 min, milled for 10 min, milled for 5 min and amorphous felodipine).

It also can be seen form Figure 5.6 that the intensity ratios of crystalline peak (3367cm^{-1}) to amorphous peak (3335cm^{-1}) in 70% (w/w) samples increased with increasing milling time periods from 5min to 30min, and plateaued after 30min. This was proved by the calculation of ratios of these two peaks from 70% (w/w) extrudates milled for different time periods as shown in Figure

5.7. The reaching plateau after 30min milling can be clearly seen. This suggests that milling could not generate more felodipine crystals in the 70% (w/w) extrudates after 30min milling processing, which explains the plateau of recrystallization enthalpy after 30min milling detected in the DSC results (Figure 5.4).

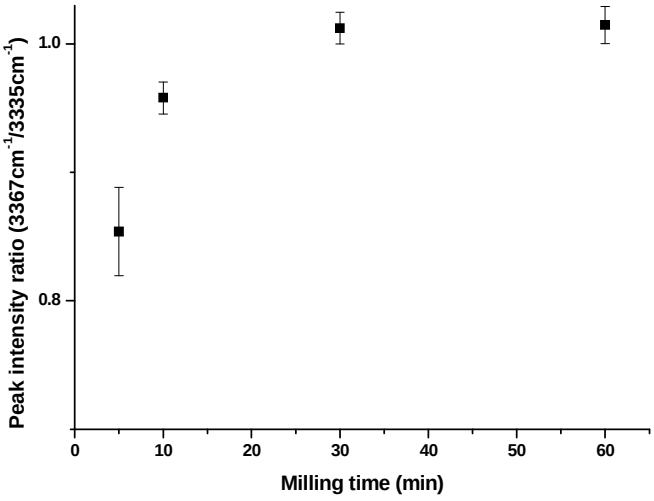

Figure 5.7: Peak intensity ratio of 3367 to 3335 from 70% (w/w) extrudates milled for different time periods.

5.3.1.3 Effect of heat-treatment after milling

As mentioned previously, amorphous phase separation can be instantly generated by milling in 70% (w/w) felodipine-EUDRAGIT® EPO melt extrudates, and the recrystallization of the generated amorphous felodipine phase can be induced by heating in DSC. In order to gain better understanding of the behaviour of the phase separated amorphous felodipine generated by milling, VT-ATR-FTIR was used to test freshly prepared strand form and 5 min milled extrudates.

5.3.1.3.1 Freshly prepared strand form extrudates

VT-ATR-FTIR was applied to 10%-70% (w/w) fresh strand form extrudates. Results showed that no recrystallization or melting was detected on heating in any sample. Therefore, only the VT-ATR-FTIR results of freshly prepared strand form 70% (w/w) extrudates are discussed here as an example to show the effect of heat-treatment on the fresh strand extrudates (Figure 5.8). It can be seen in Figure 5.8c that the NH peak from felodipine in 70% (w/w) amorphous solid dispersion shifted from 3343cm^{-1} (in between the amorphous 3335cm^{-1} and crystalline 3367cm^{-1} NH peak) at 30^{o}C to 3358cm^{-1} at 160^{o}C. After heating up to the melting point, no NH peak from crystalline felodipine (3367cm^{-1}) was detected, indicating no recrystallization or melting of crystalline felodipine occurred during heating in the 70% (w/w) fresh strand extrudates. The NH peak shift is due to the increased molecular motion on heating which results in the weakened hydrogen bonding between two felodipine molecules. The absorbance of the two peaks (3343cm^{-1} and 3358cm^{-1}) on

heating was recorded and the trend of the absorbance changing of the the two peaks was identical (Figure 5.8b). This trend can also be clearly seen in the result of 3D graph (Figure 5.8a). The VT-ATR-FTIR results showed that no recrystallization or melting in fresh strand extrudates was induced by heat-treatment. The results correlate well with the previous MTDSC tests (Figure 5.3 fresh strand form).

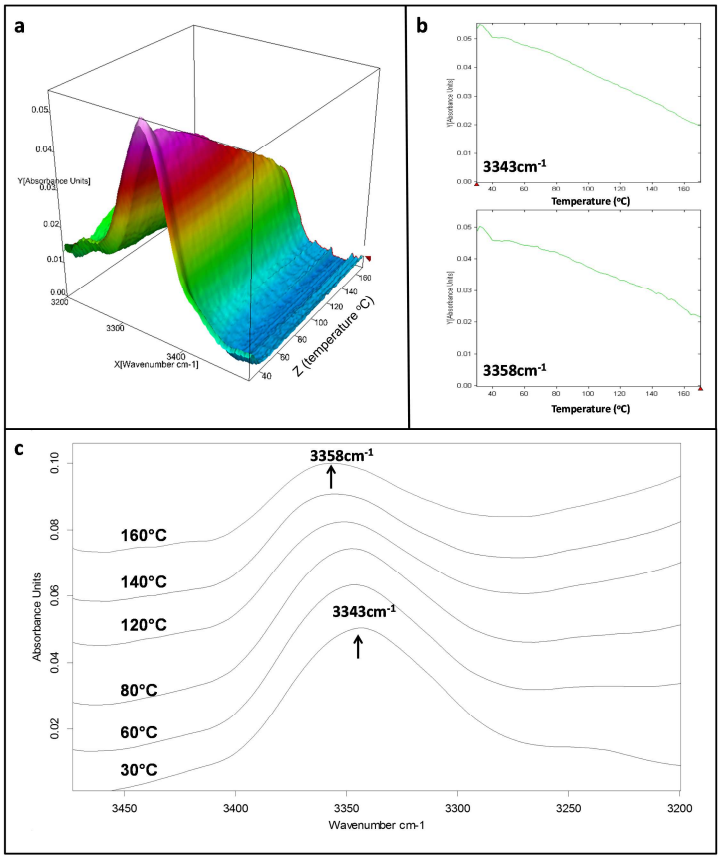

Figure 5.8: NH group of freshly prepared strand form 70% (w/w) felodipine-EUDRAGIT® EPO melt extrudates tested by heated up from 30 to 160°C at the ramp of 2°C/min (a: 3D spectra of the NH peak on heating; b: the absorbance of 3343cm^{-1} and 3358cm^{-1} on heating; C: 2D spectra the NH peak position on heating).

5.3.1.3.2 Freshly prepared and milled extrudates

Freshly prepared and milled (for 5min) felodipine-EUDRAGIT® EPO melt extrudates were tested by VT-ATR-FTIR. No crystalline felodipine was detected in 10% and 30% (w/w) sample the spectra on heating. This result is identical to the strand form samples, indicating heat-treatment could not induce phase separation in these samples.

Freshly milled 50% (w/w) extrudates showed interesting IR spectra on heating as shown in Figure 5.9. The NH peak of felodipine shifted from 3353cm^{-1} at 30°C to 3372cm^{-1} at 160°C (Figure 5.9c). A separation of the single 3353cm^{-1} peak (into 3353cm^{-1} and 3372cm^{-1}) was observed with

increasing temperature and it became evident at 140°C. This may suggest the occurrence of recrystallization in the milled 50% (w/w) induced by the heat-treatment as the 3372cm^{-1} peak was very close to crystalline felodipine NH peak (3367cm^{-1}). However, the trend of the absorbance change on heating of the two peaks (3353cm^{-1} and 3372cm^{-1}) was identical (Figure 5.9b), which indicates that there was very little recrystallization (if large recrystallization occurred on heating, an increased absorbance of crystalline felodipine NH peak should be observed on heating). Therefore, the VT-ATR-FTIR results may suggest that the physical state of the freshly milled 50% (w/w) extrudates could be affected by heating instantly but at a very low level.

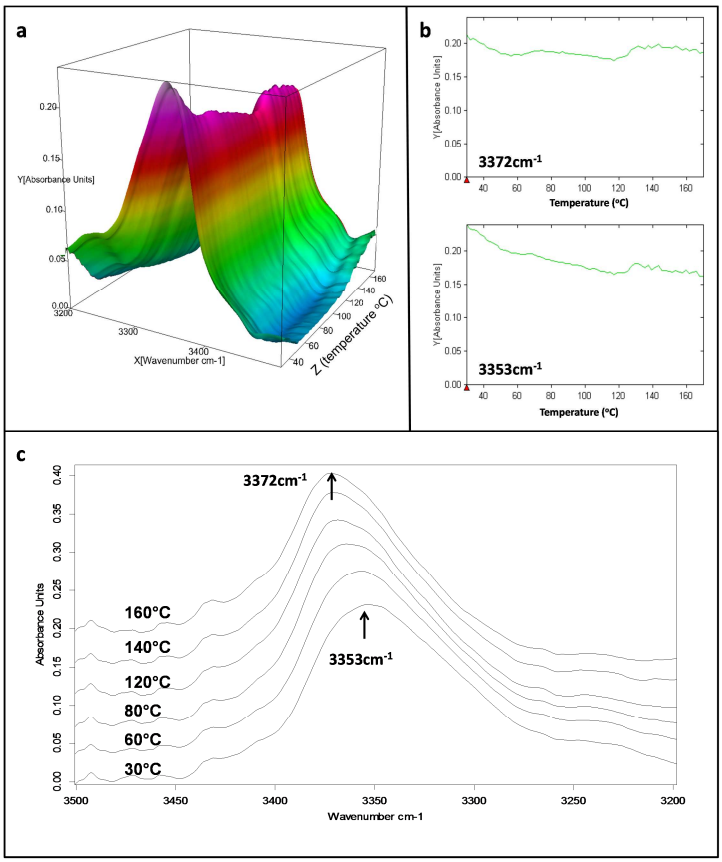

Figure 5.9: NH group of freshly prepared and milled 50% (w/w) HME felodipine-EUDRAGIT® EPO extrudates tested by heated up from 30 to 160°C at the ramp of 2°C/min (a: 3D spectra of the NH peak on heating; b: the absorbance of 3353cm^{-1} and 3372cm^{-1} on heating; C: 2D spectra the NH peak position on heating).

Freshly prepared and milled 70% felodipine-EUDRAGIT® EPO extrudates showed significantly different results in comparison to the corresponding strand form samples as seen Figure 5.10. On heating to 120°C, the intensity of 3335cm^{-1} peak which represents amorphous felodipine continued increasing with increasing temperature, indicating more and more amorphous felodipine was separating from the bulk amorphous solid dispersions on heating. When the temperature reached 140°C, the peak at 3367cm^{-1} representing crystalline felodipine became the dominant band. This

was proved by the trend of the absorbance of the two peaks (3335cm-1and 3367cm^{-1}) on heating as well. A drastic drop of 3335cm^{-1} peak (amorphous felodipine) can be observed within the temperature range from 120 to 140^{o}C. In contrast, the intensity of the 3367cm^{-1} peak kept increasing with increasing temperature within the same range (120 to 140^{o}C). The peak shift and peak intensity change demonstrates phase separation of the amorphous felodipine and solid transformation from amorphous felodipine to crystalline felodipine on heating. This confirms that there is a reasonable amount of phase separated amorphous felodipine generated by milling and the amount of which can recrystallize if induced by heating.

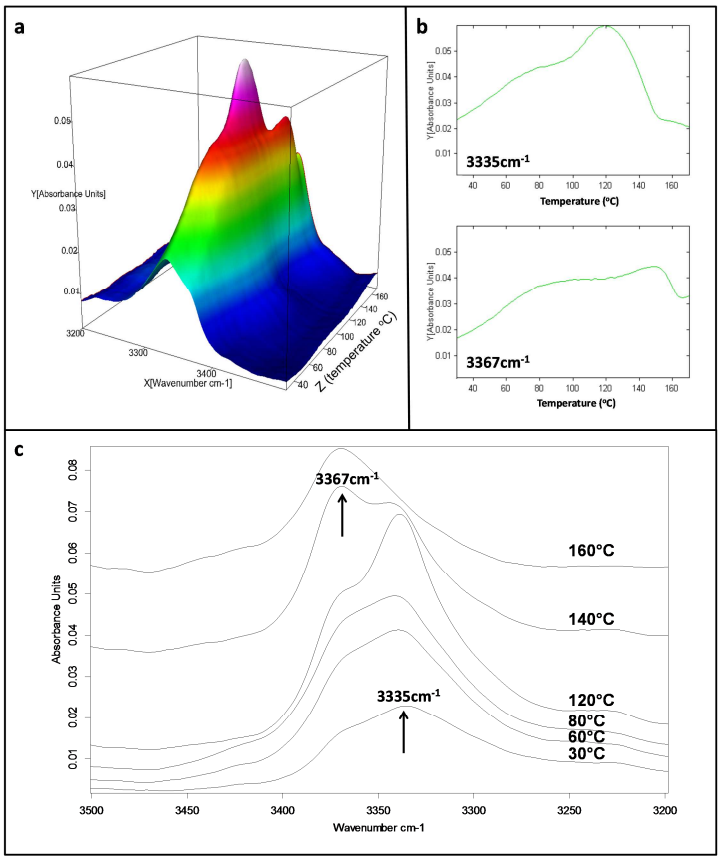

Figure 5.10: NH group of freshly prepared and milled 70% (w/w) HME felodipine-EUDRAGIT® EPO extrudates tested by heated up from 30 to 160^{o}C at the ramp of 2^{o}C/min (a: 3D spectra of the NH peak on heating; b: the absorbance of 3353cm^{-1} and 3372cm^{-1} on heating; C: 2D spectra the NH peak position on heating).

5.3.1.4 Effect of aging

The effect of milling on the physical stability of freshly prepared and milled 10%-70% (w/w) was studied and results showed that milling could instantly generate phase separation in fresh strand form 70% (w/w) extrudates. With the imposed energy on the extrudates by milling, the physical stability of amorphous solid dispersions might be affected on aging under stressed conditions (high humidity or temperature) as milled drug-polymer extrudates may exist at a higher energy level in

comparison to the strand form extrudates. Therefore, it is essential to evaluate the behaviour of the real-time physical stability of milled extrudates for a fuller understanding of the milling effect on the physical stability of felodipine- EUDRAGIT® EPO melt extrudates. Freshly prepared strand form and milled 10-70% (w/w) extrudates were stored under 75%RH/room temperature to compare the effect of aging on the milled samples.

SEM images of strand form and milled extrudates are shown in Figure 5.11. As seen in the SEM images, no particles were observed on the freshly milled extrudates. On the contrary, crystal-like small particles with the size below 10µm were observed on the surface of 50% and 70% (w/w) fresh strand form extrudates. This is possibly because after milling the small amount of particles on the surface of 50% (w/w) and 70% (w/w) fresh extrudates were diluted whereby the low quantity of the surface crystals were dispersed into the bulk by milling. After 6 months aging under 75%RH/room temperature, a large amount of particles were observed both on 50% (w/w) and 70% (w/w) strand form and milled extrudates. In comparison to strand form samples, the number density of particles from milled samples was higher than the corresponding strand form extrudates. In addition, given the fact that milled extrudates have a significantly larger surface area to volume ratio (due to the small particle size) than the strand form extrudates, it could be expected that the particle number density in total is significantly higher in milled extrudates than the strand form extrudates. It has been suggested that the appearance of particles on the surface of felodipine-EUDRAGIT® EPO melt extrudates could be a strong indicator of phase separation or recrystallization (28). Therefore, the SEM results may indicate that milled extrudates were less stable than the strand form extrudates on aging under 75%RH/room temperature.

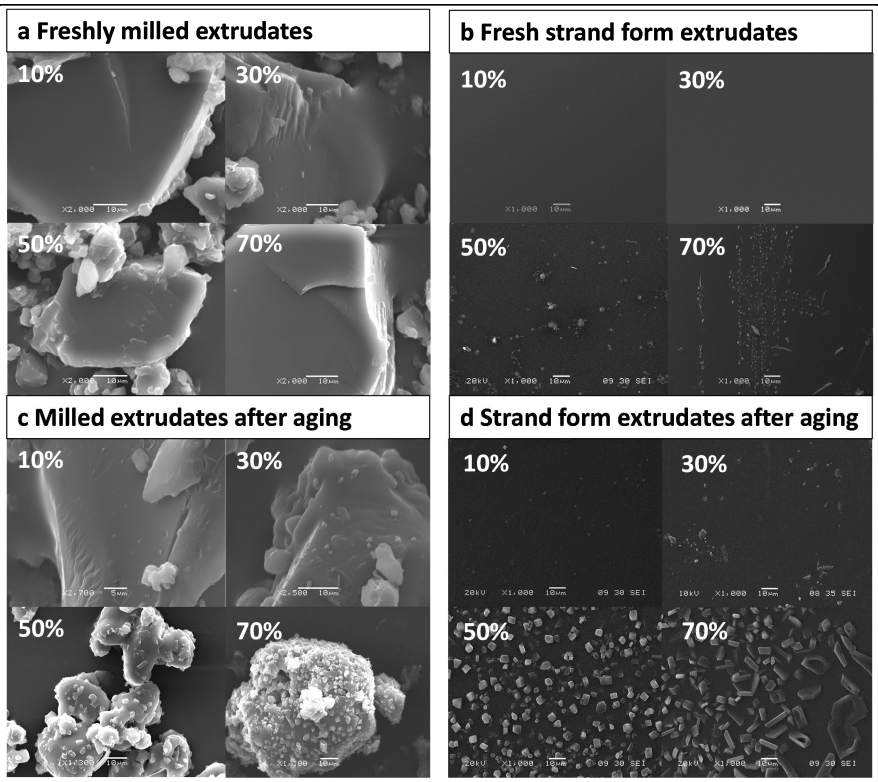

Figure 5.11: SEM images of the surface of freshly prepared and milled and felodipine-EUDRAGIT® EPO melt extrudates and 6 months aged strand form and milled felodipine-EUDRAGIT® EPO melt extrudates under 75%RH/room temperature (a: the surface of freshly prepared and milled extrudates; b: the surface freshly prepared strand form extrudates; c: the surface of milled extrudates after 6 month aging; d: the surface of strand form extrudates after 6 months aging).

Strand form and milled extrudates on aging under 75%RH/room temperature were also studied by MTDSC. For 10%-50% (w/w) strand form samples, no melting of felodipine was detected after 6 months aging. A small melting peak was detected in 70% (w/w) strand form extrudates after 6 months aging (Figure 5.12). The calculated crystallinity using *Eq 5.1* was 1.31% (w/w) after 6 months aging (Figure 5.13).

For 10%-30% (w/w) milled extrudates, no melting was detected by DSC after 6 months aging, which indicates milling had no significant impact on the physical stability of milled extrudates with drug loadings at and below 30% (w/w) on aging. However, evident melting was observed in the 50% (w/w) milled sample (depressed melting point of felodipine at 132^{o}C) after 6 months aging under 75%RH/room temperature (Figure 5.12). In addition to the detected melting in 50% (w/w) milled extrudates, an exothermic peak (recrystallisation) before the melting was also detected, which indicates that the amorphous drug phase separation generated by milling in the 50% (w/w) extrudates occurred on aging.

The effect of milling on the physical stability on aging of felodipine-EUDRAGIT® EPO extrudates was more evident in 70% (w/w) samples (Figure 5.12). The detected melting peak was significantly larger in the 70% (w/w) milled extrudates than in the corresponding strand form extrudates, which proves the influence of milling on the physical stability. It should be noted that the recrystallization peak remained evident before melting in the 70% (w/w) milled extrudates, which may indicate that the system may still mainly be amorphous solid dispersion and the phase separation needed to be induced by heating.

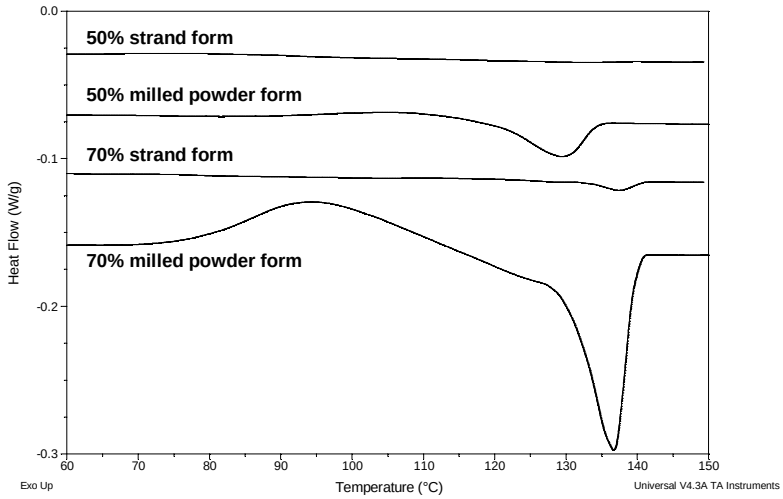

Figure 5.12: MTDSC results of strand form and milled felodipine-EUDRAGIT® EPO extrudates with 50% and 70% (w/w) drug loadings after 6 months aging under 75%RH at room temperature.

Detailed crystallinity calculation in milled and strand form extrudates on aging under 75%RH/room temperature are shown in Figure 5.13. Crystallinity of felodipine in systems was calculated using *Eq5.1*. After 6 months aging, the amount of crystalline felodipine in 70% (w/w) milled extrudates increased from 21.57% to 24.57% (w/w). The quantity of crystalline felodipine in this system reached a plateau after 2 months aging and did not increase with increasing aging time. For 50% milled extrudates, no crystalline felodipine was detected by MTDSC after 1 month aging. Evident melting can be observed in this sample after 2 months storage, but the melting enthalpy did not increase with increasing aging time periods. The crystallinity of felodipine in 50% milled extrudates was calculated as 3.42% (w/w) after 6 months aging.

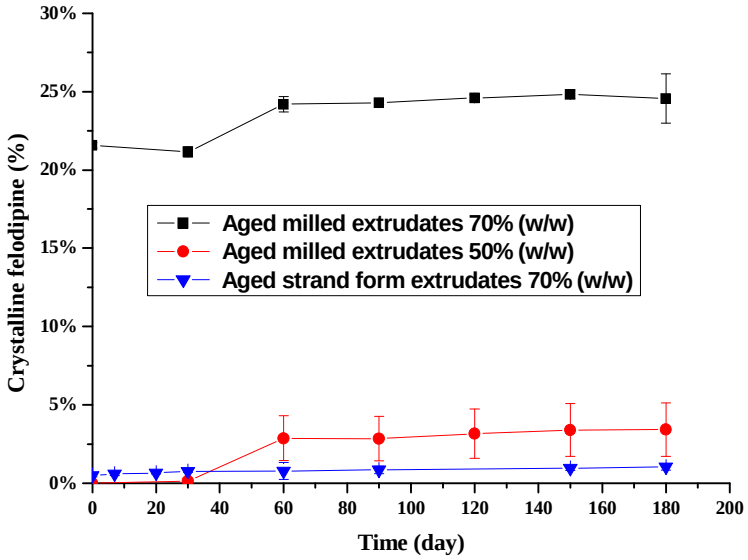

Figure 5.13: Crystallinity of felodipine in milled and strand form extrudates on aging under 75%RH at room temperature calculated by using melting enthalpy.

This phenomenon of reaching plateau of maximum amount of recrystallized drug in the milled extrudates on aging was also confirmed by ATR-FTIR study as seen in Figure 5.14. For 50% milled extrudates, after 2 months aging the peak at 3367cm^{-1} representing crystalline felodipine appeared but its intensity did not increase on aging. For 70% milled extrudates, after 2 months aging, the peak intensity ratio of crystalline felodipine peak (3365cm^{-1}) to amorphous felodipine peak (3335cm^{-1}) did not increase with increasing aging time indicating phase separation and recrystallization reached a steady state. No crystalline felodipine was detected by ATR-FTIR in 10% and 30% (w/w) milled samples after 6 months aging under 75%RH/room temperature. This suggests that after milling felodipine-EUDRAGIT® EPO solid dispersions can be maintained as amorphous solid dispersion up to 30% (w/w) drug loading after 6 months aging under 75%RH/room temperature.

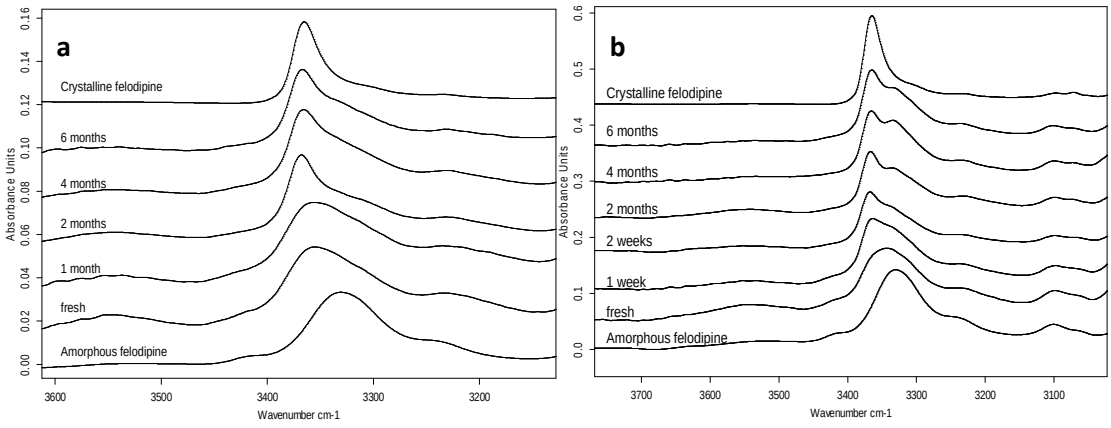

Figure 5.14: NH group from 50% (a) and 70% (b) milled felodipine-EUDRAGIT® EPO extrudates on aging under 75%RH/room temperature.

ATR-FTIR study was also applied to the 10-70% (w/w) strand form extrudates, however, after 6 months aging, no crystalline felodipine can be detected in the cross section of the strand extrudates. The spectra were identical to the freshly prepared strand form extrudates, which indicates a high level of bulk physical stability of strand form extrudates. The results of the aging effect on the milled extrudates clearly demonstrate milling can only generate a certain amount of phase separated amorphous felodipine in melt extrudates on aging.

5.3.1.5 Prediction of solid solubility using milling method-method development

The recrystallized amount of amorphous felodipine (recrystallized during heating in DSC) generated by milling in 50% and 70% (w/w) systems should be considered as an instable portion in systems at room temperature, which is very likely to phase separate and crystallise out on aging (as proved by the results of 50% w/w milled samples on aging). Therefore the stabilised amounts of felodipine remained as amorphous solid dispersions in milled extrudates after 6 months aging under 75%RH/room temperature were calculated as 45.43% (w/w) (using 70% minus 24.57% which was calculated from aging study) for 70% milled extrudates and 46.58% (w/w) for 50% samples. It is worthwhile to mention again that no crystalline felodipine can be detected by ATR-FTIR or MTDSC in milled systems with drug loadings below 50% (w/w). Thus the amount of felodipine which remained molecularly dispersed in melt extrudates was circa 45% (w/w) after 6 months aging under 75%RH/room temperature.

By evaluating the impact of milling on the physical stability of felodipine- EUDRAGIT® EPO extrudates on aging, it demonstrated that for systems with high drug loadings (50% and 70%), after a certain time periods, recrystallization and phase separation seemed to reach a plateau, and the amount of molecularly dispersed felodipine in both extrudates was similar. This may indicate the obtained equilibrium state of the molecular dispersion of felodipine into EUDRAGIT® EPO in the extrudates after long time period aging at room temperature.

In comparison to the milled extrudates, the strand form extrudates showed substantially high physical stability on aging after 6 months under 75%RH/room temperature even with 70% (w/w) drug loading, which suggests that it may require long time period for the strand form extrudates to reach equilibrium at room temperature. Consequently, it can be proposed that milling could be used as a practical and relatively fast approach to predict apparent solid solubility of drugs in solid dispersions prepared by hot melt extrusion. In the case of felodipine, the apparent solid solubility in EUDRAGIT® EPO processed by hot melt extrusion is circa 45% (w/w) (as calculated previously).

In Chapter 4, predicted solid solubility of felodipine in EUDRAGIT® EPO by theoretical approaches was all below 40% (w/w). This is because theoretical approaches were used to predict the thermodynamic solubility which did not take into account the influence of preparation

processes. Therefore, the processing-related drug-polymer solubility (apparent drug-polymer solubility) could be different from the theoretical values. It has been reported that solid solubility of drugs in solid dispersions can vary depending on preparation methods (9, 18, 29). In hot melt extrusion, the extra energy in the form of high temperature and high pressure is input into to drug-polymer mixtures, whereby drug molecules can be melted and dispersed evenly into polymer chains and form homogeneous drug-polymer solid dispersions molecularly (30). Therefore, it is reasonable to believe that apparent solid solubility of drugs in melt extrudates should be higher than theoretical values.

The application of mechanical milling in predicting apparent solid solubility of drugs in melt extrudates can be briefly described as follows. 1) An appropriate drug loading at which oversaturation in the amorphous drug-polymer solid dispersions can be generated should be identified. In the case of felodipine, for example, 70% (w/w) drug loading was considered as super-saturated drug loading since instant effect of milling on the physical state of 70% (w/w) extrudates was observed. 2) Melt extrudates should be prepared with this super-saturated drug loading. 3) Mechanical milling should be performed on the freshly prepared super-saturated melt extrudates. The applied time periods of milling may vary depending on the drug-polymer systems. For instance, as shown earlier in this chapter, after 10min milling no significant further increase of melting enthalpy can be determined in 70% felodipine-EUDRAGIT® EPO extrudates. Therefore it is suggested that the milling time should be determined depending on the individual drug-polymer system. Different time periods of milling should be used to the targeted system until the equilibrium (plateau) is achieved as shown by the study of felodipine-EUDRAGIT® EPO systems. 4) Although the instant effect of mechanical milling can be observed on super-saturated extrudates, to ensure the accuracy of the prediction of apparent solid solubility, milled extrudates should be stored under accelerated stressed condition (high temperature or high humidity, and results of felodipine-EUDRAGIT® EPO melt extrudates regarding aged under stressed temperature will be discussed in Chapter 6) until a plateau of recrystallization is achieved.

5.3.2 Prediction of solid solubility of model drugs in extrudates by milling approach-case studies

Solid solubility of model drugs in EUDRAGIT® EPO have been predicted by theoretical approaches in Chapter 4. However, as aforementioned, theoretical approaches did not take into account the effect of preparation processes which may generate a system comprising higher drug concentrations than the drug-polymer solubility. Moreover, due to assumptions, limitations and restrictions of those theoretical approaches, solid solubility predicted by which may not be sufficiently accurate and thus cannot be applied practically to improve formulation design. In this chapter so far, it has been demonstrated that mechanical milling can be used as a practical and relatively rapid method to predict the solid solubility of drugs in melt extrudates. Subsequently,

model drugs including celecoxib, fenofibrate and carbamazepine were formulated with EUDRAGIT® EPO by hot melt extrusion with high drug loadings to predict their apparent solid solubility in the polymer using this milling method.

5.3.2.1 Apparent solid solubility of celecoxib in EUDRAGIT® EPO

In Chapter 4, the apparent solid solubility of celecoxib in EUDRAGIT® EPO was predicted by theoretical approaches as 35% (solubility parameter approach), 41% (melting point depression approach) and 20%w/w (enthalpy method). As discussed in Chapter 4, these theoretical approaches did not take into account the effect of processing methods, which may lead to an underestimation of the apparent drug-polymer solubility in amorphous solid dispersions. Therefore, in order to predict the apparent drug-polymer solubility more accurately, in particular for hot melt extruded systems, milling approach was applied to calculate the solubility of celecoxib in melt extrudates. Following the procedure of using milling to predict solid solubility described above, celecoxib-EUDRAGIT® EPO extrudates with 70% (w/w) drug loading were prepared by hot melt extrusion. Freshly prepared extrudates was then milled by ball milling for 10min. Milled extrudates were stored under 75%RH at room temperature. As seen in Figure 5.15, a significant increase of melting enthalpy can be detected after milling in comparison to the freshly prepared strand form sample, indicating physical instability of 70% (w/w) celecoxib-EUDRAGIT® EPO melt extrudates was induced by mechanical milling. Using melting enthalpy to calculate crytallinity of celecoxib in 70% (w/w) celecoxib-EUDRAGIT® EPO melt extrudates (*Eq 5.1*), it increased from 13.12% for strand form sample to 27.50% (w/w) for freshly milled sample.

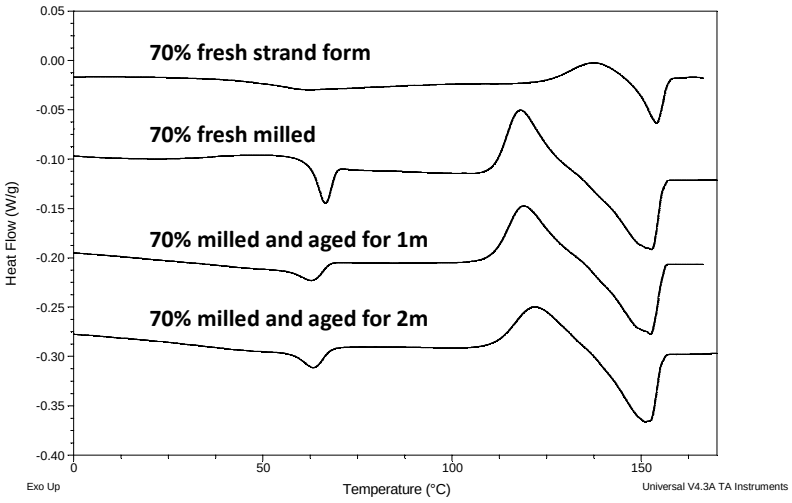

Figure 5.15: MTDSC results of fresh strand form and milled 70% (w/w) celecoxib-EUDRAGIT® EPO melt extrudates on aging under 75%RH at room temperature.

Freshly prepared and milled samples were then stored under 75%RH/room temperature up to 2 months. It can be seen in Figure 5.15 that melting enthalpy did not increase with increasing aging

time periods, indicating milling time of 10 min was sufficient to induce the physical instability of 70% celecoxib-EUDRAGIT® EPO melt extrudates. Detailed results of crystallinity of celecoxib in 70% system was carried out and shown in Figure 5.16. The amount of crystalline celecoxib detected by MTDSC in this system was circa 28% (w/w) and did not increase on aging up to 2 months, indicating equilibrium may has been achieved. Therefore, the amount of celecoxib remaining as solid dispersions in the 70% (w/w) extrudates can be calculated as 42% (w/w) (using drug loading minus 28%), which could be considered as the apparent solid solubility of celecoxib in celecoxib-EUDRAGIT® EPO solid dispersions prepared by hot melt extrusion. In comparison to the predicted solubility of celecoxib in EUDRAGIT® EPO by theoretical approaches, the value by milling method was similar to the melting point depression method (41.42%) but higher than the values by solubility parameter method (35.00% w/w) and modified melting enthalpy method (20.00% w/w). This suggests that the apparent solubility of celecoxib in EUDRAGIT® EPO can be affected by the processing method compared with the theoretical values and milling could be a more practical and accurate method for the prediction of drug-polymer solubility in melt extrudates.

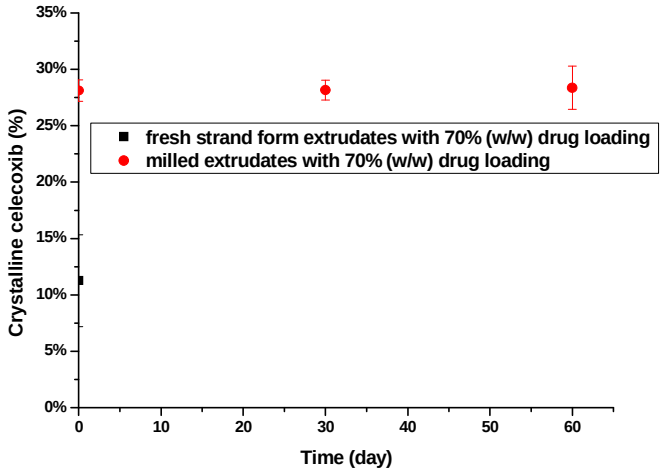

Figure 5.16: The amount of crystalline celecoxib in 70% strand form and milled celecoxib-EUDRAGIT® EPO melt extrudates.

5.3.2.2 Apparent solid solubility of fenofibrate in EUDRAGIT® EPO

The milling approach was attempted to predict fenofibrate solid solubility in EUDRAGIT® EPO. Fenofibrate-EUDRAGIT® EPO extrudates with 70% drug loading were prepared by hot melt extrusion. However, due to the low glass transition temperature of amorphous fenofibrate (-19.7°C), the glass transition temperature of 70% (w/w) was reduced to a temperature below ambient temperature. Using Fox equation to estimate the T_g of the 70% (w/w) system (31):

$$1 / T_{gmix} = w_1 / T_{g1} + (1-w_1) / T_{g2} \qquad Eq\ 5.2$$

where T_{gmix} is the glass transition temperature of the drug-polymer system, T_{g1} is the glass transition temperature of component 1 (fenofibrate, -19.5°C), T_{g2} is the glass transition temperature of component 2 (EUDRAGIT® EPO, 50°C) and w_1 is the weight fraction of component 1. The T_g of 70% fenofibrate-EUDRAGIT® EPO system was calculated as -19.01°C, which is significantly below room temperature. As calculated, the freshly prepared 70% extrudates had liquid-like state at room temperature. Thus milling is not applicable to this system. However, a rapid recrystallization in the form of samples solidifying and appearance changing from transparent to off-white was observed, if surface disruption, such as touching with a spatula, was imposed to this system. With the impact of the surface disruption, immediate recrystallization was detected by MTDSC as seen in Figure 5.17. Evident recrystallization followed by a melting was detected in freshly prepared and touched 70% (w/w) sample. Using *Eq 5.1*, the amount of crystalline fenofibrate was calculated as 57.39% (w/w) in 70% (w/w) extrudates. After 6 months aging under 75%RH at room temperature, the crystallinity of fenofibrate in this system was calculated as 57.52% (w/w) which is very close to the freshly prepared and surface-disrupted samples indicating the imposed surface disruption can induce the physical instability and rapidly lead to the equilibrium level. It should be noted that there was no recrystallization peak (exothermic peak) detected by MTDSC in the aged sample, which indicates that the portion of originally instable amorphous fenofibrate induced by surface disruption had completely converted to crystalline form on aging. The amount of fenofibrate remained in the amorphous solid dispersions, namely the solid solubility of fenofibrate, in 70% (w/w) melt extrudates was finally calculated as circa 13% (w/w).

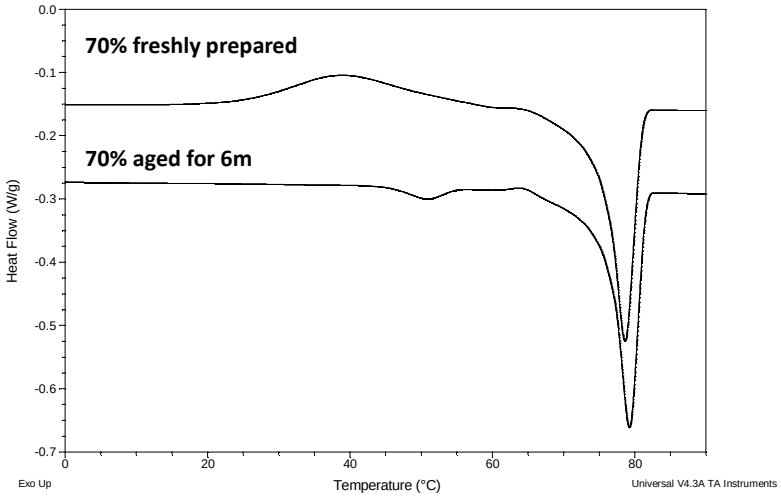

Figure 5.17: MTDSC results of freshly prepared and touched, and aged 70% fenofibrate-EUDRAGIT® EPO melt extrudates under 75%RH at room temperature.

The predicted apparent solubility of fenofibrate in melt extrudates was lower than the drug-polymer solubilities predicted by theoretical approaches. This is very likely because the T_g value of amorphous fenofibrate was very low (-20°C), which can bring the T_g value of the melt extrudates to

a low degree (lower than room temperature for 70% w/w sample). Therefore, at room temperature, high molecular mobility of fenofibrate in 70% (w/w) melt extrudates can cause the fast recrystallization, leading to the low drug-polymer solubility (at room temperature). Amorphous materials at the temperatures above their T_g value will have a great molecular mobility leading to the fast recrystallization.

5.3.2.3 Apparent solid solubility of carbamazepine in EUDRAGIT® EPO

5.3.2.3.1 Thermal stability of carbamazepine

Carbamazepine-EUDRAGIT® EPO systems with 70% (w/w) drug loading were prepared by hot melt extrusion for using milling method to predict the apparent drug-polymer solid solubility. In order to achieve a completely amorphous drug-polymer system, it is necessary to run the extruder at the melting point of the drug when preparing samples with extremely high drug loading since the small portion of polymer will not be capable to dissolve a large amount of the crystalline drug at lower temperature. However, it has been reported that carbamazepine was likely to degrade at the temperature close to its melting point (191^{o}C) (32). Therefore, in order to ensure the thermal stability of carbamazepine in processing at high temperature (close to its melting point), a thermal gravimetric analysis (TGA) test was carried out. The result (Figure 5.18) showed that after isothermal at 190^{o}C for 5min, the amount of degradation was 0.99% (w/w), indicating the processing temperature of 191^{o}C in hot melt extrusion is acceptable.

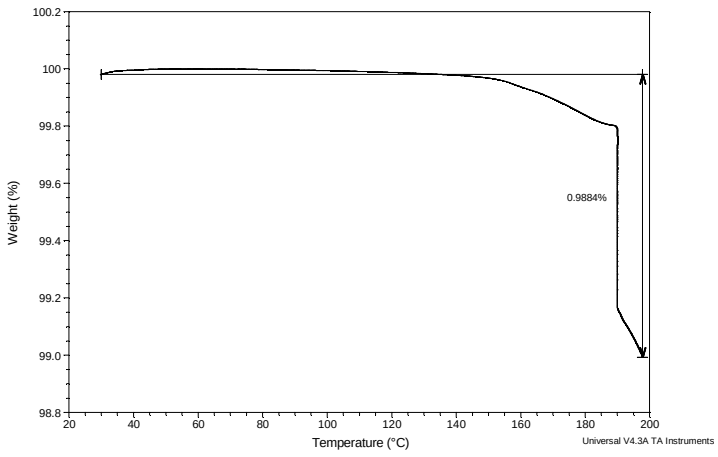

Figure 5.18: TGA result of crystalline carbamazepine tested by isothermal at melting point for 5min.

70% (w/w) carbamazepine-EUDRAGIT® EPO extrudates were prepared by hot melt extrusion at the temperature of 190^{o}C with the retention time of 5min. However, MTDSC results of freshly prepared sample showed an endothermic peak occurring at 140^{o}C as seen in Figure 5.19. The peak position of this endothermic peak does not agree with any melting point of reported carbamazepine polymorph. PXRD and ATR-FTIR was applied to characterise this sample, but characteristic peaks detected by PXRD and ATR-FTIR from this sample did not show agreement with the results

reported by the literature (33). A heating-cooling-reheating procedure was applied to investigate the thermal stability of crystalline carbamazepine. Crystalline carbamazepine was heated up to 200^{o}C at the ramp of 2^{o}C/min and then cooled down to -10^{o}C immediately and followed by a reheating to 200^{o}C at the same ramp as shown in Figure 5.20. Two endothermic peaks can be detected on first heating corresponding to the melting of form III (solid transformation from form III to form I occurred at the same temperature range) and I, which is in good agreement with the reported data (33). After cooling, an exothermic peak occurred at a temperature of 145^{o}C which is very close to the detected values from the 70% extrudates on second heating. No further endothermic peaks were detected up to 200^{o}C. No articles have reported this phenomenon so far, and thus with the thermal test it is reasonable to deduce the occurrence of thermal degradation in the process of melt extrusion. Besides, the addition of ingredients in formulations could possibly assist the APIs to be more sensitive to thermal degredation.

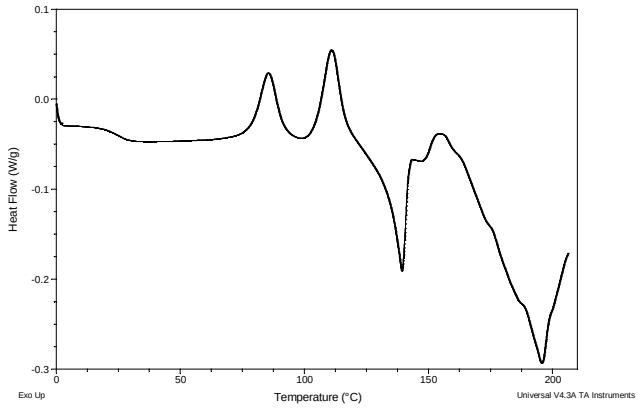

Figure 5.19: MTDSC result of freshly prepared 70% carbamazepine-EUDRAGIT® EPO melt extrudates.

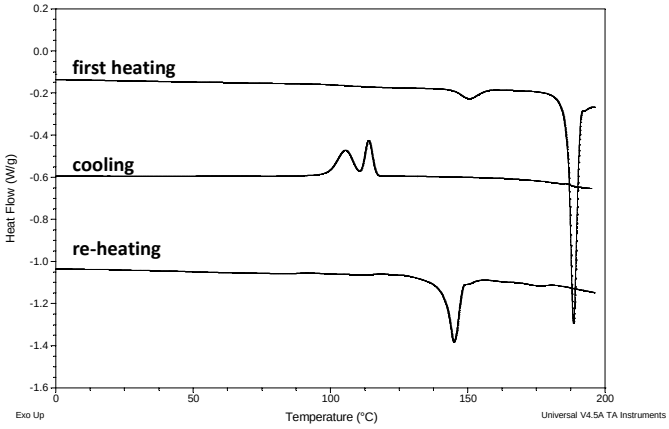

Figure 5.20: MTDSC result of crystalline carbamazepine tested by heating-cooling-reheating.

Although the TGA results showed that the degree of degradation was low at the temperature of 190^{o}C, it is still possible for carbamazepine to degrade in melt extrusion. Two reasons can be taken

account for with the first one that local temperature within the extruder barrel can be higher than the set temperature since the shearing generated by the rotation of twin screws can increase the temperature to higher degree locally. Secondly, pressure imposed by twin screws combining high temperature is possible to cause the degradation.

5.3.2.3.2 Approximate estimation of solid solubility of carbamazepine in EUDRAGIT® EPO

In order to avoid thermal degradation of carbamazepine in hot melt extrusion, a lower process temperature, 185°C was applied to prepared samples. 70% carbamazepine-EUDRAGIT® EPO melt extrudates were prepared at that temperature with a dwell time of 5min. A high torque value was observed during the process, which was caused by the high viscosity due to the fact that carbamazepine did not completely melt in preparation. This resulted in an extremely low yield, below 10% w/w. Freshly prepared sample was tested by MTDSC as seen in Figure 5.21. It can be seen that no endothermic peak was detected at 140°C, indicating the absence of thermal degradation. The detected melting point (185°C) is in agreement with the depressed melting point detected in physical mixture with same drug-polymer ratio (tested at the same heating rate, 2°C/min), and it can be confirmed as depressed melting point of form I according to the literature (33). The freshly prepared 70% (w/w) sample showed a large melting enthalpy (Figure 5.21) indicating the physical mixture of crystalline carbamazepine and EUDRAGIT® EPO was not completely transformed into amorphous solid dispersions by hot melt extrusion. Therefore, the 70% (w/w) carbamazepine-EUDRAGIT® EPO melt extrudates prepared at the temperature below the melting point cannot be guaranteed as supersaturated amorphous system. Milling was still attempted to be applied to this system to approximately estimate the solid solubility in of carbamazepine in the melt extrudates.

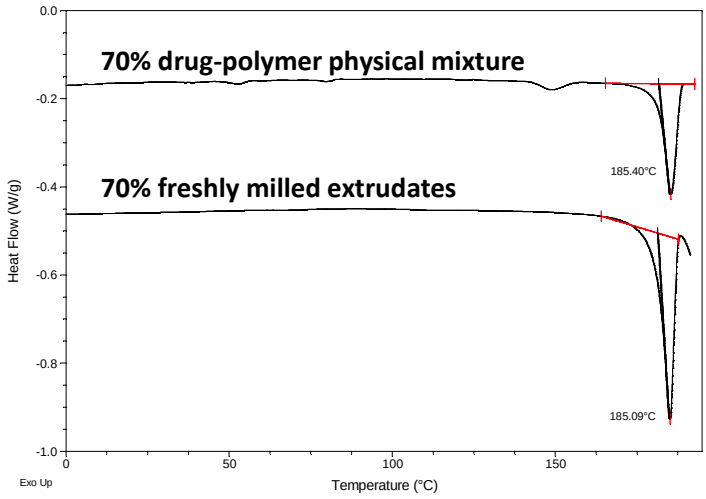

Figure 5.21: DSC results of 70% w/w freshly prepared strand form carbamazepine-EUDRAGIT® EPO melt extrudates and physical mixture.

Freshly prepared 70% (w/w) carbamazepine-EUDRAGIT® EPO extrudates were milled for 10min and then tested by MTDSC. Results are shown in Figure 5.22. By using *Eq 5.1*, the amount of crystalline carbamazepine in freshly prepared 70% (w/w) strand and milled samples was 51.92% and 52.08% (w/w), respectively. After 1 month aging at room temperature under 75%RH, melting enthalpy of milled 70% (w/w) extrudates did not increase as seen in Figure 5.22 and the calculated crystallinity was 52.10% (w/w). Therefore, the apparent solid solubility of carbamazepine in EUDRAGIT® EPO is estimated as circa 18% (w/w). Due to the thermal degradation of carbamazepine at high temperature, low operation temperature was applied in hot melt extrusion, which results in the preparation of partially crystalline melt extrudates. The predicated apparent solubility of carbamazepine by milling method may not be accurate as the method requires the preparation of super-saturated amorphous solid dispersions. In this study, therefore, only an approximate estimation of the solubility of carbamazepine in the extrudates can be achieved. This could be the disadvantage of the milling method: for drugs which are sensitive to high temperature and easy to degrade at high temperature, milling may not be applicable to predict the drug-polymer solubility as amorphous over-saturated melt extrudates cannot be prepared with these drugs. However, for those thermal sensitive drugs, hot melt extrusion may not be the appropriate processing method to prepare amorphous solid dispersions.

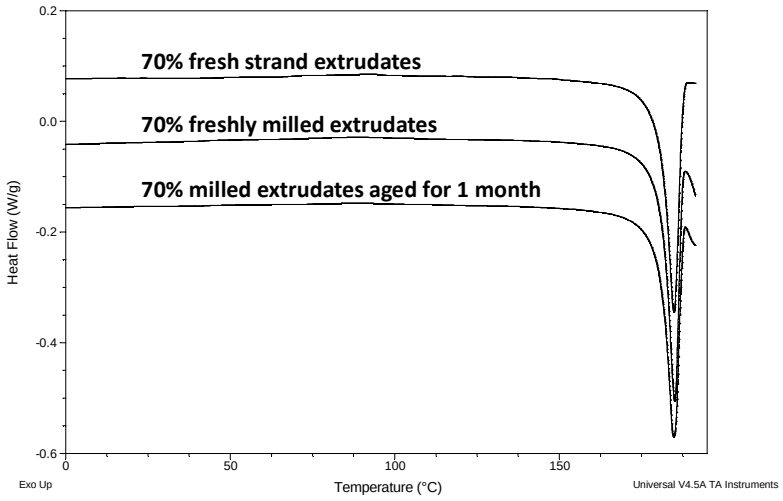

Figure 5.22: MTDSC results of 70% (w/w) freshly prepared strand carbamazepine-EUDRAGIT® EPO extrudates, and 70% (w/w) freshly milled and aged extrudates for 1 months under 75%RH at room temperature.

By using mechanical milling, solid solubility of model drugs in solid dispersions with EUDRAGIT® EPO prepared by hot melt extrusion were predicted and they are circa 45% (w/w) for felodipine, 42% (w/w) for celecoxib, 13% (w/w) for fenofibrate and 18% (w/w) for carbamazepine. In comparison to the predicted values by theoretical approaches, a significant discrepancy can be observed. For example, the measured apparent solubility of felodipine in the

extrudates was 45% (w/w), which is significantly higher than the values from all theoretical approaches. The developed mechanical milling method is more practical and more specifically applied to the solid solubility prediction of drugs in melt extrudates. Theoretical approaches could be applicable to many drug-polymer cases and may be served as a general method in predicting solid solubility. The required assumptions and limitations of those theoretical models, however, may result in a less practically accurate prediction, which might not be capable to improve the formulation development of amorphous solid dispersions. Moreover, as emphasized earlier, the apparent drug-polymer solubility can vary significantly depending on the processing methods. Therefore, it is reasonable to propose that the mechanical milling method developed in this project can predict solid solubility of drugs in melt extrudates more accurately and more concisely in the context of solid dispersions prepared by hot melt extrusion.

5.4 Conclusions

In this chapter, the impact of milling on the physical stability of felodipine- EUDRAGIT® EPO as a model system was evaluated. Four main factors (drug loading, milling period, aging, and external heating) were explored in terms of their effect on the milled hot melt extruded solid dispersions. It shows that mechanical milling can induce phase separation and recrystallization of melt extrudates with high drug loadings for as little as 5min milling. On studying the aging effect under high humidity, an equilibrium of physical state of 50% and 70% (w/w) felodipine-EUDRAGIT® EPO was observed with the crystallinity of felodipine in both systems circa 45% (w/w), which is considered as the apparent solid solubility of felodipine in melt extrudates. Therefore, mechanical milling is applied as a practical method to predict solid solubility of drugs in melt extrudates. Applying the milling method, the solid solubility of model drugs in melt extrudates with EUDRAGIT® EPO was calculated as 42% (w/w) for celecoxib, 13% (w/w) for fenofibrate and 18% (w/w) for carbamazepine.

The milling method can be used as a practical approach to predict the drug-polymer solubility in melt extruded amorphous solid dispersions accurately. It provides a tool for the selection of the "safe" range of drug loadings when developing melt extruded amorphous solid dispersions at the early stage as amorphous solid dispersions with the drug loading below the predicted solubility by milling should be physically stable. Therefore, the developed milling method may make a contribution to the prediction and enhancement of the physical stability of amorphous solid dispersions prepared by hot melt extrusion.

Reference

1. R.A. Bellantone, P. Patel, H. Sandhu, D.S. Choi, D. Singhal, H. Chokshi, A.W. Malick, and N. Shah. A method to predict the equilibrium solubility of drugs in solid polymers near room temperature using thermal analysis. Journal of Pharmaceutical Sciences. 101:4549-4558 (2012).

2. M.A. Alam, R. Ali, F.I. Al-Jenoobi, and A.M. Al-Mohizea. Solid dispersions: a strategy for poorly aqueous soluble drugs and technology updates. Expert Opinion on Drug Delivery. 9:1419-1440 (2012).
3. M. Yang, P. Wang, and C. Gogos. Prediction of acetaminophen's solubility in poly(ethylene oxide) at room temperature using the Flory–Huggins theory. Drug Development and Industrial Pharmacy. 39:102-108 (2013).
4. P. Marsac, S. Shamblin, and L. Taylor. Theoretical and Practical Approaches for Prediction of Drug–Polymer Miscibility and Solubility. Pharm Res. 23:2417-2426 (2006).
5. D.J. Greenhalgh, A.C. Williams, P. Timmins, and P. York. Solubility parameters as predictors of miscibility in solid dispersions. Journal of Pharmaceutical Sciences. 88:1182-1190 (1999).
6. S. Qi, P. Belton, K. Nollenberger, N. Clayden, M. Reading, and D.M. Craig. Characterisation and Prediction of Phase Separation in Hot-Melt Extruded Solid Dispersions: A Thermal, Microscopic and NMR Relaxometry Study. Pharm Res. 27:1869-1883 (2010).
7. H. Suwardie, P. Wang, D.B. Todd, V. Panchal, M. Yang, and C.G. Gogos. Rheological study of the mixture of acetaminophen and polyethylene oxide for hot-melt extrusion application. European Journal of Pharmaceutics and Biopharmaceutics. 78:506-512 (2011).
8. S. Janssensand G. Van den Mooter. Review: physical chemistry of solid dispersions. Journal of Pharmacy and Pharmacology. 61:1571-1586 (2009).
9. S. Janssens, A. Zeure, A. Paudel, J. Humbeeck, P. Rombaut, and G. Mooter. Influence of Preparation Methods on Solid State Supersaturation of Amorphous Solid Dispersions: A Case Study with Itraconazole and Eudragit E100. Pharm Res. 27:775-785 (2010).
10. P. Karmwar, K. Graeser, K.C. Gordon, C.J. Strachan, and T. Rades. Investigation of properties and recrystallisation behaviour of amorphous indomethacin samples prepared by different methods. International Journal of Pharmaceutics. 417:94-100 (2011).
11. J. Tang, W. Zhao, C.J. O'Connor, and S. Li. Nanocomposite formation and size reduction of Terfenol-D particles during mechanical milling. Journal of Alloys and Compounds. 250:482-485 (1997).
12. A.K. Nath, C. Jiten, and K.C. Singh. Influence of ball milling parameters on the particle size of barium titanate nanocrystalline powders. Physica B: Condensed Matter. 405:430-434 (2010).
13. K.J. Crowleyand G. Zografi. Cryogenic grinding of indomethacin polymorphs and solvates: Assessment of amorphous phase formation and amorphous phase physical stability. Journal of Pharmaceutical Sciences. 91:492-507 (2002).
14. M.K. Gupta, A. Vanwert, and R.H. Bogner. Formation of physically stable amorphous drugs by milling with neusilin. Journal of Pharmaceutical Sciences. 92:536-551 (2003).
15. J.F. Willartand M. Descamps. Solid State Amorphization of Pharmaceuticals. Molecular Pharmaceutics. 5:905-920 (2008).
16. P.N. Balani, S.Y. Wong, W.K. Ng, E. Widjaja, R.B.H. Tan, and S.Y. Chan. Influence of polymer content on stabilizing milled amorphous salbutamol sulphate. International Journal of Pharmaceutics. 391:125-136 (2010).
17. N. Trasi, S.M. Boerrigter, and S. Byrn. Investigation of the Milling-Induced Thermal Behavior of Crystalline and Amorphous Griseofulvin. Pharm Res. 27:1377-1389 (2010).
18. V. Caron, L. Tajber, O.I. Corrigan, and A.M. Healy. A Comparison of Spray Drying and Milling in the Production of Amorphous Dispersions of Sulfathiazole/Polyvinylpyrrolidone and Sulfadimidine/Polyvinylpyrrolidone. Molecular Pharmaceutics. 8:532-542 (2011).
19. M.L. Branham, T. Moyo, and T. Govender. Preparation and solid-state characterization of ball milled saquinavir mesylate for solubility enhancement. European Journal of Pharmaceutics and Biopharmaceutics. 80:194-202 (2012).
20. V. Caron, J.F. Willart, R. Lefort, P. Derollez, F. Danede, and M. Descamps. Solid state amorphization kinetic of alpha lactose upon mechanical milling. Carbohydrate Research. 346:2622-2628 (2011).
21. J.F. Willart, L. Carpentier, F. Dannede, and M. Descamps. Solid-state vitrification of crystalline griseofulvin by mechanical milling. Journal of Pharmaceutical Sciences. 101:1570-1577 (2012).

22. J.-F. Willart, M. Durand, L.-E. Briggner, A. Marx, F. Danede, and M. Descamps. Solid-state amorphization of linaprazan by mechanical milling and evidence of polymorphism. Journal of pharmaceutical sciences. 102:(2013).
23. D.A. Miller, J.T. McConville, W. Yang, R.O. Williams, and J.W. McGinity. Hot-melt extrusion for enhanced delivery of drug particles. Journal of Pharmaceutical Sciences. 96:361-376 (2007).
24. J.P. Lakshman, Y. Cao, J. Kowalski, and A.T.M. Serajuddin. Application of Melt Extrusion in the Development of a Physically and Chemically Stable High-Energy Amorphous Solid Dispersion of a Poorly Water-Soluble Drug. Molecular Pharmaceutics. 5:994-1002 (2008).
25. J. Albers, R. Alles, K. Matthée, K. Knop, J.S. Nahrup, and P. Kleinebudde. Mechanism of drug release from polymethacrylate-based extrudates and milled strands prepared by hot-melt extrusion. European Journal of Pharmaceutics and Biopharmaceutics. 71:387-394 (2009).
26. J. Albers, K. Matthée, K. Knop, and P. Kleinebudde. Evaluation of predictive models for stable solid solution formation. Journal of Pharmaceutical Sciences. 100:667-680 (2011).
27. X. Tang, M. Pikal, and L. Taylor. A Spectroscopic Investigation of Hydrogen Bond Patterns in Crystalline and Amorphous Phases in Dihydropyridine Calcium Channel Blockers. Pharm Res. 19:477-483 (2002).
28. S. Qi, P. Belton, K. Nollenberger, A. Gryczke, and D.M. Craig. Compositional Analysis of Low Quantities of Phase Separation in Hot-Melt-Extruded Solid Dispersions: A Combined Atomic Force Microscopy, Photothermal Fourier-Transform Infrared Microspectroscopy, and Localised Thermal Analysis Approach. Pharm Res. 28:2311-2326 (2011).
29. I. Weuts, F. Van Dycke, J. Voorspoels, S. De Cort, S. Stokbroekx, R. Leemans, M.E. Brewster, D. Xu, B. Segmuller, Y.T.A. Turner, C.J. Roberts, M.C. Davies, S. Qi, D.Q.M. Craig, and M. Reading. Physicochemical properties of the amorphous drug, cast films, and spray dried powders to predict formulation probability of success for solid dispersions: Etravirine. Journal of Pharmaceutical Sciences. 100:260-274 (2011).
30. M.M. Crowley, F. Zhang, M.A. Repka, S. Thumma, S.B. Upadhye, S. Kumar Battu, J.W. McGinity, and C. Martin. Pharmaceutical Applications of Hot-Melt Extrusion: Part I. Drug Development and Industrial Pharmacy. 33:909-926 (2007).
31. M. Cortázar, J.I. Eguiazábal, C. Uriarte, and J.J. Iruin. Glass transition temperatures of plasticized polyarylate. Polymer Bulletin. 18:149-154 (1987).
32. X. Liu, M. Lu, Z. Guo, L. Huang, X. Feng, and C. Wu. Improving the Chemical Stability of Amorphous Solid Dispersion with Cocrystal Technique by Hot Melt Extrusion. Pharm Res. 29:806-817 (2012).
33. A.L. Grzesiak, M. Lang, K. Kim, and A.J. Matzger. Comparison of the four anhydrous polymorphs of carbamazepine and the crystal structure of form I. Journal of Pharmaceutical Sciences. 92:2260-2271 (2003).

Chapter 6: Physical stability studies of hot melt extrudates on aging

6.1 Introduction

Amorphous solid dispersions have been widely used and proved to be effective to enhance the dissolution rate of poorly water-soluble drugs in the pharmaceutical industry (1-3). The mechanism of the dissolution enhancement by amorphous solid dispersions has been well understood that drugs in amorphous solid dispersions have higher apparent solubility in aqueous solution in comparison to their crystalline forms due to the lack of lattice crystalline structure (4-6).

However, the physical stability of amorphous solid dispersions still remains the main challenge for the formulation development of solid dispersions. As mentioned previously, molecularly dispersed drugs in amorphous solid dispersions existing at high-energy level tend to spontaneously (according to the Gibb's free energy law) revert back to the more physically stable crystalline form. Therefore, in order to enhance the physical stability of amorphous solid dispersions, it is essential to clearly understand the physical instability in great depth. In this chapter, model drugs were formulated with EUDRAGIT® EPO by hot melt extrusion. Real-time physical stability studies of the melt extrudates were carried out under different storage conditions. Therefore, comprehensive results of physical stability studies can be achieved, and the effect of the storage condition on the physical stability of amorphous solid dispersions can be understood. In addition, the validation of the milling method in predicting drug-polymer solubility developed in Chapter 5 can be tested combined with the real-time physical stability studies.

In Chapter 3, physical properties including glass transition temperatures, relaxation time of amorphous drugs, and physical stability of amorphous drugs alone have been studied. These factors have been suggested in articles to be correlated with the physical stability of amorphous solid dispersions (7-10). Therefore, by comparing the physical properties of the model drugs with the results of the real-time physical stability studies of melt extrudates, dominant factors which control the physical stability of amorphous solid dispersions can be revealed.

In Chapter 4, drug-polymer miscibility and solubility were predicted using different theoretical approaches. Predicted drug-polymer solubility of individual drug varied significantly between different approaches due to the limitations of different theoretical approaches as discussed earlier. In Chapter 5, a practical method, milling, was developed for more accurate prediction of the solubility of drugs in melt extrudates. The predicted value of individual drug by milling method was different from the values by theoretical approaches. It has been suggested that drug-polymer

solubility is one of the most significant factors which is related to the physical stability of amorphous solid dispersions. Therefore, by comparing the predicted drug-polymer solubility with the results of real-time physical stability studies, the validation of the theoretical approach and milling method in predicting drug-polymer solubility can be tested. This is based on the hypothesis that extrudates composed of model drugs (the same drug loading amongst different formulations) with higher solubility should be more physically stable on aging than those composed drugs with lower solubility.

The fundamental aims of this chapter can be divided into three aspects. Firstly, through the real-time physical stability studies of melt extrudates aged under different conditions (0%RH/room temperature, 75%RH/room temperature, 0%RH/40^{o}C and 75%RH/40^{o}C), the effect of storage condition including stressed temperature and stressed humidity on the physical stability of amorphous solid dispersions can be investigated. Secondly, combining the real-time physical stability studies with the physical properties of amorphous drugs, the key factors controlling the physical stability of amorphous solid dispersions can be found out. Thirdly, the real-time physical stability studies can be used to validate the prediction of drug solubility in melt extrudates. The completion of the three aims will substantially contribute the development of methods for the prediction and enhancement of the physical stability of amorphous solid dispersions.

Research objectives

1. To investigate the effect of storage conditions on the physical stability of solid dispersions prepared by hot melt extrusion.

2. To find out the key factors which control the physical stability of melt extruded solid dispersions.

3. To validate theoretical approaches and milling method in predicting the drug-polymer solubility.

6.2 Experimental methods

6.2.1 Hot melt extrusion

Equipment for hot melt extrusion refers to Chapter 2 (section 2.2.1.1). Physical mixtures of crystalline model drugs and EUDRAGIT® EPO with ratios of 10:90 and 70:30 (w/w) were pre-mixed in a mortar and pestle before melt extrusion. The processing temperature was set at 5 degree higher than the melting points of crystalline model drugs. For the case of carbamazepine, the operation temperature is 5 degree lower than its melting point to avoid thermal degradation. The rotating speed of twin screws was 100r/min. A round shape die with diameter of 2mm was attached to the extruder.

6.2.2 Physicochemical characterisation

Instrumental information of the characterisation techniques used and the applied parameters including MTDSC, PXRD, ATR-FTIR and SEM refers to different sections in Chapter 2 (2.2.2.1.3 for MTDSC, 2.2.2.4.2 for ATR-FTIR, 2.2.2.5.2 for PXRD, 2.2.2.6.2 for SEM)

6.2.3 Storage tests under different conditions

Freshly prepared strand form melt extrudates were stored as intact strand form without milling under four different conditions: 0%RH (provided by P_2O_5)/room temperature, 75%RH (provided by saturated sodium chloride solution)/room temperature, 0%RH/40^oC and 75%RH/40^oC for up to 6 months, and were tested by MTDSC (strand form extrudates), ATR-FTIR, SEM and PXRD (strand extrudates milled into powder before the test).

6.2.4 Kinetic study of surface recrystallisation

In order to study the kinetics of the surface recrystallization of melt extrudates, image-analysis software, Image J (National Institutes of Health, USA) was used to analyse SEM images. An example is given in Figure 6.1. Figure 6.1 (a) is an image of the surface of a melt extruded sample, and Figure 6.1 (b) is the analysed result of the SEM image by Image J. It can be seen that the size and shape of individual particle was tracked and framed by the software, and the percentage of total areas (in μm^2) occupied in the whole image (the real tested sample area be achieved from the SEM image information) can be calculated by the software. The real area of the sample tested under SEM can be achieved using the scale bar in SEM image. Therefore, the kinetics of the surface recrystallization growth of melt extrudates on aging can be studied.

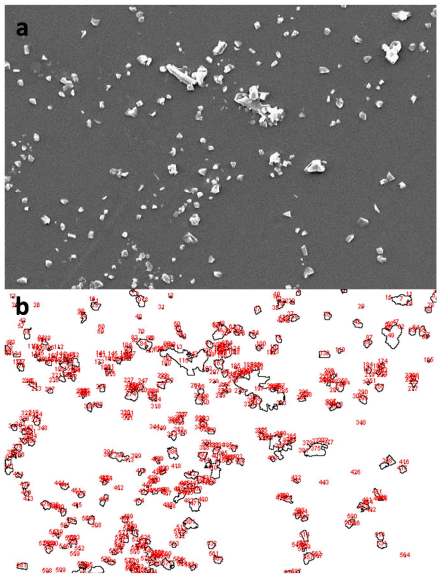

Figure 6.1: SEM image of the surface of melt extruded sample (a) and the analysed result by Image J (b).

6.3 Results and discussion

The accelerated storage conditions suggested by United Sates Pharmacopeia (USP) and British Pharmacopeia (BP) normally consist of stressed temperature (40^{o}C) and stressed humidity (75%RH). These two conditions have also been regularly used in articles concerning physical stability studies of amorphous solid dispersions as stressed humidity and temperature can increase molecular mobility of drugs in solid dispersions leading to the physical instability (11-13). Therefore, in this chapter, in order to thoroughly understand the effect of storage conditions on the physical stability of melt extruded solid dispersions, four conditions mentioned in section 6.2.4 were used. All melt extrudates were stored under four different conditions as intact strand form without milling after fresh preparation.

In Chapter 5, the predicted drug-polymer solubilities by the theoretical approaches and milling method were all within the range between 10% (w/w) to 50% (w/w). Two drug loadings including 10% (below the predicted solubility) and 70% (w/w) (above the predicted solubility, and hence super-saturated system) were selected for individual drug-EUDRAGIT® EPO melt extrudates. The two drug loadings can be used to test the accuracy of different approaches (theoretical approaches and the milling method) in predicting drug-polymer solubility. The melt extrudates with drug loadings below the predicted solubility should be physically stable whereas phase separation should be observed in super-saturated melt extrudates with drug loading above the predicted solubility on aging.

6.3.1 Physical stability study of melt extruded felodipine-EUDRAGIT® EPO systems under different conditions

6.3.1.1 Surface physical stability

For 10% (w/w) felodpine-EUDRAGIT® EPO melt extrudates aged under different conditions after 6 months, no felodipine crystals can be detected by ATR-FTIR on the surface of the samples, suggesting no surface phase separation occurred in low drug loading samples. SEM images of 6 months aged 10% (w/w) extrudates is shown in Figure 6.2. No evident particles were observed on the surface of any 10% (w/w) samples after 6 months aging under the four conditions. This indicates that the felodpine-EUDRAGIT® EPO melt extrudates with 10% (w/w) drug loading were homogeneous with high surface stability within 6 months. The results of surface physical stability study of 10% (w/w) samples showed good agreement with the predicted solubility (45% w/w) by milling method.

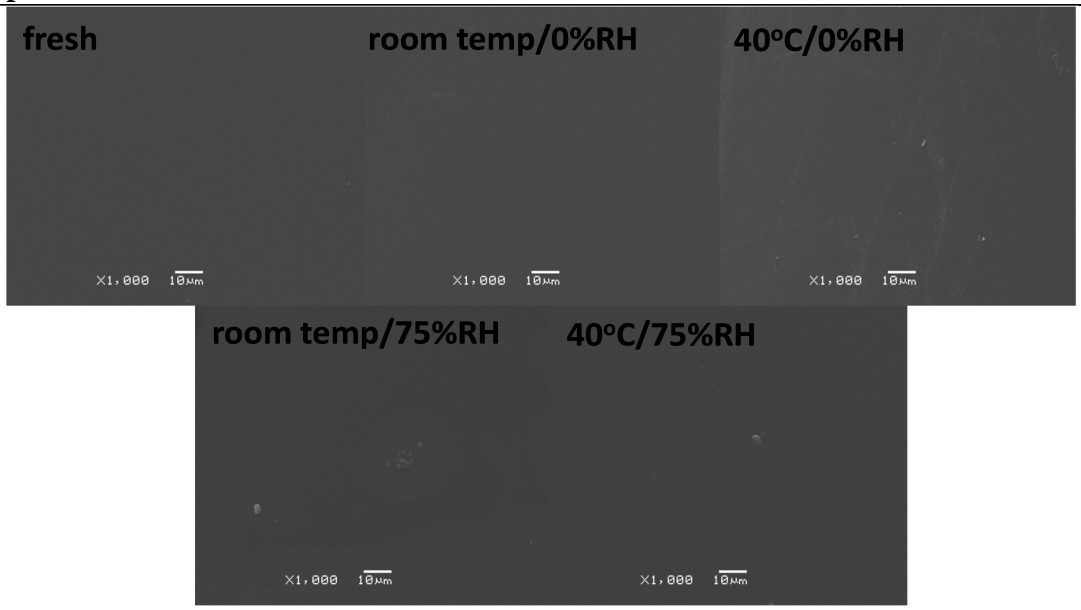

Figure 6.2: SEM images of the surface of fresh and 6 months aged 10% (w/w) felodpine-EUDRAGIT® EPO melt extrudates under different conditions.

ATR-FTIR spectra of the surface of 70% (w/w) felodipine-EUDRAGIT® EPO melt extrudates on aging under different conditions are collected and shown in Figure 6.3. As mentioned in Chapter 4, the NH group is an indicator of felodipine being crystalline or amorphous. A single peak at 3341cm^{-1} (in between the amorphous and crystalline felodipine NH peak) in the 70% (w/w) melt extrudates can be seen in the freshly prepared sample, indicating a single-phase amorphous system. On aging under 0%RH/room temperature (mildest condition) for 2 months, a peak at 3365cm^{-1} representing crystalline felodipine and a peak at 3335cm^{-1} representing phase separated amorphous felodipine can both be detected on the surface of the sample, indicating the occurrence surface phase separation and recystallisation in this sample.

For 70% (w/w) samples aged under 75%RH/room temperature, after 1 month aging, the crystalline felodipine peak (3365cm^{-1}) was observed and the amorphous felodipine peak (3335cm^{-1}) was barely evident (Figure 6.3). The absence of the amorphous felodipine peak indicates a high level of surface recrystallization occurred in samples stored under this condition.

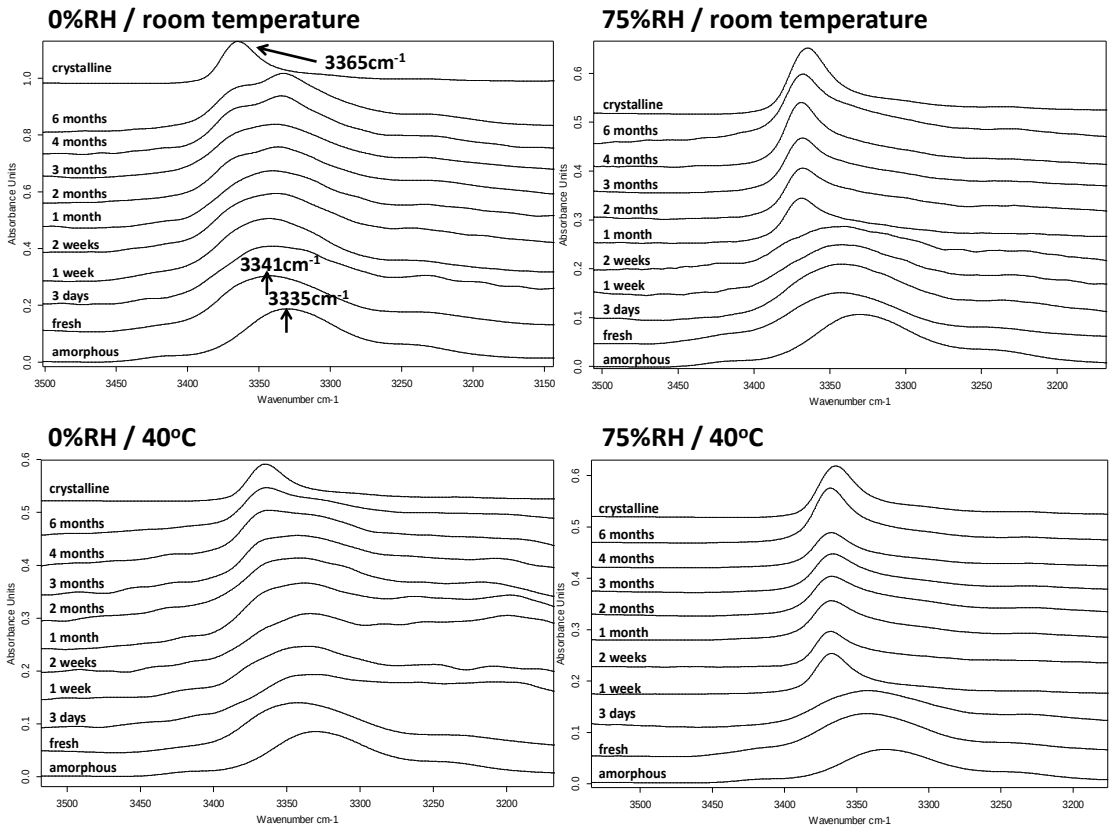

Figure 6.3: ATR-FTIR results of NH group from the surface of 70% (w/w) felodpine-EUDRAGIT® EPO melt extrudates aged under different conditions.

For 70% (w/w) samples aged under 0%RH/40°C, phase separation took place after 1 month aging as crystalline and amorphous felodipine peaks appeared (Figure 6.3). However, in comparison to samples aged under 75%RH/room temperature, the phase separation and recrystallization occurred at a significantly lower level since the peak intensity of amorphous felodipine (3335cm^{-1}) was still restively high after 4 months aging.

Aged under 75%RH/40°C, after 1 week, crystalline felodipine was detected on the surface of 70% (w/w) felodpine-EUDRAGIT® EPO melt extrudates (Figure 6.3). With increasing aging time, no amorphous crystalline felodipine was observed on the surface, indicating a significantly high level of surface recrystallization occurred in 70% (w/w) samples aged under 75%RH/40°C.

The ATR-FTIR study of 70% (w/w) felodipine-EUDRAGIT® EPO melt extrudates demonstrates that surface recrystallization occurred in samples aged under all conditions. Stressed humidity and stressed temperature can both accelerate the surface recrystallization, and stressed humidity has more significant impact on the surface recrystallization than the stressed temperature on aging.

Surface physical stability of felodipine-EUDRAGIT® EPO melt extrudates on aging under all conditions were also studied using SEM (images were taken regularly up to 6 months). It has been

reported that the appearance of particles on the surface of melt extrudates were a strong sign of phase separation and recrystallization (13, 14). SEM images of the surface of 3 months aged extrudates are shown in Figure 6.4 as an example. Rod shape particles with the size from below 10µm (0%RH/room temperature) to above 100µm (75%RH/40°C) were observed on the surface of extrudates aged under all conditions. Samples aged under 0%RH/room temperature showed the lowest particle density on the surface. Samples aged under 75%RH/room temperature showed higher particle density on the surface than samples aged under 0%/40°C. The surface of the extrudates aged under 75%RH/40°C was almost covered by particles after 3 months aging. SEM images clearly showed that stressed storage conditions could increase surface recrystallization and stressed humidity had more significant impact than stressed temperature on surface recrystallization on aging. This is in good agreement with the ATR-FTIR results.

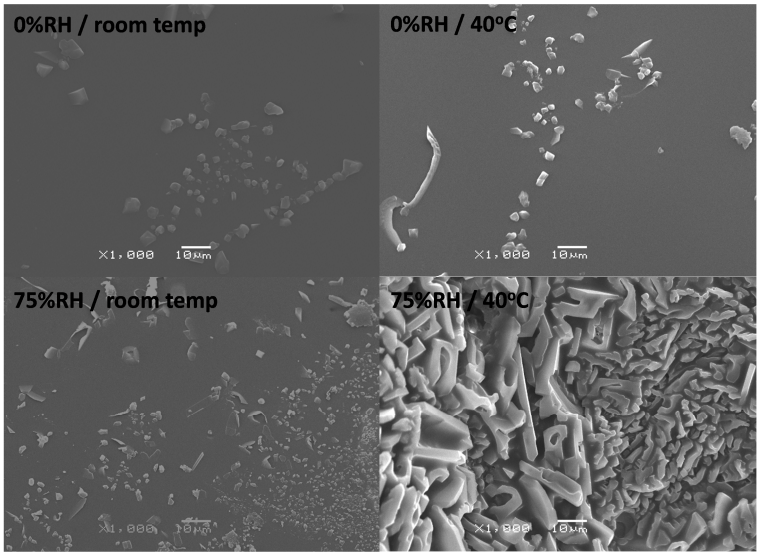

Figure 6.4: SEM images of the surface of 70% felodipine-EUDRAGIT® EPO melt extrudates after 3 months aging under different conditions.

The SEM images of the surface of 70% (w/w) melt extrudates on aging were further analysed using Imaging J (method mentioned in section 6.2.5) for the kinetic study of the surface recrystallization (Figure 6.5). After 6 months aging under 0%RH/room temperature and 0%RH/40°C, only less than 20% area (calculated using the measured total particle areas divided by the size of the whole image area) of the tested surface (whole area of the image taken by SEM) of both samples contained particles. But for samples aged under 75%RH/room temperature, more than 50% of the surface contained particles after 6 months aging, demonstrating that the physical stability of 70% (w/w) felodpine-EUDRAGIT® EPO melt extrudates was affected more by humidity than by high temperature. For samples aged under 75%RH/40°C, within 2 months aging, a fast rate of particle growth was observed resulting in more than 80% of the area covered by

particles, indicating a nearly completion (phase I) of the surface recrystallization for the sample aged under this condition within 2 months.

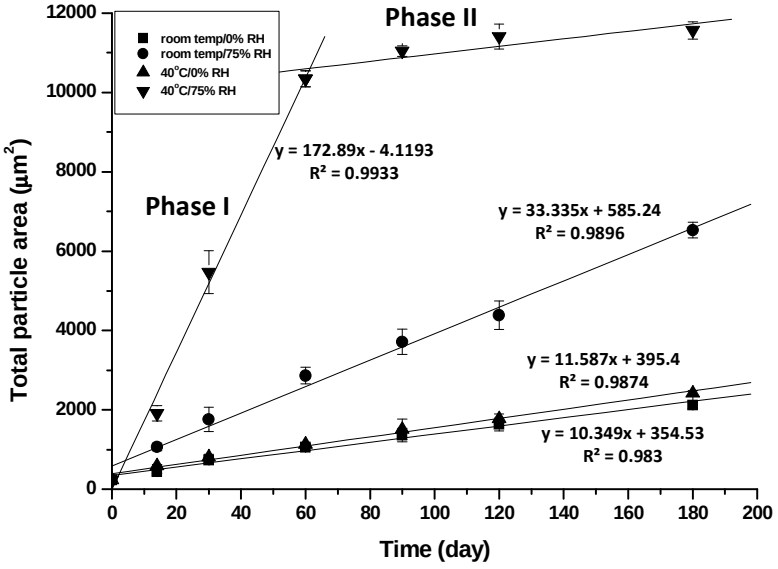

Figure 6.5: Results of total particle area (μm^2) achieved by using Image J to analyse SEM images on the surface of 70% felodpine-EUDRAGIT® EPO melt extrudates on aging under different conditions.

The classic Avrami model was introduced in this study to fit the surface rcrystallisation data (15). Avrami model has been widely used to study the kinetics of crystallisation in different research areas (12, 16-18). The kinetics of crystallisation can be derived from the assumption including the phases of nucleation, crystal growth and termination of crystal growth when two crystals meet (19). Generally, these three phases of crystallisation is well described by Avrami model and it can be written by:

$$\alpha = 1- exp-[(k(t-t_0))]^{n} \qquad Eq\ 6.1$$

where α is the fraction of crystalline drug at time t, k is the apparent crystallisation rate constant (time^{-1}), t_0 is the induction time and n is Avrami exponent depending on nucleation mechanism and the dimensions in which growth is occurring (the value of n is limited to 1,2,3 and 4).

The surface recrystallization data of samples aged under all conditions did not fit in the Avrami model as the curve in Figure 6.5 did not show the sigmoidal profile. This can be attributed to the reason that felodipine crystals already existed on the surface of fresh 70% (w/w) extrudates (as shown in Figure 6.5 that particle domains in fresh sample was not 0). Therefore, surface recrystallization of the 70% (w/w) extrudates lacked the step of nucleation, and initially started with the crystal growth and the possible appearance of new nuclei on aging. For samples aged under 0%RH/room temperature, 75%RH/room temperature and 0%RH/40^{o}C, a continuous surface recrystallization was observed up to 6 months. For samples aged under 75%RH/40^{o}C, after 2

months aging, a decreased crystallisation rate was seen indicating the near completion of the surface recrystallization in the samples. Although the kinetics of the surface recrystallization of 70% (w/w) felodipine-EUDRAGIT® EPO melt extrudates did not fit in the Avrami model, a clear linear kinetics (with acceptable regression coefficients) was observed for samples aged under all conditions (phase I for 705 w/w samples under under 75%RH/room temperature) (Figure 6.5). The slopes of individual linear plot (Figure 6.5) can be considered as the recrystallization rates of individual 70% (w/w) extrudates aged under different conditions. By comparing the recrystallization rates, it was observed that extrudates aged under 0%RH/room temperature (10.3μm^2/day) and 0%RH/40^oC (11.6μm^2/day) showed similar recrystllisation rates, which were smaller than that from the samples aged under 75%RH/room temperature (33.3μm^2/day). Extrudates aged under 75%RH/40^oC showed the highest rate (172.9μm^2/day) within the first 2 months aging, and a plateau was observed afterwards due to the near completion of surface recrystallisation.

Results of the surface stability study of felodipine-EUDRAGIT® EPO melt extrudates showed that no surface recrystallization was detected in 10% (w/w) extrudates aged under the four conditions up to 6 months. For 70% (w/w) melt extrudates, surface recrystallization in samples different conditions exhibit different crystal growth rate. Stressed humidity showed more significant effect on the surface recrystallsation than stressed temperature.

6.3.1.2 Bulk physical stability

The bulk stability of felodipine- EUDRAGIT® EPO melt extrudates was studied using MTDSC and PXRD. After 6 months aging, no recrystallization or melting was detected by MTDSC in any 10% (w/w) extrudates aged under all conditions, indicating high bulk physical stability of 10% (w/w) sample. PXRD results showed the agreement with the MTDSC results. No crystalline felodipine was detected by PXRD in 10% (w/w) samples aged under all conditions after 6 months.

The bulk physical stability of 70% (w/w) felodpine-EUDRAGIT® EPO melt extrudates was also evaluated by MTDSC and PXRD. MTDSC results (Figure 6.6, values in the figure are the calculated crystallinity using *Eq 5.1* in individual sample after 6 months aging) showed that after 6 months aging under 0%RH/room temperature, 0%RH/40^oC and 75%RH/room temperature, the amount of crystalline felodipine in 70% (w/w) melt extrudates was still below 1% (w/w), indicating extremely high bulk physical stability of these samples. Crystallinity of samples aged under 75%RH/room temperature (0.82% w/w) was slightly higher than that in samples aged under 0%RH/40^oC (0.45% w/w), which may suggest that stressed humidity had more influence on the bulk physical stability than stressed temperature.

For 70% (w/w) samples aged under 75%RH/40°C, evident melting can be detected after 6 month aging, and the quantity of felodipine crystals in the system was calculated as 24.12% (w/w). Due to the low glass transition temperature of 70% (w/w) felodpine-EUDRAGIT® EPO systems (38.7°C determined by MTDSC) combined with high humidity, the sample started to agglomerate after 2 weeks aging, and thus for further storage test, these samples required to be broken into pieces (such as chipped by spatula and gentle milling). Therefore the assessment of the physical stability of samples aged under 75%RH/40°C may be less accurate (as proved in Chapter 5, milling could induce the physical stability of felodpine-EUDRAGIT® EPO).

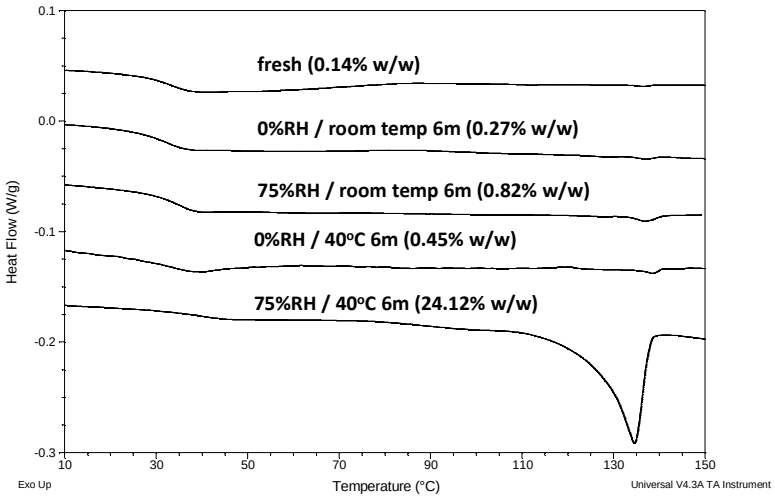

Figure 6.6: MTDSC results of freshly prepared 70% (w/w) felodpine-EUDRAGIT® EPO extrudates and aged under different conditions after 6 months (crystallinity of felodipine in differently aged systems was calculated and listed in the brackets).

More detailed MTDSC results of 70% (w/w) felodipine-EUDRAGIT® EPO melt extrudates aged under 75%RH/40°C are shown in Figure 6.7. It can be seen that the detected melting enthalpy increased with increasing aging time. Evident exothermic peak (recrystallization) was detected after 1 months aging (circled in Figure 6.7). This exothermic peak disappeared after 4 months aging. This demonstrates that a certain amount of amorphous felodipine was separated out from the bulk after 1 month aging and the recrystallization of the phase-separated amorphous felodipine can be induced by heating in DSC scanning. After 4 months aging, the absence of the recrystallization indicates that the phase separated amorphous felodipine had already completely recrystallized on aging. It should be noted that the amount of felodipine remained as solid dispersions in this system (46.88% w/w) was very close to the predicted solubility (45% w/w) by mechanical milling in Chapter 5. This proves the accuracy of milling method in predicting apparent solid solubility of felodipine in felodpine-EUDRAGIT® EPO melt extrudates.

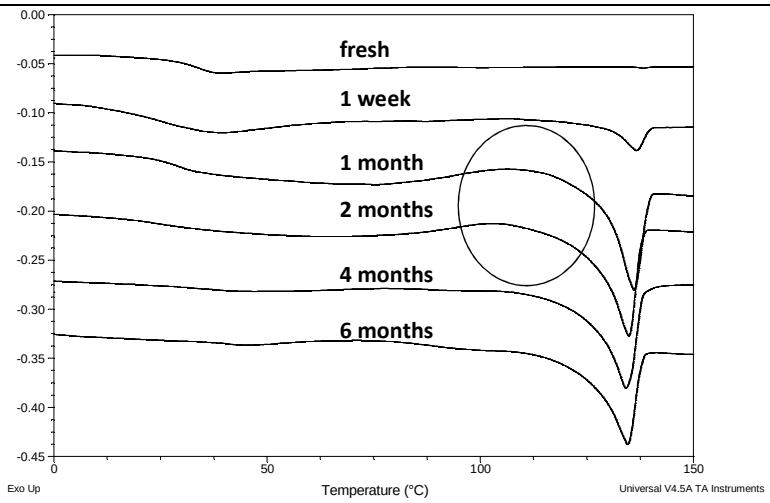

Figure 6.7: MTDSC results of 70% (w/w) felodpine-EUDRAGIT® EPO extrudates aged under 75%RH/40°C.

The bulk physical stability of 70% (w/w) felodpine-EUDRAGIT® EPO melt extrudates was tested by PXRD after 6 months aging under different conditions as seen in Figure 6.8 (samples were stored as intact strand form and milled just before the PXRD test). Results showed that crystalline felodipine features can be only detected in samples aged under 75%RH/40°C, which is in good agreement with MTDSC results. By comparing with the PXRD feature of form I felodipine, it can be confirmed that amorphous felodipine in 70% (w/w) samples aged under 75%RH/40°C recrystallized into form I on aging.

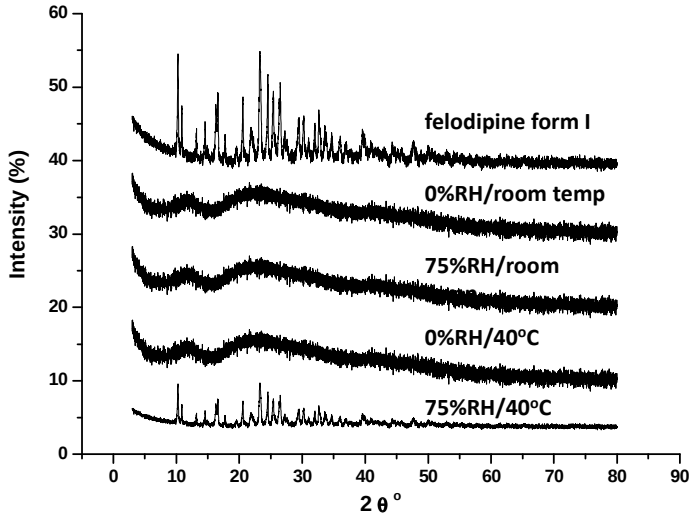

Figure 6.8: PXRD results of 70% (w/w) felodpine-EUDRAGIT® EPO melt extrudates after 6 months aging under different conditions.

Results of the bulk physical stability studies showed that 10% (w/w) felodpine-EUDRAGIT® EPO melt extrudates were highly stable irrespective of storage conditions. The overall bulk

physical stability of 70% (w/w) samples aged under 0%RH/room temperature, 0%RH/40°C and 75%RH/room temperature was still relatively high as proved by low crystallinity in individual samples after 6 months aging. 70% (w/w) melt extrudates aged under 75%RH/40°C showed high level of bulk phase separation and recrystallization. This can possibly be explained by the involved stress for breaking the samples. However, the ultimate amount of felodipine remaining as amorphous solid dispersion (46.88% w/w) in this sample was very close to the predicted solubility by milling method, which proves the accuracy of the milling method in predicting drug-polymer solubiliy.

In short summary, the physical stability of felodipine-EUDRAGIT® EPO melt extrudates showed good agreement with the predicted solubility by milling method. Samples with the drug loading (10% w/w) below the predicted solubility (45% w/w) showed extremely high surface and bulk physical stability irrespective of different aging conditions. Super-saturated 70% (w/w) extrudates showed poor surface physical stability on aging under all conditions. In addition, physical stability study of felodipine-EUDRAGIT® EPO melt extrudates also proved that stressed humidity had more significant impact on aging on the physical stability of 70% (w/w) extrudates than stressed temperature, especially on the surface stability.

6.3.2 Physical stability study of melt extruded celecoxib-EUDRAGIT® EPO systems under different conditions

6.3.2.1 Surface physical stability

No celecoxib crystals were detected by ATR-FTIR on the surface of 10% (w/w) celecoxib-EUDRAGIT® EPO melt extrudates after 6 months aging under all conditions. SEM images showed similar results that no evident particles were observed on the surface of 10% (w/w) extrudates after 6 months aging (Figure 6.9). These results demonstrate that 10% (w/w) celecoxib-EUDRAGIT® EPO melt extrudates had high surface physical stability against stressed conditions on aging. This good physical stability of 10% (w/w) celecoxib-EUDRAGIT® EPO melt extrudates validates the predicted solubility by milling method (42% w/w).

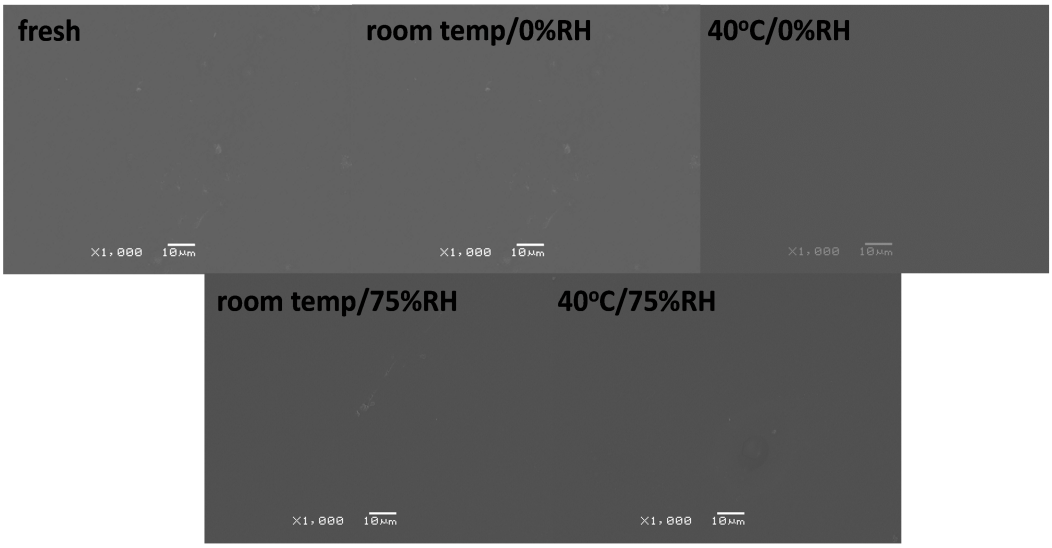

Figure 6.9: SEM images of the surface of 10% (w/w) celecoxib-EUDRAGIT® EPO melt extrudates after 6 months aging under different conditions.

ATR-FTIR spectra of the surface of 70% (w/w) celecoxib-EUDRAGIT® EPO melt extrudates aged under different conditions are shown in Figure 6.10. It has been reported that the SO_2 group is a good indicator to distinguish the physical state of celecoxib (20). Upon transformation from the crystalline to amorphous state, the SO_2 peak shifted from 1345cm^{-1} to 1336cm^{-1} as shown in Figure 6.10. Freshly prepared 70% (w/w) celecoxib-EUDRAGIT® EPO melt extrudates showed a single broad peak at 1338 cm^{-1} indicating a single phase amorphous system of the surface of extrudates.

After 1 month aging under 0%RH/room temperature, two peaks can be observed on the surface of 70% (w/w) melt extrudates with one at 1347cm^{-1} (very close to crystalline celecoxib peak, 1345cm^{-1}) representing crystalline celecoxib and the other one at 1338cm^{-1} representing amorphous solid dispersion, suggesting the occurrence of surface recrystallization in this sample (Figure 6.10).

For 70% (w/w) melt extrudates aged under 75%RH/room temperature, surface recrystallization took place after 3 days aging as proved by the presence of 1347cm^{-1} peak, and on aging the crystalline peak become more dominant in comparison to the amorphous solid dispersion peak (1338cm^{-1}) (Figure 6.10).

For 70% (w/w) melt extrudates aged under 0%RH/40^{o}C, crystalline celecoxib peak (1347cm^{-1}) was detected after 1 week aging. This demonstrates that in comparison to the same sample aged under 75%RH/room temperature, surface recrystallization was slightly delayed, indicating stressed humidity had more significant impact on the surface recrystallization of 70% (w/w) celecoxib-EUDRAGIT® EPO melt extrudates than stressed temperature (Figure 6.10).

Evident crystalline celecoxib was detected on the surface of 70% (w/w) melt extrudates after 3 days aging under 75%RH/40°C. The peak representing amorphous solid dispersions (1338cm^{-1}) disappeared after 1 month aging indicating a high level of surface recrystallization occurred in this sample on aging (Figure 6.10). In comparison to the corresponding samples aged under 75%RH/room temperature and 0%RH/40°C, samples aged under 75%RH/40°C showed the highest level of surface recrystallization.

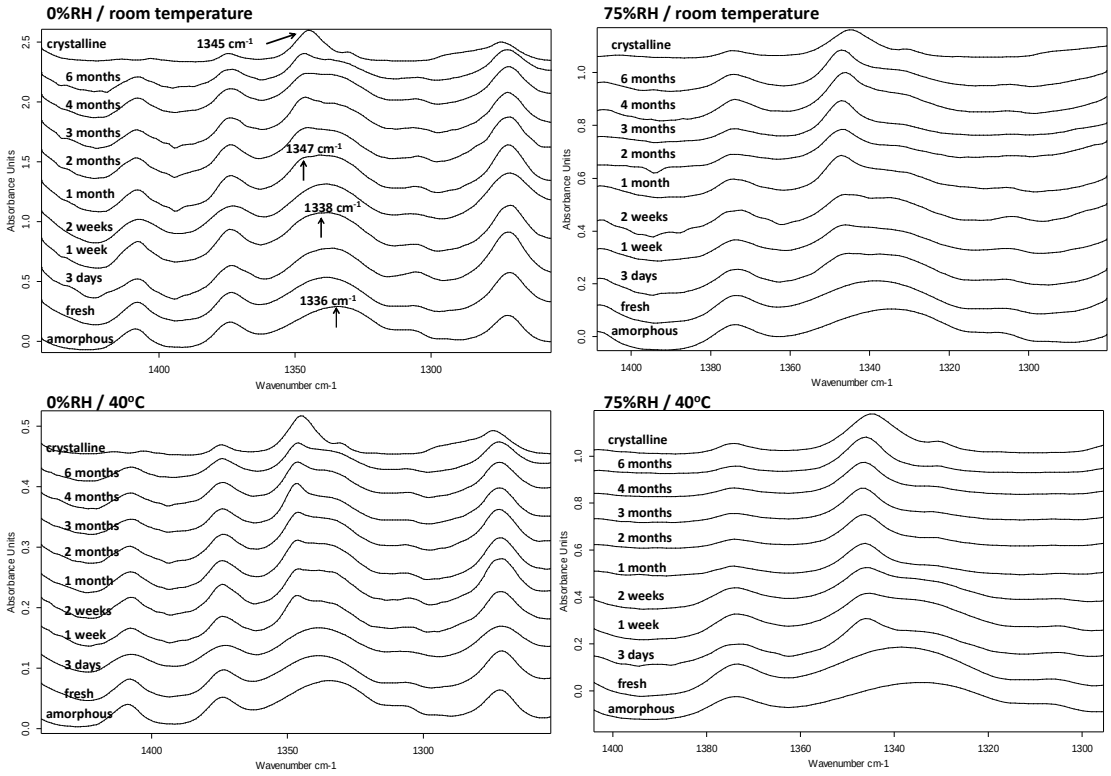

Figure 6.10: ATR-FTIR results of SO_2 group from the surface of 70% (w/w) celecoxib-EUDRAGIT® EPO melt extrudates on aging under different conditions.

Surface recrystallization in 70% (w/w) celecoxib-EUDRAGIT® EPO melt extrudates was also confirmed by SEM studies. SEM images of 3 months aged 70% (w/w) melt extrudates are shown in Figure 6.11. Rod-shaped particles can be observed on the surface of 70% (w/w) samples aged under 0%RH/room temperature and 0%RH/40°C. For samples aged under 75%RH/room temperature, particles showed a needle shape, and the size and density of particles were significantly larger and higher than the same samples aged under 0%RH/40°C, indicating stressed humidity had more impact on the surface recrystallization of 70% (w/w) extrudates than stressed temperature. The two observed crystals habits (needle and rod shape) may indicate polymorphism of crystalline celecoxib. However, the ATR-FTIR results did not show crystalline polymorphs. For 70% (w/w) extrudates aged under 75%RH/40°C, particles grew together to from clusters with the diameter of circa 30µm and the fibre shpae particles on the surface grew to as long as 50µm which was significantly larger than the same samples aged under other conditions.

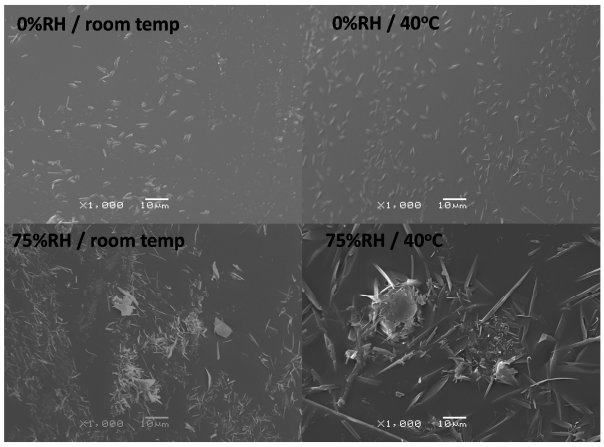

Figure 6.11: SEM images of the surface of 70% celecoxib-EUDRAGIT® EPO melt extrudates after 3 months aging under different conditions.

The kinetics of surface recrystallization of 70% (w/w) celecoxib-EUDRAGIT® EPO melt extrudates on aging was also studied using Image J to analyse SEM images (Figure 6.12). Again, the data did not fit in the Avrami model (*Eq 6.1*) as it lacked of the nucleation phase leading to recrystallization starting with existed nuclei initially. However, a linear relationship of kinetics with acceptable coefficient was observed in individual extrudates aged under all conditions (Figure 6.12). The slope of individual linearity can be considered as the growth rate of surface recrystallisation on aging. Thus it can be seen that temperature has less impact on surface physical stability on aging in comparison to high humidity since samples stored under 0%RH/40^{o}Cshowed a slower rate (36.0µm^2/day) than samples aged under 75%RH/room temperature (12.6µm^2/day). Samples aged under 75%RH/40^{o}C showed the highest rate amongst samples aged under all conditions.

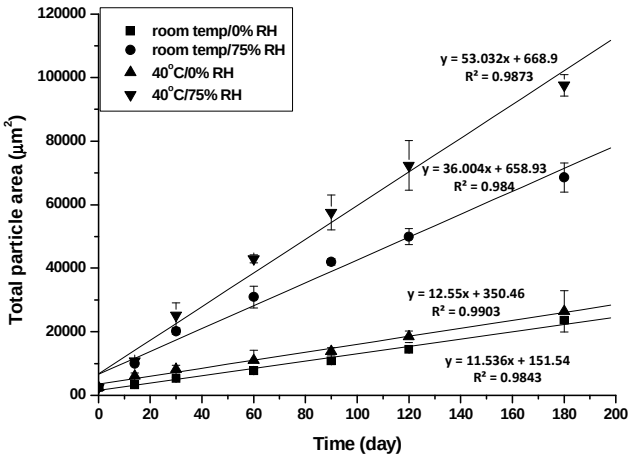

Figure 6.12: Results of total particle area (µm^2) achieved by using Image J to analyse SEM images on the surface of 70% celecoxib-EUDRAGIT® EPO melt extrudates on aging under different conditions.

Results of surface physical stability study showed that no surface recrystallization was detected in any 10% (w/w) melt extrudates aged under all conditions, indicating 10% (w/w) system was highly stable on aging. For 70% (w/w) melt extrudates, surface recrystallization was detected in samples aged under all conditions, indicating low level of surface physical stability of 70% (w/w) extrudates. Moreover, for 70% (w/w) celecoxib-EUDRAGIT® EPO extrudates, stressed humidity also showed significantly more influence on surface recrystallization than stressed temperature.

6.3.2.2 Bulk physical stability

Bulk physical stability of celeocixb-EUDRAGIT® EPO melt extrudates was studied using MTDSC and PXRD. After 6 months aging under different conditions, no melting was detected by MTDSC in any 10% (w/w) melt extrudates. No crystalline celecoxib feature was observed using PXRD. These results indicate that 10% (w/w) melt extrudates were physically stable as bulk after 6 months aging under different conditions.

Bulk physical stability of 70% (w/w) celecoxib-EUDRAGIT® EPO melt extrudates was also studied by MTDSC and PXRD. MTDSC results of fresh and 6 months aged 70% (w/w) melt extrudates are shown in Figure 6.13. Crystallinity of celecixib in different 70% (w/w) systems was calculated using *Eq 5.1* and listed in the figure. Freshly prepared 70% (w/w) melt extrudates showed the amount of crystalline celecoxib of 13.12% (w/w). An exothermic peak (very likely to be recrystallization on heating in MTDSC) was detected in the freshly prepared samples. This indicates that there was already a certain amount of phased separated amorphous celecoxib in the fresh 70% (w/w) extrudates and their recrystallisation could be induced by heating in DSC. After 6 months aging, no significant increase of crystallinity was observed in samples aged under different conditions. For instance, after 6 months aging under 75%RH/40^{o}C, the amount of detected crystalline only increased to 14.58% (w/w), and the recrystallisation peak was still evident. This demonstrates that although phase separation can be detected in 70% (w/w) fresh extrudates, the overall bulk recrystallisation only increased with low level after 6 months aging under different conditions.

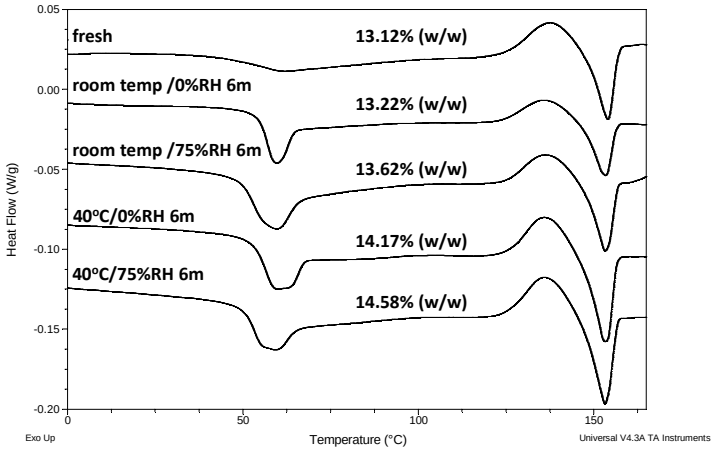

Figure 6.13: MTDSC results of freshly prepared 70% (w/w) celecoxib-EUDRAGIT® EPO extrudates and aged under different conditions after 6 months (crystallinity of celecoxib in differently aged systems was calculated and listed in the brackets).

However, broad endothermic peaks detected by MTDSC at the glass transition areas can be seen for different aged 70% (w/w) samples which did not appear in the freshly prepared 70% (w/w) samples (Figure 6.13). This endothermic peak at glass transition area can be attributed to the overlapped relaxation of amorphous celecoxib and EUDRAGIT® EPO on aging. Relaxation is a procedure occurs to amorphous materials on aging whereby amorphous materials will relax the extra thermodynamic properties, such as enthalpy, to approach to the equilibrium on aging. These relaxed thermodynamic properties can be compensated on heating in DSC as amorphous materials need to re-establish the volume and enthalpy of the liquid state. The increased relaxation enthalpy in aged 70% (w/w) extrudates indicated increased molecular motion in the systems (relationship between relaxation and molecular mobility has been described in Chapter 1), which may potentially affect the bulk physical stability.

A more detailed MTDSC result with non-reversing signals is shown in Figure 6.14 to study the relaxation. It can be seen that after 6 months aging under 75%RH/room temperature, 0%RH/40°C and 75%RH/40°C, two partially overlapped relaxation peaks were detected by MTDSC, and they can be attributed to the relaxation of amorphous celecoxib and the relaxation of EUDRAGIT® EPO. The two separated relaxations suggest that an amorphous phase separation in which drugs and polymers separated into individual amorphous phase occurred in samples aged under these three conditions. Although crystallinity in 6 months aged 70% (w/w) samples under all conditions did not increase significantly, the amorphous phase separation demonstrated that 70% (w/w) celecoxib-EUDRAGIT® EPO melt extrudates as bulk were not physically stable on aging under 75%RH/room temperature, 0%RH/40°C and 75%RH/40°C. The physical instability mainly manifested as amorphous phase separation.

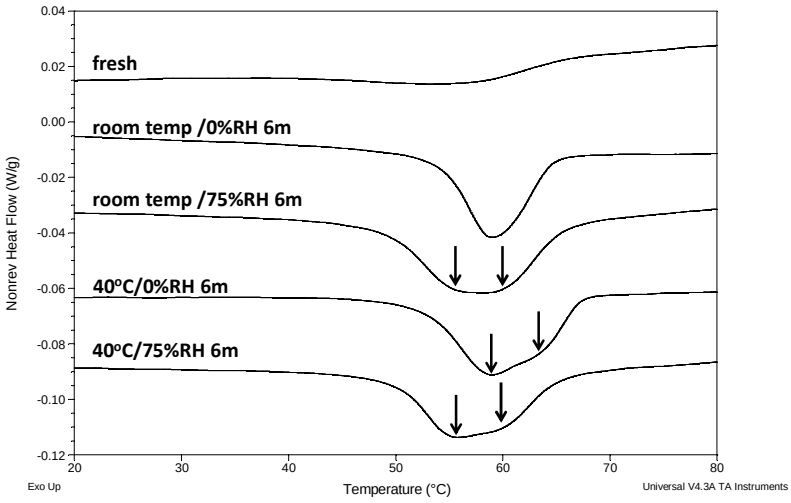

Figure 6.14: MTDSC results in non-reversing signals of freshly prepared and 6 months 70% (w/w) celecoxib-EUDRAGIT® EPO extrudates (crystallinity of felodipine in differently aged systems was calculated and listed in the brackets).

PXRD results showed that no celecoxib was detected in any 70% (w/w) melt extrudates after 6 months aging under all conditions (Figure 6.15). This correlates well with the MTDSC results that phase separation in 70% (w/w) melt extrudates after 6 months aging still remained at amorphous phase separation level. The detected crystalline drug were attributed to the recrystallization of amorphous drug induced on heating in DSC.

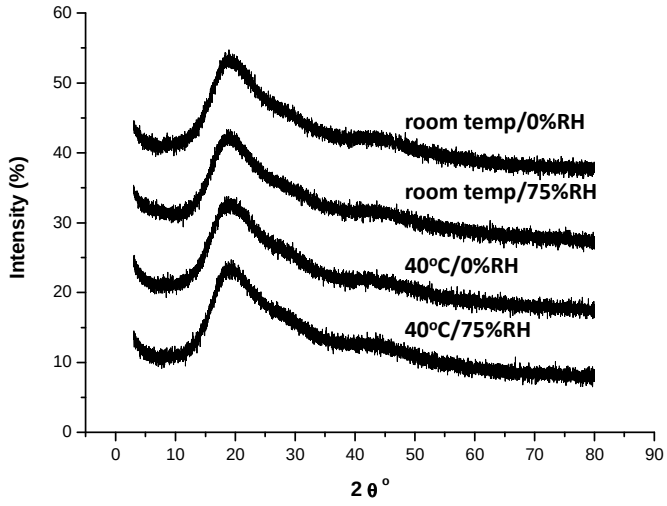

Figure 6.15: PXRD results of 70% (w/w) celecoxib-EUDRAGIT® EPO melt extrudates after 6 months aging under different conditions.

Results of bulk physical stability studies of celecoxib-EUDRAGIT® EPO melt extrudates showed that 10% (w/w) samples were highly stable after 6 months aging under different conditons they were still amorphous solid dispersions. For 70% (w/w) melt extrudates, although no crystalline celecoxib was detected by PXRD after 6 months aging under different conditions, amorphous

phase separation was confirmed using MTDSC in the same aged samples. This indicates that 70% (w/w) celecoxib-EUDRAGIT® EPO melt extrudates were not physically stable on aging under the four conditions.

In summary, the physical stability studies of celecoxib-EUDRAGIT® EPO melt extrudates demonstrated that 10% (w/w) samples were extremely stable after 6 months aging under the four conditions. Both the surface and the bulk of 10% (w/w) extrudates were still amorphous solid dispersions. However, for 70% (w/w) melt extrudates, a high level of surface recrystallisation was observed on aging under all conditions. Stressed humidity showed more impact on surface recrystallization in 70% (w/w) samples than stressed temperature on aging. The bulk physical stability study showed that amorphous phase separation occurred in 70% (w/w) samples aged under 75%RH/room temperature, 0%RH/40^{o}C and 75%RH/40^{o}C. Physical stability studies of celecoxib-EUDRAGIT® EPO melt extrudates agreed well with the predicted solubility using milling method. Samples with the drug loading (10% w/w) below the predicted solubility (42% w/w) remained amorphous solid dispersions after 6 months aging under different conditions, whereas surface and bulk phase separation was confirmed in super-saturated samples (70% w/w). The bulk physical instability was amorphous phase separation and the surface instability was surface recrystallization. This again proves the accuracy of milling method in predicting the solubility of celecoxib in celecoxib-EUDRAGIT® EPO melt extrudates.

6.3.3 Storage test of melt extruded fenofibrate-EUDRAGIT® EPO systems under different conditions

6.3.3.1 Surface physical stability

Surface physical stability of 10% (w/w) fenofibare-EUDRAGIT® EPO melt extrudates under different conditions were studied using SEM and ATR-FTIR. No particles were observed on the surface of freshly prepared 10% (w/w) samples. After 6 months aging, particles were observed on the surface of 10% (w/w) melt extrudates aged under all conditions (Figure 6.16), which indicates the physical instability on the surface of the 10% (w/w) samples. Particle size and density of the crystalline like features on the surface of samples aged under different conditions were similar. This may suggest that surface recrystallisation of 10% (w/w) melt extrudates occurred at early stage of aging and no further increase of surface recrystallization was affected by aging conditions. This was also confirmed by the kinetic study of the surface recrystallization of the 10% (w/w) samples aging under different conditions (Figure 6.17). As seen in Figure 6.17, the surface crystal growth rates of samples aged under different did not show significant different. After 3 months aging, crystal growth reached a plateau for all 10% (w/w) samples, and nearly 12% (calculated using the measured total particle areas divided by the size of the whole image area) of the tested area was covered by particles (crystals). The kinetics of the surface recrystallization did not fit in the Avrami model or linear relationship.

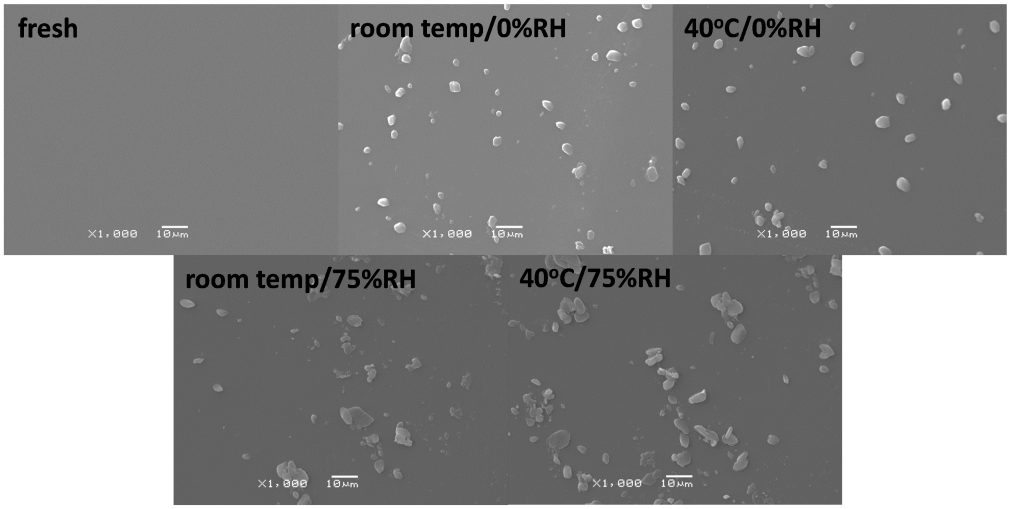

Figure 6.16: SEM images of the surface of 10% (w/w) fenofibrate-EUDRAGIT® EPO melt extrudates after 6 months aging under different conditions.

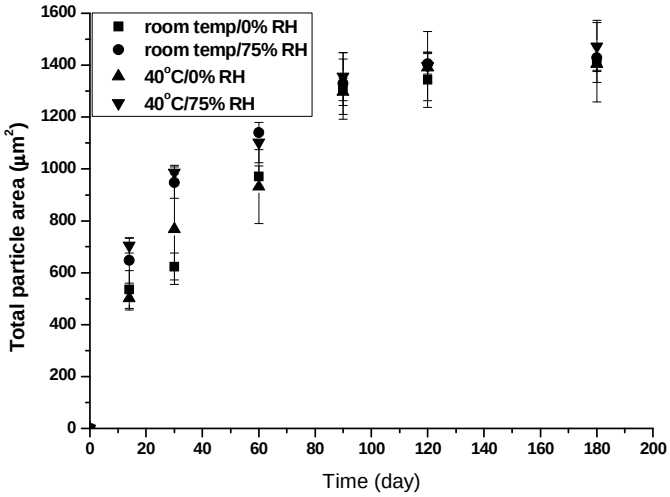

Figure 6.17: Results of total particle area (µm^2) achieved by using Image J to analyse SEM images on the surface of 10% fenofibrate-EUDRAGIT® EPO melt extrudates on aging under different conditions.

Surface recrystallisation of 10% (w/w) samples on aging different conditions was also confirmed using ATR-FTIR (Figure 6.18). A single carbonyl peak at 1657cm^{-1}, which is very close to the carbonyl peak (1656cm^{-1}) from amorphous fenofibrate was detected on the surface of freshly prepared 10% (w/w) sample, suggesting an amorphous drug-polymer system on the surface of the freshly prepared samples. On aging under different conditions, this peak shifted progressively towards the carbonyl peak (1648cm^{-1}) from crystalline fenofibrate. After 6 months aging under all conditions, the carbonyl peak from 10% (w/w) samples all ended at 1651cm^{-1} which is close to the crystalline peak. This gradual carbonyl peak shift indicates phase separation and recrystallization on aging. The ATR-FTIR study on the surface of 10% (w/w) sample demonstrates the surface physical instability of fenofibrate-EUDRAGIT® EPO melt extrudates on aging even with low drug loading.

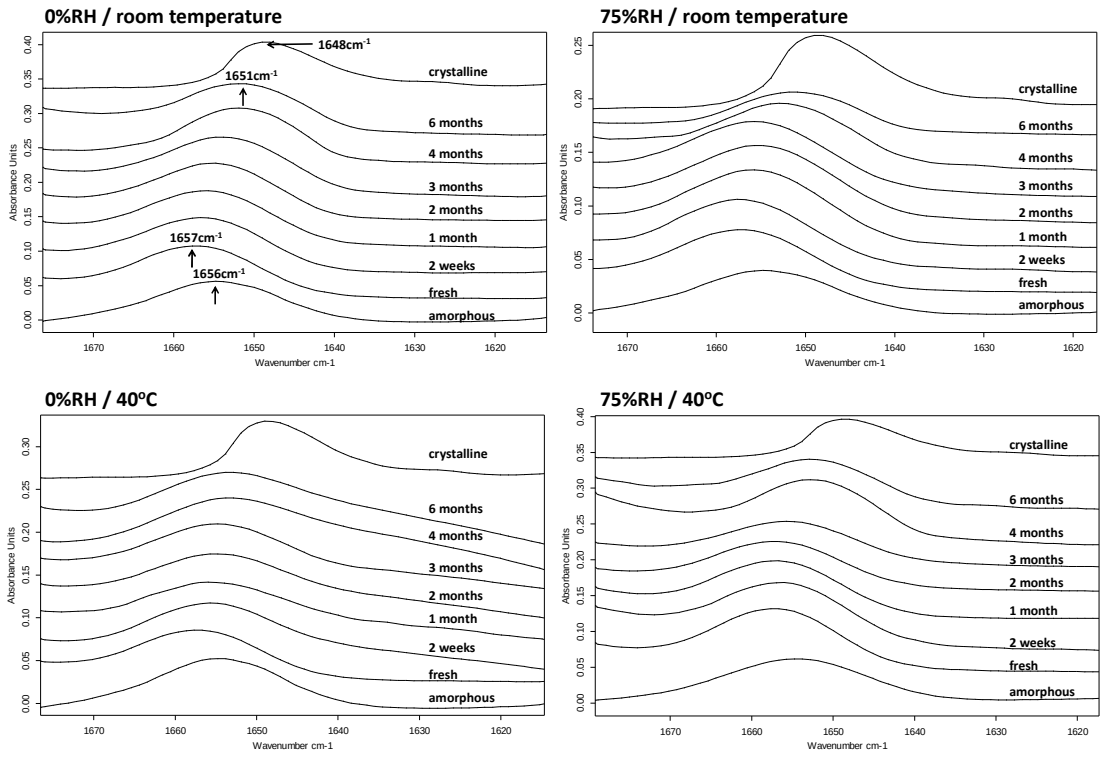

Figure 6.18: ATR-FTIR results of carbonyl group from the surface of 10% (w/w) fenofibrate-EUDRAGIT® EPO melt extrudates on aging under different conditions up to 6 months.

Due to the low glass transition temperature of 70% (w/w) fenofibare-EUDRAGIT® EPO melt extrudates (-19.7°C) as mentioned in Chapter 5, freshly prepared samples were liquid-like and the recrystallization of this sample can be triggered by surface disruption such as touched by tweezers. This fast surface recrystallisation of 70% (w/w) samples under ambient condition was recorded using ATR-FTIR (Figure 6.19 a and b). 70% (w/w) sample was placed in contact with the ATR-FTIR diamond after fresh preparation, and multiple scanning was carried out for a certain time period. Freshly prepared 70% (w/w) fenofibare-EUDRAGIT® EPO melt extrudates showed a single carbonyl group at 1656cm^{-1} which has the same position as amorphous fenofibrate indicating an amorphous drug-polymer system. With increasing time periods under ambient condition, a gradual peak shift can be observed from 1656cm^{-1} to 1648cm^{-1} which is at the same position as crystalline fenofibrate, indicating the occurrence of recrystallization on the surface in contact with the ATR diamond. The peak shift was clearly reflected by the change of intensity ratio of the two peaks (1648cm^{-1} to 1656cm^{-1}) with increasing time (Figure 6.19b). For the first 150min, 70% (w/w) system remained as amorphous solid dispersions, and then recrystallization was triggered (Figure 6.19b). The whole process of the surface recrystallization in 70% (w/w) fenofibare-EUDRAGIT® EPO melt extrudates detected by ATR-FTIR occurred circa in 200min (Figure 6.19b), suggesting that 70% (w/w) fenofibrate extrudates with high drug loading were highly instable.

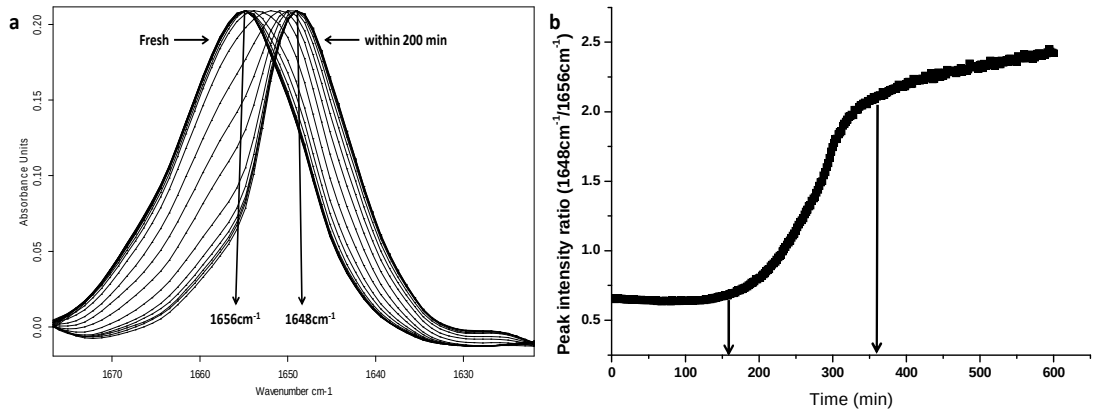

Figure 6.19: ATR-FTIR results of carbonyl group shift in freshly prepared 70% (w/w) fenofibare-EUDRAGIT® EPO melt extrudates (a) and the change of the peak intensity ratio (1648cm^{-1} to 1656cm^{-1}) with increasing time.

6.3.3.2 Bulk physical stability

The bulk physical stability of 10% (w/w) fenofibare-EUDRAGIT® EPO melt extrudates was studied using MTDSC. After 6 months aging under different conditions, no recrystallisation or melting was detected in any 10% (w/w) samples, suggesting a high bulk physical stability of the 10% (w/w) extrudates. This also suggests that the surface recrystallization of 10% (w/w) was at a low level.

The bulk recrystallization of 70% (w/w) fenofibare-EUDRAGIT® EPO melt extrudates was also studied using MTDSC (Figure 6.20). As mentioned earlier, the recrystallisation of 70% (w/w) extrudates can be easily triggered by surface disruption. Therefore, a certain amount of fenofibrate could be induced to recrystallize already during MTDSC sample preparation due to the contact with the sample, and this was reflected by the detected melting peak in fresh 70% (w/w) samples. Using *Eq 5.1*, the amount of crystalline fenofibrate in freshly prepared 70% (w/w) was calculated as 57.39% (w/w). It was also noted that an exothermic peak (recrystallization) was detected before melting, which indicates there was still a certain quantity of amorphous fenofibrate in fresh 70% (w/w) samples before the heating in DSC. After 6 months aging under different conditions, fenofibrate crystallinity in 70% (w/w) samples did not increase significantly in comparison to that in fresh samples (values listed in Figure 6.20). No recrystallization peak (exothermic peak) was detected in any aged 70% (w/w) samples in DSC, indicating phase separated amorphous fenofibrate had recrystallized out completely on aging.

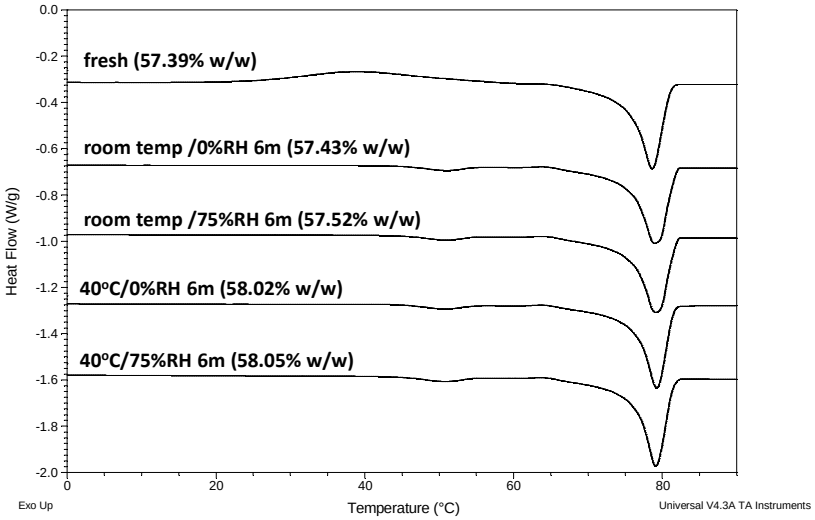

Figure 6.20: MTDSC results of freshly prepared and 6 months aged 70% (w/w) fenofibare-EUDRAGIT® EPO melt extrudates under different conditions (crystallinity of fenofibrate in differently aged systems was calculated and listed in the brackets).

The physical stability study of fenofibrate-EUDRAGIT® EPO melt extrudates showed that both 10% and 70% (w/w) samples had poor surface physical stability, Once triggered, the surface recrystallisation of 70% (w/w) samples could complete within 200min under ambient condition. 10% (w/w) showed high bulk physical stability and after 6 months aging under different conditions, 10% (w/w) samples were still amorphous solid dispersions. For 70% (w/w) extrudates, low bulk physical stability was observed as recrystallisation and melting was detected in the freshly prepared samples by MTDSC. The physical stability study of fenofibrate-EUDRAGIT® EPO melt extrudates showed good agreement with the predicted solubility by surface disruption that 10% (w/w) samples showed significantly high bulk physical stability on aging under different conditions.

6.3.4 Physical stability studies of melt extruded carbamazepine-EUDRAGIT® EPO systems under different conditions

As mentioned in Chapter 5, thermal degradation of carbamazepine was found when preparing carbamazepine-EUDRAGIT® EPO with 70% (w/w) drug loading at the temperature of its melting point using hot melt extrusion. By decreasing the operation temperature in hot melt extrusion, whilst thermal degradation was avoided, the yield was extremely low, leading to the failure of producing a sufficient amount of 70% (w/w) samples for storage tests. In addition, at low operation temperature, super-saturated samples cannot be prepared as proved in Chapter 5. Therefore the physical stability study was only carried out on 10% (w/w) carbamazepine-EUDRAGIT® EPO melt extrudates under different aging conditions.

6.3.4.1 Surface physical stability

Surface recrystallization of 10% (w/w) carbamazepine-EUDRAGIT® EPO melt extrudates was studied using SEM and ATR-FTIR. SEM images of fresh and 6 months aged 10% (w/w) extrudates are shown in Figure 6.21. Compared with freshly prepared samples, after 6 months aging under different conditions, particles of rod and needle shapse can be observed on the surface of all samples, suggesting the occurrence of surface recrystallisation on aging. It can be seen that particle size and density on the surface of 10% (w/w) samples aged under 75%RH/room temperature is significantly higher than that of the samples aged under 0%RH/40^{o}C. This indicates stressed humidity had more significant impact on the surface recrystallisation of 10% (w/w) samples than stressed temperature.

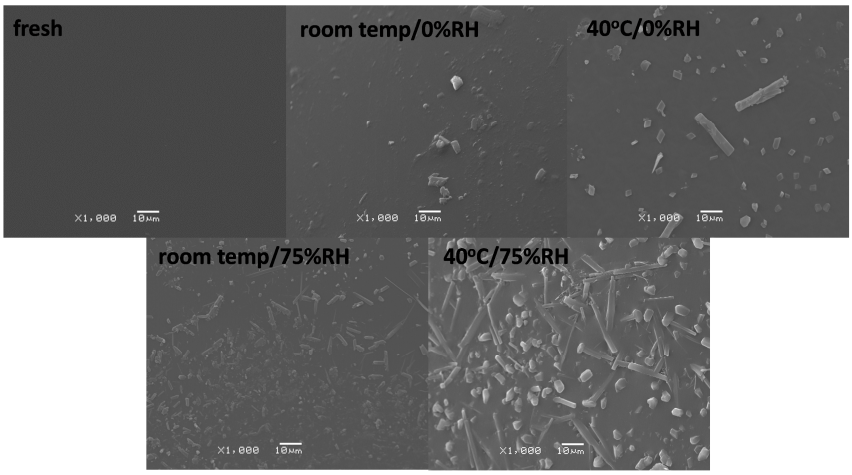

Figure 6.21: SEM images of the surface of fresh and 6 months aged 10% (w/w) carbamazepine-EUDRAGIT® EPO melt extrudates under different conditions.

The kinetics of surface recrystallization of 100% (w/w) carbamazepine-EUDRAGIT® EPO melt extrudates on aging was studied using Image J to analyse SEM images (Figure 6.22). The data did not fit in the Avrami model (*Eq 6.1*). A linear relationship of kinetics with acceptable coefficient was observed in individual extrudates aged under all conditions (Figure 6.22). The slope of individual linearity can be considered as the growth rate of surface recrystallisation on aging. It clearly shows that high temperature has less impact on surface physical stability on aging in comparison to high humidity since samples stored under 0%RH/40^{o}C showed a slower rate (6.2µm^{2}/day) than samples aged under 75%RH/room temperature (12.5µm^{2}/day). Samples aged under 75%RH/40^{o}C showed the highest rate amongst samples aged under all conditions.

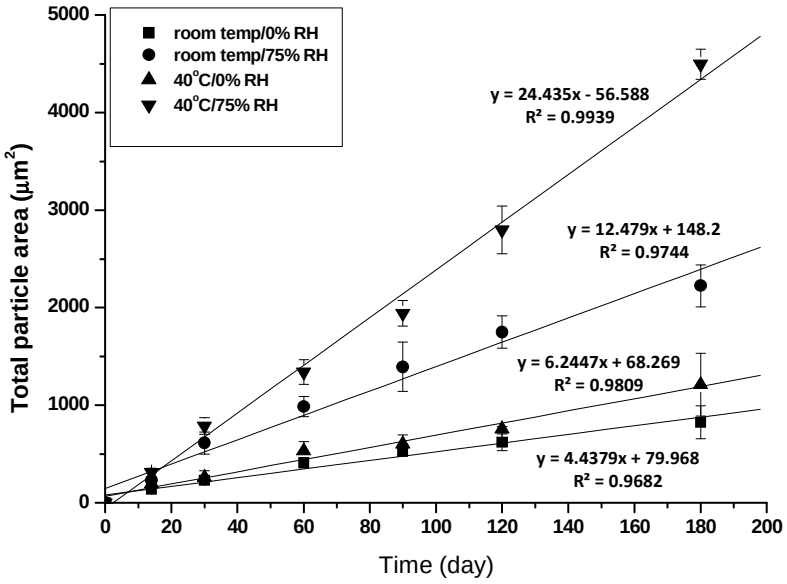

Figure 6.22: Results of total particle area (μm^2) achieved by using Image J to analyse SEM images on the surface of 10% carbamazepine-EUDRAGIT® EPO melt extrudates on aging under different conditions.

Surface recrystallization was also confirmed using ATR-FTIR as shown in Figure 6.23. Due to the low drug loading, the NH_2 group from amorphous carbamazepine in the freshly prepared 10% (w/w) melt extrudates was difficult to be detected since the peak intensity in amorphous state can be lower than in the crystalline state (21). After aging under 75%RH/room temperature, a peak with a relatively high intensity at 3464cm^{-1} was detected, which has the identical NH_2 peak position of that from form III crystalline carbamazepine, indicating the recrystallization into form III on aging under high humidity at room temperature (22). After 3 months aging under the same condition, another peak at 3486cm^{-1} appeared and it was confirmed as form I crystalline carbamazepine (22), and thus amorphous carbamazepine on the surface of 10% (w/w) samples recrystallisaed into a mixture of form I and III under 75%RH/room temperature. Similar recrystallization occurred on the surface of 10% (w/w) samples aged under 75%RH/40^{o}C, in which amorphous carbamazepine recrystallisaed into a mixture of form I and III. For 10% (w/w) melt extrudates aged under 0%RH/40^{o}C, only form III carbamazepine was detected after 2 months storage. For 10% (w/w) samples aged under 0%RH/room temperature, no carbamazepine crystals were detected after 6 months storage. It also can be noticed in this sample that the NH peak was hardly detected after 6 months aging under 0%RH/room temperature. This is because the intensity of the NH peak from amorphous solid dispersions was low as mentioned earlier.

To summarise these findings, it can be concluded that stressed aging condition, including high temperature and humidity, can induce recrystallization into a mixture of form I and III by high humidity rather than high temperature. If stored under dry condition at room temperature, the 10%

(w/w) carbamazepine-EUDRAGIT® EPO melt extrudates can be physically stable for up to 6 months.

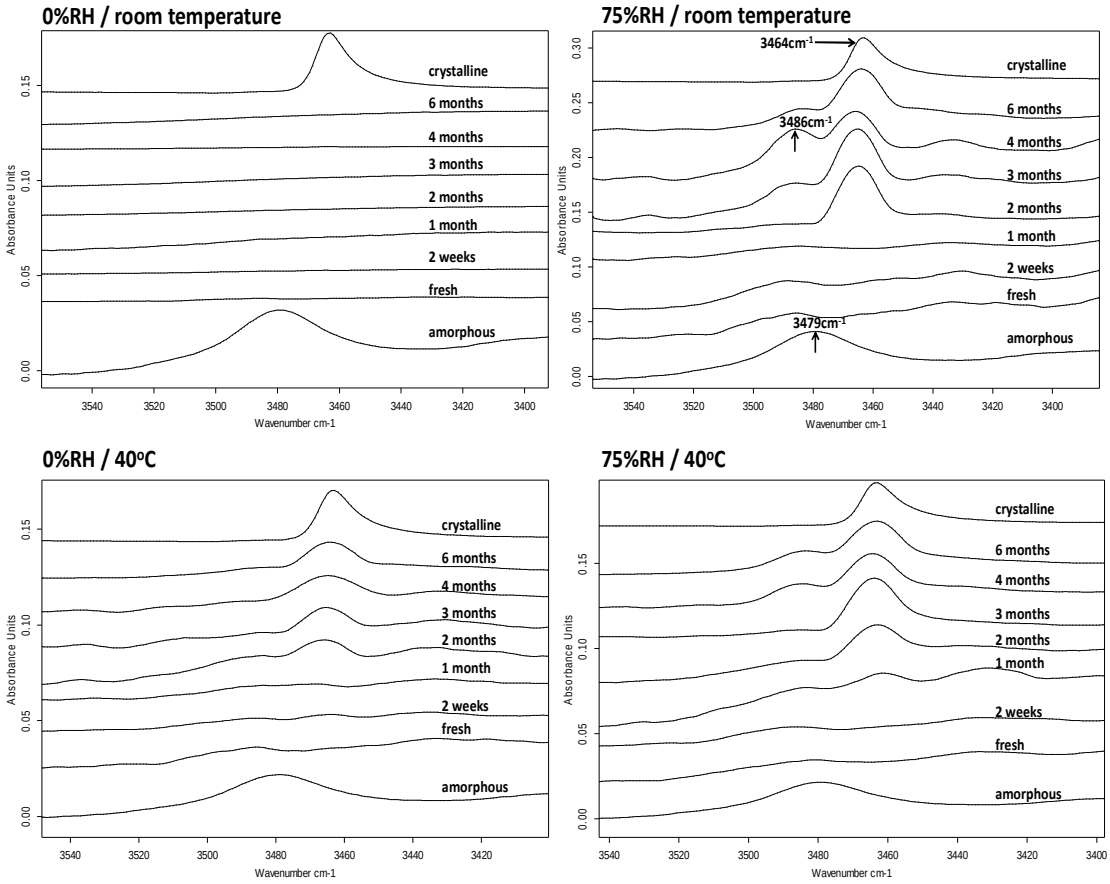

Figure 6.23: NH_2 groups on the surface of 10% (w/w) carbamazepine-EUDRAGIT® EPO melt extrudates aged under different conditions for up to 6 months.

6.3.4.2 Bulk physical stability

The bulk physical stability of 10% (w/w) carbamazepine-EUDRAGIT® EPO melt extrudates was evaluated using MTDSC. After 6 months aging, no crystalline carbamazepine was detected in 10% (w/w) melt extrudates aged under all conditions, which indicates high bulk physical stability of this system.

Physical stability studies of 10% (w/w) carbamazepine-EUDRAGIT® EPO melt extrudates showed that physical instability only occurred on the surface of the samples. The high bulk physical stability on aging was in good agreement with the predicted solubility (18% w/w) by the milling method.

6.3.5 Comparison of physical stability studies between different melt extrudates

The significance of the physical stability of solid dispersions has been substantially emphasised by pharmaceutical researchers due to its important role in affecting the dissolution rate of poorly water soluble drugs and hence bioavailability. As mentioned earlier, factors such as glass transition temperatures of solid dispersions, molecular mobility of amorphous drugs and drug-polymer miscibility and solid solubility have been evaluated and considered to be key factors that control the physical stability. Due to the large variety of the selection of drugs and polymers and different processing methods for the preparation of solid dispersions, it is difficult to establish a general rule for the improvement of formulation design of solid dispersions in the pharmaceutical industry. In this work, by investigating different properties associated with the physical stability of solid dispersions, three fundamental aims as mentioned in the introduction can be accomplished.

Results of the physical stability studies of melt extrudates prepared with model drugs and EUDRAGIT® EPO are summarised in Table 6.1. Stressed temperature and stressed humidity have been considered as the two main storage factors which can potentially affect the physical stability of amorphous solid dispersions on aging. Molecular mobility in amorphous solid dispersions can be substantially increased if the storage temperature is close to or above the T_g of the solid dispersions, which can lead to phase separation and recrystallisation. Stressed humidity can also affect the physical stability as water sorption in amorphous solid dispersions can act as plasticizers which can decrease the T_g of the system and increase the molecular mobility. In this chapter, results of physical stability studies of individual system clearly revealed that stressed humidity had more significant impact on the physical stability of amorphous solid dispersions than stressed temperature, especially on the surface physical stability. For instance in Table 6.1, surface recrystallisation rate of 70% (w/w) felodipine-EUDRAGIT® EPO aged under 75%RH/room temperature (33.3μm^2/day) was almost three times higher than that of the samples aged under 0%RH/40^oC (11.6μm^2/day). This was also the case for 70% (w/w) celecoxib- EUDRAGIT® EPO and 10% (w/w) carbamazepine-EUDRAGIT® EPO melt extrudates. This phenomenon was not evident for 10% (w/w) fenofibrate-EUDRAGIT® EPO systems, which might be attributed to the reason that surface recrystallisation occurred at early stage of aging to a saturated level irrespective of aging conditions as proved by the kinetics of crystal growth on aging (Figure 6.16). Nevertheless, physical stability studies still conclude that stressed humidity (refers to accelerated conditions in USP, 75%RH) has stronger effect on the surface recrystallization of melt extrudates than stressed temperature (refers to accelerated conditions in USP, 40^oC).

This stronger effect by stressed humidity is not clearly understood. It might be accounted for by the fact that extrudates were aged as intact strand, and thus the adsorbed water on the surface can be relatively high (although difficult to measure). Therefore, the “local” water content on the surface can be very high, leading to the faster recrystallisation rate in comparison to samples aged under 0%RH/40^oC.

Table 6.1: Summary of the physical stability studies of melt extrudates prepared with model drugs and Eudragit® EPO aged under different conditions.

Drugs	Melt extrudates		0%RH/room temp	75%RH/room temp	0%RH/40°C	75%RH/40°C
felodipine	**10%**	**surface**	A*	A	A	A
		bulk	A	A	A	A
	70%	**surface (μm²/day)***	10.3	33.3	11.6	172.9
		bulk* (w/w)	0.27%	0.82%	0.45%	24.12%
celecoxib	**10%**	**surface**	A	A	A	A
		bulk	A	A	A	A
	70%	**surface(μm²/day)***	11.5	36.0	12.6	53.0
		bulk	13.22%	14.17%	13.62%	14.58%
fenofibrate	**10%**	**surface**	A, C*	A, C	A, C	A, C
		bulk	A	A	A	A
	70%	**surface**	fast recrystallization (completed within 200min under ambient condition)			
		bulk* (w/w)	57.43%	57.52%	58.02%	58.05%
carbamazepine	**10%**	**surface(μm²/day)***	4.4	12.5	6.2	24.4
		bulk	A	A	A	A

A*:amorphous solid dispersion; C*: crystalline drug; surface*: surface crystal growth rate; bulk*: crystallinity (w/w) in individual system after 6 months aging calculated using *Eq 5.1*.

A clear order of physical stabilities of different melt extruded formulations on aging can be made by comparing the results between different model drug-polymer systems. For 10% (w/w) extrudates, felodipine and celecoxib showed extremely high physical stability both on surface and as bulk under all conditions (Table 6.1). However, as seen in SEM images, particles were observed on the surface of both 10% carbamazepine and fenofibrate extrudates on aging under all conditions (Figure 6.15 and 6.20). For 70% (w/w) samples, felodipine and celecoxib showed high bulk physical stability but poor surface physical stability. Comparing the crystallinity between felodipine and celecoxib melt extrudates in Table 6.1, it can be seen that after 6 months aging crystallinity in 70% (w/w) felodipine melt extrudates was significantly lower than that in 70% (w/w) celecoxib melt extrudates (the exception of felodipine extrudates aged under 75%RH/room temperature has been discussed and was attributed to the involved breaking strength). 70% (w/w) fenofibrate showed the fastest recrystallisation rate under ambient condition (within 200min). Consequently, based on the findings from the physical stability studies, it is reasonable to conclude the order of the physical stability of melt extrudates under all conditions is felodipine melt > celecoxib > carbamazepine ≥ fenofibrate melt extrudates.

In previous chapters, several factors of model drugs associated with physical stability of solid dispersions have been studied. Several theoretical approaches were applied to predict drug-polymer miscibility and solubility. In addition, a practical mechanical milling approach was developed to predict the apparent solid solubility of drugs in melt extrudates. In order to reveal the key factors which control the physical stability of amorphous solid dispersions, the results which are considered to be related with the physical stability of amorphous solid dispersions from previous chapters are summarised in Table 6.2. Glass transition temperatures of different amorphous drugs, calculated molecular mobility of amorphous drugs, theoretically predicted drug-polymer solid solubility do not show the same order as the order of physical stabilities of different formulations. Amongst all investigated factors so far, the physical stability of amorphous drugs and predicted apparent solid solubility of drugs in melt extrudates by mechanical milling seem to be the two key factors associated with physical stability of melt extrudates and they both showed the same order as the order of the physical stability order of different formulations. Based on the achieved results, it may generally suggest that melt extruded amorphous solid dispersions formulated with a drug which is physically stable in amorphous state alone can be expected to have a good physical stability. More significantly, a drug loading below the predicted drug-polymer solubility (by milling method) is essential for preparing a physically stable melt extruded amorphous solid dispersion. Glass transition temperatures and molecular mobility of amorphous drugs did not show direct relationship with the physical stability of amorphous solid dispersions. These two factors are commonly associated with the physical stability of amorphous drugs alone. After formulated with polymers, the physical stability can be enhanced significantly in comparison to that of the amorphous drugs alone. It also demonstrates that the milling method is a more accurate and valid

method for the prediction of drug-polymer solubility in melt extrudates than the theoretical approaches. Thus the developed milling method has the potential to be generalised as a common method to predict drug-polymer solubility in melt extrudates. As mentioned in Chapter 5, milling can be a relatively fast method for the prediction of drug-polymer solubility in melt extrudates. Therefore, the developed milling method can be beneficial and useful for the formulation design of melt extrudates in the pharmaceutical industry.

Table 6.2: Summary of drug-polymer solubilities (model drugs in EUDRAGIT® EPO) predicted by different approaches and physical properties of model drugs.

Drugs	Solubility by milling approach (w/w)	Solubility by solubility parameter approach (w/w)	Solubility by melting point depression approach (w/w)	Solubility by enthalpy measurement approach (w/w)	T_g (^oC)	Relaxation time at 25^oC (s)	Ranking of the physical stability of amorphous drugs under 0%RH/room temp and 75%RH/room temp
felodipine	45 %	25%	31%	20%	46.5	2.47×10^{3}	1
celecoxib	42%	35%	41%	20%	58.2	1.31×10^{4}	2
carbamazepine	18%	15%	46%	30%	50.1	1.78×10^{3}	3
fenofibrate	13%	40%	-	40%	-19.7	3.51×10^{-1}	4

One may consider another key factor in influencing the physical stability, the formation of hydrogen bonding between drugs and polymers in amorphous solid dispersions. Although three model drugs have hydrogen bonding donor groups (NH for felodipine, NH_2 for celecoxib and NH_2 for carbamazepine) and EUDRAGIT® EPO has acceptor groups, there was no evidence showing the formation of hydrogen bonding between drugs and the polymer since the EUDRAGIT® EPO carbonyl peak position did not shift after formulation with the three drugs. Therefore one may argue that the physical stability could behave better if hydrogen bonding formed between drugs and polymers since it has been considered as the strength in restricting molecular motion and the key factor that affects solid solubility (23). On one hand, hydrogen bonding cannot be universally formed between any drug and polymer, therefore the development of methods for enhancing physical stability of solid dispersions lacking of hydrogen bonding is still necessary. On the other hand, hydrogen bonding is normally formed in formulations with polymers as acceptors, and thus the physical stability can be significantly influenced if formulations with hydrogen bonding were exposed to high humidity since water molecule is a very strong competitor against drug molecules to form hydrogen bonding with polymers in formulations (24, 25). The involvement of hydrogen bonding in melt extruded formulation will also be discussed in Chapter 7.

6.4 Conclusions

In this chapter, physical stability studies under different aging conditions of melt extrudates prepared with model drugs and EUDRAGIT® EPO were investigated. By comparing the physical stability of individual drug-polymer formulation under different aging conditions, it was proved that humidity had more significant impact than high temperature on the physical stability of melt extrudates, especially on the surface physical stability. In addition, for individual drug-polymer system with the two drug loadings, the bulk physical stability was significantly higher than the surface physical stability.

By comparing the results of physical stability studies between different melt extrudates, the order of physical stability (bulk and surface) of melt extruded formulations containing model drugs can be concluded as felodipine > celecoxib > carbamazepine ≥ fenofibrate. Combined with the results from previous chapters, physical stability of amorphous drugs and predicted apparent solid solubility of drugs in melt extrudates using the milling method were the two key factors which were most relevant to the physical stability of melt extruded solid dispersions.

Results of physical stability studies also validated the milling method as a more accurate method for predicting drug-polymer solubility than the three theoretical approaches. Therefore, the developed milling method can be a useful and fast tool to predict safe drug loading and thus enhance the physical stability when developing melt extruded formulations in the pharmaceutical industry.

Reference

1. E. Karavas, E. Georgarakis, M.P. Sigalas, K. Avgoustakis, and D. Bikiaris. Investigation of the release mechanism of a sparingly water-soluble drug from solid dispersions in hydrophilic carriers based on physical state of drug, particle size distribution and drug–polymer interactions. European Journal of Pharmaceutics and Biopharmaceutics. 66:334-347 (2007).
2. H. Konno, T. Handa, D.E. Alonzo, and L.S. Taylor. Effect of polymer type on the dissolution profile of amorphous solid dispersions containing felodipine. European Journal of Pharmaceutics and Biopharmaceutics. 70:493-499 (2008).
3. H. Bley, B. Fussnegger, and R. Bodmeier. Characterization and stability of solid dispersions based on PEG/polymer blends. International Journal of Pharmaceutics. 390:165-173 (2010).
4. K. Kogermann, A. Penkina, K. Predbannikova, K. Jeeger, P. Veski, J. Rantanen, and K. Naelapää. Dissolution testing of amorphous solid dispersions. International Journal of Pharmaceutics.
5. G. Chawlaand A.K. Bansal. A comparative assessment of solubility advantage from glassy and crystalline forms of a water-insoluble drug. European Journal of Pharmaceutical Sciences. 32:45-57 (2007).
6. G. Van den Mooter. The use of amorphous solid dispersions: A formulation strategy to overcome poor solubility and dissolution rate. Drug Discovery Today: Technologies. 9:e79-e85 (2012).
7. B. Hancock, S. Shamblin, and G. Zografi. Molecular Mobility of Amorphous Pharmaceutical Solids Below Their Glass Transition Temperatures. Pharm Res. 12:799-806 (1995).
8. M. Kennedy, J. Hu, P. Gao, L. Li, A. Ali-Reynolds, B. Chal, V. Gupta, C. Ma, N. Mahajan, A. Akrami, and S. Surapaneni. Enhanced Bioavailability of a Poorly Soluble VR1 Antagonist Using an Amorphous Solid Dispersion Approach: A Case Study. Molecular Pharmaceutics. 5:981-993 (2008).
9. F. Qian, J. Huang, and M.A. Hussain. Drug-polymer solubility and miscibility: Stability consideration and practical challenges in amorphous solid dispersion development. Journal of Pharmaceutical Sciences. 99:2941-2947 (2010).
10. Y.C. Ng, Z. Yang, W.J. McAuley, and S. Qi. Stabilisation of amorphous drugs under high humidity using pharmaceutical thin films. European Journal of Pharmaceutics and Biopharmaceutics(2013).
11. S.-M. Khoo, C.J.H. Porter, and W.N. Charman. The formulation of Halofantrine as either non-solubilising PEG 6000 or solubilising lipid based solid dispersions: Physical stability and absolute bioavailability assessment. International Journal of Pharmaceutics. 205:65-78 (2000).
12. S. Narine, K. Humphrey, and L. Bouzidi. Modification of the Avrami model for application to the kinetics of the melt crystallization of lipids. J Amer Oil Chem Soc. 83:913-921 (2006).
13. S. Qi, P. Belton, K. Nollenberger, N. Clayden, M. Reading, and D.M. Craig. Characterisation and Prediction of Phase Separation in Hot-Melt Extruded Solid Dispersions: A Thermal, Microscopic and NMR Relaxometry Study. Pharm Res. 27:1869-1883 (2010).
14. S. Qi, P. Belton, K. Nollenberger, A. Gryczke, and D.M. Craig. Compositional Analysis of Low Quantities of Phase Separation in Hot-Melt-Extruded Solid Dispersions: A Combined Atomic Force Microscopy, Photothermal Fourier-Transform Infrared Microspectroscopy, and Localised Thermal Analysis Approach. Pharm Res. 28:2311-2326 (2011).
15. M. Avrami. Kinetics of phase change. I general theory. Journal of chemical physics. 7:(1939).
16. E.A. Schmitt, D. Law, and G.G.Z. Zhang. Nucleation and crystallization kinetics of hydrated amorphous lactose above the glass transition temperature. Journal of Pharmaceutical Sciences. 88:291-296 (1999).
17. T. De Cock, C. Capdevila, F.G. Caballero, and C. García de Andrés. Global recrystallisation model of low carbon sheet steels with different cementite contents. Materials Science and Engineering: A. 519:9-18 (2009).

18. W. Sinclair, M. Leane, G. Clarke, A. Dennis, M. Tobyn, and P. Timmins. Physical stability and recrystallization kinetics of amorphous ibipinabant drug product by fourier transform raman spectroscopy. Journal of Pharmaceutical Sciences. 100:4687-4699 (2011).
19. D. Zhou, G.G.Z. Zhang, D. Law, D.J.W. Grant, and E.A. Schmitt. Thermodynamics, Molecular Mobility and Crystallization Kinetics of Amorphous Griseofulvin. Molecular Pharmaceutics. 5:927-936 (2008).
20. G. Chawla, P. Gupta, R. Thilagavathi, A.K. Chakraborti, and A.K. Bansal. Characterization of solid-state forms of celecoxib. European Journal of Pharmaceutical Sciences. 20:305-317 (2003).
21. A.A. Ambike, K.R. Mahadik, and A. Paradkar. Stability study of amorphous valdecoxib. International Journal of Pharmaceutics. 282:151-162 (2004).
22. A.L. Grzesiak, M. Lang, K. Kim, and A.J. Matzger. Comparison of the four anhydrous polymorphs of carbamazepine and the crystal structure of form I. Journal of Pharmaceutical Sciences. 92:2260-2271 (2003).
23. M. Vasanthavada, W.-Q. Tong, Y. Joshi, and M.S. Kislalioglu. Phase Behavior of Amorphous Molecular Dispersions II: Role of Hydrogen Bonding in Solid Solubility and Phase Separation Kinetics. Pharm Res. 22:440-448 (2005).
24. L. Taylorand G. Zografi. Spectroscopic Characterization of Interactions Between PVP and Indomethacin in Amorphous Molecular Dispersions. Pharm Res. 14:1691-1698 (1997).
25. H. Konnoand L. Taylor. Ability of Different Polymers to Inhibit the Crystallization of Amorphous Felodipine in the Presence of Moisture. Pharm Res. 25:969-978 (2008).

Chapter 7: Enhancement of the physical stability of hot melt extruded solid dispersions using immiscible polymer blends

7.1 Introduction

Hot melt extrusion has been proved as an effective processing method for the preparation of amorphous solid dispersions to improve the dissolution rate of poorly water-soluble drugs (1-4). However, with the physical structure of being amorphous solid dispersions, amorphous formulations prepared by hot melt extrusion inevitably have the physical stability issue, which can potentially affect dissolution performance (5-7). To improve the physical stability of amorphous solid dispersions, formulation strategies such as using polymers with high drug-polymer miscibility and solubility, have been highly suggested (8-10).

In Chapter 6, a high degree of surface recrystallization was observed in felodipine-EUDRAGIT® EPO melt extrudates under stressed conditions (high humidity and temperature). In this chapter, in order to enhance the physical stability of felodipine amorphous solid dispersions, immiscible polymer blends were applied as a formulation strategy in hot melt extrusion.

The hypothesis of the polymer blend formulation strategy for the enhancement of the physical stability was originated from two aspects. Firstly, the incorporation of a polymer (Kollidon® VA 64) which may have higher solubility of felodipine than EUDRAGIT® EPO into the binary felodipine-EUDRAGIT® EPO systems can increase the overall drug-polymer solubility in amorphous solid dispersions. It has been reported in articles that hydrogen bonding can play a significant role in drug-polymer solubility (8, 11-13). As discussed in Chapter 6, no evidence of the formation of hydrogen bonding between felodipine and EUDRAGIT® EPO was seen. However, Kollidon® VA 64 has been reported to form hydrogen bonding with felodipine in solid dispersions (14). Therefore, the addition of Kollidon® VA 64 into felodipine-EUDRAGIT® EPO systems may potentially increase the overall solubility of felodipine in melt extrudates.

However, the drawback of using such polymers (PVP or PVPVA 64) is that they are highly hygroscopic, which can increase the risk of physical instability on aging especially under stressed humidity (14, 15). This was also proved in Chapter 6 that humidity could significantly affect the surface physical stability of melt extruded solid dispersions. This is attributed to the reason that the drug-polymer hydrogen bonding in solid dispersions can be disrupted upon exposure to high humidity by adsorbed and absorbed water molecules as they have a high potential to act as hydrogen bonding donors and accepters (16). Therefore, by blending the hydrophilic polymer (Kollidon® VA 64 with high hygroscopicity) and the hydrophobic polymer (EUDRAGIT® EPO),

the overall moisture sorption of amorphous solid dispersions can be reduced, leading to a higher physical stability.

The illustration of the formulation design is shown in Figure 7.1. Since the two polymers are immiscible, two separated phases including hydrophobic phase and hydrophilic phase will exist in the amorphous solid dispersion. With higher drug-polymer solubility, the hydrophilic polymer will dissolve more drug molecules than the hydrophobic polymer. Meanwhile, the separated hydrophilic domains can be protected from moisture uptake by the hydrophobic domains. Therefore, the immiscible polymer blends may enhance the physical stability of amorphous solid dispersions by the combined effect of increasing the saturated level of the amorphous solid dispersions and reducing moisture sorption.

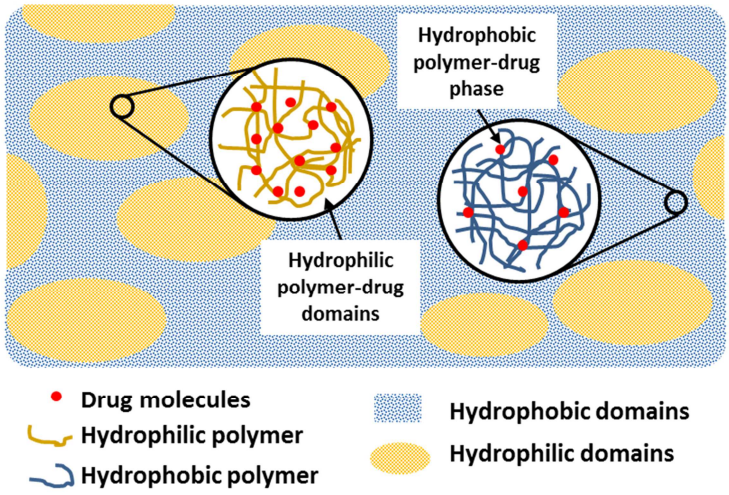

Figure 7.1: Proposed schematic illustration of the micro-strucutre of the immiscible polymer blend formulation loaded with model drug.

Research objective

1. To predict the apparent solid solubility of felodipine in Kollidon® VA by mechanical milling and melting point depression approaches.

2. To enhance the physical stability of melt extruded felodipine amorphous solid dispersions against stressed conditions (high temperature and humidity) by the application of the polymer blends of EUDRAGIT® EPO and Kollidon® VA matrices in hot melt extrusion.

3. To investigate the micro-structure of felodipine-polymer blend melt extrudates to confirm the hypothesis of the enhancement of the physical stability.

7.2 Experimental methods

7.2.1 Hot melt extrusion

Instrumental information refers to Chapter 2 (2.2.1.1). Crystalline felodipine and EUDRAGIT® EPO powder with ratios of 10:90, 30:70, 50:50, and 70:30 (w/w), crystalline felodipine and Kollidon® VA 64 powder with ratios of 10:90, 30:70, 50:50, and 70:30 (w/w), and crystalline felodipine, EUDRAGIT® EPO and Kollidon® VA 64 with ratios of 10:45:45, 30:35:35, 50:25:25 and 70:15:15 were pre-mixed in mortar. These physical mixtures were prepared into melt extrudates at 150^{o}C with a dewell time of 5min.

7.2.2 Milling of melt extrudates

To predict apparent solid solubility of felodipine in extrudates of felodipine-EUDRAGIT® EPO, felodipine-Kollidon® VA 64 and felodipine-polymer blend systems, samples of different extrudates with 70% (w/w) drug loading were milled by Retsh MM400 Ball Miller (RETSH, Haan, Germany). Samples were milled for 5, 10, 30, 60 minutes at a frequency of 30Hz by a single 7mm stainless steel ball. Milled samples were tested by MTDSC immediately after milling.

7.2.3 Physicochemical characterisation

Instrumental information of characterisation techniques and the applied parameters for MTDSC, PXRD, ATR-FTIR, SEM, ATF, TTM, PT-MS, DVS, and ssNMR refers to different sections in Chapter 2 (2.2.2.1.3 for MTDSC, 2.2.2.3.2 for DVS, 2.2.2.4.2 for ATR-FTIR, 2.2.2.5.2 for PXRD, 2.2.2.6.2 for SEM, 2.2.8.1.2 for AFM, 2.2.8.5 for TTM, 2.2.8.6 for PT-MS and 2.2.9.2 for ssNMR)

7.2.4 Effect of polymers on the solubility of crystalline felodipine in acidic solution

The effect of polymers on the solubility of crystalline and amorphous felodipine in 0.1MHCl solution was studied. Different amounts of EUDRAGIT® EPO and Kollidon® VA 64 powders were dissolved in 0.1MHCl solution respectively, to prepare polymer-HCl solutions with concentrations from 0.004 to 0.038 g/ml (saturated for EUDRAGIT® EPO but not for PVPVA). Physical mixtures of polymer blend (with ratio of 50:50 w:w in each sample) were dissolved in 0.1MHCl to prepare solutions with the same concentrations as single polymer-HCl solutions.

To investigate the effect of polymers on the solubility of crystalline felodipine in 0.1MHCl solution, excess amounts of crystalline felodipine were added to these solutions and vigorously stirred for 72 hours. Samples were filtered using 0.22μm membrane and the concentrations of felodipine in different solutions were determined by a Lambda XLS UV Spectrometer (PerkinElmer LTD, UK) at the wavelength of 363nm (maximum absorption peak).

7.2.5 Effect of EUDRAGIT® EPO on inhibiting recrystallization of amorphous felodipine in acidic solution

The effect of polymers on inhibiting recrystallisation of amorphous felodipine in the dissolution media was also studied. Amorphous felodipine was prepared using melt-cool method. Excess amount of freshly prepared amorphous felodipine was added into the prepared EUDRAGIT® EPO-HCl solutions (as mentioned in 7.2.4), and the concentration of felodipine in the solution were measured at different time points up to 72 hours using the same UV method. Samples were filtered by 0.22μm membrane before testing.

7.2.6 In vitro dissolution testing

Dissolution testing was carried out on a Copley CIS 8000 dissolution bath (Copley Scientific, UK). The withdrawn solution was measured by Perkin Elmer Series 200 HPLC equipped with a UV/Vis detector and an auto sampler (PerkinElmer LTD, UK). Mobile phase was composed of methanol: acetonitrile: water (50:15: 35). The column was ODS C18 column (150mm×4.6mm, 5μm) (SUPELCO INC, Bellefonte, USA). The flow rate of the mobile phase was 1.0 ml/min. The wavelength was 363 μm. Strand form extrudates of freshly prepared felodipine-EUDRAGIT® EPO, felodipine- Kollidon® VA 64 and felodipine-polymer blend systems were milled before dissolution test by mortar and pestle and particle size was controlled by sieve to between 63 and 106μm. Different samples with an equivalent dose of 10mg (commercial dose) of felodipine was added for the individual dissolution test. Drug release from formulations was tested under non-sink condition (0.1MHCl). Paddle method with the speed of 100r/min was employed, and 900mL media at the temperature of 37°C was used. Dissolution samples were filtered by 0.22μm membrane before testing.

7.3 Results and discussion

7.3.1 Prediction of solid solubility of felodipine in Kollidon® VA

The application of polymer blends in melt extrusion is firstly hypothesised on the difference of the capability of the two polymers to dissolve felodipine. In Chapter 4, the solubility of felodipine in EUDRAGIT® EPO by melting point depression method was 31.72% (w/w). In Chapter 5, the solubility of felodipine in felodipine- EUDRAGIT® EPO melt extrudates was predicted as 45% (w/w) using the milling method. In this chapter, the melting point depression approach and the milling method were applied as a theoretical and a practical method, respectively, to predict solid solubility of felodipine in Kollidon® VA64 in order to confirm whether the solubility of felodipine in Kollidon® 64 is higher than in EUDRAGIT® EPO.

7.3.1.1 Prediction of apparent solid solubility of felodipine in Kollidon® VA 64 by melting point depression approach

The melting point depression approach was applied to predict solid solubility of felodipine in Kollidon® VA64. Details of the method have been described in Chapter 4. Physical mixtures of felodipine and Kollidon® VA64 with the ratios from 10:90 to 90:10 (w/w) were prepared and tested by DSC at a heating rate of 1°C/min. The calculated interaction parameter from the approach by regression analysis is shown in Figure 7.2. Using the achieved interaction parameter, the solid solubility of felodipine in Kollidon® VA64 was calculated as 41.71% (w/w), which is higher than the predicted solid solubility of felodipine in EUDRAGIT® EPO (31.72% w/w) by the same approach.

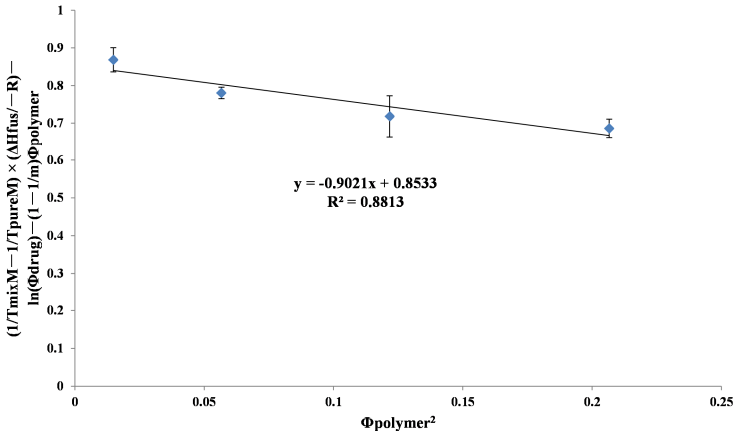

Figure 7.2: Calculation of interaction parameter form the melting point depression approach.

7.3.1.2 Prediction of apparent solid solubility of felodipine in melt extrudates using milling method

As discussed in Chapter 5, the solid solubility predicted by theoretical approaches did not take into account the effect of the preparation process, which may lead to the deviation of the theoretically predicted value from the practical value related to the drug-polymer dispersions prepared by certain process. Therefore the mechanical milling approach, as a practical method, was applied to predict apparent solid solubility of felodipine in felodipine-Kollidon® VA64 melt extrudates. Melt extrudates of felodipine-EUDRAGIT® EPO**,** felodipine-Kollidon® VA 64 and felodipine-polymer blend systems with 70% (w/w) drug loading were milled from 5min to 60min by ball milling. The milled extrudates were tested by MTDSC immediately after milling. The MTDSC results of the 70% (w/w) melt extrudates milled for 60min are shown in Figure 7.3. Significant differences of melting enthalpies can be measured by MTDSC between the 70% (w/w) samples with different polymer matrices. A substantially low degree of melting enthalpy was detected in 70% (w/w) felodipine-Kollidon® VA64 (4.72J/g) samples in comparison to the corresponding EUDRAGIT® EPO sample (26.36J/g), indicating higher apparent solid solubility of felodipine in melt extrudates with Kollidon® VA64 than in that with EUDRAGIT® EPO. Although

a higher melting enthalpy (10.66J/g) was detected in the polymer blend system compared with the Kollidon® VA64 binary system, it is still significantly smaller than the felodipine-EUDRAGIT® EPO binary system, suggesting more felodipine molecularly dispersed in polymer blends than in EUDRAGIT® EPO in melt extrudates. It should be noted that exothermic peaks (recrystallisation) before melting were detected in 70% (w/w) felodipine-polymer blend (110°C) and felodipine-EUDRAGIT® EPO (96°C) systems. This indicates that after 1 hour milling time, a certain amount of amorphous felodipine had already phase separated from the bulk systems. However, the exothermic peak from 70% (w/w) felodipine-polymer blend system was significantly smaller than that from 70% (w/w) felodipine-EUDRAGIT® EPO systems. This demonstrates polymer blends can decrease the level of amorphous phase separation of the 70% (w/w) formulations generated by milling.

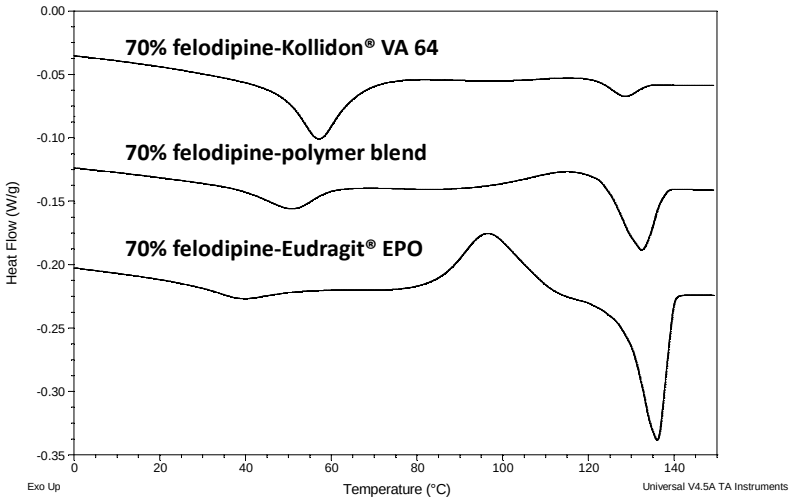

Figure 7.3: MTDSC results of freshly prepared 70% (w/w) melt extrudates milled for 60min.

70% (w/w) milled extrudates were also studied using PXRD as seen in Figure 7.4. After 1 hour milling, crystalline features can only be detected in the 70% (w/w) felodipine-EUDRAGIT® EPO melt extrudates by PXRD, whereas the other two corresponding melt extrudates only showed an amorphous halo detected by PXRD. By comparing with the PXRD patterns of crystalline felodipine form I, felodipine crystals generated by milling in 70% (w/w) felodipine-EUDRAGIT® EPO was confirmed as form I.

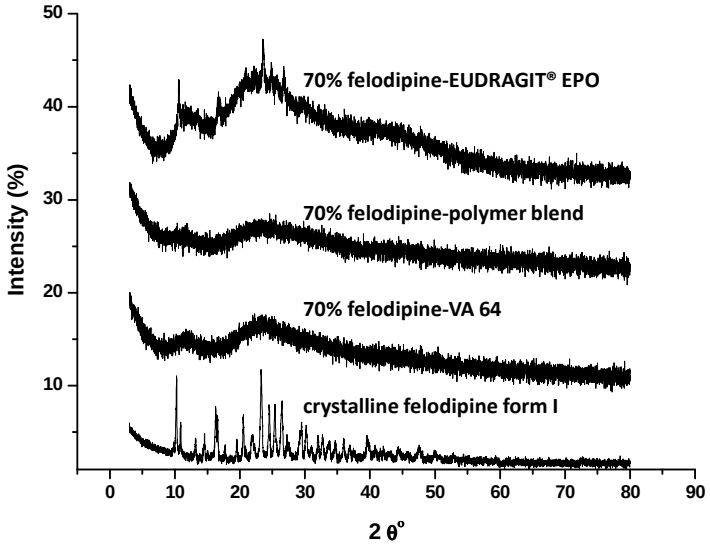

Figure 7.4: PXRD results of different 70% (w/w) felodipine melt extrudates after 1 hour milling.

The amount of crystalline felodipine (calculated using *Eq.5.1*) in different 70% (w/w) melt extrudates generated by different milling time periods is summarised in Figure 7.5. It can be seen that a plateau of crystallinity of felodipine has reached after 10min milling in all 70% (w/w) extrudates. The amount of crystalline felodipine in different 70% (w/w) systems after 60min milling was calculated as 23.12% (w/w) in EUDRAGIT® EPO, 9.58% (w/w) in polymer blend and 4.11% (w/w) in Kollidon® VA64. Therefore the apparent solid solubility of felodipine in polymer blend and Kollidon® VA64 was 60.42% (w/w) (crystallinity subtracted by the drug loading of 70% w/w) and 65.89% (w/w), respectively, which are significantly higher than that in EUDRAGIT® EPO, 45% (w/w).

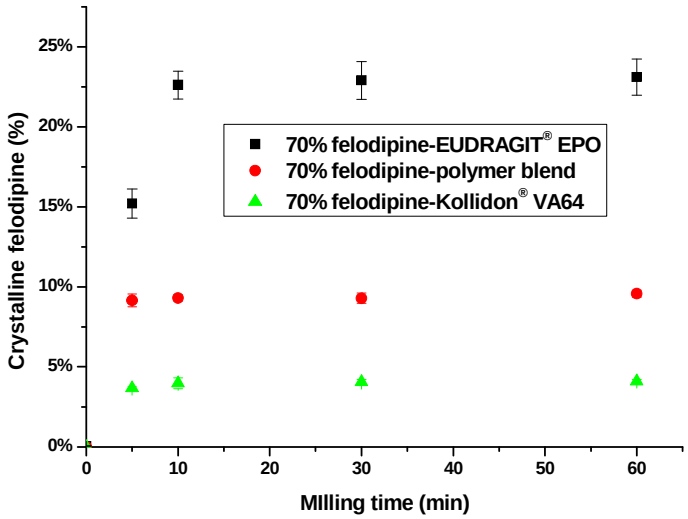

Figure 7.5: Crystallnity of felodipine calculated by using measured melting enthalpy in different 70% (w/w) melt extrudates milled for different time periods.

By using theoretical and practical mechanical milling approaches, they both showed that Kollidon® VA64 can increase the solubility of felodipine in melt extruded formulations than EUDRAGIT® EPO. Accordingly, it can be expected that in felodipine-polymer blend systems more felodipine may molecularly dispersed in Kollidon® VA64 and the physical stability of felodipine-polymer blend melt extrudates can be better on aging in comparison to the binary felodipine-EUDRAGIT® EPO melt extrudates.

7.3.2 Moisture uptake

The hypothesis of using polymer blends in hot melt extrusion to enhance physical stability of solid dispersions was also based on the assumption that blending the two polymers can reduce the overall moisture uptake of amorphous solid dispersions in comparison to felodipine-Kollidon® VA64 systems. Therefore, the moisture uptake behaviour of different melt extrudates with different matrices was studied by DVS in this section.

The moisture uptake capacities of the formulations were tested using isohumic tests (temperature maintained at 25°C) at 75%RH and it can be seen that Kollidon® VA64 can up take as much as 16.8% (w/w) moisture, whereas EUDRAGIT® EPO only up take less than 1.3% (w/w) under 75%RH/25°C (Figure 7.6). The 50:50 (w:w) physical mixture of the two polymers takes approximately 9% (w/w) which is close to half of the amount that Kollidon® VA64 takes. This value was further reduced to 4.1% (w/w) (within 600min) after formulating the two polymers without drug by hot melt extrusion. It was also noted that the water uptake plateau was not obtained even after 600min upon exposure to high humidity.

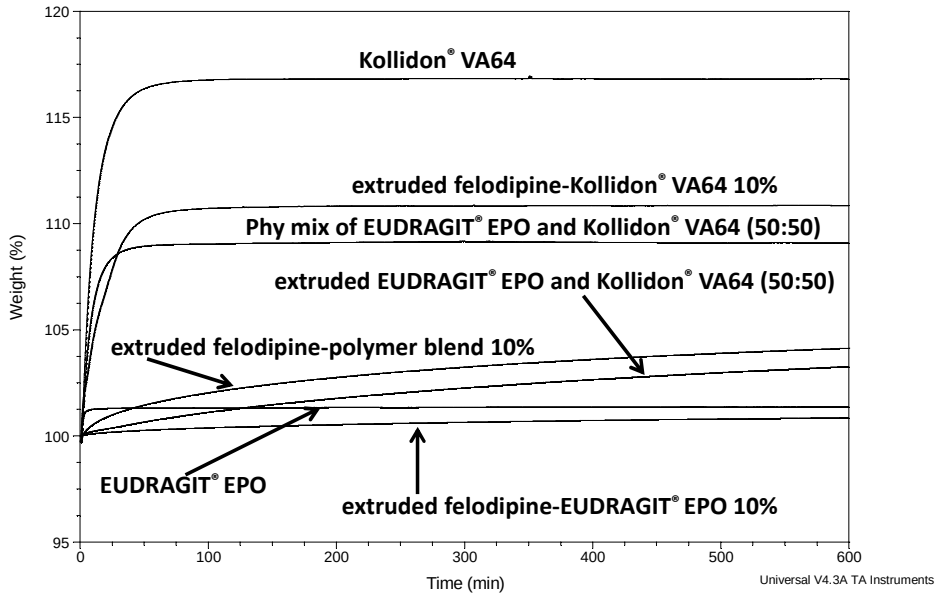

Figure 7.6: DVS results of the polymer alone (as received powder form), the physical mixture of the two polymers and freshly prepared melt extrudates of the polymer blend with and without drug (10% w/w drug loading).

After incorporation with 10% (w/w) drug, the moisture uptake of felodipine-Kollidon® VA64 extrudates was circa 10.8% (w/w) when equilibrium was achieved. For 10% (w/w) felodipine-EUDRAGIT® EPO extrudates, the moisture uptake further decreased from 1.3% (w/w) EUDRAGIT® EPO alone to 0.85% (w/w) after 600min isohumic test. The moisture sorption of 10% (w/w) felodipine-polymer was only 3.3% (w/w) in total after 600min upon exposure to 75%RH at 25°C, which was intermediate between the two binary systems. It was also noted that similar to polymer blend melt extrudates without drug, at 600min the moisture uptake of felodipine-EUDRAGIT® EPO and felodipine-polymer blend melt extrudates still gradually increase at extremely slow rates.

It has been reported that materials such as amorphous glasses or polymers moisture uptake was mainly dominated by diffusion (17-19). A Fickian diffusion model was introduced to fit with the experimental data to test if diffusion is the mechanism of water uptake of samples. Assuming particles are homogeneous spheres, the diffusion model can be expressed by (17):

$$\frac{M_t}{M_e} = 1 - \frac{6}{\pi^2}\sum_{n=1}^{\infty}\left(\frac{1}{n}\right)\exp\left(\frac{-Dn^2\pi^2 t}{a^2}\right) \qquad \textit{Eq 7.1}$$

where M_t is the moisture uptake at time t, M_e is the moisture uptake at equilibrium, D is the diffusion coefficient, a is the radius of the solid spheres and n is a numerical index. The moisture sorption profiles of the melt pre-processed Kollidon® VA64 powder, physical mixtures of Kollidon® VA64 and EUDRAGIT® EPO, polymer blend melt extrudates with and without drug all fit well with the diffusion model with different coefficients. A fitting test example of 10% (w/w) felodipine-polymer blend melt extrudates is shown in Figure 7.7.

The well-fitting with Fickian diffusion model in these systems indicates the moisture uptake was dominated by a diffusion mechanism in which concentration gradient of water gradually built up over time as the moisture adsorbs to the surface and further moved into the material across a diffusion gradient. Although all controlled by diffusion mechanism, diffusion rates in polymer blend systems (with and without drug) were significantly lower than that in felodipine-Kollidion® VA 64 systems. As suggested in Figure 7.1, phase separation already existed in freshly prepared polymer blend samples due to the immiscibility between the two polymers. Therefore, the overall diffusion rate in the polymer blend system was significantly slower than that in felodipine-Kollidion® VA 64 systems since the phase separation can lead to distorted diffusion path length of the moisture while it is being taken up. Thus the time to reach equilibrium for felodpine-polymer blend systems takes much longer than for felodipine-Kollidion® VA 64 systems.

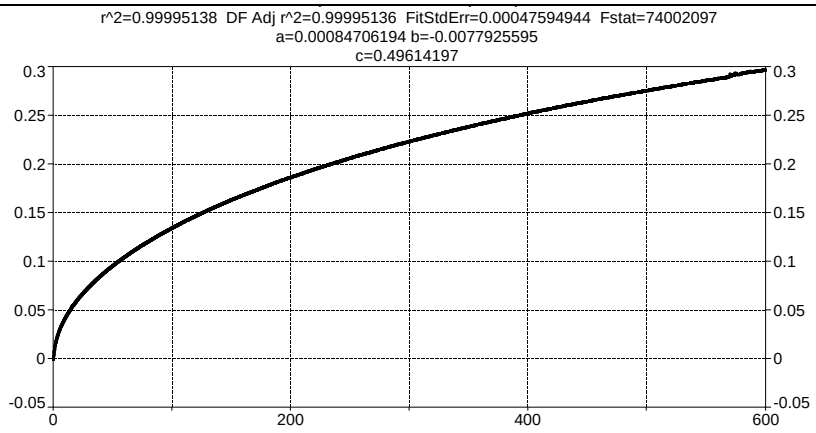

Figure 7.7: Fickian diffusion model fitting of 10% (w/w) felodipine-polymer blend upon exposure to 75%RH at 25°C up to 600min.

7.3.3 Physical stability studies of melt extruded polymer blend systems under stressed conditions

In order to individually evaluate the stabilisation effect of the polymer blend in comparison to the corresponding binary melt extrudates against stressed temperature and humidity, melt extruded formulations were aged under 75%RH/room temperature (stressed humidity) and 23%RH/40°C (stressed temperature), respectively.

7.3.3.1 Stressed humidity

For all melt extrudates with 50% (w/w) drug loading and below including the polymer blends and the two binary systems, no crystalline felodipine can be detected on the surface after 1 months aging under stressed humidity by ATR-FTIR.

For formulations with 70% (w/w) drug loading, the polymer blend system showed a much lower level of surface recrystallization after 1 month aging under 75%RH/room temperature in comparison to the two corresponding binary systems. This was proved by SEM images (Figure 7.8) that after 1 month aging, significantly fewer particles were observed on the surface of 70% (w/w) felodipine-polymer blend extrudates than those on the surface of the two 70% (w/w) binary extrudates (w/w).

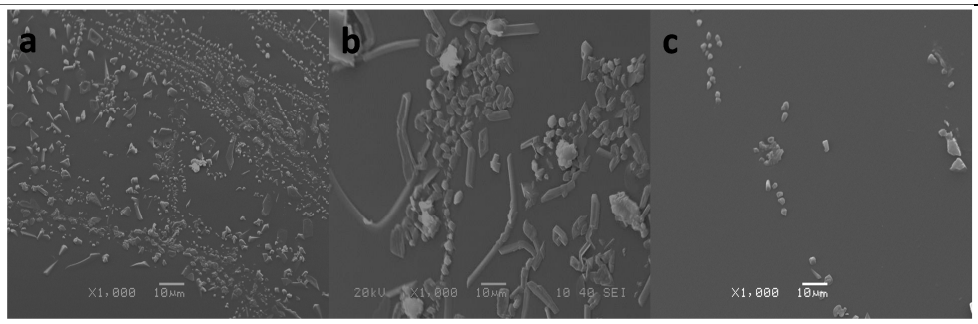

Figure 7.8: SEM images of the surfaces of 70% (w/w) different melt extrudates after 1 month aging under 75%RH/room temperature (a:felodipine-EUDRAGIT® EPO, b: felodipine-Kollidon® VA64 and c: felodipine-polymer blend).

The higher physical stability of 70% (w/w) felodipine-polymer blend extrudates in comparison to the two binary systems was also proved by ATR-FTIR study (Figure 7.9). After 1 month aging, the NH group from the two freshly prepared binary extrudates both shifted to 3365cm^{-1}, which had the same position as crystalline felodipine indicating the occurrence of surface recrystallization. Although the predicted apparent solid solubility of felodipine in melt extrudates with Kollidon® VA64 was higher than that in the polymer blend extrudates, a high level of surface recrystallization was still observed in the binary 70% (w/w) felodipine-Kollidon® VA64 system, indicating the formulation was not physically stable against stressed humidity. The reason can be attributed to the hygroscopicity of Kollidon® VA64 (as proved by the DVS study earlier) leading to the adsorbed moisture on the surface of the 70% (w/w) binary felodipine-Kollidon® VA64 and eventually causing the surface recrystallization.

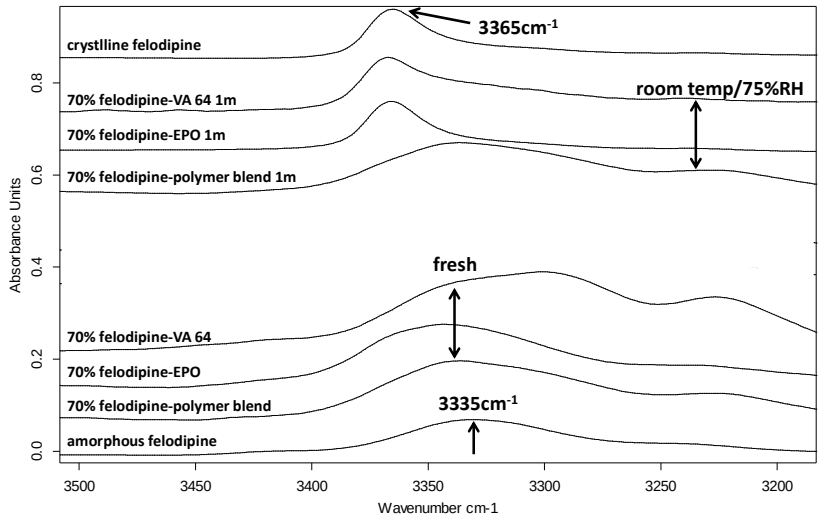

Figure 7.9: ATR-FTIR results of the NH groups from felodipine in different 70% (w/w) melt extrudates aged under different conditions for 1month.

A more detailed surface physical stability study of 70% (w/w) polymer blend system against stressed humidity by ATR-FTIR is shown in Figure 7.10. It can be seen that after as long as 4

months aging, phase separation was detected with the appearance of the crystalline and amorphous NH peaks. Compared to the two binary melt extrudates, it demonstrates that the polymer blend was able to inhibit surface recrystallization in the samples with high drug loadings (70% w/w) for at least 4 months under stressed humidity.

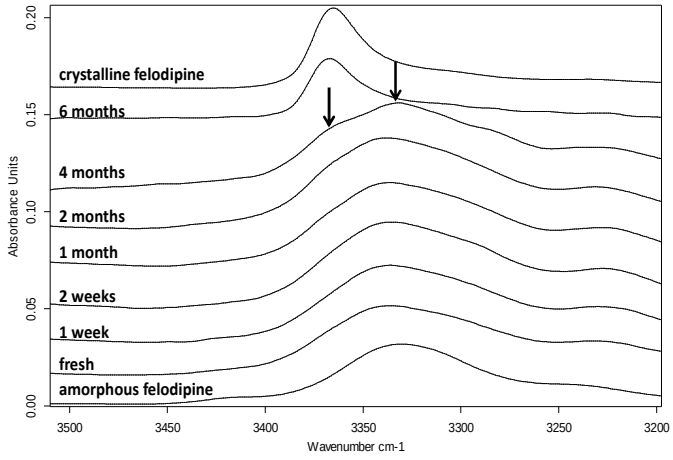

Figure 7.10: ATR-FTIR results of the NH group from the surface of 70% (w/w) felodipine-polymer blend on aging under 75%RH/room temperature (left arrow: crystalline felodipine, 3365cm^{-1}; right arrow: amorphous felodipine, 3335cm^{-1}).

Bulk physical stability of 70% (w/w) polymer blend and the two binary melt extrudates were studied using MTDSC. After 6 months aging under 75%RH/room temperature, the melting of crystalline felodipine can be only detected in 70% (w/w) felodipine-EUDRAGIT® EPO melt extrudates as seen in Figure 7.11. The absence of detecting melting by MTDSC in 70% (w/w) felodipine-Kollidon® VA64 melt extrudates can be attributed to the higher apparent solid solubility of felodipine in Kollidon® VA64 as predicted earlier, leading to the dissolution of felodipine crystals into the polymer on heating in MTDSC.

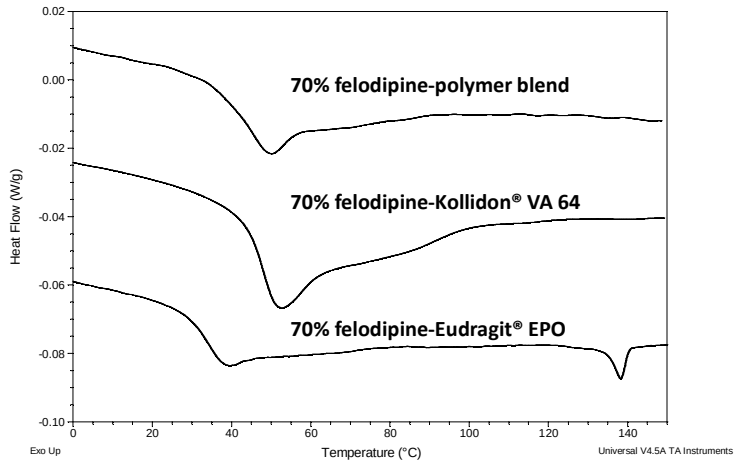

Figure 7.11: MTDSC results of different 70% (w/w) melt extrudates after 6 months aging under 75%RH/room temperature.

The MTDSC study shows that the polymer blend presented a higher bulk physical stability on aging under stressed humidity than the binary felodipine-EUDRAGIT® EPO melt extrudates with 70% (w/w) drug loading. By using *Eq 5.1*, crystallinity of felodipine in this system on aging was studied and results are shown in Figure 7.12. The crystallinity of felodipine in this system increased from 0.69% (fresh) to 1.31% (w/w) after 6 months aging indicating a high bulk physical stability on aging despite the severe surface recrystallization. The kinetics of the crystallisation of 70% (w/w) felodipine-EUDRAGIT® melt extrudates did not fit in the Avrami model (described in Chapter 6) due to the lack of nucleation phase as proved by the existence of crystals in fresh samples.

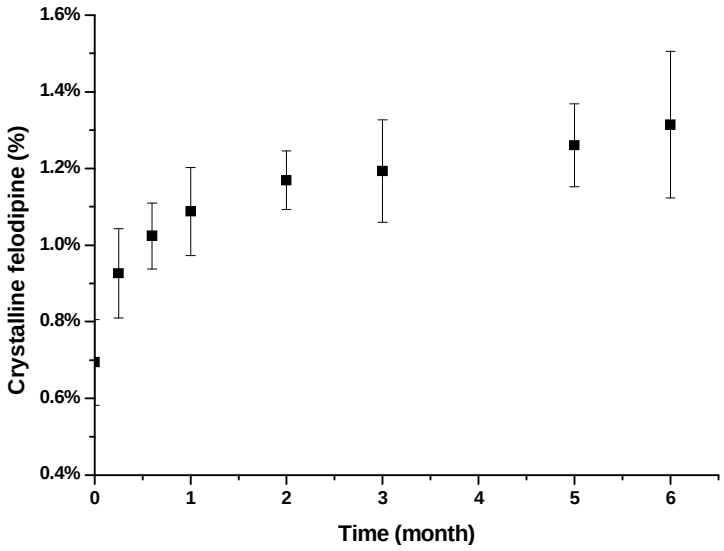

Figure 7.12: The amount of crystalline felodipine in 70% (w/w) felodipine- EUDRAGIT® EPO melt extrudates on aging under 75%RH/room temperature calculated by using measured melting enthalpy.

7.3.3.2 Stressed temperature

In order to study the physical stability against stressed temperature, the polymer blend and the two binary melt extrudates were aged under 23%RH/40°C. No crystalline felodipine can be detected on the surface of any melt extrudates with 50% (w/w) drug loading and below aged under this condition up to 6 months.

Similar to the stressed humidity results, no obvious evidence of recrystallisation of felodipine was detected on the surface of the 70% (w/w) polymer blend melt extrudates up to 6 months aging as shown in Figure 7.13. But crystalline felodipine on the surface of 70% (w/w) binary felodipine-EUDRAGIT® EPO melt extrudates was detected after 1 months aging at 40°C. For 70% (w/w) binary felodipine-Kollidon® VA64 melt extrudates, no recrystallization of felodipine was detected on the surface after 1 month aging. This behaviour of enhanced physical stability in comparison to the stressed humidity results can be attributed to the lower surrounding humidity leading to a lower amount of water sorption in the sample. The physical stability of the surface of different 70% (w/w)

melt extrudates demonstrates that 70% (w/w) felodipine-polymer blend systems could maintain as amorphous solid dispersions for at least 6 month under 23%RH/40^{o}C.

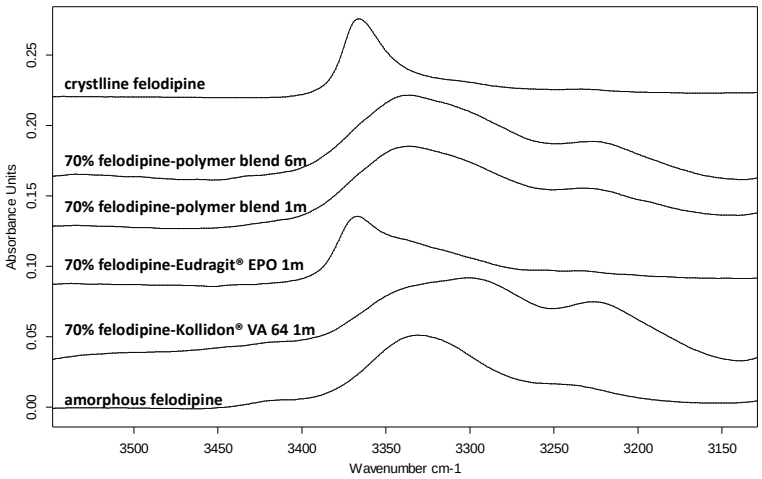

Figure 7.13: ATR-FTIR results of NH groups of the surface of different 70% (w/w) melt extrudates aged under 23%RH/40^{o}C for different time periods.

The bulk physical stability of the polymer blend and the two binary melt extrudates was evaluated using MTDSC. MTDSC results show that after 6 months aging, melting can be only detected in 70% (w/w) binary felodipine-EUDRAGIT® EPO samples (Figure 7.14).

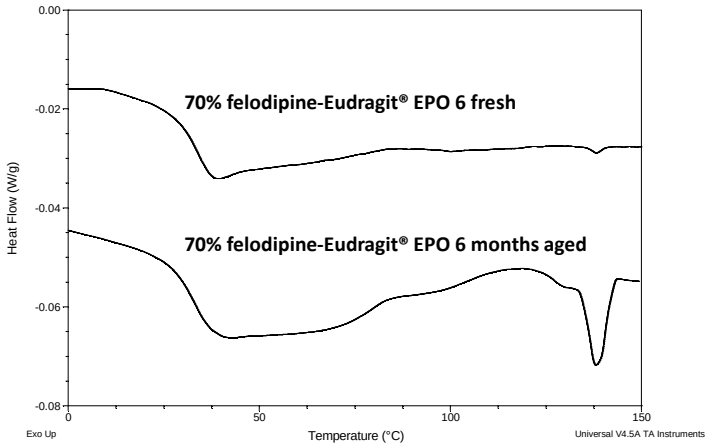

Figure 7.14: MTDSC results of fresh and 6 months aged (under 23%RH/40^{o}C) 70% (w/w) felodipine-EUDRAGIT® EPO melt extrudates.

The crystallinity of felodipine in this sample on aging is shown in Figure 7.15 and it increased from 0.11% (fresh) to 2.21% (w/w) after 6 months aging. The kinetics did not fit in the Avrami model as the recrystallization started with existed nuclei in freshly prepared sample, and therefore lack of the phase of nucleation.

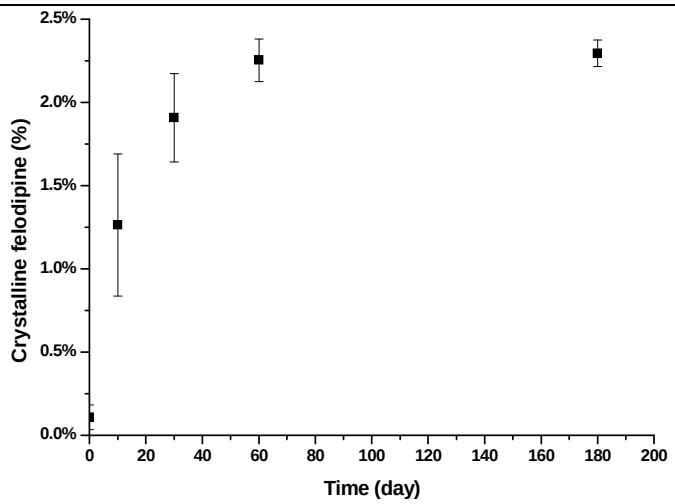

Figure 7.15: The amount of crystalline felodipine in 70% (w/w) felodipine- EUDRAGIT® EPO melt extrudates on aging under 23%RH / room temperature (calculated by using measured melting enthalpy).

Physical stability studies of polymer blend and the two binary melt extrudates under stressed conditions demonstrate that the polymer blend can enhance the physical stability of felodipine melt extrdates in comparison to the both binary felodipine melt extrudates, especially with high drug loading. It is very likely to attribute this better physical stability behaviour to the combined effects of polymer blends including the higher apparent solid solubility of felodipine in Kollidon® VA64 and the protection effect of EUDRAGIT® EPO against stressed humidity.

7.3.3.3 Drug release performance

Dissolution studies of the freshly prepared polymer blend and the two binary melt extrudates with different drug loadings were carried out under non-sink condition (0.1MHCl). Freshly prepared strand form extrudates were milled into powder before dissolution tests. The drug release profile of the freshly prepared polymer blend melt extrudates with 10% (w/w) drug loading shows the most significant enhancement in maximum drug release, in comparison to the corresponding two binary melt extrudates as seen in Figure 7.16. The maximum drug release can reach as high as 70% (equivalent to a felodipine concentration of 7.5µg/ml). The equilibrium solubility of crystalline felodipine in this media was measured as 0.69µg/ml, which indicates the apparent solubility was increased 10 times higher by polymer blends. However, after 12 hours, the drug release form 10% (w/w) felodipine-polymer blend systems decreased to circa 30% (w/w) (equivalent to a felodipine concentration of 3.33µg/ml) , which was close to the drug release from the two corresponding binary extrudates. With increasing the drug loadings to 30% (w/w) and above, the drug release pattern showed subtle differences between polymer blend and binary formulations. After 12 hours, all formulations with drug loadings of 30% (w/w) and above all ended with a drug release of circa 15% to 20% (equivalent to felodipine concentrations from 1.67 to 2.22µg/ml).

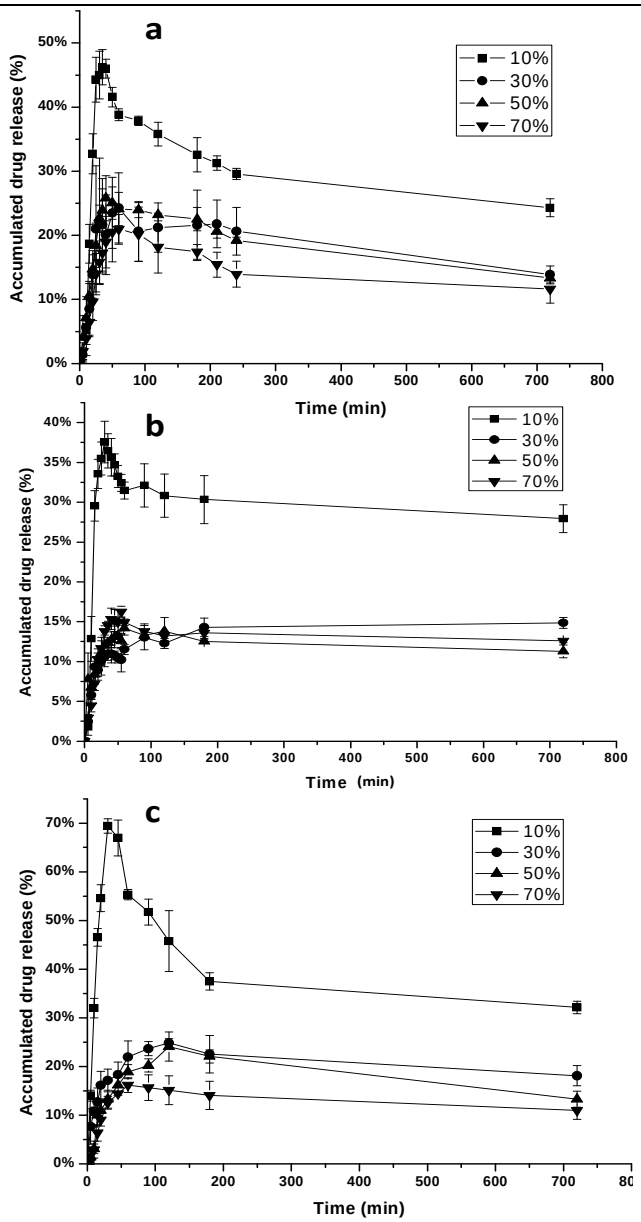

Figure 7.16: Drug release from freshly prepared polymer blend and binary melt extrudates with drug loadings from 10% to 70% (w/w) under non-sink condition (a: felodipine-Kollidon® VA64 melt extrudates, b: felodipine-EUDRAGIT® EPO and c: felodipine-polymer blend melt extrudates).

Aged formulations showed very similar dissolution profiles to the freshly prepared formulations. This is because although a high level of surface recrystallization was observed in the binary formulations on aging, the bulk crystallinity was still extremely low as proved by the MTDSC study. In addition, the milling process before dissolution test could dilute recrystallized drugs to a very low bulk concentration. Therefore the little influence of aging on the dissolution performance of formulations could be expected.

The mechanism of the different dissolution behaviours including the substantially increased maximum drug release from fresh 10% (w/w) polymer blend extrudates, the drug release equilibrium for all 30% to 70% (w/w) samples are still not completely understood (will be

discussed in the next section). Nevertheless it still demonstrates the application of polymer blends in hot melt extrusion can not only enhance the physical stability of felodipine formulations, but it also can improve dissolution performance.

7.3.3.4 Effect of polymers on the solubility of felodipine in solutions

7.3.3.4.1 Effect of polymers on the solubility of crystalline felodipine

In order to understand different dissolution behaviours between polymer blend and the two binary melt extrudates, the effect of polymers on the equilibrium solubility of crystalline felodipine in 0.1MHCl was studied. A series of 0.1MHCl solutions containing different concentrations of EUDRAGIT® EPO, Kollidon® VA64 and the physical mixture of the two with the ratio of 50:50 (w : w) were prepared. Excess amount of crystalline felodipine was added into these solutions. As seen in Figure 7.17, the apparent solubility of felodipine increases with increasing the EUDRAGIT® EPO concentration in the 0.1MHCl media up to a plateau drug concentration of 200µg/ml. EUDRAGIT® EPO concentrations at and above 20mg/ml all reach this maximum drug concentration. In contrast, Kollidon® VA64 shows very little solubilisation effect on crystalline felodipine in this media. Physical mixtures of the polymer blend dissolved in the media showed linear solubilisation enhancement of crystalline felodipine which can reach 155µg/ml with a polymer concentration of 38 mg/ml. This represents an over 200-fold increase in solubility in comparison to that of crystalline felodipine alone in this media. It should be noted that the increased apparent solubility of crystalline felodipine in 0.1MHCl solution by polymer blend was mainly contributed by EUDRAGIT® EPO. Therefore, the concentration of EUDRAGIT® EPO in 0.1MHCl can play a significant role in influencing the dissolution behaviour of the drug-loaded melt extrudtes

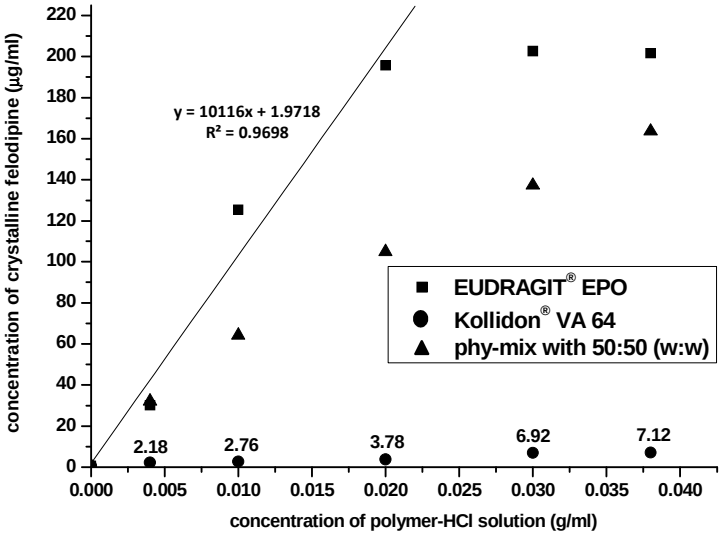

Figure 7.17: Apparent solubilities of felodipine in Kollidon® VA64, EUDRAGIT® EPO and the blend of the two polymers (50:50) solutions with different polymer concentrations in 0.1MHCl media at room temperature.

Assuming a linear relationship between EUDRAGIT® EPO concentrations in 0.1MHCl and the corresponding apparent solubility of felodipine, an equation with acceptable coefficient can be achieved as shown in Figure 7.17. For 10% (w/w) felodipine-EUDRAGIT® EPO extrudates in dissolution test, the concentration of EUDRAGIT® EPO was 0.1mg/ml, and using the linear relationship the equilibrium solubility of crystalline felodipine was calculated as 2.98µg/ml. The value was very close to the observed drug release from fresh 10% (w/w) felodipine-EUDRAGIT® EPO extrudates after 12 hours (3.33µg/ml). For 30%-70% (w/w) felodipine-EUDRAGIT® EPO extrudates, the calculated equilibrium solubility was 2.23 (for 30% w/w sample), 2.08 (for 50% w/w sample), and 1.97µg/ml (for 70% w/w sample). These values were also very close to the drug release from 30%-70% (w/w) extrudates after 12 hours (1.67 to 2.22µg/ml). These findings well explained dissolution profiles of felodipine-EUDRAGIT® EPO melt extrudates in 0.1MHCl.

Kollidon® VA64 did not show a high ability of increasing apparent solubility of crystalline felodipine in 0.1MHCl. It can be seen in Figure 7.17 that with increased concentration of Kollidon® VA64 in the solution, apparent solubility of crystalline felodipine only increased from 2.18 to 7.12µg/ml. However, the value of 2.18µg/ml is very close to the drug release from 30%-70% (w/w) felodipine-Kollidon® VA64 melt extrudates after 12 hours (1.67 to 2.22µg/ml). This may explain the drug release profiles from felodipine-Kollidon® VA64 melt extrudates, although the concentration of Kollidon® VA64 generated by melt extrudates in dissolution test was below 40mg/ml.

The increased maximum drug release from 10% (w/w) felodipine-polymer blend extrudates was still not clearly understood. The possible reason can be attributed to two aspects. Firstly, the incorporation of Kollidon® VA 64 into the polymer blend extrudates may increase the wettability of the formulation, which could lead to a faster contact with the dissolution media. This was observed during dissolution test that 10% (w/w) felodipine-polymer blend extrudates disappeared faster in dissolution media than 10% (w/w) felodipine-EUDRAGIT® EPO samples. Secondly, EUDRAGIT® EPO may also be able to inhibit recrystallization of amorphous felodipine in 0.1MHCl in addition to solubilising crystalline felodipine. This will be discussed in the next section.

7.3.3.4.2 Effect of EUDRAGIT® EPO on inhibiting recrystallization of amorphous felodipine in the dissolution media

In addition to solubilising crystalline felodipine in 0.1MHCl media, EUDRAGIT® EPO can also inhibit recrystallization of amorphous felodipine in the media. Excess amounts of amorphous felodipine (prepared by melt-cool method) were added into the same EUDRAGIT® EPO-0.1MHCl solution and the concentrations of felodipine were measured at different time points up to 72 hours. As seen in Figure 7.18, the felodipine concentration continued increasing within the first 2 hours in all solutions. Subsequently, the concentration started to decrease, but within 6 hours the felodipine concentration was still 1.5-2 times higher (felodipine concentration in saturated EUDRAGIT® EPO

solution was 7 times higher) than the apparent solubility of crystalline felodipine measured in the same solution (200µg/ml). This demonstrates that EUDRAGIT® EPO can inhibit recrystallization of amorphous felodipine in 0.1MHCl solution for a certain time period.

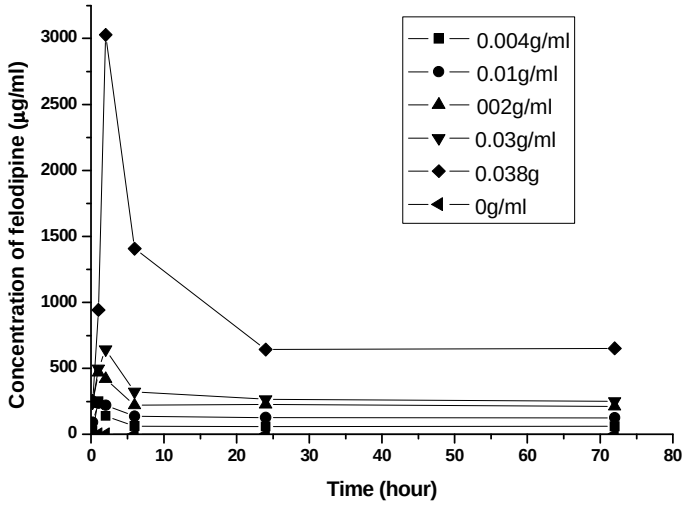

Figure 7.18: Felodipine concentration in 0.1MHCl media containing different concentrations of EUDRAGIT® EPO within 72 hours.

The ability of EUDRAGIT® EPO in solubilising crystalline felodipine and inhibiting recrystallization of amorphous felodipine in 0.1MHCl media was further proved by the dissolution study of extremely low drug loading felodipine-EUDRAGIT® EPO melt extrudates (Figure 7.19). Melt extrudates of felodipine-EUDRAGIT® EPO with 2.5% (w/w) drug loading were prepared for the dissolution study. The quantity of 400mg of this formulation (equals to 10mg of felodipine as commercial dose) was added for the dissolution study, this gave a polymer concentration of 0.43mg/ml in 0.1MHCl media in dissolution. A maximum drug release with 70% was observed in dissolution test, and after 10hours, the drug release still maintained at 60% (6.67µg/ml). Using the linear relationship in Figure 7.17, the equilibrium concentration of felodipine in this EUDRAGIT® EPO solution was calculated as 6.32µg/ml. This dissolution profile of reaching maximum and reducing to equilibrium demonstrates that EUDRAGIT® EPO can inhibit recrystallization of amorphous felodipine only for short time period. However, the drug release can still be maintained at a high level if the amount of EUDRAGIT® EPO was sufficient in solution. In comparison to the corresponding formulation with 10% (w/w) drug loading, a significant increase of maximum drug release and a higher stable drug concentration was achieved.

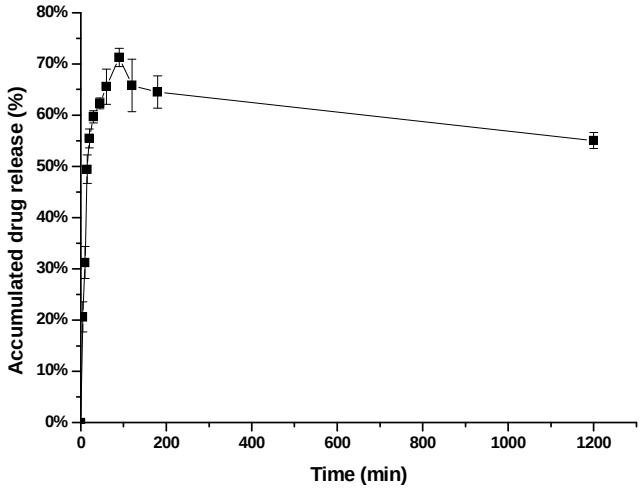

Figure 7.19: Drug release from 2.5% (w/w) felodipine-EUDRAGIT® EPO melt extrudates under non-sink condition (0.1MHCl).

A great depth of the understanding on the enhancement of maximum drug release from 10% (w/w) polymer blend melt extrudates has not been gained yet. However, the results demonstrate that EUDRAGIT® EPO not only can solubilise crystalline felodipine but it can inhibit recrystallization of amorphous felodipine in the 0.1MHCl media. Therefore, the two proposed explanations (inhibiting recrystallization of amorphous felodipine in 0.1MHCl by EUDRAGIT® EPO and increasing wettability of the formulation by Kollidon® VA 64) mentioned above for the increased maximum drug release from 10% (w/w) felodipine-polymer blend extrudates may seem reasonable.

7.3.4 Investigation into the micro-structure of polymer blend extrudates

Polymer blends can be homogeneous or heterogeneous depending on the miscibility between the two polymers. A homogeneous polymer blends can be achieved if the two polymers are completely miscible. On the contrary, if the two polymers are partially miscible and immiscible, the polymer blends will be typically heterogeneous after processing (20-22). Phase separation with different domains could be expected if polymer blends were formed by two immiscible polymers. The size and morphology of these domains can be affected by the composition of the blend (23-25). For immiscible polymer blends, the morphology of the domains of one polymer can be manipulated from phase separated spherical domains to interconnected islands by changing the ratio between the two polymers close to 50:50 (24, 25). Furthermore, if the polymer blends are processed under biaxial stress, such as air-blowing, the separated domains can be shaped to flat layers instead of the spherical domains. If polymer blends are processed under one-directional stress, such as hot melt extrusion, the domains are likely to be rod-like shape and act as a fibrotic composite in the blend (26-28).

In this study, polymer blends have demonstrated the ability of enhancing the physical stability of melt extruded solid dispersions. The improved physical stability was attributed to the overall

increased drug-polymer solubility in melt extrudates and decreased moisture sorption. These two aspects have been clearly proved so far, and the two advantages provided by polymer blends were highly correlated with the micro-structure as proposed in Figure 7.1. Therefore, it is essential to gain a full understanding of the micro-structure of the polymer blends.

7.3.4.1 Phase behaviour of polymer blends without drug

To understand the micro-structure of melt extrudates prepared with polymer blends, the miscibility between the two polymers was evaluated. The phase behaviour of the polymer blends of EUDRAGIT® EPO and Kollidon® VA64 was first investigated using MTDSC to determine the T_gs of the two polymers which can be used as a typical indicator of the degree of phase separation. In order to mix the two polymers, the physical mixtures of the two polymers with ratios of EUDRAGIT® EPO: Kollidon® VA64 from 10:90 to 90:10 (w/w) were heated to 140°C and cooled to 20°C. After thermal mixing in the DSC pans, each blend sample was tested using MTDSC on reheating. Two distinct at 50°C and 107°C were seen in all polymer blend physical mixtures (Figure 7.20a), and the two T_gs correspond well to the T_gs of the pure EUDRAGIT® EPO and Kollidon® VA64, respectively. This indicates the significant level of immiscibility between the two polymers. However, there is no external processing/mixing involved in these physical mixtures, which may lead to the physical state of physical mixtures being different from that of polymer blends prepared by hot melt extrution. The heat capacity changes at the T_g transitions of the blends were further analysed to confirm the immiscibility of the two polymers. If the polymers are highly immiscible, no additional phases with an intermediate T_g between the T_gs of the two polymer should be detected, and the heat capacity change at the two separated T_gs should be proportional to the intrinsic ΔC_p values at T_g of the each pure polymer and a linear correlation should be observed between the ΔC_p values at the T_g of each polymer in each blend. This is the case for both Kollidon® VA64 and EUDRAGIT® EPO as seen in Figure 7.20b. The ΔC_p value of each polymer in the blends is linearly proportional to the ΔC_p of the pure polymer (Figure 7.20b). Based on the miscibility study of the two polymers, it demonstrates that the applied polymer blends in this study is immiscible.

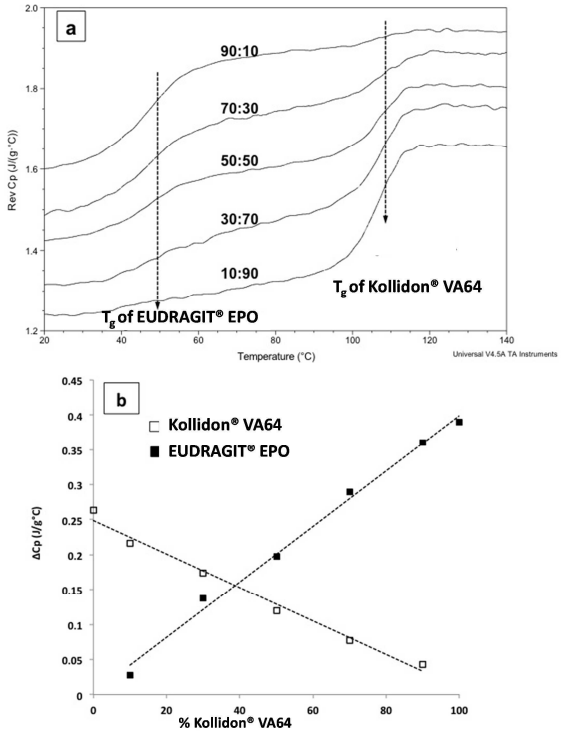

Figure7.20: a: DSC results of the polymer blend with EUDRAGIT® E PO: Kollidon® VA64 ratios from 90:10 (top) to 10:90 (bottom) without drug; b: plot of ΔC_p at the two T_gs of each blend vs. percentage of Kollidon® VA64 in the blend.

To further investigate phase separation of polymer blends and take into account the effect of processing method, polymer blends with the ratio of 50:50 (w/w) (the same as the ratio in melt extrudates with felodipine) without drug were prepared by hot melt extrusion. Samples were studied using AFM phase imaging (tapping mode) and transition temperature microscopy. As shown in Figure 7.21b, phase separated domains with a long strip morphology was dispersed into a continuous phase. It also can be noted in Figure 7.21a that phase separation detected by tapping mode were not all presented in the topography image, which suggests that the roughness of the sample has little influence on the features of AFM phase image. Using Image J to analyse the phase image (method has been described in Chapter 5), the ratio of the continuous phase to separated phase was 52:48, which was close to polymer blend ratio in formulation (50:50). However, the observed two phases by AFM tapping mode cannot be assigned to the two polymers. Therefore, to identify the two separated phases, transition temperature microscopy (TTM) was used to characterise the polymer blend extrudates. It can be seen in Figure 7.21c that a higher transition temperature around 100-110^{o}C was detected in the continuous phase (red), the temperature in which was very close to the glass transition temperature of Kollidon® VA64, indicating Kollidon® VA64 was the continuous phase. A transition temperature around 40-50^{o}C was detected in the separated domains (blue), and the temperature was in agreement with the T_g of EUDRAGIT® EPO. This indicates that EUDRAGIT® EPO was the separated phase in the polymer blend extrudates. Some domains with transition temperatures between 65-85^{o}C were also detected as shown with the

colour of yellow to green in Figure 7.21c. These domains were very likely to be the miscible polymer blends. Although high immiscibility between the two polymers was proved by the DSC study, given the high temperature and high pressure in hot melt extrusion, a small amount of miscible polymer blend could be generated during processing. But as shown in Figure 7.21c, the portion of these miscible domains was small, which demonstrates that the two polymers were still immiscible even after processing. Using Fox equation (29), the percentage of two polymers in these partially miscible phases can be estimated. With a T_g of 65°C, the ratio of EUDRAGIT® EPO to Kollidon® VA64 was approximately 63% to 37%. For regions with a T_g of 85°C, there should be nearly 30% EUDRAGIT® EPO and 70% Kollidon® VA64. It was also noted that most of the blue EUDRAGIT® EPO regions were surrounded by green miscible regions. This indicates that the polymer domains were partially inter-connected but largely immiscible. The micro-structure of polymer blend composed of EUDRAGIT® EPO and Kollidon® VA64 by hot melt extrusion is schematically illustrated in Figure 7.21d.

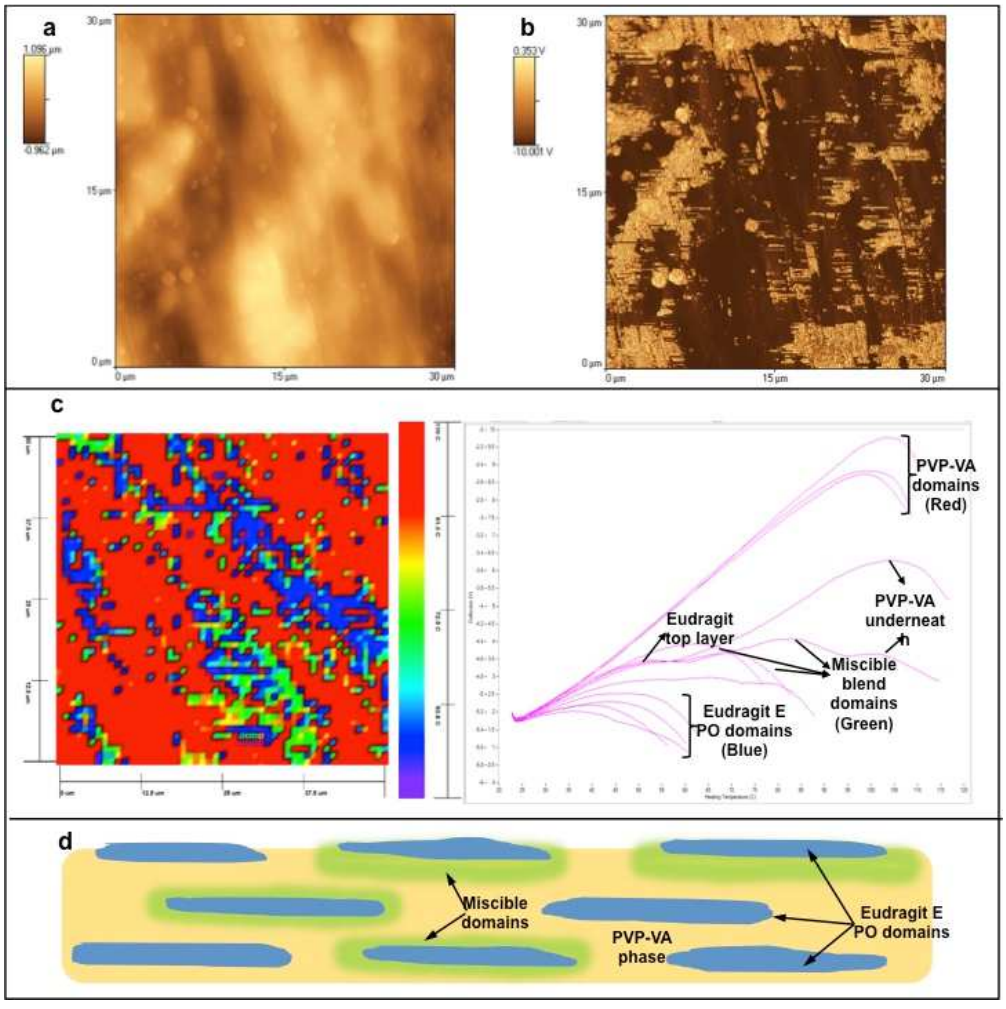

Figure 7.21: a: AFM toppography and b: phase image of the polymer blend; c: Nano-thermal imaging mapping of the 50:50 EUDRAGIT® EPO-Kollidon® VA64 (PVP-VA) polymer blend extrudates and the corresponding nano-thermal transition profiles of the 12 slected data point at the bottom of the

TTM map; d: schemetic illustration of the micro-strucutre of the EUDRAGIT E PO- Kollidon® VA64 blend.

7.3.4.2 Phase behaviour of polymer blend with drug

7.3.4.2.1 MTDSC results

Phase separation in freshly prepared melt extruded polymer blend with felodipine was studied using MTDSC as seen in Figure 7.22. Two separated glass transitions can be seen in the freshly prepared 10%-50% (w/w) felodipine-polymer blend melt extrudates. Only one glass transition was detected in the freshly prepared 70% (w/w) extrdates, and this was because the extremely high drug loading brings the T_g value of this system closely down to the T_g value of pure amorphous felodipine (45^{o}C).

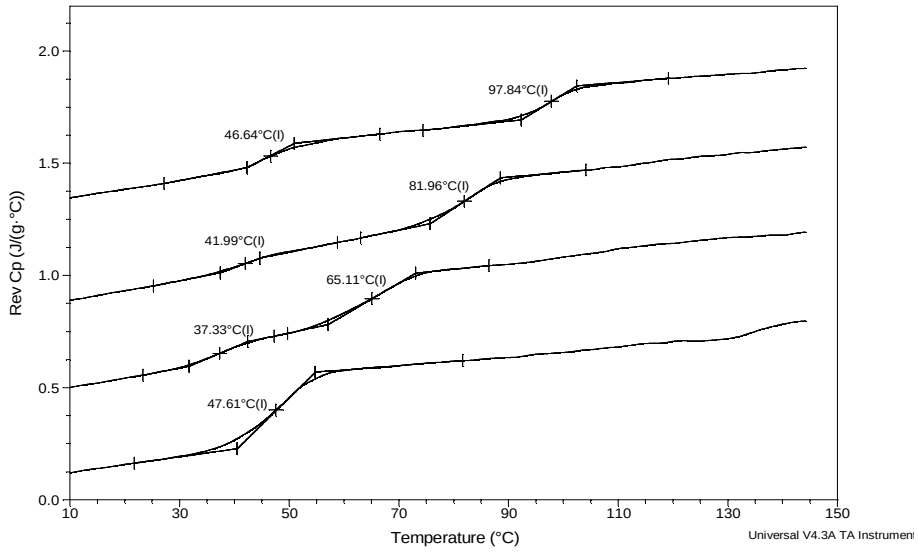

Figure 7.22: MTDSC results in reversing heat capacity signal of freshly prepared felodipine-polymer blend melt extrudates.

The amount of felodipine molecularly dispersed in each polymer can be estimated using Fox equation with the detected T_g values. The calculated results are summarised in Table 7.1. It can be seen that more felodipine molecularly dispersed in Kollidon® VA64 than in EUDRAGIT® EPO in all samples (only one T_g value presented in 70% w/w sample leading to the failure of the calculation), which is in good agreement with the apparent solid solubility prediction by milling method. With increasing drug loading, higher amount of drug partitioned into the Kollidon® VA64 phase rather than EUDRAGIT® EPO phase. The calculation concludes that in the felodipine-polymer blend melt extrudates, felodipine dispersed in the two polymers unevenly with a higher concentration in Kollidon® VA64 and a lower concentration in EUDRAGIT® EPO.

Table 7.1: Calculated drug distribution of felodipine in different polymer domains using MTDSC results.

Polymer Blend Systems (w/w)	$W_{felo\ in\ EPO}$[a] (w/w)	$W_{felo\ in\ VA\ 64}$[b] (w/w)	Ratio of W_{felo}[c] $_{in\ EPO}$ To $W_{felo\ in\ VA\ 64}$
10%	3.73%	6.27%	1:1.68
30%	7.24%	22.76%	1:3.14
50%	9.96%	40.04%	1:4.02

7.3.4.2.2 Drug-polymer interactions in polymer blend melt extrudates

The higher felodipine concentration in Kollidon® VA64 and higher apparent solid solubility of felodipine in Kollidon® VA64 were very likely associated with the ability of forming hydrogen bonding with felodipine by Kollidon® VA64. As discussed in Chapter 6, no evidence of formed hydrogen bonding between felodipine and EUDRAGIT® EPO was shown by ATR-FTIR. In contrast, hydrogen bonding was confirmed in the polymer blend melt extrudates as seen in Figure 7.23. A blue shift of NH peak in felodipine from 3335cm^{-1} (amorphous felodipine) to 3292cm^{-1} was observed after formulating with Kollidon® VA64 which indicates the formation of hydrogen bonding between the drug and the polymer. Instead of a blue shift, a red shift of NH peak was observed in the corresponding felodipine-EUDRAGIT® EPO formulation, and the reason has been discussed in Chapter 5 that the formed hydrogen bonding between two felodipine molecules was affected by the carbonyl groups from EUDRAGIT® EPO. Thus it may suggest that the order of the potential of forming hydrogen bonding is felodipine with Kollidon® VA64 > two felodipine molecules > felodipine with EUDRAGIT® EPO. In the corresponding polymer blend formulation, these two NH peaks were both observed, suggesting the existence of the two separated phases: amorphous felodipine-EUDRAGIT® EPO phase and amorphous felodipine- Kollidon® VA64 phase. Fourier self deconvolution was applied to analyse the polymer blend formulation with the attempt to distinguish the two peaks. However it was impossible to completely separate them, and thus quantitative analysis of the drug distribution cannot be achieved. Nevertheless, it still can be concluded that hydrogen bonding was formed between felodipine and Kollidon® VA64 and the two phases both contained drug molecules.

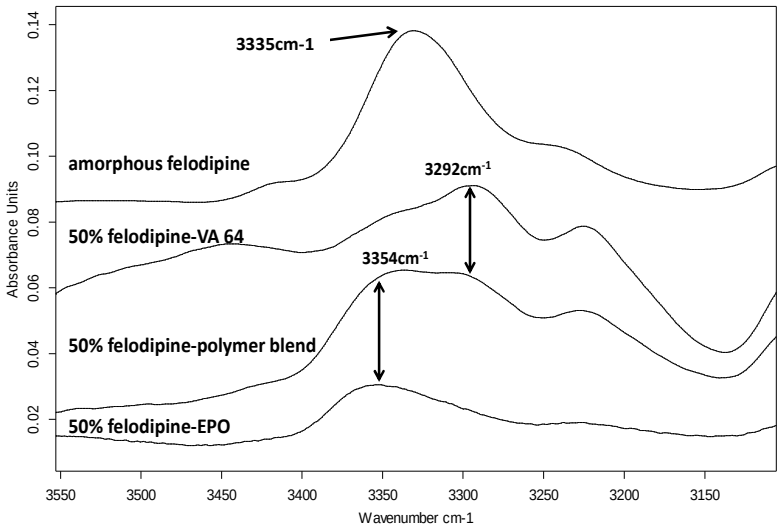

Figure 7.23: ATR-FTIR results of NH groups from amorphous felodipine and 50% (w/w) melt extruded formulations.

7.3.4.2.3 Transition temperature mapping analysis

Phase separation of felodipine-polymer blend melt extrudates with all drug loadings was also studied using transition temperature mapping (TTM) as seen in Figure 7.24. Due to the roughness of the cross section of felodipine-polymer blend extrudates, only the surface of the samples was tested. Two separated phases were observed on the surface of the 10%-50% (w/w) felodipine-polymer blend melt extrudates and only one phase was detected on the surface of 70% (w/w) sample, which is in good agreement with the MTDSC results. It can be seen that in 10% (w/w) sample domains (blue spots) with a transition temperature of around 55^{o}C are separated phases and domains (green spots) with a transition temperatures of 95^{o}C are continuous phases. The two detected transition temperatures were close to the two T_gs measured by DSC in the same sample. This demonstrates that, similar to the polymer blend melt extrudates without drug, in felodipine-polymer blend melt extrudates, Kollidon® VA64-felodipine is the continuous phase and EUDRAGIT® EPO-felodipine is the separated phase. Two separated phase with different transition temperatures was also observed on the surface of 30% and 50% (w/w) systems. The percentage of the two detected phases (as shown in blue and green areas) deviates from 50:50, which is possibly because the tested areas were too small (30µm×30 µm) to represent the intact phase separation of the samples. It is also possible that the surface has different phase behaviour from the bulk.

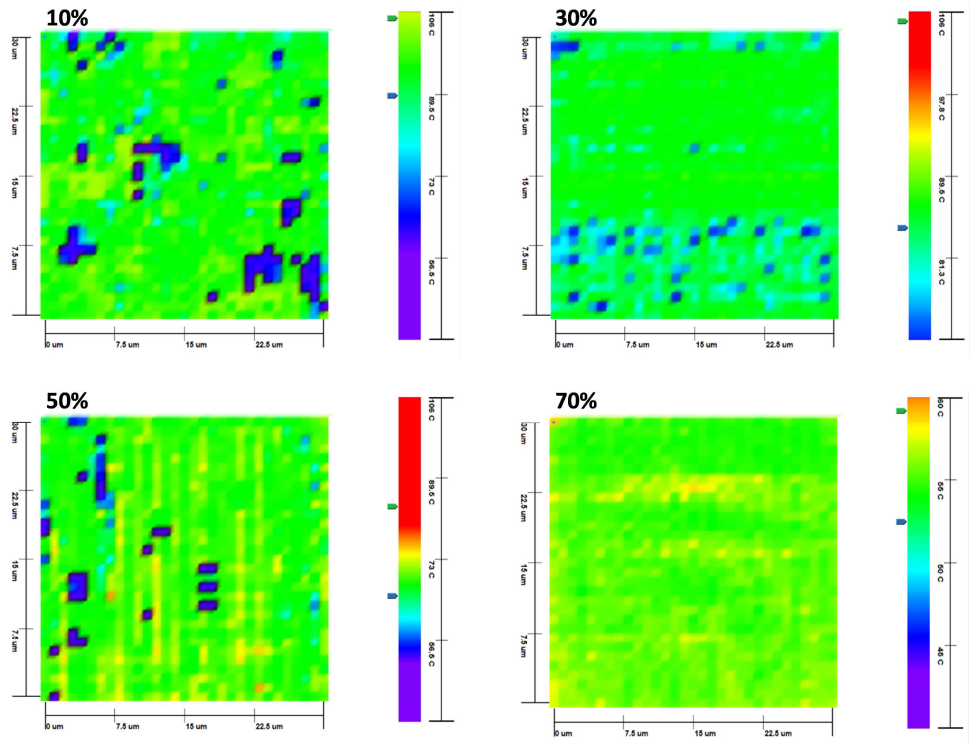

Figure 7.24: TTM results of the surface of freshly prepared felodipine-polymer blend melt extrudates.

7.3.4.2.4 Photothermal-microspectroscopy analysis

Phase separation of felodipine-polymer blend melt extrudates was also studied by photothermal-microspectroscopy (PT-MS). As transition temperature microscopy could not be applied to the bulk of felodipine-polymer blend extrudates, PT-MS was used to study the bulk phase behaviour. The analysis of fresh 10 % (w/w) felodipine-polymer blend extrudates is discussed here as an example. 10% (w/w) felodipine-polymer blends melt extrudates were gently milled into particles by mortal and pestle. A single particle from the milled 10% (w/w) samples was attached to the probe for the analysis of the bulk phase behaviour. Due to the multi-components in felodipine-polymer blend melt extrudates, it is difficult to clearly conclude the phase behaviour of the system as a unique peak assigning to the individual component cannot be selected. However, it still shows the uneven drug distribution in 10% (w/w) polymer blend systems (Figure 7.25). Three peaks were selected to study the phase behaviour of 10% (w/w) systems including 3335cm^{-1} representing amorphous felodipine, 1715cm^{-1} which is the overlapped peak from EUDRAGIT® EPO and Kollidon® VA64 and 1681cm^{-1} (carbonyl groups) which is the contribution from amorphous felodipine-Kollidon® VA64 phase in the sample. It can be seen that with normalisation to the 1715cm^{-1} peak, the relative peak intensity of 3335cm^{-1} (amorphous felodipine) varies among different tests of the 10% (w/w) sample, which suggests the uneven drug distribution in 10% (w/w) felodipine-polymer blend system. It may also suggest that amorphous felodipine dispersed more in the Kollidon® VA64 rather than EUDRAGIT® EPO since the PT-MS results showed that with increasing relative intensity of amorphous felodipine, the intensity of 1681cm^{-1} (amorphous felodipine-Kollidon®

VA64 phase) increased as well. This demonstrates that phase separation also exists in the bulk of the sample, and more felodipine molecularly dispersed in Kollidon® VA64 than in EUDRAGIT® EPO in bulk, which is in good agreement with MTDSC results.

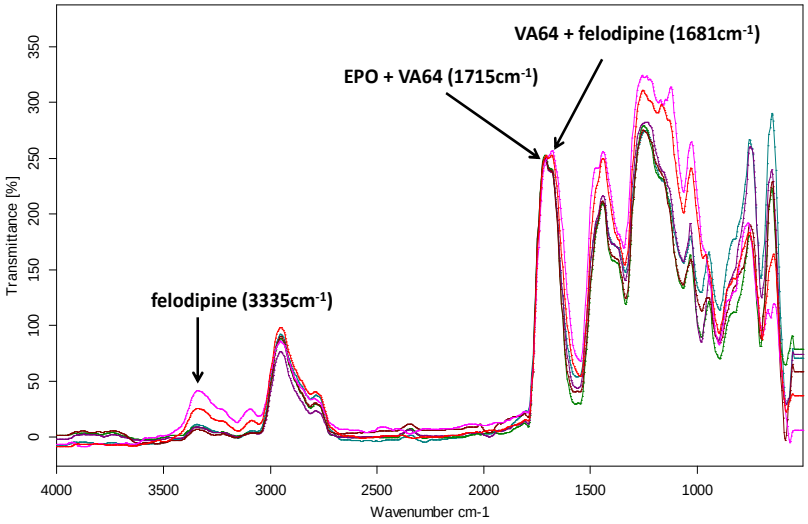

Figure 7.25: PT-MS results of freshly prepared and milled particles of 10% (w/w) felodipine-polymer blend melt extrudates.

7.3.4.2.5 Solid state NMR analysis

Solid state NMR (ss-NMR) relaxometry is a powerful technique for detecting phase separation with sub-micro dimensions (30, 31). In this study, proton solid state NMR relaxometry was used to study the bulk phase behaviour of the felodipine-polymer blend melt extrudates. Samples of the polymer blend and the two binary melt extrudates with 10% and 70% (w/w) drug loadings (lowest and highest in the study) aged under ambient condition for 4 months were tested by solid state NMR. The ^{1}H spin-lattice relaxation times, T_1 are summarised in Table 7.2. For the two binary systems with different drug loadings, a single relaxation of T_1 was detected, indicating a molecular single-phase system. Although surface recrystallization was observed in the two binary melt extrudates with 70% (w/w) drug loading, the bulk crystallinity was still extremely low according to the calculated results by MTDSC study, leading to the undetectable phase separation by solid state NMR. It should be noted that the relaxation time T_1 of all samples was measured by collabrators in China (Wuhan Insititute of Physics and Mathematics, Chinese Academy of Sciences, Wuhan, China) and data analysis was carried out by the author.

Table 7.2: ^{1}H T_1 spin-lattice relaxation time of 10% and 70% (w/w) felodipine-polymer blend and the two binary extrudates.

Samples	T_1 (1) (ms)	T_1 (2) (ms)
felodipine-EPO 10%	81.7	-
felodipine-EPO 70%	166.4	-
felodipine-VA 64 10%	950	-
felodipine-VA 64 70%	1024	-
felodipine-blend 10%	79	787
felodipine-blend 70%	160	502

However, two spin-lattice relaxation times, T_1, were detected in the 10% and 70% (w/w) felodipine-polymer blend melt extrudates, suggesting the presents of two phases in the dispersions. By comparing the relaxation time of the polymer blend melt extrudates to the two binary melt extrudates with the same drug loadings, it is reasonable to confirm the separated phases in felodipine-polymer blend melt extrudates as felodipine-EUDRAGIT® EPO and felodipine-Kollidon® VA64. For instance, in 10% (w/w) felodipine-polymer blend extrudates, the $T_1(1)$ value (79ms) was very close to the $T_1(1)$ *value* (81.7ms) in the binary 10% (w/w) felodipine-EUDRAGIT® EPO sample, and the $T_1(2)$ value (787ms) was also close to the $T_1(1)$ value (950ms) in the binary 10% (w/w) felodipine-Kollidon® VA64. For a heterogeneous system, the relaxation time of different phases can be further used to estimate the dimension of the separated phases (32). The observation of two separated relaxation processes for T_1 indicates the existence of at least two separated domains. Assuming the process of exchange is by spin diffusion, the following relationship is valid (33):

$$2\sqrt{2}(A^2 / (\pi^2 D)) \, |\Delta\gamma| \; > 1 \qquad \textit{Eq 7.1}$$

where A is the dimension over which diffusion takes place and is indicative of the smallest dimension of the separated domains, D is the spin diffusion coefficient mediating exchange between the two phases, and $\Delta\gamma$ is the difference in the relaxation rates of the separated phases. The spin-diffusion coefficient D has a typical value in polymeric systems as $10^{-16} m^2 s^{-1}$ (33). The $\Delta\gamma$ can be calculated using *Eq 7.2*:

$$\Delta\gamma = 1/T_A - 1/T_B \qquad \textit{Eq 7.2}$$

where T_A and T_B represent the relaxation time of phase A and B. By using *Eq 7.1*, the size of domains can be estimated. The average values of the long T_1 (T_1 (2)) and short T_1 (T_1 (1)) of the felodipine-polymer blend melt extrudates were used to estimate the domain sizes measured in the T_1 experiments. The values obtained by *Eq 7.1* for 10% (w/w) felodipine-polymer blend melt extrudates was greater than 5.5nm, and for 70% (w/w) sample was greater than 9.0nm. As proved by TTM study, felodipine-EUDRAGIT® EPO was the continuous phase in the polymer blend dispersions. Therefore, the calculated domain size was assigned to that phase. The results cannot be interpreted as the accurate size measurement, but an approximate estimation. Also it should be noted that the estimated domain size in felodipine-polymer blend melt extrudates by ss-NMR was not comparable to the dimension detected by TTM as TTM applied in this study only has a highest spatial resolution of 1µm (the smallest distance between the two tested points).

7.3.5 Immiscible polymer blends as a formulation strategy in amorphous solid dispersions

In this chapter, immiscible polymer blends were proposed as a formulation strategy for the enhancement of the physical stability of amorphous solid dispersions prepared by hot melt extrusion. In comparison to the conventional binary drug-polymer solid dispersions, two advantages can be provided by polymer blends. They are the overall increased apparent solubility of drugs in solid dispersions and the reduced moisture sorption. The key factor of the formulation design is based on the immiscibility between the two polymers, which ideally should form a configuration of phase separation as illustrated in Figure 7.1. With this structure, the polymer which has higher solubility will dissolve the majority of drug molecules and form the separated phase. The polymer with higher drug solubility is normally hygroscopic which can lead to physical instability by moisture sorption. By blending with a hydrophilic polymer, the separated phase can be protected from moisture uptake by the continuous phase formed by the hydrophilic polymer with low quantity of drugs. Consequently, the physical stability of amorphous solid dispersions can be enhanced.

The concept of immiscible polymer blend was applied to felodipine amorphous solid dispersions by blending felodipine with Kollidon® VA64 (hydrophilic but with higher drug solubility) and EUDRAGIT® EPO (hydrophobic) using hot melt extrusion. Although the micro-structure study showed an inversed structure (Figure 7.20d) to the proposed phase configuration (Figure 7.1), the physical stability was still significantly enhanced both against stressed temperature and stressed humidity in comparison to the two binary melt extrudates. The phase configuration of the immiscible polymer blends can vary depending on their physical properties. For instance, the surface tension of the two polymers at operation temperature in hot melt extrusion may affect the phase distribution. Nevertheless, the study proves that in practice even with inversed configuration the polymer blend matrix still offers better stabilisation effect.

With a great depth of the understanding of polymer properties, a desired phase configuration can be achieved. In addition, using polymer blends can also save the effort for the development of new polymers as polymer blends can combine the desired physical properties of individual polymer. This immiscible polymer blend proposal may be generalised as a formulation strategy for the enhancement of the physical stability of amorphous solid dispersions.

7.4 Conclusions

In this chapter, immiscible polymer blends as a formulation strategy for the enhancement of the physical stability of amorphous solid dispersions was introduced. The polymer blend of Kollidon® VA64 and EUDRAGIT® EPO was applied in hot melt extrusion with felodipine. The proposed formulation concept of this study was the combination of increasing apparent solid solubility of the drug by the incorporation of Kollidon® VA64 in the formulation and the moisture protection against high humidity by the addition of EUDRAGIT® EPO in the formulation.

Higher apparent solid solubility of felodipine in Kollidon® VA64 than in EUDRAGIT® EPO was predicted by melting point depression and milling approaches. On aging under stressed temperature and humidity, respectively, felodipine-polymer blend melt extrudates with 70% (w/w) drug loading showed significantly higher physical stability than the corresponding two binary melt extrudates, demonstrating the success of the polymer blend formulation design. It also consequently proves the validation of the mechanical milling as a reliable approach in predicting apparent solid solubility. The polymer blend formulation dramatically reduced moisture uptake to below 5% (in comparison to the 12% moisture uptake by the binary felodipine-Kollidon® VA64 formulation), which also contributes to the improved physical stability.

The phase separation configuration of felodipine-polymer blend extrudates was confirmed as felodipine-Kollidon® VA64 being the continuous phase and felodipine-EUDRAGIT® EPO being the separated phase. Felodipine was proved to disperse in both polymers in the polymer blend extrudates but a higher felodipine concentration in Kollidon® VA64 phase and a lower concentration in EUDRAGIT® EPO was observed, which was in good agreement with the predicted apparent solid solubility.

In addition to the enhanced physical stability, the application of the polymer blend in melt extrusion can also improve dissolution profile of felodipine. A significantly higher maximum drug release was achieved from the 10% (w/w) felodipine-polymer blend melt extrudates in comparison to the corresponding two binary extrudates. It might be explained by the enhanced wettability provided by Kollidon® VA64 and the combined effects of EUDRAGIT® EPO on felodipine in 0.1MHCl media including the solubilisation effect on crystalline felodipine and the recystallisation inhabitation effect on amorphous felodipine.

The polymer blend concept in formulation design in hot melt extrusion may broaden the application of the commercially available polymers rather than developing new polymers. The concept may also be generalised as a formulation strategy to enhance the physical stability of solid dispersions

Reference

1. C. De Brabander, C. Vervaet, and J.P. Remon. Development and evaluation of sustained release mini-matrices prepared via hot melt extrusion. Journal of Controlled Release. 89:235-247 (2003).
2. M.M. Crowley, B. Schroeder, A. Fredersdorf, S. Obara, M. Talarico, S. Kucera, and J.W. McGinity. Physicochemical properties and mechanism of drug release from ethyl cellulose matrix tablets prepared by direct compression and hot-melt extrusion. International Journal of Pharmaceutics. 269:509-522 (2004).
3. U. Quintavalle, D. Voinovich, B. Perissutti, F. Serdoz, G. Grassi, A. Dal Col, and M. Grassi. Preparation of sustained release co-extrudates by hot-melt extrusion and mathematical modelling of in vitro/in vivo drug release profiles. European Journal of Pharmaceutical Sciences. 33:282-293 (2008).
4. S. Shah, S. Maddineni, J. Lu, and M.A. Repka. Melt extrusion with poorly soluble drugs. International Journal of Pharmaceutics(2012).
5. C.M. Adeyeye, J. Rowley, D. Madu, M. Javadi, and S.S. Sabnis. Evaluation of crystallinity and drug release stability of directly compressed theophylline hydrophilic matrix tablets stored under varied moisture conditions. International Journal of Pharmaceutics. 116:65-75 (1995).
6. S.K. Dordunoo, J.L. Ford, and M.H. Rubinstein. Physical Stability of Solid Dispersions Containing Triamterene or Temazepam in Polyethylene Glycols. Journal of Pharmacy and Pharmacology. 49:390-396 (1997).
7. I. Bravo-Osuna, C. Ferrero, and M.R. Jiménez-Castellanos. Drug release behaviour from methyl methacrylate-starch matrix tablets: Effect of polymer moisture content. European Journal of Pharmaceutics and Biopharmaceutics. 69:285-293 (2008).
8. P. Marsac, T. Li, and L. Taylor. Estimation of Drug–Polymer Miscibility and Solubility in Amorphous Solid Dispersions Using Experimentally Determined Interaction Parameters. Pharm Res. 26:139-151 (2009).
9. S.-u. Yoo, S.L. Krill, Z. Wang, and C. Telang. Miscibility/stability considerations in binary solid dispersion systems composed of functional excipients towards the design of multi-component amorphous systems. Journal of Pharmaceutical Sciences. 98:4711-4723 (2009).
10. F. Qian, J. Huang, Q. Zhu, R. Haddadin, J. Gawel, R. Garmise, and M. Hussain. Is a distinctive single Tg a reliable indicator for the homogeneity of amorphous solid dispersion? International Journal of Pharmaceutics. 395:232-235 (2010).
11. L.A. Wegiel, L.J. Mauer, K.J. Edgar, and L.S. Taylor. Crystallization of amorphous solid dispersions of resveratrol during preparation and storage—Impact of different polymers. Journal of Pharmaceutical Sciences. 102:171-184 (2013).
12. M. Maniruzzaman, D.J. Morgan, A.P. Mendham, J. Pang, M.J. Snowden, and D. Douroumis. Drug–polymer intermolecular interactions in hot-melt extruded solid dispersions. International Journal of Pharmaceutics. 443:199-208 (2013).
13. P. Hoppu, S. Schantz, and A. Juppo. A solid-state NMR study of physical stability and molecular interactions in citric acid and paracetamol blends. European Journal of Pharmaceutical Sciences. 34:S38 (2008).
14. A.C.F. Rumondorand L.S. Taylor. Effect of Polymer Hygroscopicity on the Phase Behavior of Amorphous Solid Dispersions in the Presence of Moisture. Molecular Pharmaceutics. 7:477-490 (2009).
15. S. Qi, J.G. Moffat, and Z. Yang. Early Stage Phase Separation in Pharmaceutical Solid Dispersion Thin Films under High Humidity: Improved Spatial Understanding Using Probe-Based Thermal and Spectroscopic Nanocharacterization Methods. Molecular Pharmaceutics. 10:918-930 (2013).

16. A.F. Rumondor, I. Ivanisevic, S. Bates, D. Alonzo, and L. Taylor. Evaluation of Drug-Polymer Miscibility in Amorphous Solid Dispersion Systems. Pharm Res. 26:2523-2534 (2009).
17. S. Qi, P. Belton, W. McAuley, D. Codoni, and N. Darji. Moisture Uptake of Polyoxyethylene Glycol Glycerides Used as Matrices for Drug Delivery: Kinetic Modelling and Practical Implications. Pharm Res.30: 1123-1136 (2012).
18. H.M.L. Thijs, C.R. Becer, C. Guerrero-Sanchez, D. Fournier, R. Hoogenboom, and U.S. Schubert. Water uptake of hydrophilic polymers determined by a thermal gravimetric analyzer with a controlled humidity chamber. Journal of Materials Chemistry. 17:4864-4871 (2007).
19. A.M. Ribeiro, T.P. Sauer, C.A. Grande, R.F.P.M. Moreira, J.M. Loureiro, and A.r.E. Rodrigues. Adsorption Equilibrium and Kinetics of Water Vapor on Different Adsorbents. Industrial & Engineering Chemistry Research. 47:7019-7026 (2008).
20. R. Paul Dand W. Barlow J. A Brief Review of Polymer Blend Technology. Multiphase Polymers, Vol. 176, AMERICAN CHEMICAL SOCIETY1979, pp. 315-335.
21. K. Sakurai, T. Maegawa, and T. Takahashi. Glass transition temperature of chitosan and miscibility of chitosan/poly(N-vinyl pyrrolidone) blends. Polymer. 41:7051-7056 (2000).
22. A. Sionkowska. Interaction of collagen and poly(vinyl pyrrolidone) in blends. European Polymer Journal. 39:2135-2140 (2003).
23. D.R. Paul. Polymer Blends: Phase Behavior and Property Relationships. Multicomponent Polymer Materials, Chapter 1 3-19, American Chemical Society 1985.
24. M.L. Ruegg, B.J. Reynolds, M.Y. Lin, D.J. Lohse, and N.P. Balsara. Microphase and Macrophase Separation in Multicomponent A/B/A−C Polymer Blends with Attractive and Repulsive Interactions. Macromolecules. 39:1125-1134 (2006).
25. C.R. Lopez-Barronand C.W. Macosko. Characterizing Interface Shape Evolution in Immiscible Polymer Blends via 3D Image Analysis. Langmuir. 25:9392-9404 (2009).
26. C.Z. Chuai, K. Almdal, I. Johannsen, and J. Lyngaae-Jørgensen. Morphology evolution of polycarbonate–polystyrene blends during compounding. Polymer. 42:8217-8223 (2001).
27. M. Pracella. Micro- and Nanostructured Multiphase Polymer Blend Systems: Phase Morphology and Interfaces. Macromolecular Chemistry and Physics. 208:233-233 (2007).
28. F. Teyssandier, P. Cassagnau, J.F. Gérard, N. Mignard, and F. Mélis. Morphology and mechanical properties of PA12/plasticized starch blends prepared by high-shear extrusion. Materials Chemistry and Physics. 133:913-923 (2012).
29. P.J.F. Thomas G. Fox. Second‐Order Transition Temperatures and Related Properties of Polystyrene. I. Influence of Molecular Weight. Journal of Applied Physics. 21:11 (1950).
30. C. Gao, M. Stading, N. Wellner, M.L. Parker, T.R. Noel, E.N.C. Mills, and P.S. Belton. Plasticization of a Protein-Based Film by Glycerol: A Spectroscopic, Mechanical, and Thermal Study. Journal of Agricultural and Food Chemistry. 54:4611-4616 (2006).
31. Y. Aso, S. Yoshioka, T. Miyazaki, T. Kawanishi, K. Tanaka, S. Kitamura, A. Takakura, T. Hayashi, and N. Muranushi. Miscibility of Nifedipine and Hydrophilic Polymers as Measured by H-NMR Spin-Lattice Relaxation. Chemical and Pharmaceutical Bulletin. 55:1227-1231 (2007).
32. P. Belton. Spectroscopic Approaches to the Understanding of Water in Foods. Food Reviews International. 27:170-191 (2011).
33. S. Qi, P. Belton, K. Nollenberger, N. Clayden, M. Reading, and D.M. Craig. Characterisation and Prediction of Phase Separation in Hot-Melt Extruded Solid Dispersions: A Thermal, Microscopic and NMR Relaxometry Study. Pharm Res. 27:1869-1883 (2010).

Chapter 8: Enhancement of the physical stability of solid dispersions using different processing methods: spin coating vs. hot melt extrusion

8.1 Introduction

Solid dispersions have been widely used in the pharmaceutical industry as a formulation strategy for increasing dissolution rate of poorly water soluble drugs and hence the bioavailability (1, 2). As mentioned in previous chapters, the main challenge of commercialising pharmaceutical formulations of solid dispersions is the physical stability issue, which is highly potential to affect dissolution performance of amorphous solid dispersions (3-5). To achieve a physically stable amorphous drug-polymer formulation, several factors were recommended by pharmaceutical researchers including a certain degree of miscibility between drugs and polymers, apparent solid solubility of drugs in polymers and some thermodynamic properties such as glass transition temperatures of amorphous drugs and polymers (6-8). In addition to these factors mentioned above, processing methods have also been reported to be related to the physical stability of amorphous solid dispersions (9-11)

The fundamental theory of preparing amorphous drug-polymer solid dispersions in general is to destroy the lattice structure (long range order) of the crystalline form drugs, and thus amorphous drugs with short range order will be formed and be stabilised by the added polymers (12). The lattice structure in crystalline drugs can be broken by either dissolving drugs in solutions or melting them to temperatures above their melting points (or below melting points depending on the drug-polymer ratios in formulations) (13). Accordingly, two main methods of preparing solid dispersions were introduced in the pharmaceutical industry including solvent evaporation based methods, such as film casting or spray drying, and melting based methods, such as hot melt extrusion.

Similar to film casting, spin coating is a typical solvent evaporation based preparation process whereby crystalline drugs and polymers dissolve mutually in a solvent or co-solvent (14). Unlike film casting in which solvent evaporates naturally under either ambient or lower pressure environment, solvent evaporation in spin coating occurs due to the fast spinning within a short time of preparation (15). It is a technology originated from semi-conductor industry for preparing thin film coatings with various thicknesses depending on the applied solvent (16). Due to the precise control and high consistency of the processing in preparation, spin coating has been used in the pharmaceutical research in areas such as the investigation of crystallisation tendency of amorphous drugs and the understanding of recrystallisation behaviour of amorphous drugs (17-19). It also has been reported that spin coating was an effective processing method of preparing physically stable solid dispersions containing amorphous drugs with different crystallisation tendency (17).

Studies from articles have showed that solid dispersions with the same drug-polymer compositions but prepared by different processes exhibited significantly different physical stability on aging, which may indicate that the apparent solid solubility of drugs in solid dispersions may vary depending on different preparation processing (9-11). In Chapter 6, a high level of surface recrystallisation was observed in hot melt extruded felodipine-EUDRAGIT® EPO dispersions aged upon exposure to high humidity. In Chapter 7, with the addition of the polymer Kollidon® VA64 into the binary formulation to increase the overall apparent solid solubility of felodipine in the extrudates, the physical stability of amorphous solid dispersions was substantially improved. In this chapter, another formulation strategy of enhancing the physical stability of felodipine-EUDRAGIT® EPO solid dispersions, using spin coating as an alternative rapid solvent evaporation preparation process was introduced. With a different mechanism of preparing solid dispersions to hot melt extrusion, solid dispersions prepared by spin coating may show different physical stability behaviour. Although the reason has not been deeply understood, drug-polymer miscibility and solubility may vary depending on different processing methods, leading to an enhanced physical stability (9). In this chapter, the comparison of physical stability between spin coated and hot melt extruded felodipine-EUDRAGIT® EPO solid dispersions was reported. Results showed that the physical stability of amorphous solid dispersions could be significantly enhanced by spin coating in comparison to hot melt extrusion.

Research objectives

1. Using spin coating to prepare felodipine-EUDRAGIT® EPO solid dispersions.

2. Comparing with melt extruded felodipine-EUDRAGIT® EPO formulations to investigate if physical stability of solid dispersions can be enhanced by using spin coating.

3. Investigation into the phase separation of spin coated and melt extruded felodipine-EUDRAGIT® EPO solid dispersions in order to understand the potential mechanism of the enhanced physical stability.

8.2 Experimental methods

8.2.1 Hot melt extrusion

Instrumental information and operation parameters refer to Chapter 2 (session 2.2.1.1). Drug-polymer ratio (felodipine:EUDRAGIT® EPO) in melt extrudates included 10:90, 30:70, 50:50, 70:30 and 90:10 (w/w). The prepared extrudates were stored under 75%RH at room temperature up to 10 months.

8.2.2 Spin coating

Instrumental information and sample preparation refer to Chapter 2 (session 2.2.1.2). Drug-polymer ratio in spin coated samples included: 10:90, 30:70, 50:50, 70:30 and 90:10 (w/w). The prepared spin coated films were stored under 75% RH at room temperature up to 10 months.

8.2.3 Physicochemical characterisation

Instrumental information of the characterisation techniques and the used parameters for MTDSC, PXRD, ATR-FTIR, SEM, LTA refer to different sessions in Chapter 2 (2.2.2.1.3 for MTDSC, 2.2.2.4.2 for ATR-FTIR, 2.2.2.5.2 for PXRD, 2.2.2.6.2 for SEM, and 2.2.8.2 for LTA)

8.2.4 Kinetic study of surface recrystallization

Method for the kinetic study of surface recrystallization of smelt extruded and spin coated felodipine-EUDRAGIT® EPO solid dispersions refers to Chapter 6 (session 6.2.5).

8.2.5 Neutron Reflectivity

Neutron reflectivity was used to investigate the phase separation behaviour of ultra-thin spin coated films. It was performed on the SURF neutron reflectometer at the ISIS facility of the Rutherford Appleton Laboratory (Oxfordshire, UK). A well-collimated incident neutron beam at a glancing angle of less than 2^o was shined on the surface of spin coated films and reflected into the detector. The neutron beam was polychromatic containing a range of neutron wavelengths from 0.5 to 6.5 Å. The magnitude of momentum transfer Q was calculated by:

$$Q = 4\pi sin\theta/\lambda \qquad Eq\ 8.1$$

where λ is the wavelength of the incident neutron beam and θ is the incident beam angle. The reflected intensity as a function of time-to-arrival were normalised for the incident beam spectrm and converted to reflectivity *versus Q* using a standard data reduction routine (QUICK) provided by the ISIS laboratory. Data measurement and analysis were both carried out by ISIS laboratory.

To increase the signal contrast, deuterated felodipine (felodipine-d_3(2,3-dichlorophenyl-d_3), CDM Isotopes, Pointe-Claire, Canada) was used to prepare spin coated thin films with EUDRAGIT® EPO. To ensure the flatness of the thin films, spin coating was carried out on silicon wafers rather than microscope glass slide for neutron reflectivity study only.

8.2.6 Dissolution test of melt extrudates

Dissolution instrumental information (session 7.2.5) and UV method (session 7.2.4) refer to Chapter 7. Freshly prepared and aged strand form extrudates (tested as intact strand) were tested in sink-condition media consisting of 0.3% sodium dodecyl sulphate (SDS) in 0.1MHCl. Dissolution

samples were filtered using 0.22µm membrane. Strand form extrudates with the same drug loading were maintained with the same dimensions between the fresh and aged samples.

8.3 Results and discussion

8.3.1 Physical stability studies of hot melt extruded vs. spin coated felodipine-EUDRAGIT® EPO solid dispersions

8.3.1.1 Surface physical stability

In terms of the ability of preparing amorphous felodipine-EUDRAGIT® EPO solid dispersions, significant difference was observed between spin coating and hot melt extrusion. This was particularly evident for 90% (w/w) sample preparation as proved by PXRD results in Figure 8.1. It can be seen in Figure 8.1 that freshly prepared 90% (w/w) felodipine-EUDRAGIT® EPO melt extrudates showed typical crystalline features (felodipine form I) detected by PXRD, indicating the system contains significant amount of felodipine crystals. However, only an amorphous halo was observed in the corresponding spin coated sample. This proves spin coating can prepare amorphous felodipine-EUDRAGIT® EPO solid dispersions with extremely high drug loading. This may also possibly indicate that the apparent solid solubility of felodipine in spin coated solid dispersions was higher than that in melt extruded dispersions.

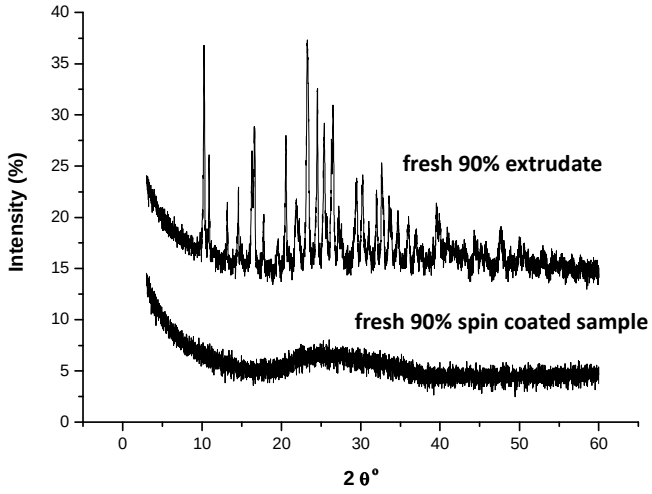

Figure 8.1: PXRD results of freshly prepared 90% (w/w) melt extruded and spin coated felodipine-EUDRAGIT® EPO samples.

In order to compare the difference of the physical stability, 10%-70% (w/w) melt extruded and 10%-90% (w/w) spin coated felodipine-EUDRAGIT® EPO solid dispersions were aged under 75%RH/room temperature up to 10 months (90%w/w melt extrudates were not studied as the fresh sample showed a significant amount of crystalline drug). After 10 months aging under 75%RH at room temperature, no crystalline felodipine was detected on the surface of 10% (w/w) felodipine-EUDRAGIT® EPO melt extrudates by ATR-FTIR, indicating significantly high physical stability of this sample against stressed humidity.

However, surface recrystallization appeared in 30%-70% (w/w) melt extrudates after aged for different time periods by monitoring NH peak position using ATR-FTIR. For 30% (w/w) samples, it can be seen that freshly prepared extrudates show an identical NH peak position as the aged sample which was very close the NH peak position in crystalline felodipine (Figure 8.2). But this did not mean crystalline felodipine was detected on the surface of fresh 30% (w/w) sample. The reason has been discussed in Chapter 5 that carbonyl groups from EUDRAGIT® EPO can disturb the hydrogen bonding between two felodipine molecules leading to the NH peak shift in the melt extrudates. It has been reported that peaks of certain chemical groups (e.g. NH or OH) in drugs in crystalline state detected by FTIR can become broader with a lower intensity (in amorphous state) after they are changed to amorphous state, and this was the case here with the NH group from felodipine (20). It can be seen that after 6 months aging, the NH peak from 30% (w/w) felodipine-EUDRAGIT® EPO melt extrudates became sharper in comparison to the freshly prepared samples, which may suggest the occurrence of surface recrystallization on aging under75%RH/room temperature.

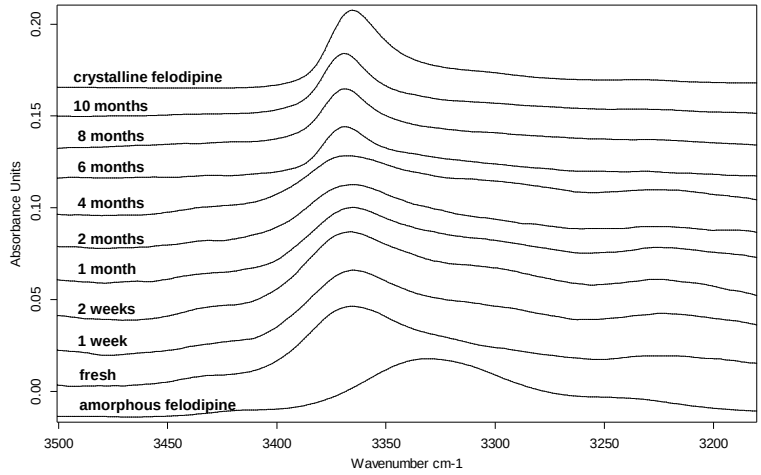

Figure 8.2: ATR-FTIR results of the NH group from the surface of 30% (w/w) felodipine-EUDRAGIT® EPO melt extrudates on aging under 75%RH/room temperature.

Surface recrystallization in 50% (w/w) melt extrudates were detected after 4 months aging under 75%RH/room temperature as shown in Figure 8.3. A single NH peak at 3358cm^{-1} was detected in the fresh 50% (w/w) samples, indicating amorphous solid dispersions of the surface. After 4 months aging, the NH peak shifted to 3365cm^{-1} which was identical to the NH peak from crystalline felodipine, indicating the occurrence of surface recrystallization.

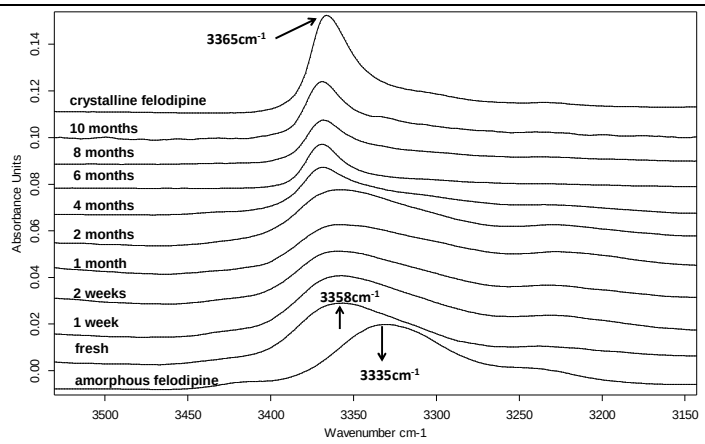

Figure 8.3: ATR-FTIR results of the NH group from the surface of 50% (w/w) felodipine-EUDRAGIT® EPO melt extrudates on aging under 75%RH/room temperature.

Surface recrystallization in 70% (w/w) extrudates was confirmed after 1 month aging under 75%RH/room temperature as seen in Figure 8.4. NH peak at 3345cm^{-1} in freshly prepared 70% (w/w) sample shifted to 3365cm^{-1} after 1 month aging which was identical to the NH peak in crystalline felodipine indicating the surface recrystallization on in 70% (w/w) extrudates. The ATR-FTIR results showed that 30%-70% (w/w) melt extrudates were not physically stable against stressed humidity, and surface recrystallization occurred in these samples after different aging time periods.

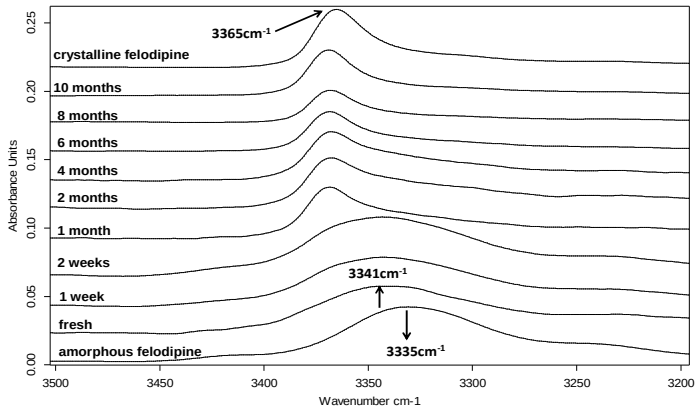

Figure 8.4: ATR-FTIR results of the NH group from the surface of 70% (w/w) felodipine-EUDRAGIT® EPO melt extrudates on aging under 75%RH/room temperature.

However, spin coated felodipine-EUDRAGIT® EPO thin films presented substantially different surface physical stability by ATR-FTIR tests as seen in Figure 8.5. After 10 months aging, the NH peak did not shift in any spin coated samples even including the 90% (w/w) sample, indicating no crystalline felodipine appeared on the surface of any spin coated systems and all spin coated samples still remained as amorphous solid dispersions. This proves that spin coated felodipine-EUDRAGIT® EPO were physically stable with the level of the sensitivity of detecting felodipine

crystals by conventional ATR-FTIR technology. The ATR-FTIR results demonstrate that the physical stability of felodipine-EUDRAGIT® EPO solid dispersions prepared by spin coating was significantly higher than prepared by hot melt extrusion, especially the surface physical stability.

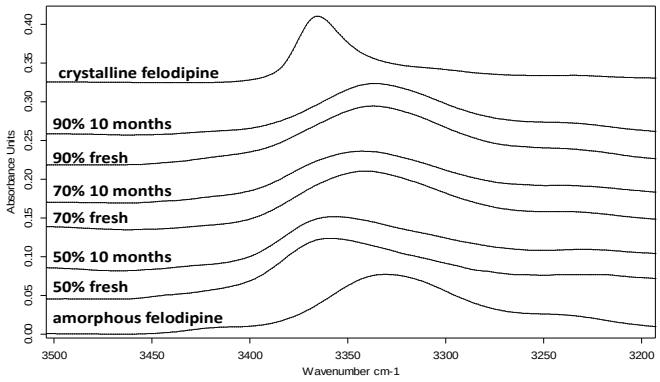

Figure 8.5: ATR-FTIR results of the NH group from 50%-90% (w/w) spin coated felodipine-EUDRAGIT® systems on aging under 75%RH/room temperature.

Surface recrystallization of felodipine-EUDRAGIT® EPO melt extrudates was also studied by SEM as seen in Figure 8.6. No particles was observed on the surface of fresh 10% and 30% (w/w) extrudates, and few particles were seen on the surface of freshly prepared 50% and 70% (w/w) melt extrudates. However, after 10 month aging under 75%RH/room temperature, particles with the size of approximately 10µm were seen on the surface of 30% (w/w) extrudates. For 50% (w/w) samples, after 10 months aging particles with the size of 30-40 µm were observed. The surface of 10months aged 70% (w/w) was nearly covered by particles. Only the surface of 10% (w/w) extrudates was still as smooth as the fresh 10% (w/w) sample. SEM results showed that 30%-70% (w/w) extrudates had poor surface physical stability on aging under 75%RH/room temperature, which is in good agreement with the ATR-FTIR results.

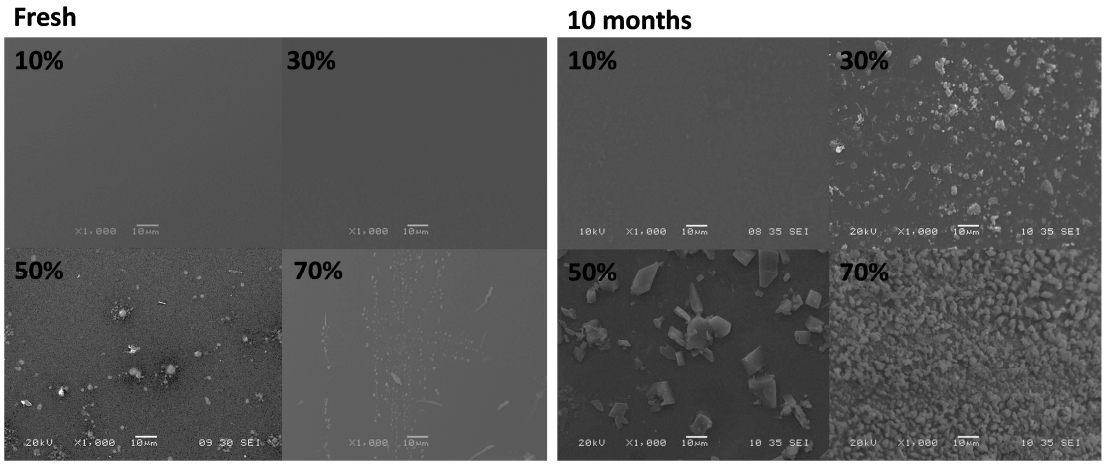

Figure 8.6: SEM images of the surface of fresh and 10 months aged felodipine-EUDRAGIT® EPO melt extrudates.

Spin coated thin films showed completely different surface morphology. No particles were seen on any freshly prepared thin films. After 10 months aging, only very few particles with the size below 30µm were observed on the surface of 50%-90% (w/w) thin films (Figure 8.7). Compared with the surface of the corresponding melt extrudates, the particle size and density was significantly smaller and lower. This indicates a significantly higher level of physical stability of spin coated thin films than that of corresponding melt extrudates. The observed particles in the spin coated samples suggest that surface phase separation in spin coated film only occurred at a very low level, and it could not be detected by conventional ATR-FTIR.

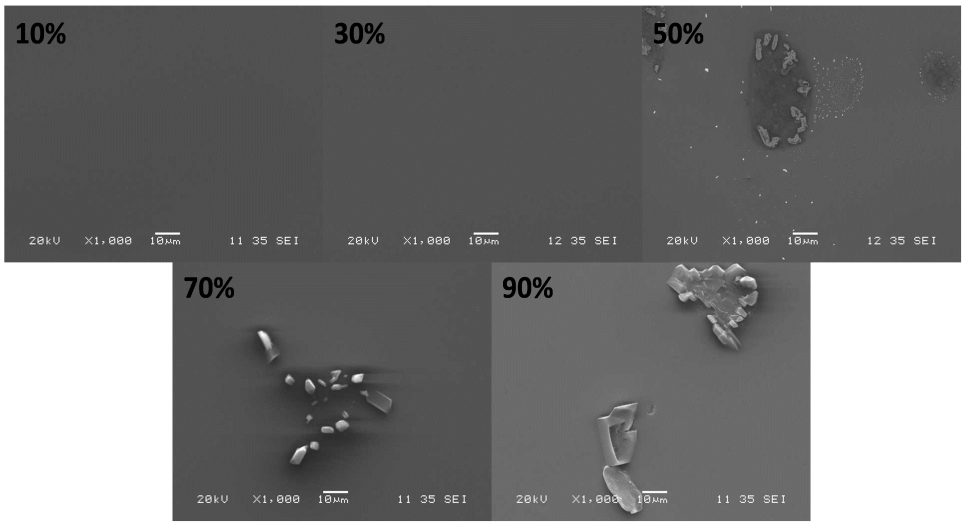

Figure 8.7: SEM images of the surface of spin coated 10%-90% (w/w) felodipine-EUDRAGIT® EPO films after 10 months aging under 75%RH/room temperature.

Kinetics of surface recrystallisation in hot melt extruded felodipine-EUDRAGIT® EPO solid dispersions on aging were studied using the analysis of SEM images on aging by Image J (Figure 8.8). After 10 months aging, approximately 10% (calculated using the measured total particle areas divided by the size of the whole image area) of the surface area tested by SEM was covered by particles (drug crystals) in 30% (w/w) melt extrudates, and for 50% (w/w) extrudates the particles-covered area was circa 30%. For 70% (w/w) extrudates, nearly 90% of the surface area tested by SEM was covered by particles, indicating a high level of surface recrystallization in this sample. Kinetics of surface recrystallization of 30%-70% (w/w) melt extrudates did not fit in the Avrami model (described in Chapter 6) as it lacked of the nucleation phase and the phase of the completion of the nucleation. Instead, linear relationships with acceptable regression coefficients were found for the kinetics of surface recrystallization of 30%-70% (w/w) extrudates (Figure 8.8). The slope of individual linearity can be considered as the surface crystal growth rate of each sample on aging. It clearly showed that the recrystallization rate increased with increasing drug loading on aging (5.48µm^2/day for 30%w/w extrudates, 13.67µm^2/day for 50%w/w extrudates, and 34.24µm^2/day for 70%w/w extrudates).

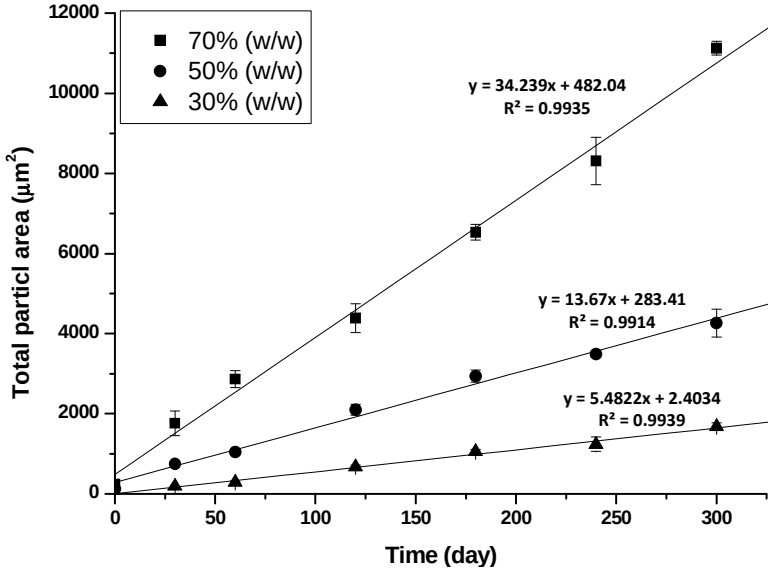

Figure 8.8: Results of total particle domain area (%) achieved by using Image J to analyse SEM images on the surface of felodipine-EUDRAGIT® EPO melt extrudates with different drug loadings.

Kinetics of surface recrystallization of spin coated thin films was also studied. For 50%-90% (w/w) spin coated solid dispersions, no particles were observed on the surface after 2 months aging under 75%RH/room temperature. After 10 months aging, the percentage of the surface area covered by particles (drug crystals) was below 10% (calculated using the measured total particle areas divided by the size of the total image area) for all samples even including the 90% (w/w) spin coated film. For spin coated thin films, the nucleation phase was observed as proved by the absence of particles on the surface within the first 2 months aging time period. However, kinetics of the surface recrystallization of spin coated thin films still did not fit in the Avrami model. This is because the crystals growth on the surface occurred at a slow rate on aging and after 10 months aging the overall surface recrystallization was still significantly below completion, leading to the unfitting in the sigmoidal of the Avrami model. The kinetics surface recrystallization in spin coated films on aging showed a linear relationship as seen in Figure 8.9 (form 2 months to 10 months aging time). The slope of the linearity can be considered as the surface crystal growth rate in individual spin coated thin film, and it can be seen that the rate increased with increasing drug loading. This can also provide a clear comparison of recrystallization rates between melt extrudates and spin coated films. Surface recrystallization rate of 70% (w/w) melt extrudates (34.24μm^2/day) was nearly 10 times faster than the rate of 90% (w/w) spin coated films (3.88μm^2/day). This again demonstrates that the physical stability of felodipine-EUDRAGIT® EPO solid dispersions prepared by spin coating was significantly higher than prepared by hot melt extrusion, especially the surface physical stability.

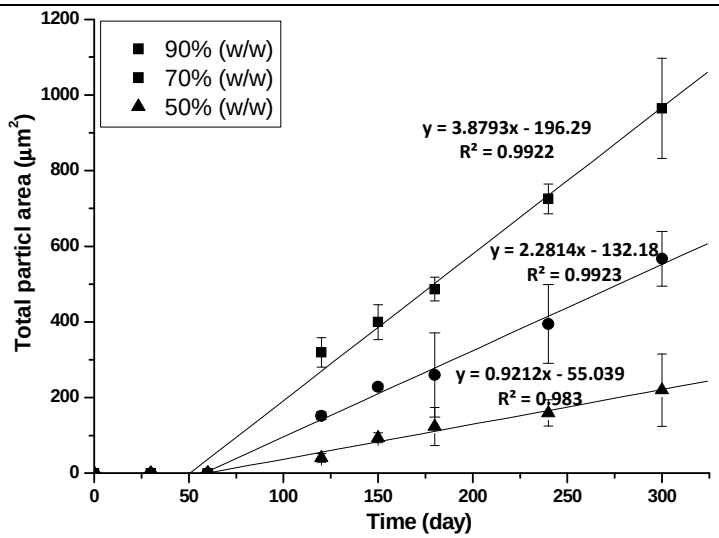

Figure 8.9: Results of total particle domain area (%) achieved by using Image J to analyse SEM images on the surface of spin coated felodipine-EUDRAGIT® EPO thin films with different drug loadings.

8.3.1.2 Bulk physical stability

Due to the extremely low sample mass and the difficulties of removing the thin films from the coating substrate, bulk physical stability of spin coated felodipine-EUDRAGIT® EPO cannot be studied using MTDSC. The bulk physical stability was studied using PXRD. After 10months aging under 75%RH/room temperature, no crystalline felodipine was detected by PXRD in any spin coated samples, indicating all spin coated samples remained as amorphous solid dispersions as bulk. This demonstrates high bulk physical stability of spin coated felodipine-EUDRAGIT® EPO thin films.

Bulk physical stability of melt extrudates was studied using MTDSC. No melting of crystalline felodipine was detected by MTDSC in the extrudates with the drug loading of 50% (w/w) and below after 10 months aging under 75%RH/room temperature. This can be attributed to the reason that the amount of recrystallised felodipine in those formulations was below the detection sensitivity of MTDSC. Felodipine crystals were very likely to re-dissolve into the polymer on heating as proved in the melting point depression study of felodipine in EUDRAGIT® EPO in Chapter 4. This also proves the surface recrystallization level of these samples was low.

Melting of crystalline felodipine was detected by MTDSC in 70% (w/w) melt extrudates on aging, and using *Eq 5.1* the crystallinity in this sample can be analysed quantitatively as seen in Figure 8.10. The amount of crystalline felodipine increased from 0.7% (w/w) in freshly prepared sample to 1.8% (w/w) after 10 months aging under 75%RH at room temperature, indicating extremely high bulk physical stability despite the high degree of surface recrystallization. The recrystallization

profile does not fit in the classic Avrami model due to the existing heterogeneous nuclei in freshly prepared samples.

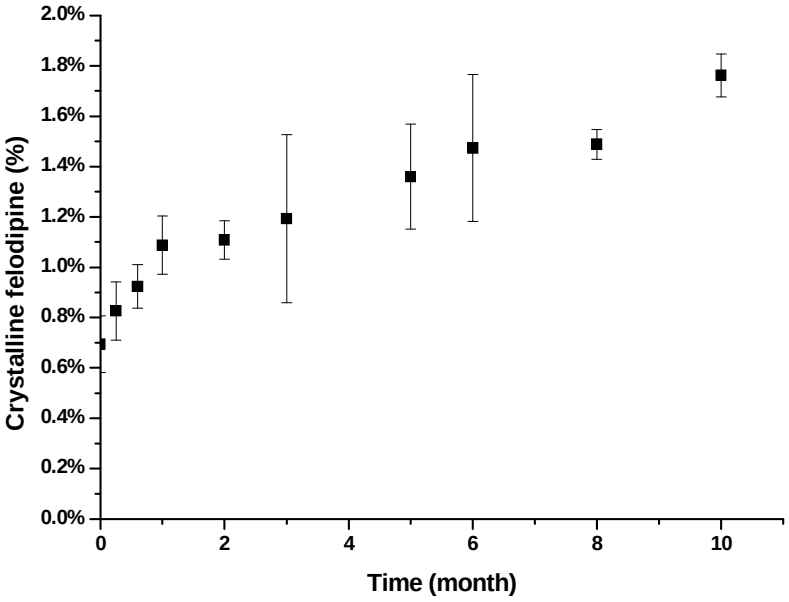

Figure 8.10: The amount of crystalline felodipine in 70% (w/w) felodipine-EUDRAGIT® EPO melt extrudates on aging under 75%RH at room temperature calculated using the measured melting enthalpy.

The physical stability study of felodipine-EUDRAGIT® EPO solid dispersions clearly demonstrated that spin coating can significantly enhance the physical stability against stressed humidity in comparison to hot melt extrusion, especially the surface physical stability. The mechanism of the physical stability enhancement will be discussed later in this chapter.

8.3.2 Investigation into the underpinning mechanisms of the observed physical stability difference of melt extruded and spin coated solid dispersions

Results of physical stability studied showed that felodipine-EUDRAGIT® EPO solid dispersions prepared by spin coating were significantly more stable than by hot melt extrusion. No surface recrystallization was detected in any spin coated thin films after 10 months aging under 75%RH/room temperature by conventional characterisation technology (ATR-FTIR and PXRD). However, particles were observed on the surface of 50%-90% (w/w) spin coated thin films on aging using SEM, which indicates that surface recrystallization already occurred in spin coated thin films but it remained at a low level. Therefore, in order to understand the surface physical stability of spin coated and melt extruded felodipine-EUDRAGIT® EPO solid dispersions in greater depth, LTA was used to analyse the both aged systems.

8.3.2.1 Methodology validation of LTA

To confirm the transition temperatures of amorphous and crystalline felodipine detected by LTA, a validation study was carried out before the sample tests. To summarise, a spin coated pure felodipine thin film (confirmed as amorphous as discussed in Chapter 2) and compressed crystalline felodipine tablet were tested by LTA to measure their thermal transition temperatures. Results are shown in Figure 8.11. It can be seen that a thermal transition at circa 45^{o}C was detected for amorphous felodipine (spin coated thin film of pure felodipine) which is in good agreement with the DSC results. However, a consistent transition temperature at circa 120^{o}C was detected for crystalline felodipine (compressed tablet of pure crystalline felodipine) which is 25^{o}C lower than the melting point (145^{o}C) detected by DSC. This is possibly because the surface defects of crystalline felodipine caused by compression, leading to the depressed melting points (21, 22). It is also possible that the thermal transition of a material detected by LTA on heating is the transition occurs at the temperature where the thermo-mechanical properties of the material change (23). Therefore transition temperatures, such as glass transition temperatures (T_g) and melting points (T_m) detected by LTA can be lower or higher than those measured by DSC if thermo-mechanical properties change on heating occurred at different temperatures from T_g or T_m (24, 25). These two reasons are why the reference test of amorphous and crystalline felodipine was carried out before testing samples. With the results of reference tests, it was then possible to identify potential phase separation and recrystallization on the surface of the thin films and melt extrudates.

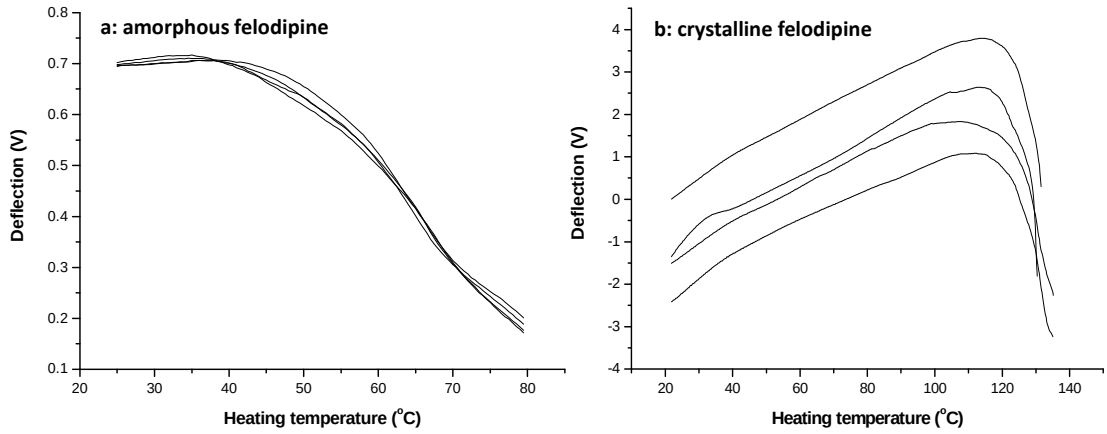

Figure 8.11: LTA results of freshly prepared spin coated pure amorphous felodipine (a) and compressed crystalline felodipine tablet (b).

8.3.2.2 LTA studies of spin coated thin films

8.3.2.2.1 Surface phase separation in aged spin coated thin films detected by LTA

The AFM and LTA results of 10 months aged 10% and 30% (w/w) spin coated felodipine-EUDRAGIT® EPO thin films are shown in Figure 8.12. Only one transition temperature (circa 80^{o}C for both samples) was detected for both thin films, indicating an amorphous single-phase

dispersion for both samples after 10 month aging under 75%RH/room temperature, which is in good agreement with the observation by SEM. In addition, it can be seen from the AFM topography images that these two samples had very smooth surfaces with a roughness within 150nm, indicating a significantly low level of heterogeneity. Transition temperatures detected for 10% (w/w) and 30% (w/w) samples (glass transition temperatures) were close at circa 80°C, which were different from the values of the corresponding melt extruded solid dispersions measured by DSC (46°C for 10% w/w and 39°C for 30%w/w). This temperature difference may be speculated with two reasons. Firstly, this can be explained by the reason that the thermo-mechanical properties of the spin coated thin films were different from the corresponding melt extruded solid dispersions. Secondly, it is possible that glass transition temperatures of solid dispersions with the same composition prepared by different processing methods can be different, although the mechanism has not been clearly understood. However, these two speculations can not be proved. Nevertheless, with the detected single transition temperatures of 10% and 30% (w/w) spin coated thin films in between the reference amorphous and crystalline felodipine transition temperatures, it proves that these two systems showed extremely high physical stability against stressed humidity at room temperature.

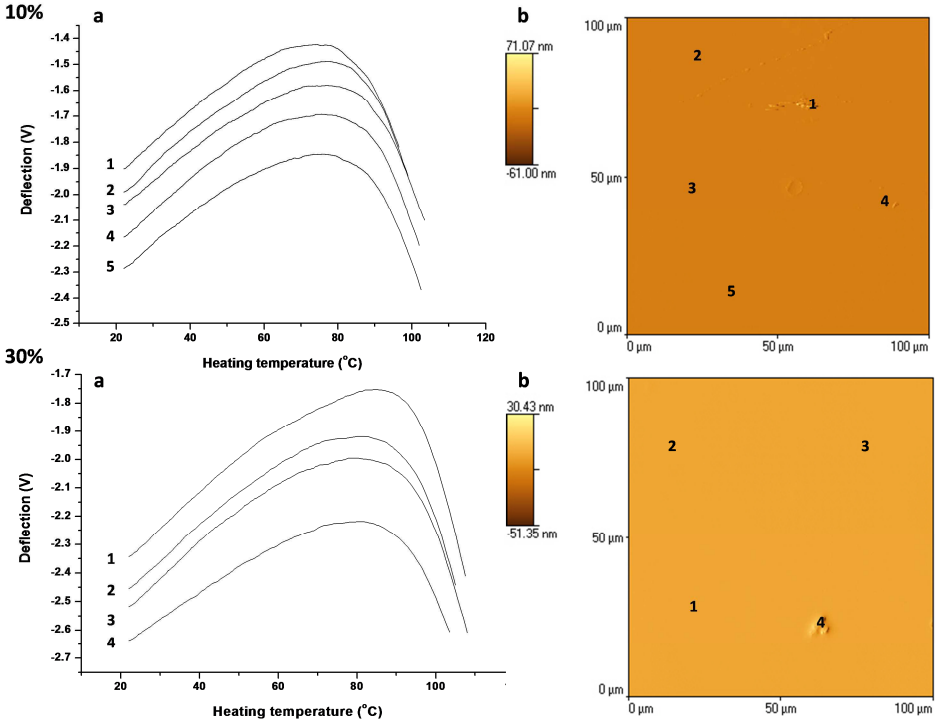

Figure 8.12: LTA results (a) and AFM topography images (b) of 10months aged 10% and 30% (w/w) spin coated felodipine-EUDRAGIT® EPO thin films (numbers in LTA results refer to the testing points in AFM topography image).

Phase separation at different levels were detected in 10 months aged 50%-90% (w/w) spin coated thin films as seen in Figures 8.13 and 14. Surface features were observed in 50%-90% (w/w) aged

thin films. The sizes of the particles observed in AFM topography images (below 5µm for 50% w/w, circa 10µm for 70% w/w, and circa 20 µm for 90% w/w thin films) were in agreement with those observed in SEM images. Two phases with the transition temperature of circa 50°C and 65°C were detected in 50% (w/w) sample (Figure 8.13), and by comparing the transition temperatures in the sample with the reference tests they can be confirmed as amorphous felodipine phase (50°C) and miscible felodipine-EUDRAGIT® EPO phase (65°C). Although few particles were scanned by AFM in the 50% (w/w) sample, no crystalline felodipine was detected, and they could be the early-stage phase separated amorphous felodipine from underneath the surface layer of the film as reported in the literature (19).

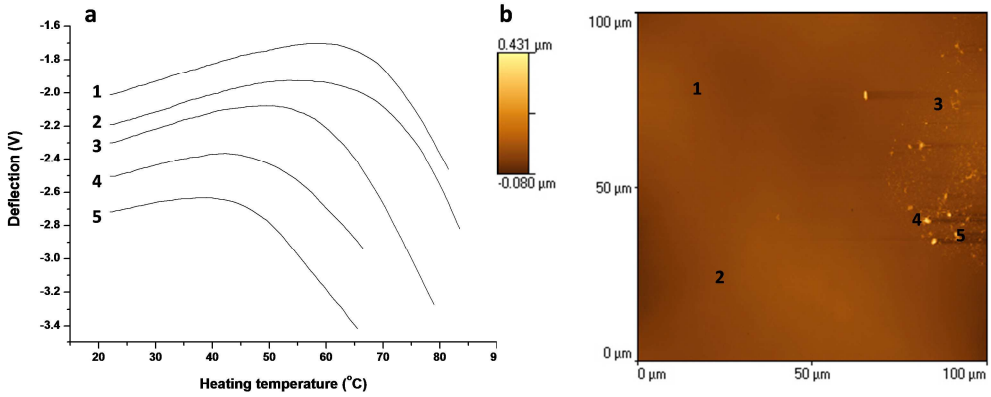

Figure 8.13: LTA results (a) and AFM topography image (b) of 10 months aged 50 (w/w) spin coated thin films (numbers in LTA results refer to the testing points in AFM topography image).

Crystalline felodipine was detected in 70% and 90% (w/w) thin films as seen in the Figure 14. The detected higher transition temperatures (110°C) in both samples were close to the transition temperature of crystalline felodipine (120°C) in the reference tests. Therefore it is reasonable to conclude the occurrence of recrystallization of felodipine in both samples after 10 months aging under 75%RH/room temperature. The detected lower transition temperatures in both samples (70°C for 70% w/w sample and 60°C for 90% w/w sample) showed consistent and the two values in between the transition temperatures of amorphous (45°C) and crystalline felodipine (120°C) in the reference tests. Thus they were very likely to be the miscible drug-polymer phase. In addition, those detected transitions of crystalline felodipine only occurred on the scanned particles, confirming these particles being felodipine crystals.

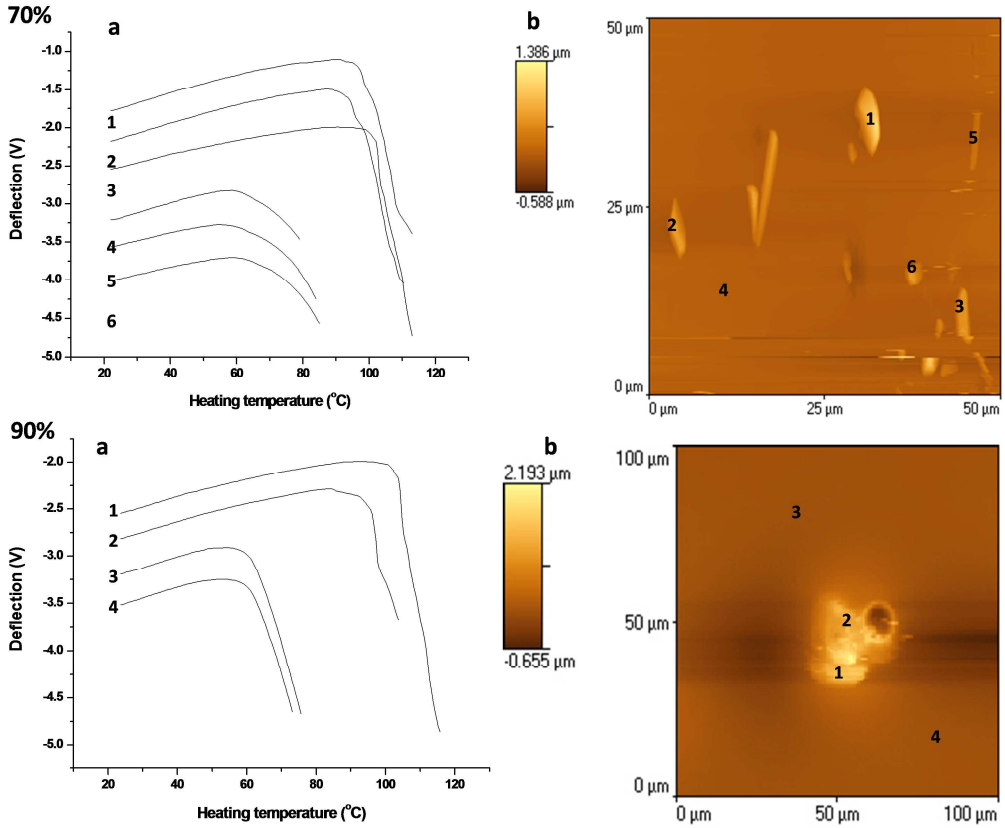

Figure 8.14: LTA results (a) and AFM topography images (b) of 10 months aged 70% and 90% (w/w) spin coated thin films (numbers in LTA results refer to the testing points in AFM topography image).

In summary, the LTA results of the aged spin coated thin films showed that phase separation and recrystallization were only detected in 50%-90% (w/w) samples after 10 months aging under 75%RH/room temperature, and they all occurred at a low level (as proved by the AFM topography images). Amorphous felodipine was detected in 50% (w/w) samples, and crystalline felodipine was detected in 70% and 90% (w/w) thin films. These findings possibly indicate that three steps were involved with regards to phase separation in spin coated felodipine-EUDRAGIT® EPO thin films on aging and they are 1) freshly prepared miscible drug-polymer, 2) followed by the appearance of phase separated amorphous drug in the possible drug-rich phase on aging and 3) completed in the form of recrystallized drugs. The absence of detecting amorphous drug phase in 70% and 90% (w/w) films could be attributed to the reason that separation in terms of the presence of amorphous felodipine in both systems had already accomplished at an earlier stage on aging.

8.3.2.2.2 Attempt of using neutron reflectivity to study phase behaviour of ultra-thin spin coated films

Spin coated thin films showed extremely high physical stability against stressed humidity, and only a low level of phase separation was detected in 50%-90% (w/w) samples. This may suggest that solid dispersions prepared by spin coating may result in a molecular dispersion, whereby drugs dissolve into to polymers in solid dispersions forming a solid solution. However, due to the

thickness of the spin coated films (500nm-10µm), very limited technologies can be applied to investigate drug-polymer distribution in the spin coated films. Neutron reflectivity has been reported as a successful tool to study thin films (26). It is based on the classic specular reflection approach which analyses the beam energy change as a function of incident angle. The information regarding the structure and composition of thin films particularly in molecular dimensions can be provided (27, 28). Although it is normally applied to study films composed of single layer of molecules, an initial attempt of using neutron reflectivity to investigate drug polymer distribution in spin coated thin films was carried out in this study. For neutron reflectivity study, ultra-thin films were prepared.

90% (w/w) spin coated samples showed very good data fitting as shown in Figure 8.15. After data fitting, a felodipine layer with the thickness of approximately 300nm was confirmed to cover the surface of 90% (w/w) spin coated thin film. The reason for this separated drug layer on top was still not clearly understood. The 10% (w/w) sample showed an almost identical pattern to pure EUDRAGIT® EPO, and this might be due to the low drug concentration in this system. The 30%-70% (w/w) spin coated d-felodipine-EUDRAGIT® EPO showed very poor data fitting, indicating drug molecules distributed into small patches in the systems instead of complete phase separation by layers as in 90% (w/w) sample.

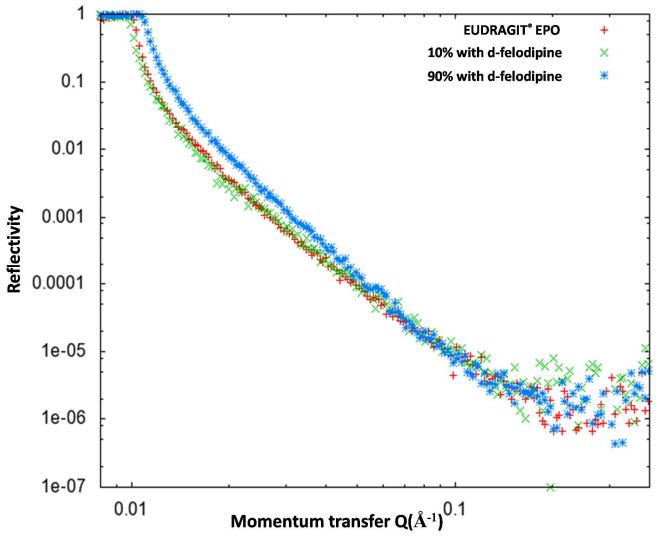

Figure 8.15: Neutron reflectivity patterns of fresh 10% and 90% (w/w) d-felodipine-EUDRAGIT® EPO and pure EUDRAGIT® EPO spin coated samples.

According to the neutron reflectivity results, the proposed drug-polymer distribution in fresh spin coated films is shown in Figure 8.16. The covered drug layer was not detected in 90% (w/w) spin coated films by LTA. This is because the thickness of the film can significantly influence the phase behaviour in thin films (29-31). Spin coated films on microscope slide gave a thickness of circa 10µm whereas using silicon wafer the thickness of the spin coated films was decreased to sub-

micron level. Therefore, spin coated felodipine-EUDRAGIT® EPO films with different thickness showed different phase behaviour.

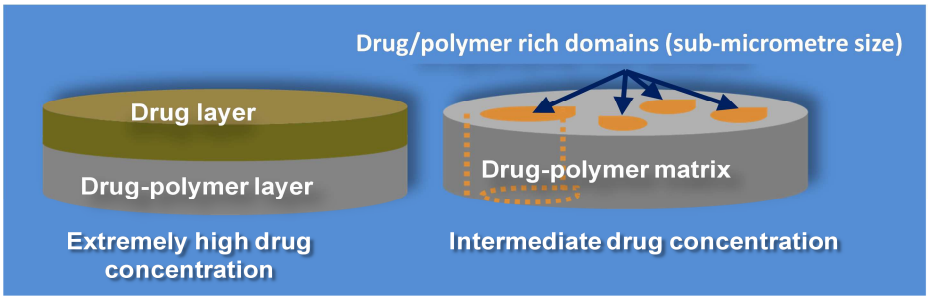

Figure 8.16: Proposed drug-polymer distribution in fresh spin coated felodipine- EUDRAGIT® EPO thin films.

8.3.2.3 LTA studies of hot melt extrudates

8.3.2.3.1 Bulk physical stability

LTA was first applied to investigate the bulk physical stability of aged hot melt extruded felodipine-EUDRAGIT® EPO dispersions. As discussed earlier, MTDSC results showed that the bulk physical stability of melt extrudates was still extremely high after 10 months aging under 75%RH at room temperature. Crystallintiy in 70% (w/w) extrudates only increased form 0.7% w/w (fresh) to 1.8% w/w after 10 months aging. This was further confirmed using LTA to test the cross section of the 10 months aged melt extrudates. It should be mentioned that AFM imaging cannot be performed on the cross section of the extrudates due to the roughness (caused by using a scalpel to cut the strand form extrudates), and therefore the topographyare not provided. It can be seen in Figure 8.17 that only one transition temperature (60^{o}C for 10% w/w, 55^{o}C for 30%w/w, 50^{o}C for 50%w/w and 45^{o}C for 70%w/w extrudates) was detected on the cross section of all melt extrudates after 10 months aging under 75%RH/room temperature, indicating 10%-70% (w/w) melt extrudates as bulk were still physically stable. The detected transition by LTA in all samples can to be confirmed as the miscible drug-polymer phases as these transition temperatures were in between the amorphous and crystalline felodipine transition temperatures in the reference study. Melting of crystalline felodipine in fresh and aged 70% (w/w) extrudates was detected by DSC. However, as proved by the surface morphology study of 70% (w/w) extrudates, felodipine crystals were likely to stay on the surface rather than the cross section. Therefore, no crystalline felodipine was detected on the cross section of aged 70% (w/w) extrudates.

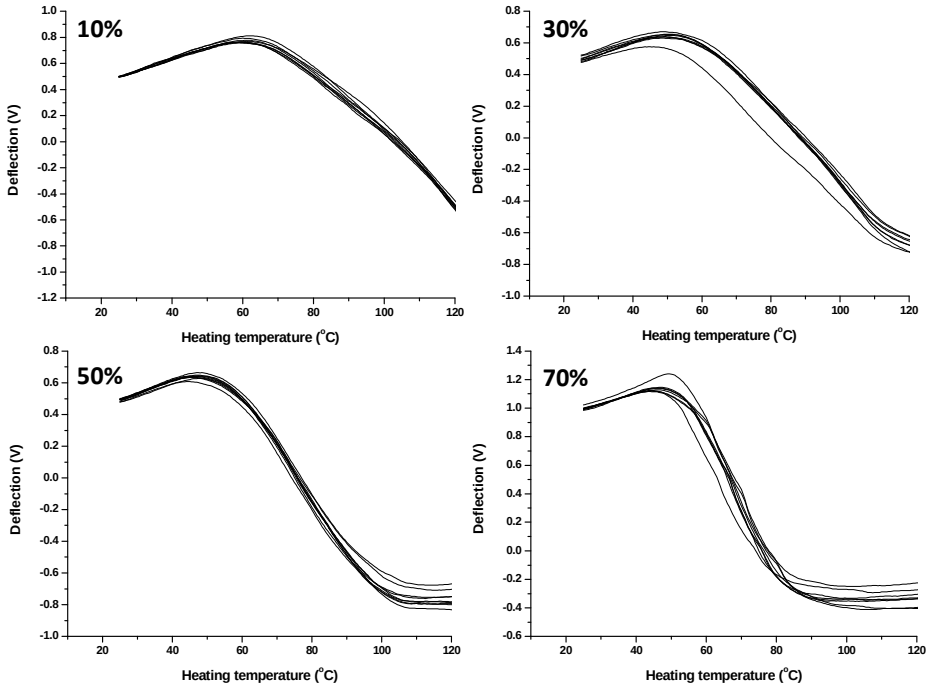

Figure 8.17: LTA results of the cross section of 10months aged 10%-70% (w/w) felodipine-EUDRAGIT® EPO.

8.3.2.3.2 Surface recrystallization

Surface recrystallization of 10 months aged (under 75%RH/room temperature) melt extrudates was studied by LTA. Due to the roughness of the surface of the aged melt extrudates, AFM imaging area was only restricted to 10µm ×10µm. It can be seen that even with the small scanning area (Figure 8.18 and 8.19), the roughness of the surfaces was still high (with a range between 0.6-2.1µm between 10%-70% w/w extrudates), which suggests a great level of surface phase separation after 10 months aging. Although no crystalline felodipine was detected on the surface of 10% (w/w) extrudates by ATR-FTIR, thermal transition of crystalline felodipine was confirmed by LTA as seen in Figure 8.18. Two separated phases were detected within the scanned area and they can be assigned to the miscible drug-polymer phase (60°C) and crystalline felodipine (110°C). This demonstrates that phase separation still occurred locally on the surface of the 10% (w/w) sample but with a low level as proved by the size of the particles (felodipine crystals) in the topography image (below 5µm).

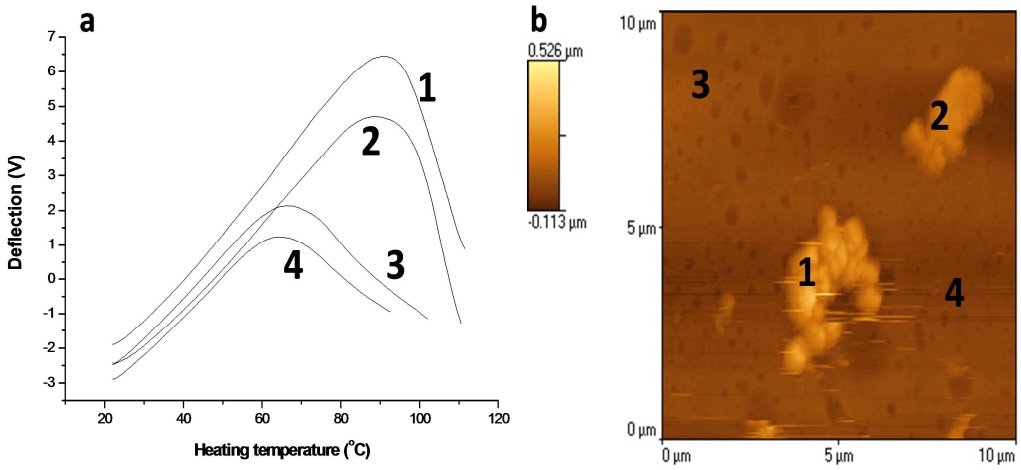

Figure 8.18: LTA results (a) and AFM topography image (b) of the surface of 10 months aged 10% (w/w) felodipine-EUDRAGIT® EPO melt extrudates (numbers in LTA results refer to the testing points in AFM scanning image).

Surface recrystallization in 10 months 30%-70% (w/w) extrudates was also confirmed using LTA (Figure 8.19). Miscible drug-polymer (with the transition temperatures of 55°C for 30%w/w, 50°C for 50%w/w and 45°C for 70%w/w extrudates) and crystalline drug (with the transition temperature of circa 120°C) were both detected on the surface of 30%-70% (w/w) melt extrudates. In addition, taking into account the significantly smaller imaging areas (10µm ×10µm for extrudates and 100µm ×100µm for thin films), particle (felodipine crystals) density on the surface of melt extrudates should be significantly higher than that on the surface of spin coated thin films.

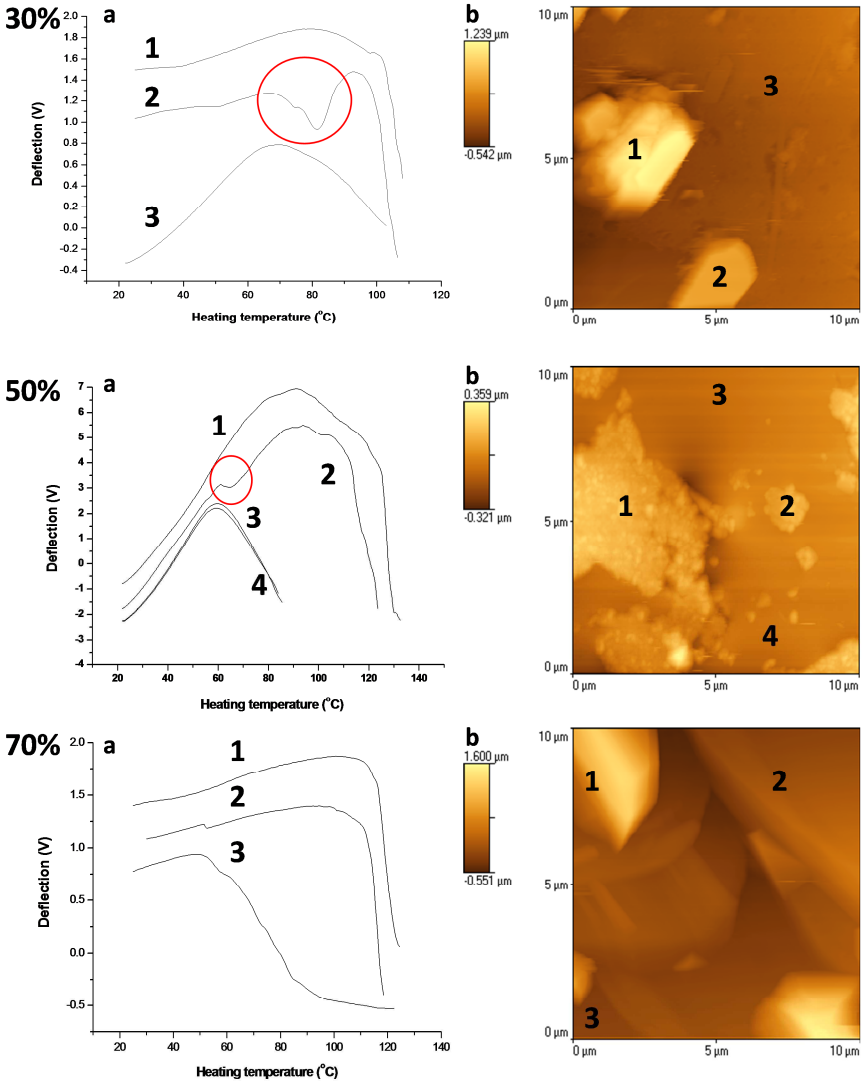

Figure 8.19: LTA results (a) and AFM scanning images (b) of the surface of 10 months aged 30%-70% (w/w) felodipine-EUDRAGIT® EPO melt extrudates (numbers in LTA results refer to the testing points in AFM scanning image) (the red circles refer to the detected first reansition in samples with double transitions).

Double thermal transitions in one test were detected on the surface of 30% and 50% (w/w) melt extrudates (as highlighted by red circle in Figure 8.19). For instance, in the LTA result of 30% (w/w) melt extrudates, a double transition was detected in Test 2. The first transition occurred with a decrease of the deflection signal at the temperature identical to the temperature where the thermal transition of miscible drug-polymer occurred (Test 3). Subsequently, following the first transition another transition was detected in the same test, which showed a transition temperature close to the LTA-detected melting of crystalline felodipine and it was also very close to Test 1. This suggests that, in Test 2 the thermal probe was first in contact with the miscible drug-polymer layer and after penetration the first layer on heating, it touched the second layer, crystalline drug. Similar results were achieved in 50% (w/w) samples as shown in Figure 8.19. Consequently, this may suggest that

surface recrysllisation may occur from the layer underneath the surface and the crystals grew upwards rather than inside of the extrudates on aging.

8.3.2.4 Possible mechanisms of surface recrystallization of hot melt extrudates

Surface crystallisation of pure amorphous drugs has been investigated in articles (32-34). By evaluating the surface recrystallization of indomethacin, nifedipine, it was concluded that surface recrystallization rate could be 1 to 2 orders of magnitude faster than the bulk recrystallization rate at the temperature below their glass transition temperatures (33). The reason was attributed to the greater molecular mobility of amorphous drugs on the surface than in the bulk, leading to the higher surface recrystallization rate, and using gold nano-coating to cover the surface the recrystallization rate was significantly reduced (32). These researches made a great contribution to the confirmation of higher surface recrystallization rate of amorphous drugs in comparison to the bulk. However, it did not discuss surface recrystallization behaviour of drug-polymer solid dispersions. Recently, Qi et al reported a study concerning early stage phase separation of felodipine-PVP solid dispersions prepared by spin coating (19). In this literature, it was confirmed that surface recrystallization of felodipine-PVP solid dispersions initiated in the layer underneath the surface rather than on the surface, and a drug concentration gradient towards the surface was observed on aging due to the drug migration (19). In this study, similar surface recrystallization progress to Qi et al report was observed in felodipine-EUDRAGIT® EPO melt extrudates.

Surface recrystallization behaviour of melt extrudates was studied by analysing ATR-FTIR data of the surface of melt extrudates on aging (Figure 8.20 and 8.21). Results of 70% (w/w) melt extrudates was discussed here as an example (Figure 8.20a). As can be seen in the figure the spectra were normalised to the intensity of the carbonyl group from the drug ($1696cm^{-1}$), and subsequently a trend of decreased intensity of carbonyl group from the polymer ($1727cm^{-1}$) in the same extrudates with increasing aging time periods was observed. This was also observed in 30% and 50% (w/w) extrudates on aging (Figure 8.21).

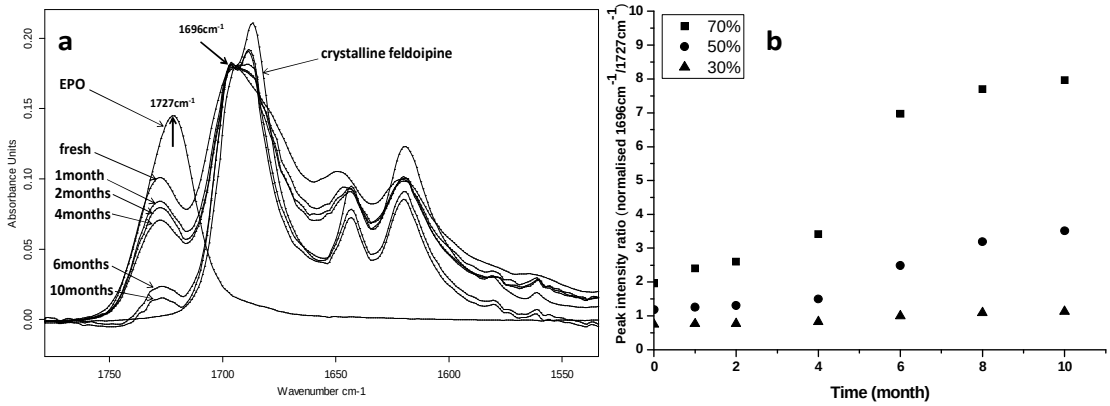

Figure 8.20: a:ATR-FTIR results of carbonyl groups in 70% (w/w) felodipine-EUDRAGIT® EPO melt extrudates on aging under 75%RH/room temperature; b: peak intensity ratio of normalised 1696cm^{-1} to 1727cm^{-1} in 30%-70% (w/w) melt extrudates on aging.

Peak intensity ratio of the normalised 1696cm^{-1} (carbonyl group form crystalline felodipine) to 1727cm^{-1} (carbonyl group from EUDRAGIT® EPO) against aging time is shown in Figure 8.20b. With increasing aging time, gradually increased drug concentration was detected on the surface of 30%-70% (w/w) extrudates. This may indicate the procedure of the surface recrystallization of melt extrudates. Firstly, the reduced relative peak intensity form the polymer indicates the increased drug concentration towards the surface on aging. Secondly, the gradually increased drug concentration on the surface demonstrates that migration of drug molecules in the extrudates occurred from the inner core part towards the surface layer on aging.

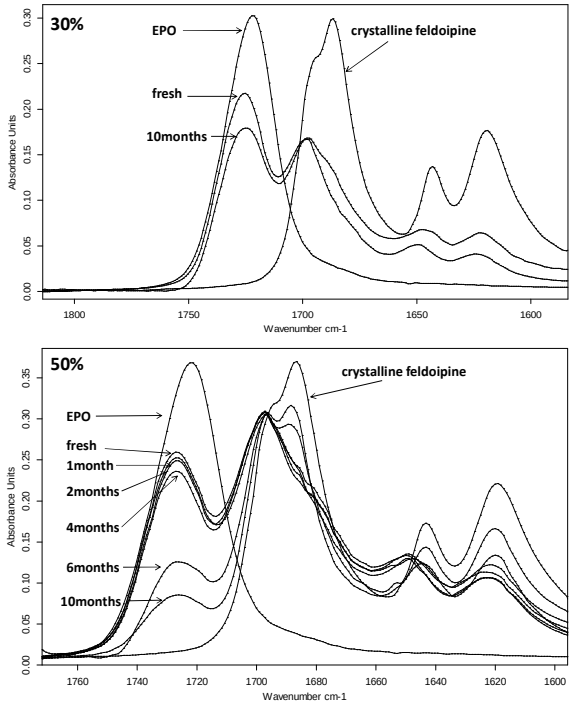

Figure 8.21: ATR-FTIR results of carbonyl groups in 30% and 50% (w/w) felodipine-EUDRAGIT® EPO melt extrudates on aging under 75%RH at room temperature.

However, drug migration towards the surface was not detected in spin coated samples on aging (Figure 8.22). It can be seen that after 10 months aging under 75%RH/room temperature the peak intensity ratio of 1696cm^{-1} to 1727cm^{-1} did not change in 70% and 90% (w/w) spin coated thin films in comparison to the corresponding samples. This demonstrates that within 10 months aging under 75%RH/room temperature, there was no drug migration towards the surface in any spin coated films, indicating the molecular mobility in spin coated thin films was extremely slow in comparison to the corresponding melt extrudates.

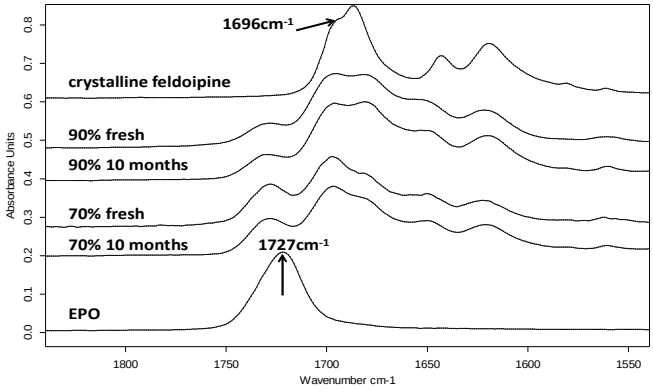

Figure 8.22: ATR-FTIR results of carbonyl groups in fresh and 10 months aged 70% and 90% (w/w) spin coated felodipine-EUDRAGIT® EPO thin films.

Combined with the LTA results, the possible progress of surface recrystallization in felodipine-EUDRAGIT® EPO melt extrudates on aging under stressed humidity at room temperature could be described by the scheme in Figure 8.23. As demonstrated by the LTA measurements on the cross section of the melt extrudates, a single phase amorphous solid dispersion was confirmed even after 10 months aging, it is therefore reasonable to assume that a molecular solid dispersion of felopdipine-EUDRAGIT® EPO was formed as bulk after fresh preparation. On aging under 75%RH at room temperature, drug molecules in the solid dispersions tended to migrate towards the surface to form amorphous drug-rich phase (amorphous phase separation in the layer underneath the surface), and subsequently within the amorphous drug-rich phase recrystallization of amorphous felodipine occurred. Finally, recrystallized felodipine stayed on the surface and at the layer underneath the surface. For ATR-FTIR spectroscopy, the IR beam within the mid-infrared region can penetrate approximately 1-3µm, which indicates the recrystallization progress occurred in the layer 1-3µm underneath the surface (35).

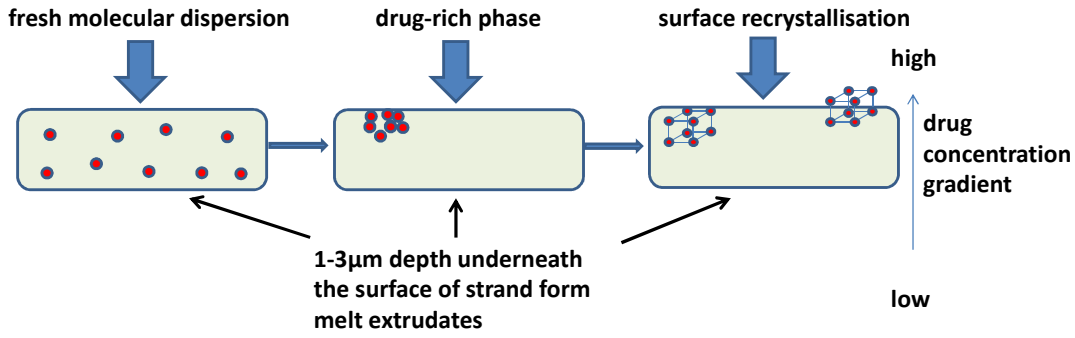

Figure 8.23: Schematic illustration of surface recrystallization in felodipine-EUDRAGIT® EPO melt extrudates on aging.

In Chapter 5, the apparent solid solubility of felodipine in felodipine-EUDRAGIT® EPO was predicted by the milling method as approximate 45% (w/w). The milling method was only applicable to measure the bulk drug-polymer solubility. The occurrence of surface recrystallization in the melt extrudates with the drug loading (30% w/w) below the predicted solubility could be attributed to the proposed recrystallization progress (Figure 8.22). The amorphous drug migration towards the surface on aging is very likely to contribute to the surface recrystallization. Due to the accumulation of amorphous drugs on the layers underneath the surface on aging, an amorphous drug-rich phase was formed (amorphous phase separation in the layer underneath the surface), in which the local drug concentration can be higher than the predicted apparent solid solubility. This localised higher drug concentration could be the driving force for the surface recrystallization. The impetus of the molecular motion at the layer underneath the surface was still not clearly understood, and it could be associated with the lower molecular diffusion barrier at the interface between the surface of extrudates and the ambient, resulting in higher local molecular motion (32). However, this drug migration was not observed in any spin coated solid dispersions on aging (Figure 8.22). This is possibly because surface phase separation in all spin coated thin films was still at early stage, and therefore drug migration may only occur at a substantially low level.

The investigation into surface recrystallisaon of spin coated and melt extruded solid dispersions demonstrates the physical stability of felodipine-EUDRAGIT® EPO solid dispersions was significantly enhanced by spin coating, especially the surface physical stability. For felodipine-EUDRAGIT® EPO solid dispersions with the same drug loading, in this study the transition temperature of amorphous drug-polymer phase (T_g of amorphous solid dispersion) detected by LTA in spin coated thin film was always higher than that detected in melt extrudates (e.g. 10% w/w spin coated thin film showed a transition temperature of 80^{o}C whereas the corresponding melt extrudates showed a transition temperature of 60^{o}C). Although the amorphous drug-polymer transition temperatures of melt extrudates by LTA were different from the value of T_gs measured by DSC, given the fact that two systems were both tested using the same technique (LTA), it is reasonable to believe that glass transition temperatures of spin coated thin films were higher than

the corresponding melt extrudates. As both systems were stored at room temperature which was lower than the T_g of any sample, this increased glass transition temperatures by spin coating contributed significantly to reduce the molecular mobility of drugs in amorphous solid dispersions (36). This reduced molecular mobility of drugs in spin coated thin films in comparison to the molecular mobility of drugs in melt extrudates was proved by the ATR-FTIR analysis (Figure 8.20). Evident drug migration towards the surface was observed in 30%-70% (w/w) extrudates whereas no drug migration was detected in spin coated thin films on aging. Eventually, this reduced molecular mobility by spin coating significantly enhanced the surface physical stability of felodipine-EUDRAGIT® EPO solid dispersions.

8.3.3 Effect of surface recrystallization on dissolution performance of melt extrudates

Bulk recrystallisation in amorphous drug-polymer solid dispersions on aging has been reported to have impact on dissolution performance from formulations (37). However, very few articles focused on the effect of surface recrystallization on drug release from solid dispersion formulations. If melt extrudates were tested as intact strand, it could be expected that surface recrystallisation may reduce overall drug release rate. This is because the dissolution of the inner core part (amorphous solid dispersion) can be delayed due to the slower dissolution rate (in comparison to amorphous drug) of the drug crystals on the surface. In order to investigate the effect of surface recrystallization on drug release from the extrudates, freshly prepared and 10 months aged 10%-70% (w/w) strand form (intact strands without milling) extrudates were tested and compared. It should be mentioned that due to the low mass of spin coated thin films, dissolution test cannot be carried out using conventional dissolution bath with 900ml media.

Preliminary study showed that under non-sink condition (0.1MHCl), drug release was undetectable for any freshly prepared strand form formulation after 3 hours. This is possibly because the significantly smaller surface area (in comparison to the milled extrudates in dissolution test) delayed the dissolution of the drug and the polymer. As proved in Chapter 7, drug release from felodipine-EUDRAGIT® EPO melt extrudates in 0.1MHCl was dominated by the concentration of dissolved EUDRAGIT® EPO in the media, and therefore the insufficient dissolution of polymer (after 3 hours, the tested strand samples were still intact strand) could lead to the extremely low drug concentration in dissolution test. Therefore, sink-condition composed of 0.3% (w/v) SDS in 0.1MHCl (solubility of felodipine in this solution was measured as 273.83µg/ml at 37^{o}C) were used for the dissolution test.

No significant difference of accumulated drug release was seen between 10%-50% (w/w) freshly prepared and 10months aged felodipine-EUDRAGIT® EPO melt extrudates in strand form as seen in Figure 8.24. Maximum drug release was achieved after 20min dissolution of 10%-50% (w/w) fresh and aged melt extrudates, indicating surface recrystallization on aging did not have any impact on the drug release from formulations with drug loadings of 50% (w/w) and below.

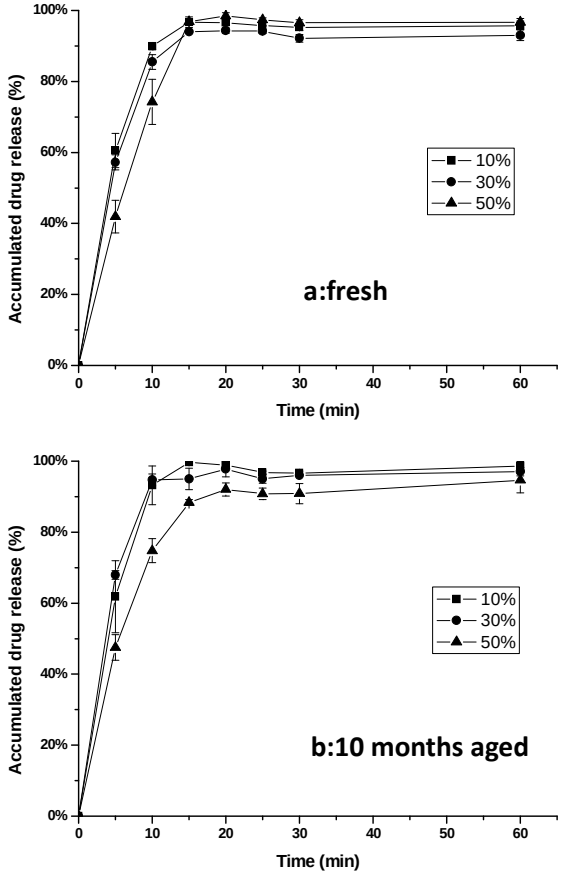

Figure 8.24: Results of dissolution test of 10%-50% (w/w) freshly prepared (a) and 10 months aged (b) felodipine-EUDRAGIT® EPO strand form extrudates under sink condition.

However, evident differences of dissolution performance between 70% (w/w) fresh and 10 months aged extrudates were observed as seen in Figure 8.25. Freshly prepared extrudates showed a higher dissolution rate than the corresponding 10 months aged sample. In addition, after 24 hours dissolution test, maximum drug release from the freshly prepared sample can reach as high as 65%, whereas the 10 months aged extrudates only had a maximum release of 38%. This clearly demonstrates that surface recrystallization can decrease drug release from intact strand extrudates with higher level of recrystallization.

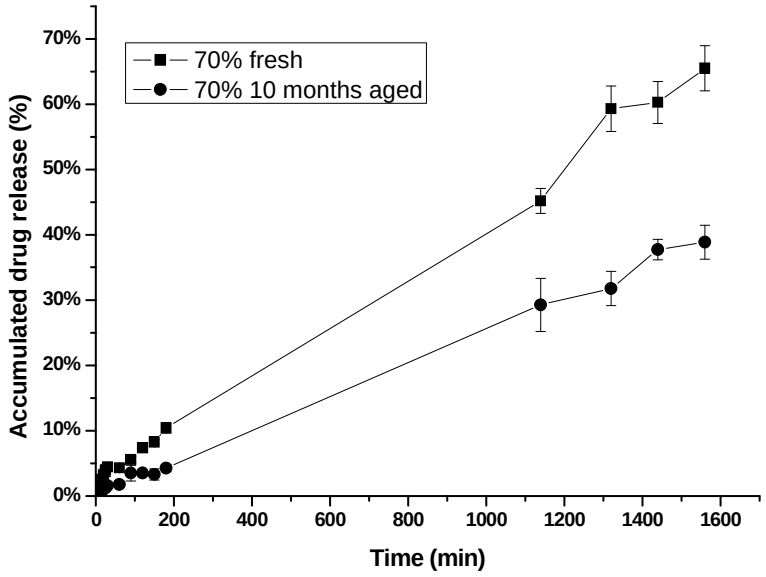

Figure 8.25: Results of dissolution test of 70% (w/w) freshly prepared (a) and 10 months aged (b) felodipine-EUDRAGIT® EPO strand form extrudates under sink condition.

Drug release from formulations can be described by Noyes-Whitney dissolution equation (38):

$$dW / dt = DA (C_s - C) / L \qquad Eq\ 8.1$$

where dW / dt is the dissolution rate, A is the surface area, C is the concentration of the drug in the bulk media, C_s is the concentration of the drug in the surrounding diffusion layer and L is the diffusion layer thickness. Given the fact that the dimensions of the freshly prepared and 10 months aged strand extrudates were controlled by the die of the extruder, the surface area A can be considered identical in dissolution between the two samples. Therefore, the main factor that affects dissolution rate is the difference of drug concentration in the diffusion layer and the bulk media. Since a significantly high degree of surface recrystallization occurred in the 70% (w/w) aged sample, the dissolution driving force in aged sample was the dissolution rate of crystalline felodipine, whereas in freshly prepared strand sample, dissolution rate of felodipine in amorphous solid dispersions became the driving force. The higher dissolution rate of the drug from amorphous solid dispersions in comparison to the crystalline counterpart resulted in the higher drug release rate in freshly prepared strand extrudates. Accordingly, given the same dissolution time period, the higher dissolution rate from fresh 70% (w/w) formulations could lead to a higher maximum drug release at the end of dissolution test. It can be noted that drug release plateau was not achieved even after 24 hours dissolution for fresh and 10 months aged 70% (w/w) strand extrudates. This is possibly because the total surface area of the sample in contact with dissolution media was not sufficiently large leading to a relatively slow dissolution rate in comparison to 10%-50% (w/w) strand extrudates.

It was also noted that fresh and 10 months aged 70% (w/w) strand extrudates showed linear drug release profile, which was significantly different from 10%-50% (w/w) extrudates (fresh and 10 months aged). This linear drug release profile indicates drug release from fresh and aged 70% (w/w) strand extrudates followed a nearly zero-order kinetics whereby the drug release rate was constant throughout the entire dissolution test (39). This zero-order drug release might be attributed to the reason that both fresh and 10 months aged 70% (w/w) extrudates served as a reservoir in dissolution in which drug concentration was super-saturated and drug was constantly released by diffusion into the media though the pathway generated by the dissolved drugs and polymers (40). Since EUDRAGIT® EPO was soluble in 0.1 MHCl, the mechanism of dissolution of 70% (w/w) extrudates may follow a combination of diffusion and erosion. This could be supported by the observation that after 24 hours dissolution test, fresh and 10 months aged 70% (w/w) extrudates remained as stand extrudates but with smaller dimension.

The dissolution study proved that a high level of surface recrystallization on aging can have a significant influence on drug release from intact strand extrudates with high drug loading (70% w/w). Aged strand form samples with 70% (w/w) drug loading showed a reduced drug release rate leading to a lower maximum drug release under sink condition.

8.3.4 Potential explanations for the improved physical stability by spin coating

In articles, it has been reported in case studies that the rate of surface recrystallization of amorphous nifedipine, indomethacin and grisefulvin can be 1-2 orders of magnitude faster than that of bulk recrystallization since the molecular mobility at the interface between the bulk and the ambient was significantly faster than that in the bulk (32-34). However, given the fact that the melt extrudates and spin coated felodipine-EUDRAGIT® EPO solid dispersions were both aged under 75%RH/room temperature and the volume to mass ratio of spin coated thin films were substantially larger than that of the corresponding melt extrudates, it eventually demonstrates that felodipine-EUDRAGIT® EPO solid dispersions prepared by spin coating were significantly more stable than those prepared by hot melt extrusion.

Spin coating as a processing method for the preparation of solid dispersions was limited in the pharmaceutical industry and the application was mainly focused on the understanding of the fundamental mechanism of physical instability of solid dispersions prepared by spin coating alone (19, 41). In this study, by comparing with hot melt extrusion, spin coating was developed into a processing method which can be used to enhance the physical stability of amorphous solid dispersions. The mechanism of the differences in the physical stability of solid dispersions prepared between spin coating and hot melt extrusion was still not clearly understood. However, although lack of literature support, based on the nature of spin coating process and the achieved results from this study, there still could be several speculations explaining the differences.

Firstly, a more intimate mixing in preparation processing between felodipine and EUDRAGIT® EPO by spin coating than by hot melt extrusion could be expected. The drug and the polymer were dissolved in a co-solvent before spin coating, which results in a molecular level of mixing between the drug and the polymer. Whereas in hot melt extrusion, mixing between drugs and polymers was performed by the co-rotating twin screws which may not blend drugs and polymers as intimately as the spin coating method. This was possibly because despite drugs and polymers were melted in hot melt extrusion, the relatively higher viscosity of melted drug-polymer mixtures in comparison to that of pre-spin coating solution may limit the mixing. Secondly, a local "quench" cooling effect in spin coating, which is caused by the fast evaporation of the organic solvent during processing, may contribute to the preparation of a physically stable solid dispersion. In contrast, the melt extruded products were cooled down naturally by the ambient, and thus molecular motion was not as "frozen" in melt extrudates as that in spin coating. These two speculations may possibly lead to higher apparent drug-polymer solubility in solid dispersions prepared by spin coating than by hot melt extrusion. This higher apparent drug-polymer solubility by spin coating could be proved by the successful preparation of amorphous felodipine-EUDRAGIT® EPO solid dispersions with extremely high drug (90% w/w) whereas hot melt extrusion failed to prepare amorphous solid dispersions with the same drug loading. Thirdly, as demonstrated earlier, molecular mobility of drugs in amorphous solid dispersions prepared by spin coating was significantly lower than by hot melt extrusion, which leads to the enhanced surface physical stability of spin coated thin films.

Although a complete understanding of the higher ability of spin coating in stabilising amorphous felodipine in comparison to hot melt extrusion has not been achieved, possibilities discussed above are very likely to explain the observed results. Nevertheless, the study still proved that spin coating was an effective processing method for enhancing the physical stability of felodipine-EUDRAGIT® EPO solid dispersions in comparison to hot melt extrusion.

8.4 Conclusions

In this chapter, a fast solvent evaporation (with no heating involvement which is different from spray drying) based method, spin coating, was applied to enhance the physical stability of felodipine-EUDRAGIT® EPO solid dispersions. Upon exposure to stressed humidity (75%RH) at room temperature on aging, physical stability of formulations prepared by spin coating were significantly higher than those prepared by hot melt extrusion, especially the surface physical stability. A high degree of surface recrystallization was observed in 30%-70% (w/w) melt extrudaes on aging after different time periods using conventional characterisation techniques. In contrast, surface recrystallization in 50%-90% (w/w) spin coated samples was only confirmed at a low level using LTA after 10 months aging.

Upon exposure to stressed humidity (75%RH) at room temperature, drug migration towards the surface of melt extrudates to form a drug-rich phase was observed, which was considered as the

contribution to the surface recrystallization in extrudates with drug loading (30% w/w) below the predicted apparent solid solubility (45%w/w). Drug migration was not seen in spin coated samples indicating lower drug molecular motion in spin coated samples than in melt extrudates. This reduced drug migration in spin coated thin films was believed to be one of the main reasons for the higher surface physical stability provided by spin coating.

Surface recrystallization in 70% (w/w) extrudates showed significant impact on dissolution performance. The maximum drug release decreased from 65% in fresh samples to 38% in 10months aged sample. For extrudates with 10%-50% (w/w) drug loadings, no significant difference of drug release was observed between fresh and 10 months aged samples.

Reference

1. H.N. Joshi, R.W. Tejwani, M. Davidovich, V.P. Sahasrabudhe, M. Jemal, M.S. Bathala, S.A. Varia, and A.T.M. Serajuddin. Bioavailability enhancement of a poorly water-soluble drug by solid dispersion in polyethylene glycol–polysorbate 80 mixture. International Journal of Pharmaceutics. 269:251-258 (2004).
2. N.A. Urbanetzand B.C. Lippold. Solid dispersions of nimodipine and polyethylene glycol 2000: dissolution properties and physico-chemical characterisation. European Journal of Pharmaceutics and Biopharmaceutics. 59:107-118 (2005).
3. D.J. van Drooge, W.L.J. Hinrichs, M.R. Visser, and H.W. Frijlink. Characterization of the molecular distribution of drugs in glassy solid dispersions at the nano-meter scale, using differential scanning calorimetry and gravimetric water vapour sorption techniques. International Journal of Pharmaceutics. 310:220-229 (2006).
4. S. Qi, A. Gryczke, P. Belton, and D.Q.M. Craig. Characterisation of solid dispersions of paracetamol and EUDRAGIT® E prepared by hot-melt extrusion using thermal, microthermal and spectroscopic analysis. International Journal of Pharmaceutics. 354:158-167 (2008).
5. J. Zhang, M. Bunker, A. Parker, C.E. Madden-Smith, N. Patel, and C.J. Roberts. The stability of solid dispersions of felodipine in polyvinylpyrrolidone characterized by nanothermal analysis. International Journal of Pharmaceutics. 414:210-217 (2011).
6. P. Marsac, T. Li, and L. Taylor. Estimation of Drug–Polymer Miscibility and Solubility in Amorphous Solid Dispersions Using Experimentally Determined Interaction Parameters. Pharm Res. 26:139-151 (2009).
7. J.A. Bairdand L.S. Taylor. Evaluation of amorphous solid dispersion properties using thermal analysis techniques. Advanced Drug Delivery Reviews. 64:396-421 (2012).
8. P. Ke, S. Hasegawa, H. Al-Obaidi, and G. Buckton. Investigation of preparation methods on surface/bulk structural relaxation and glass fragility of amorphous solid dispersions. International Journal of Pharmaceutics. 422:170-178 (2012).
9. S. Janssens, A. Zeure, A. Paudel, J. Humbeeck, P. Rombaut, and G. Mooter. Influence of Preparation Methods on Solid State Supersaturation of Amorphous Solid Dispersions: A Case Study with Itraconazole and Eudragit E100. Pharm Res. 27:775-785 (2010).
10. I. Weuts, F. Van Dycke, J. Voorspoels, S. De Cort, S. Stokbroekx, R. Leemans, M.E. Brewster, D. Xu, B. Segmuller, Y.T.A. Turner, C.J. Roberts, M.C. Davies, S. Qi, D.Q.M. Craig, and M. Reading. Physicochemical properties of the amorphous drug, cast films, and spray dried powders to predict formulation probability of success for solid dispersions: Etravirine. Journal of Pharmaceutical Sciences. 100:260-274 (2011).
11. P. Karmwar, K. Graeser, K.C. Gordon, C.J. Strachan, and T. Rades. Investigation of properties and recrystallisation behaviour of amorphous indomethacin samples prepared by different methods. International Journal of Pharmaceutics. 417:94-100 (2011).
12. L. Yu. Amorphous pharmaceutical solids: preparation, characterization and stabilization. Advanced Drug Delivery Reviews. 48:27-42 (2001).

13. W.L. Chiouand S. Riegelman. Pharmaceutical applications of solid dispersion systems. Journal of Pharmaceutical Sciences. 60:1281-1302 (1971).
14. H. Konnoand L. Taylor. Ability of Different Polymers to Inhibit the Crystallization of Amorphous Felodipine in the Presence of Moisture. Pharm Res. 25:969-978 (2008).
15. D. Schubertand T. Dunkel. Spin coating from a molecular point of view: its concentration regimes, influence of molar mass and distribution. Mat Res Innovat. 7:314-321 (2003).
16. R.W. Carr. Process engineering analysis in semiconductor device fabrication. By Stanley Middleman and Arthur K. Hochberg, McGraw-Hill, Inc., 1993, 774 pp. + xvii. AIChE Journal. 41:200-201 (1995).
17. M.A. Repka, S.K. Battu, S.B. Upadhye, S. Thumma, M.M. Crowley, F. Zhang, C. Martin, and J.W. McGinity. Pharmaceutical Applications of Hot-Melt Extrusion: Part II. Drug Development and Industrial Pharmacy. 33:1043-1057 (2007).
18. A.F. Rumondor, H. Wikström, B. Van Eerdenbrugh, and L. Taylor. Understanding the Tendency of Amorphous Solid Dispersions to Undergo Amorphous–Amorphous Phase Separation in the Presence of Absorbed Moisture. AAPS PharmSciTech. 12:1209-1219 (2011).
19. S. Qi, J.G. Moffat, and Z. Yang. Early Stage Phase Separation in Pharmaceutical Solid Dispersion Thin Films under High Humidity: Improved Spatial Understanding Using Probe-Based Thermal and Spectroscopic Nanocharacterization Methods. Molecular Pharmaceutics. 10:918-930 (2013).
20. X. Tang, M. Pikal, and L. Taylor. A Spectroscopic Investigation of Hydrogen Bond Patterns in Crystalline and Amorphous Phases in Dihydropyridine Calcium Channel Blockers. Pharm Res. 19:477-483 (2002).
21. P. Bergese, I. Colombo, D. Gervasoni, and L.E. Depero. Melting of Nanostructured Drugs Embedded into a Polymeric Matrix. The Journal of Physical Chemistry B. 108:15488-15493 (2004).
22. M. Alcoutlabiand G.B. McKenna. Effects of confinement on material behaviour at the nanometre size scale. Journal of Physics Condensed Matter. 17:R461-R524 (2005).
23. X. Dai, J.G. Moffat, J. Wood, and M. Reading. Thermal scanning probe microscopy in the development of pharmaceuticals. Advanced Drug Delivery Reviews. 64:449-460 (2012).
24. D.Q.M. Craig, V.L. Kett, C.S. Andrews, and P.G. Royall. Pharmaceutical applications of micro-thermal analysis. Journal of Pharmaceutical Sciences. 91:1201-1213 (2002).
25. L. Harding, M. Reading, and D.Q.M. Craig. The development of heated tip force–distance measurements as a novel approach to site-specific characterization of pharmaceutical materials. Journal of Pharmaceutical Sciences. 97:2768-2779 (2008).
26. S. Qi, S.J. Roser, D. Deutsch, S.A. Barker, and D.Q.M. Craig. A laser imaging and neutron reflection investigation into the monolayer behaviour of fatty acids used for taste masking microspheres. Journal of Pharmaceutical Sciences. 97:1864-1877 (2008).
27. R.K. Thomas. Neutron reflectometry in solid state and materials science. Current Opinion in Solid State and Materials Science. 1:636-644 (1996).
28. R.K. Thomas. NEUTRON REFLECTION FROM LIQUID INTERFACES. Annual Review of Physical Chemistry. 55:391-426 (2004).
29. Y. Liao, J. You, T. Shi, L. An, and P.K. Dutta. Phase Behavior and Dewetting for Polymer Blend Films Studied by In Situ AFM and XPS: From Thin to Ultrathin Films. Langmuir. 23:11107-11111 (2007).
30. J. You, S. Hu, Y. Liao, K. Song, Y. Men, T. Shi, and L. An. Composition effect on dewetting of ultrathin films of miscible polymer blend. Polymer. 50:4745-4752 (2009).
31. J. You, Y. Liao, Y. Men, T. Shi, and L. An. Film Thickness Dependence of Phase Separation and Dewetting Behaviors in PMMA/SAN Blend Films. Langmuir. 26:14530-14534 (2010).
32. T. Wu, Y. Sun, N. Li, M.M. de Villiers, and L. Yu. Inhibiting Surface Crystallization of Amorphous Indomethacin by Nanocoating. Langmuir. 23:5148-5153 (2007).
33. L. Zhu, L. Wong, and L. Yu. Surface-Enhanced Crystallization of Amorphous Nifedipine. Molecular Pharmaceutics. 5:921-926 (2008).
34. L. Zhu, J. Jona, K. Nagapudi, and T. Wu. Fast Surface Crystallization of Amorphous Griseofulvin Below T g. Pharm Res. 27:1558-1567 (2010).

35. J.G. Van Alstenand S.R. Lustig. Polymer mutual diffusion measurements using infrared ATR spectroscopy. Macromolecules. 25:5069-5073 (1992).
36. B. Hancock, S. Shamblin, and G. Zografi. Molecular Mobility of Amorphous Pharmaceutical Solids Below Their Glass Transition Temperatures. Pharm Res. 12:799-806 (1995).
37. M.M. Crowley, F. Zhang, M.A. Repka, S. Thumma, S.B. Upadhye, S. Kumar Battu, J.W. McGinity, and C. Martin. Pharmaceutical Applications of Hot-Melt Extrusion: Part I. Drug Development and Industrial Pharmacy. 33:909-926 (2007).
38. A.A. Noyesand W.R. Whitney. THE RATE OF SOLUTION OF SOLID SUBSTANCES IN THEIR OWN SOLUTIONS. Journal of the American Chemical Society. 19:930-934 (1897).
39. R. Wada, S.-H. Hyon, and Y. Ikada. Kinetics of diffusion-mediated drug release enhanced by matrix degradation. Journal of Controlled Release. 37:151-160 (1995).
40. Y. Fuand W.J. Kao. Drug release kinetics and transport mechanisms of non-degradable and degradable polymeric delivery systems. Expert Opinion on Drug Delivery. 7:429-444 (2010).
41. Y.C. Ng, Z. Yang, W.J. McAuley, and S. Qi. Stabilisation of amorphous drugs under high humidity using pharmaceutical thin films. European Journal of Pharmaceutics and Biopharmaceutics(2013).

Chapter 9 Concluding remarks

The physical stability of amorphous solid dispersions has been the most emphasized topic in articles regarding solid dispersions since the concept of the solid dispersion was introduced (1-4). The physical instability has been considered as the main obstacle for the formulation development and commercialization of amorphous solid dispersions in the pharmaceutical industry (3, 4). It is generally accepted that the physical stability can have significant influence on *in-vitro* and *in-vivo* performance from amorphous solid dispersions containing poorly water-soluble drugs. Therefore, from the view of the formulation development of amorphous solid dispersions, it is essential to gain a comprehensive understanding of the physical stability in order to better predict and control the physical stability. This project was fundamentally designed for the understanding, prediction and enhancement of the physical stability of amorphous solid dispersions. By using four model drugs (felodipine, celecoxib, carbamazepine and fenofibrate) and three polymeric matrices (EUDRAGIT® EPO and Kollidon® VA 64 and the blend of the two polymers) to be formulated by hot melt extrusion (main method) and spin coating, three main achievements were obtained from the project:1) a clear understanding of factors which dominate the physical stability of amorphous solid dispersions; 2) development of a practical method (milling) for more accurate prediction of processing-related apparent drug-polymer solubility; 3) development of two methods for the enhancement of the physical stability of amorphous solid dispersions.

9.1 Understanding of the dominant factors controlling the physical stability of amorphous solid dispersions

In order to find out the key factors associated with the physical stability of amorphous solid dispersions, a series of physical properties including glass transition temperatures of amorphous drugs, relaxation time (molecular mobility) of amorphous drugs, physical stability of amorphous drugs alone and drug-polymer miscibility and solubility were studied. These factors have been suggested in articles to be related with the physical stability of amorphous solid dispersions (4-8). However, there have been few studies evaluating all these factors together and revealing which of these factors are dominating the physical stability of amorphous solid dispersions.

In Chapter 3, physical characterization of model drugs and polymers was carried out. Results showed that the glass transition temperatures of the model drugs used in this study varied in a broad range from (-19^{o}C for fenofibrate) to (58^{o}C for celecoxib). Calculated relaxation time also showed a wide range amongst amorphous model drugs. In order to evaluate the physical stability of amorphous model drugs thoroughly, amorphous drugs were prepared using melt-cool and spin coating, respectively. On aging under 0%RH/room temperature and 75%RH/room temperature up to 2 weeks, irrespective of preparation methods, the order of the physical stability of amorphous model drugs alone was felodipine > celecoxib > carbamazepine > fenofibrate. However, the T_gs

and calculated relaxation time of the model drugs did not show this order, demonstrating these two factors may not always correlate with the physical stability of amorphous materials.

In Chapter 4, different theoretical approaches including solubility parameter method, melting point depression method and an enthalpy based method were used to predict the drug-polymer miscibility and solubility (Table 4.5). Predicted solubilities of the model drugs in EUDRAGIT® EPO varied with the different theoretical methods used. In Chapter 5, a processing-related method, milling, for more accurately predicting apparent drug-polymer solubility was developed. Using the milling method, the apparent solubility of the model drugs in melt extrudates was predicted and they were felodipine (45%w/w), celecoxib (42%w/w), carbamazepine (18%w/w) and fenofibrate (13%w/w). Compared with the solubilities predicted by the theoretical approaches, solubilities predicted by the milling method were proved to be more accurate by the real-time physical stability studies. This is attributed to the reason that the milling method took into account the effect of processing method.

In Chapter 6, the real-time physical stability of melt extrudates prepared with model drugs and EUDRAGIT® EPO were studied under 4 conditions: 0%RH/room temperature, 75%RH/room temperature, 0%RH/40^{o}C and 75%RH/40^{o}C. All melt extrudates were prepared with drug loadings below (10% w/w) and above (70%w/w super-saturated) the individual predicted solubility (by theoretical and milling methods). Results showed that for individual drug-polymer systems with the two drug loadings, stressed humidity had more significant impact on the physical stability than stressed temperature. It has been well-known that storage conditions of stressed temperature and stressed humidity both have effect on the physical stability of amorphous solid dispersions (3, 9, 10). However, few studies have disclosed which one had more significant influence on the physical stability. Results from the real-time physical stability study clearly revealed that even for systems with low water sorption stressed humidity had more significant impact on the physical stability of amorphous solid dispersions than stressed temperature. Comparing different drug-polymer systems with the same drug loading aged under the condition of 0%RH/room temperature, 75%RH/room temperature, 0%RH/40^{o}C, the order of the physical stability of melt extrudates was felodipine > celecoxib > carbamazepine ≥ fenofibrate. Only aged under 75%RH/40^{o}C, 70% (w/w) celecoxib-EUDRAGIT® EPO showed higher physical stability than 70% (w/w) felodipine-EUDRAGIT® EPO. The reason can be attributed to the lower glass transition temperature of the 70% (w/w) felodipine-EUDRAGIT® EPO systems (38^{o}C) in comparison to the corresponding celecoxib systems (58^{o}C), resulting in a high molecular mobility in 70% (w/w) felodipine-EUDRAGIT® EPO systems under the aging condition (75%RH/40^{o}C).

Combining the physical stability study and the physical characterization study, a comprehensive understanding of the physical stability behavior of amorphous solid dispersions prepared by hot melt extrusion can be achieved. Amongst all the evaluated factors, only the physical stability of

amorphous drugs alone and the predicted drug-polymer solubility by milling method showed the same order as the order of the physical stability of different systems. Therefore, it can be concluded that these two factors are the dominant factors which control the physical stability of amorphous solid dispersions.

The results from the project significantly enriched the understanding of the behavior of the physical stability of amorphous solid dispersions. The practical implications of these finds can be useful for the formulation development of amorphous solid dispersions. In terms of selecting storage conditions for amorphous solid dispersions, it should avoid high humidity. When screening drug candidates for the formulation develop, highly stable amorphous drugs may lead to highly stable amorphous solid dispersions.

9.2 Prediction of apparent drug-polymer solubility in melt extrudates

Drug-polymer solid solubility has been suggested as one of the most significant factors associated with the physical stability of amorphous solid dispersions (6, 9). However, due to the extremely high viscosity of amorphous solid dispersions at room temperature (temperature below the T_g of the solid dispersion), it can take years for super-saturated systems to reach the equilibrium state, resulting in the difficulty of measuring the equilibrium drug-polymer solid solubility (11).

Therefore, instead of measuring the equilibrium drug-polymer solubility, a few attempts by using theoretical models have been made to predict the apparent drug-polymer solubility. Solubility parameter method, melting point depression method and an enthalpy based method have been reported in articles to predict the drug-polymer solubility and they are currently widely used for in the area of solid dispersions (6, 12, 13). However, the predicted values by all theoretical approaches did not show the same order as the order of the physical stability of different melt extrudates on aging. This indicates that these theoretical approaches may not be capable to predict drug-polymer solubility accurately due to their limitations (limitations have been discussed in Chapter 4 and 5). More importantly, these methods did not take into account the effect of processing method on the apparent solubility of drugs in amorphous solid dispersions (14).

In this project, a novel milling-based method was developed to more accurately predict the processing-related apparent solubility of drugs in melt extrudates. In Chapter 5, by studying the effect of milling on the physical state of felodipine-EUDRAGIT® EPO melt extrudates, it demonstrated that using milling can significantly accelerate the procedure of super-saturated melt extrudates to reach the equilibrium state, which enables the fast prediction of apparent drug-polymer solubility. The accuracy of the milling method in predicting apparent drug-polymer solubility was assessed by comparing the real-time physical stability studies of different systems under different conditions. Results showed that systems with higher predicted drug-polymer

solubility were more physically stable than systems with lower predicted solubility under most conditions.

The developed milling method demonstrated its high potential to be practically used in melt extruded amorphous solid dispersions for the prediction of drug-polymer solubility and physical stabilization. It can be used to rapidly screen a "safe" range of drug loadings to enhance the physical stability on aging at the pre-formulation stage. With drug loadings in formulations below the predicted solubility by the milling method, melt extruded amorphous solid dispersions are expected to have good physical stability on aging.

9.3 Enhancement of the physical stability of amorphous solid dispersions

The enhancement of the physical stability can enhance the shelf life of an amorphous solid dispersion. The application of polymers which can potentially form hydrogen bonding with drugs are expected to improve the physical stability as the hydrogen bonding may improve the drug-polymer miscibility and solubility and hence the physical stability. However, as discussed in Chapter 7, those polymers can be hygroscopic and amorphous formulations prepared with them have high propensity to take up moisture on aging leading to drug phase separation and recrystallization. In this project, two methods based on the formulation design and processing effect were developed for the enhancement of the physical stability of amorphous solid dispersions, and they were the application of immiscible polymer blends in melt extrusion and the development of spin coating into a processing method.

9.3.1 Enhancement of the physical stability of amorphous solid dispersions using immiscible polymer blends

Polymer blends of EUDRAGIT® EPO and Kollidon® VA64 combined the advantages of the two polymers whereby Kollidon® VA64 has higher apparent drug- polymer solubility (proved by the milling method) and EUDRAGIT® EPO is hydrophobic which does not take up moisture upon exposure to high humidity. Therefore, in felodipine-polymer blend extrudates the overall drug-polymer solubility was increased in comparison to the binary felodipine-EUDRAGIT® EPO systems and the overall moisture uptake was decreased in comparison to the binary felodipine-Kollidon® VA64 systems. These combined advantages significantly enhanced the physical stability of the amorphous solid dispersions on aging under stressed humidity and stressed temperature compared with the two binary systems.

The developed immiscible polymer blends concept may be generalized as a common formulation strategy which can be applied widely in amorphous solid dispersions for the enhancement of the physical stability, and may not just be restricted in hot melt extrusion. The fundamental conception of polymer blends is to take advantage of the merits of individual polymer and "silence" their disadvantage. Ideally, in drug-polymer blend amorphous solid dispersions, more drugs will

dissolve into the polymer phase having higher solubility. Due to the immiscibility between the two polymers, phase separation will exist in the polymer blend systems. The phase separation can effectively protect the high drug concentration phase by increasing the diffusion length of the water sorption into the system, and thus decrease the overall moisture uptake of the blend system. Therefore, the application of immiscible polymer blends may generally be effective in enhancing the physical stability of amorphous solid dispersions prepared by different methods.

9.3.2 Enhancement of the physical stability using spin coating as a processing method

In this project, spin coating was successfully developed into a processing method for the enhancement of amorphous solid dispersions. In comparison to the corresponding melt extrudates, felodipine-EUDRAGIT® EPO systems prepared by spin coating showed extremely low level of surface recrystallisation on aging under 75%RH/room temperature up to 10 months.

The enhanced physical stability by spin coating was still not clearly understood, and it may be attributed to the decreased molecular mobility as discussed in Chapter 8. Nevertheless, results from this part of the project still proved using spin coating can be an effective process to prepare amorphous solid dispersions with improved physical stability. The enhanced physical stability by spin coating provides several implications to the formulation development of amorphous solid dispersions. It clearly demonstrated that physical stability of amorphous solid dispersions can vary depending on different processing methods. More importantly, with the growing interest in formulating drugs into thin films, such as buccal/sublingual oral films (15-17), spin coating can be used as a practical film preparation method to produce amorphous drug-polymer films with high physical stability.

9.4 Recommended future work

Results collected from this project provided a comprehensive understanding of the physical stability of amorphous solid dispersions, a practical tool for the prediction of apparent drug-polymer solubility, and two methods for the enhancement of the physical stability of amorphous solid dispersions. However, as there were still several results from the project without clear explanation, the continuation related to this project might be needed. The recommended future work is listed as follows:

1. Investigation into the underpinning mechanism of the solubilizing effect of EUDRAGIT® EPO in 0.1MHCl solution on poorly water-soluble drugs.

2. Correlating the enhanced in-vitro performance from the polymer blend formulations to the in-vivo performance by animal test.

3. Investigation into the mechanisms of the enhanced physical stability by spin coating.

Reference

1. O.N. Sekiguchi K. Studies on Absorption of Eutectic Mixture. I. A Comparison of the Behavior of Eutectic Mixture of Sulfathiazole and that of Ordinary Sulfathiazole in Man. Chem Pharm Bull:866-872 (1961).
2. W.L. Chiouand S. Riegelman. Preparation and dissolution characteristics of several fast-release solid dispersions of griseofulvin. Journal of Pharmaceutical Sciences. 58:1505-1510 (1969).
3. A.T.M. Serajuddin. Solid dispersion of poorly water-soluble drugs: Early promises, subsequent problems, and recent breakthroughs. Journal of Pharmaceutical Sciences. 88:1058-1066 (1999).
4. T. Vasconcelos, B. Sarmento, and P. Costa. Solid dispersions as strategy to improve oral bioavailability of poor water soluble drugs. Drug Discovery Today. 12:1068-1075 (2007).
5. B. Hancock, S. Shamblin, and G. Zografi. Molecular Mobility of Amorphous Pharmaceutical Solids Below Their Glass Transition Temperatures. Pharm Res. 12:799-806 (1995).
6. P. Marsac, S. Shamblin, and L. Taylor. Theoretical and Practical Approaches for Prediction of Drug–Polymer Miscibility and Solubility. Pharm Res. 23:2417-2426 (2006).
7. Y.C. Ng, Z. Yang, W.J. McAuley, and S. Qi. Stabilisation of amorphous drugs under high humidity using pharmaceutical thin films. European Journal of Pharmaceutics and Biopharmaceutics(2013).
8. S. Dudduand P. Dal Monte. Effect of Glass Transition Temperature on the Stability of Lyophilized Formulations Containing a Chimeric Therapeutic Monoclonal Antibody. Pharm Res. 14:591-595 (1997).
9. P. Marsac, T. Li, and L. Taylor. Estimation of Drug–Polymer Miscibility and Solubility in Amorphous Solid Dispersions Using Experimentally Determined Interaction Parameters. Pharm Res. 26:139-151 (2009).
10. C. Telang, S. Mujumdar, and M. Mathew. Improved physical stability of amorphous state through acid base interactions. Journal of Pharmaceutical Sciences. 98:2149-2159 (2009).
11. F. Qian, J. Huang, and M.A. Hussain. Drug–polymer solubility and miscibility: Stability consideration and practical challenges in amorphous solid dispersion development. Journal of Pharmaceutical Sciences. 99:2941-2947 (2010).
12. B.C. Hancock, P. York, and R.C. Rowe. The use of solubility parameters in pharmaceutical dosage form design. International Journal of Pharmaceutics. 148:1-21 (1997).
13. S. Qi, P. Belton, K. Nollenberger, N. Clayden, M. Reading, and D.M. Craig. Characterisation and Prediction of Phase Separation in Hot-Melt Extruded Solid Dispersions: A Thermal, Microscopic and NMR Relaxometry Study. Pharm Res. 27:1869-1883 (2010).
14. S. Janssens, A. Zeure, A. Paudel, J. Humbeeck, P. Rombaut, and G. Mooter. Influence of Preparation Methods on Solid State Supersaturation of Amorphous Solid Dispersions: A Case Study with Itraconazole and Eudragit E100. Pharm Res. 27:775-785 (2010).
15. P.K.N. Arani Bose. Endovascular thin film devices and methods for treating and preventing stroke, Vol. US6666882 B1, United States, 2003.
16. J.B. Ciolino, T.R. Hoare, N.G. Iwata, I. Behlau, C.H. Dohlman, R. Langer, and D.S. Kohane. A Drug-Eluting Contact Lens. Investigative Ophthalmology & Visual Science. 50:3346-3352 (2009).
17. A.C. Arun Arya, Vijay Sharma, Kamla Pathak. Fast Dissolving Oral Films: An Innovative Drug Delivery System and Dosage Form. International Journal of ChemTech Research. 2:8 (2010).